UNIVERSITEIT VAN PRETORIA
UNIVERSITY OF PRETORIA
YUNIBESITHI YA PRETORIA

Development and evaluation of a bi-enzymatic nitric oxide reduction system

Seike Garny

Submitted in partial fulfilment of the requirements for the degree

Philosophiae Doctor Biochemistry

in the Faculty of Natural and Agricultural Science

University of Pretoria

Pretoria

South Africa

December 2013

Supervisors:

Prof. Jan Verschoor (University of Pretoria)

Dr Justin Jordaan (Council of Scientific and Industrial Research)

Submission Declaration

I, Seike Garny, declare that this dissertation, which is herewith submitted for the degree Philosophiae Doctor at the University of Pretoria, is my own work and has not previously been submitted by me for a degree at this or any other tertiary institution.

Signature:_____ Date:_____

Plagiarism Declaration

University of Pretoria

Faculty of Natural and Agricultural Sciences

Department of Biochemistry

Full name:	Seike Garny
Student number:	10680022
Title of work:	Development and evaluation of a bi-enzymatic nitric oxide reduction system

Declaration

1. I understand what plagiarism entails and I am aware of the University's policy in this regard.
2. I declare that this thesis is my own, original work. Where someone else's work was used (whether from a printed source, the internet or any other source) due acknowledgement was given and reference was made according to departmental requirements.
3. I did not make use of another student's previous work and submit it as my own.
4. I did not allow and will not allow anyone to copy my work with the intention of presenting it as his or her own work.

Signature: _____ Date: _____

Acknowledgements

I wish to express my sincere gratitude to the following individuals and institutions:

My supervisors Prof. Verschoor and Dr Justin Jordaan for their mentorship and guidance as well as their willingness to invest in me.

My collaborators at the University of Stellenbosch: Prof. Emile van Zyl and Dr Shaunita Rose for providing the *Aspergillus niger* expression host and plasmid.

The Protein Expression group of the CSIR Bioscience: Dr Michael Crampton, Dr Eldi Burger for providing the *Escherichia coli* expression host and plasmid.

The Protein Technology group of the CSIR Bioscience in Modderfontein: Dr Dean Brady, Dr Daniel Visser and colleges for their assistance in their laboratory.

MS-MS analysis: Dr Stoyan Stoychev

Helpful discussions with Helen Seals, Dr Sean Tuling, Dr Natasha Beeton-Kempen, Dr Raksha Boohra, Dr Isak Gerber and Dr Neil Gardiner regarding various aspects of this thesis.

My family and friends for their continuous encouragement and support.

CSIR ReSyn Bio Team for all the fun in the lab.

Funding bodies: Parliamentary grant of the CSIR and DST grant for the Emerging Health Technologies

CSIR Human Capital Development and studentship program for financial support

Abstract

Nitric oxide is a small diatomic molecule and is part of the nitrogen radical species. As a gas, it diffuses easily across cell membranes and is involved in numerous physiological processes and inflammation. This peculiar molecule has a dual role in inflammation. NO is one of the first signals to commence an innate immune response and it is involved in the resolution of inflammation. In the control of inflammation it is crucial to resolve NO bursts to promote tissue healing. The failure thereof results in the progression of inflammation with potentially catastrophic consequences for the host.

This study aimed to develop a nitric oxide reduction system as a research tool which could facilitate the understanding of the intricate role of NO in inflammation. Numerous chemical tools have been used to study NO biology, but were found to interfere in other metabolic pathways; thereby masking the role of NO. The nitric oxide reduction system entails the reduction of NO by nitric oxide reductase (NOR) with the concomitant oxidation of glucose by glucose dehydrogenase (GDH). The latter enzyme recycles the cofactor NADH in such a way that NO is continuously reduced. This bi-enzymatic cofactor recycling system presents the advantage of NO removal without any interference of metabolic pathways. Here, we propose that the continuous reduction of NO by the NOR system could be used to elucidate the role of NO in an innate immune response.

The construction of the NOR system commenced with development of fast and reliable spectrophotometric NADH-enzyme activity assay. This assay was essential for the quantification of enzyme activity and was used throughout the study for the purification of NOR, characterisation of NOR as well as the determination of enzyme activity maintenance after enzyme immobilisation. Both enzymes were immobilised onto five carriers with two different functional group chemistries and three functional group densities. The carboxyl functionalised carrier with the lowest functional group density was the most suitable immobilisation carrier by maintaining the highest enzyme activity for NOR and GDH. Upon co-immobilisation of both enzymes, an average of 0.088 µmoles $NADH.min^{-1}$ for NOR and 0.077 µmoles $NAD.min^{-1}$ for GDH cofactor oxidation rate was achieved. Furthermore, the cofactor was recycled six times with the concomitant consumption of the enzymes' substrates. Subsequently, the NOR system was evaluated for its potential as a research tool in an *in vitro* inflammation model.

The continuous reduction of NO was established which highlights the NOR system suitability as a research tool. However, its evaluation as a potential anti-inflammatory reagent indicated that the chosen carrier has immunogenic properties of its own. The inflammation response

elicited by this carrier alone was in part abrogated by the immobilisation of enzymes in the eventual NOR system assembly, thereby providing a scope for future work and further optimisation of this anti-inflammatory reagent.

Table of Content

˚C	degree Celsius
2MM	double strength medium
AL	Argininosuccinate lysate
AmpR	Ampicillin resistance
AP-1	Activator protein 1
AS	Argininosuccinate synthase
Asp	Asparagine
ATP	Adenosine 5′-triphosphate
BGG	bovine gamma globulin
BH_4	tetrahydrobiopterin
BioMatSA	Biomaterials Society of South Africa
BSA	bovine serum albumin
C/EPBb	CCAAT-enhancer-binding proteins
cAMP	cyclic adenosine 3′,5′-cyclic monophosphate
CAT	cationic amino acid transporters
cGMP	cyclic guanosine monophosphate
CO	Carbon monoxide
cPTIO	2-(4-Carboxyphenyl)-4,4,5,5-tetramethylimidazoline-1-oxyl-3-oxide potassium salt
CSIR	Council of Science and Industrial Research
CYP	cytochrome P450 family
Cyt	cytochrome
DAF-FM	4-Amino-5-methylamino- 2′,7′-difluorofluorescein
DAF-FM DA	4-Amino-5-methylamino- 2′,7′-difluorofluorescein diacetate
dd H_2O	double distilled water
Dex	Dexamethasone
DMSO	Dimethyl sulfoxide
DNA	Dioxyribonucleic acid
DTT	Dithiothreitol
e.g.	for example
EDC	1-Ethyl-3-(3-dimethylaminopropyl)carbodiimide
EDTA	Ethylenediaminetetraacetic acid
eNOS	endothelial Nitric Oxide Synthase
Erk	extracellular signal-regulated kinases
EU	Endotoxin units
FAD	Flavin adenine dinucleotide
FBS	Foetal bovine serum
FMN	Flavin mononucleotide
GC	Gas chromatography
GDH	Glucose dehydrogenase
GFP	Green fluorescence protein
GTP	Guanosine 5′-triphosphate
GTP-CH: I	GTP cyclohdrolase I

HEPES	4-(2-hydroxyethyl)-1-piperazineethanesulfonic acid
HuR	human RNA binding protein
i.e.	in other words"that is" from latin
IEC	Ion exchange chromatography
IFNγ	Interferon gamma
IL	Interleukin
iNOS	induced nitric oxide synthase
IPTG	Isopropyl β-D-1-thiogalactopyranoside
JNK	Jun Kinases
KanR	Kanamycin resistance
kbps	kilo basepairs of DNA
k_{cat}	catalytic turnover constant/number
K_{cat}/K_m	enzyme efficiency
kDa	kilo Dalton of protein
KLF6	Kruppel-like factor 6
K_m	Michelis-Menten constant
Kunits	Kilo units of DNase I
LB plot	Lineweaver-Burk double reciprocal plot
L-NAME	L-NG-Nitroarginine methyl ester
LPS	Lipopolysaccharide
M	Molar
Mo	monocytes
MØ	macrophages
MAPK	mitogen activated protein kinases
MES	2-(*N*-morpholino)ethanesulfonic acid
MIF	macrophage migration inhibitory factor
min	minute(s)
mM	milli Molar
MM	minimal media
MM+H	minimal media with haemoglobin
mRNA	messenger Ribonucleic acid
MS-MS	tandem mass spectrophotometry
MW	molecular weight
na	not applicable
NAD	Nicotinamide adenine dinucleotide
NADH	Nicotinamide adenine dinucleotide hydrogen
NANC	non-adrenergic and non-cholinergic nerves
NADPH	Nicotinamide adenine dinucleotide phosphate hydrogen
NF-κB	nuclear factor kappa-light-chain-enhancer of activated B cells
NHS	*N*-hydroxysuccinimide
N-L analysis	non-linear regresssion analyis
nm	nano meters
nNOS	neural Nitric Oxide Synthase
NO	Nitric oxide
NOC-5	3-(2-hydroxy-1-(methylethyl)-2-nitrosohydrazino)-1-propanamine
NOR	Nitric Oxide Reductase
NORsys	Nitric Oxide Reductase System
NOS	Nitric Oxide Synthase
NTA	Ni^{2+}-nitrilotriacetic acid
NTP	Nucleotide triphosphate

OD	optical density
ODC	Ornithine decarboxylase
P	probability value
PBS	phosphate buffered saline
PCI	phenol chloroform isopropyl alcohol
PCR	Polymerase chain reaction
PDE	Phosphodiesterases
PE	phycoerythrin
PEG	Polyethylene glycol
PEI	Polyethylenimine
PI3K	Protein tyrosine phosphatases
PKCδ	Protein kinase C delta
PKG	cGMP-dependent protein kinases (also cGK)
PMA	Phorbol 12-myristate 13-acetate
Raf-1 protein kinases	serine/threonine specific kinase
RFU	felative fluorescence unit
RNA	Ribonucleic acid
rpm	rotations per minutes
RPMI	Roswell Park Memorial Institute medium
SASBMB	South African Society of Biochemistry and Molecular Biology
SDS-PAGE	sodium dodecyl sulfate polyacrylamide gelelectrophoresis
SEC	Size exclusion chromatography
sen	sensitivity of RFU
Ser	Serine
sGC	soluble guanylyl cyclase
SLE	systemic lupus erythematosus
SNAP	S-Nitroso-N-acetyl-DL-penicillamine
SOC	super optimal catabolite repression media
STAT1	signal transducers and activators of transcription family 1
STE	Sodium chloride TRIS EDTA buffer
T/O	turnover rates
TAE	TRIS Acetate EDTA buffer
TE	Trace elements
TEA	Triethanolamine
Thr	Threonine
TGFβ	Transforming growth factor-beta
TNFα	Tumour necrosis factor alpha
TRIS	Tris(hydroxymethyl)aminomethane
UK	United Kingdom
USA	United States of America
v/v	volume/volume
w/v	weight/volume
V_{max}	maximum velocity
V_{max}/K_m	specificity constant
vs.	versus

Chapter 1
Introduction

1.1. Introduction to Nitric Oxide

Nitric oxide is a small diatomic gaseous molecule with a relative short halfe-life as it reacts with numerous targets in biolobical systems [1]. This simple molecule is an important regulator and plays fundamental roles in neuroscience, physiology and immunology [1]. With this peculiear molecule at the centre of this study, it was aimed to develop a nitric oxide reduction system as a research tool which could be used to improve the understanding of NO in biology.

1.1.1. Nitric Oxide, small but potent messenger

The significance of nitric oxide (NO) led to its acclaim as 'Molecule of the Year' in 1992 [1]. In 1998, the Nobel Price of Physiology or Medicine was awarded to Robert F. Furchgott, Louis J. Ignarro, Ferid Murad for their discoveries regarding nitric oxide as a signalling molecule [2]. The physiological role of this molecule subsequently received much scientific attention in which the entothelial relaxing factor was defined as nitric oxide as well its affect on cyclic GMP levels in cells [2, 3, 4, 5, 6, 7, 8, 9], shedding light on the plurality of its biological functions mediated by cGMP signal transduction system [10, 11, 12, 13]. Nitric oxide is a reactive nitrogen and its role as an antibacterial reagent in the immune response has been described by Dugas *et al.* (1995) [14] and reviewed by Moncada *et al.* (1991) [13], Whittle (1995) [15] and Pacher *et al.* (2007) [17] who elaborate on nitric oxide's role in various pathologies [13, 14, 15, 16, 17].

Nitric oxide (NO) is a biologically important signalling molecule in many cellular processes [18]. Its mechanism of action is affected by its reaction with transition metals of enzymes (such as soluble guanylate cyclase, cytochrome *c* oxidase and

catalase), or results in the S-nitrosylation of target proteins (transcription factors, caspases, ion channels and metabolic proteins) and generating other reactive nitrogen species which oxidise proteins, lipids and nucleotides [19, 20, 21] as outlined in Scheme 1.1.

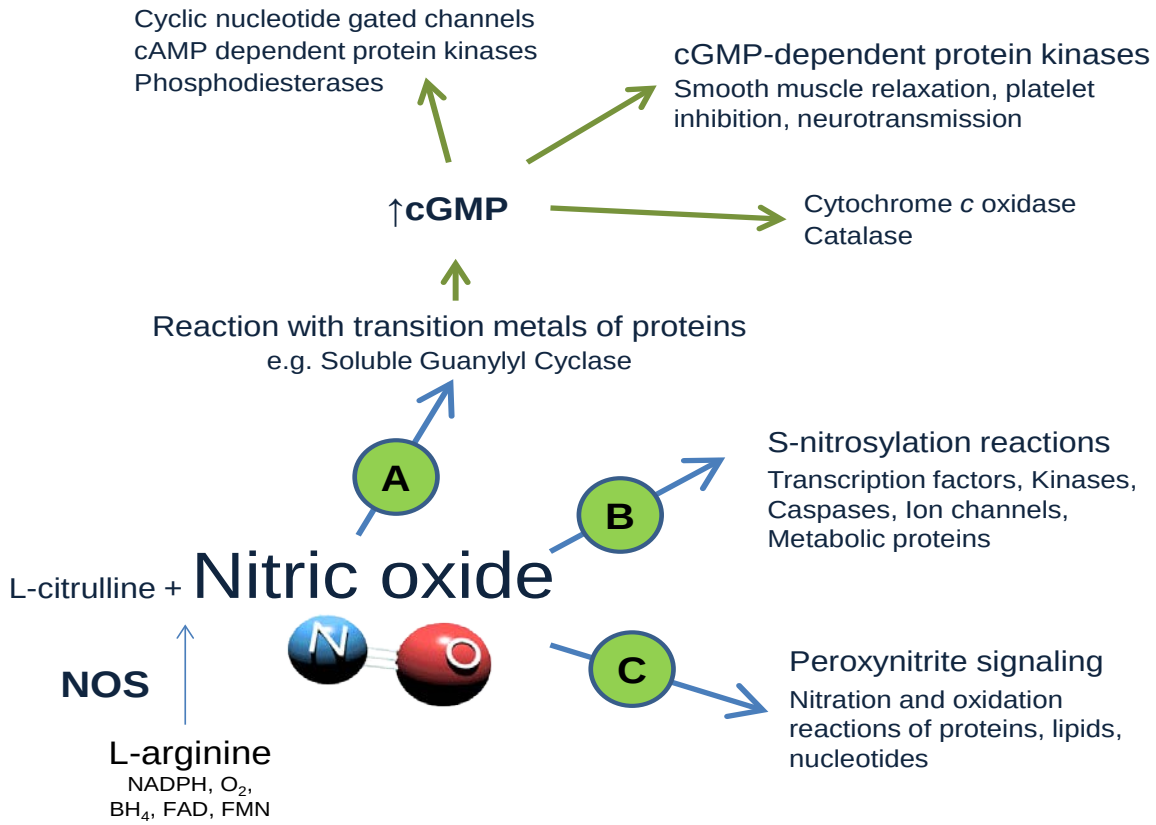

Scheme 1.1. The three major signalling pathways of NO. NO produced by nitric oxide synthase (NOS) reacts with transition metals such as iron, copper and zinc (A). This interaction is a direct effect of NO to cellular responses mostly at low concentrations. Alternatively, NO signalling can be conveyed by the formation of S-nitrosothiols from cysteine residues (B) or it reacts with superoxide anion producing peroxynitrite (C). The latter two responses are an indirect effect of NO at higher concentrations [19, 20, 21].

Due to its hydrophobic nature, NO is capable of diffusing across membranes with little resistance and can move between cells within its half-life of few milli seconds [16, 20, 22]. This property makes nitric oxide a relative fast intra- and extracellular messenger [16]. Nitric oxide initiates a signalling cascade by activating soluble guanylyl cyclase (sGC), which increases the synthesis of cyclic guanosine monophosphate (cGMP) [3]. Cyclic GMP activates downstream cGMP dependent kinases [6], protein phosphorylation [4] or decreases intracellular calcium levels in target cells [23]. Nitric Oxide–cGMP signal transduction system has been observed in diverse tissues and can result in multiple effects [18, 24] including smooth muscle

relaxation [7, 25]; platelet adhesion [26, 27]; neurotransmission [28, 29, 30]; and immune response [14, 31, 32, 33, 34, 35, 36, 37]. These effects are depicted in Scheme 1.2.

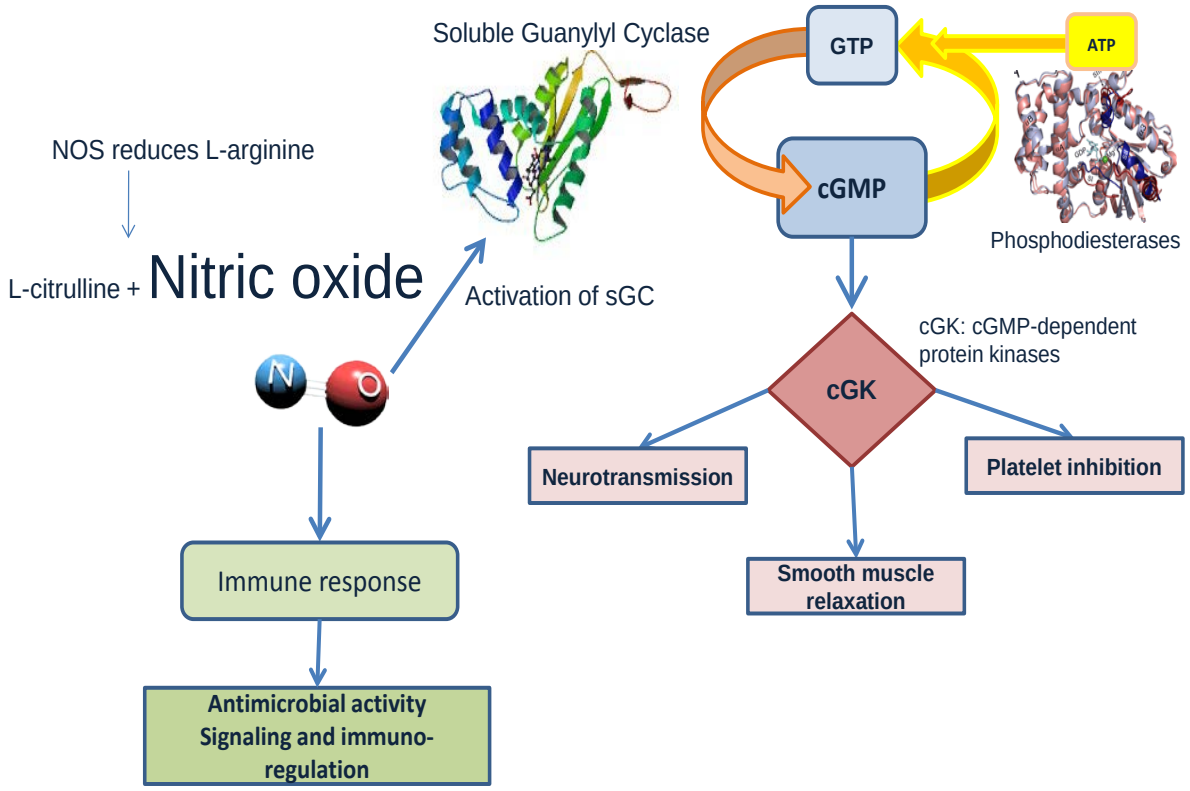

Scheme 1.2. The various physiological effects of NO induced signal transduction cascades. NO signalling commences with NO binding to a soluble guanylyl cyclase (sGC) which increases the synthesis of cyclic GMP. Intracellular cGMP modulates cGMP-dependent protein kinases (cGK, also PKG) and phosphodiesterases (PDE) which results in various cellular responses [10, 18, 24, 38].

1.1.2. Physiological role of NO

In 1987, Palmer and colleagues discovered that NO had identical biological properties to the endothelium relaxing factor and initiated research into nitric oxide's physiological role [4, 5, 7, 8, 9]. In the vasculature, NO is a paracrine agent and acts as a vasodilator. It is secreted by the endothelial cells and stimulates adjacent smooth muscles to relax [7, 8, 25]. In blood, NO inhibits platelet adhesion [26, 27, 39] and platelet aggregation [27, 39, 40] mediated by the NO-cGMP signalling pathways (refer Scheme 1.1). Nitric oxide is synthesised from L-arginine by the endothelial nitric oxide synthase (eNOS), which is located in endothelial cells [13] and platelets [39].

NO has been observed to act as an inhibitory neurotransmitter from the non-adrenergic and non-cholinergic (NANC) nerves in the gastro-intestinal tract [28, 41]. The neural Nitric oxide synthesising enzyme (nNOS) has been identified in enteric neurons [28]. It has been shown that NO hyperpolarizes smooth muscle cells and results in NANC relaxation [28]. Another example of NO acting as a neuromodulator is the expression of nNOS in the brain [30, 42], in cells of the cerebellum and the myenteric plexus [12].

In the innate immune defence system, an inducible nitric oxide synthase (iNOS) in macrophages and neutrophils produce NO in response to foreign molecules and micro-organisms [12, 43]. The production of NO is considered a major microcidal strategy [31, 33]. Nitric oxide is produced by an inducible nitric oxide synthase (iNOS or NOS2) in response to microbial products and pro-inflammatory cytokines [31]. This inducible nitric oxide enzyme (iNOS) synthesis NO over a prolonged period at higher amounts than the other two alternate nitric oxide synthesising enzymes, nNOS and eNOS [12]. During the innate defence mechanism, NO and superoxide react with each other to form the bactericidal peroxynitrite, which has also been implicated in promoting tissue injury [16, 17, 44, 45, 46].

The innate immune system acts as the first line of defence against harmful materials which is followed by the adaptive immune system to mount a response, subsequently followed by tissue repair [47, 48]. The latter immune response refers to inflammation resolution in which the pro-inflammatory mediators are suppressed and inflammatory cell-apoptosis and phagocytosis are induced [47, 48, 49, 50]. The resolution of inflammation is an active process which involves complex pathways in which nitric oxide has been shown to play a role [35, 51, 52].

1.1.3. Regulation of NO synthesis by NOS

The synthesis of NO is dependent on the transcription of the enzyme NOS [61]. The binding of various transcription factors such as NF-κB, Stat1, C/EPBb, KLF6 and AP-1 have been shown to effect the transcription of NOS [34, 53, 348]. NOS transcription has also have been shown to be controlled by mRNA stability [19]. Factors such as HuR, PKCδ, JNK, TGFβ, cGMP, cAMP as well as chemical

reagents such as dexamethasone and forskolin have shown to alter the mRNA stability [19]. The expression of iNOS is also under the control of its substrate availability and affinity in which intracellular arginine concentration have shown to affect iNOS expression [19, 53]. Besides regulation of iNOS expression on a transcriptional and post-transcriptional level, iNOS expression is regulated by various signalling pathways [19]. These include the regulation of transcription factors for iNOS expression, cAMP activation, signalling pathways regulated by cytokines or intracellular calcium, as well as the activation of mitogen activated protein kinases [19]. The regulation of NO synthesis by the upstream signalling pathway is dependent on the stimuli (microbial or cytokine) and the cell type, where some pathways promote (Janus kinases, Raf-1 protein kinases, MAP kinases p38, Erk1/2-JNK, PKC) or inhibit (PI3K, protein tyrosine phosphatases) NOS expression [53]. Furthermore, NO itself also has a regulatory effect on iNOS expression, where a low NO concentration mediates iNOS expression via NF-κB activation and high NO exerts a negative feedback regulating its own production [53, 54, 55, 56]. The signalling control of NO synthesis and its cellular effects are therefore complex and extensive. Scheme 1.4. outlines an example of NO synthesis regulation by iNOS in a macrophage in response to microbial infection.

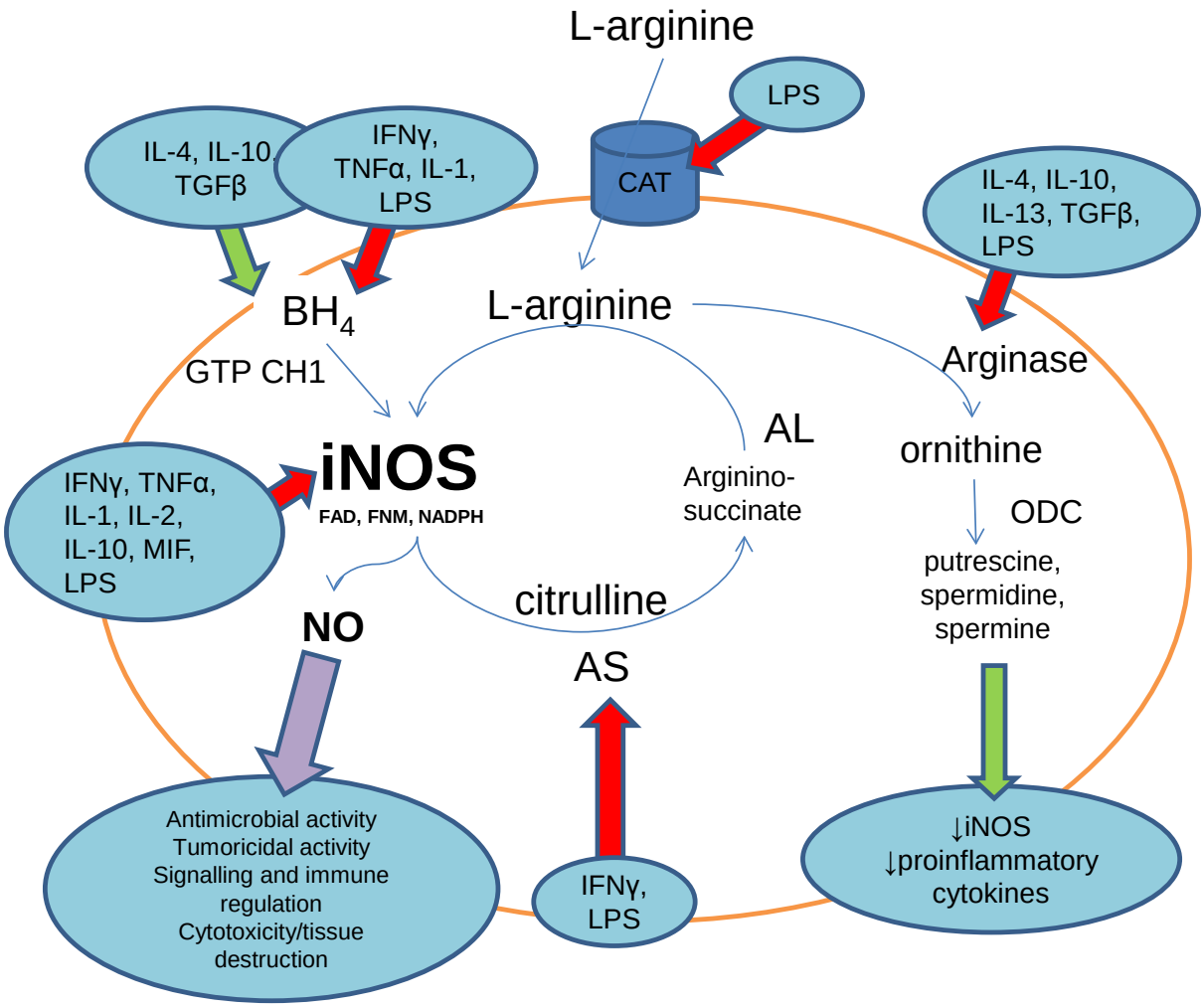

Scheme 1.3. Regulation of NO synthesis by iNOS in a macrophage to microbial stimuli. Cytokines and lipopolysaccharides (LPS) effect iNOS activity by increasing the uptake of arginine via cationic amino acid transporters (CAT), the synthesis of cofactors (BH_4) by GTP cyclohydrolase I (GTP-CH: I), iNOS mRNA stability, the enzymatic recycling of citrulline back to arginine by argininosuccinate synthase (AS) and argininosuccinate lysate (AL). Arginase activity reduces arginine concentration, which reduces iNOS activity. The arginase product, ornithine is converted to polyamines (putrescine, spermine and spermidine) by ornithine decarboxylase (ODC) which have immune suppressing properties. Red arrows indicate increase or activation where green arrows reduce or suppress the activation of the target. The purple arrow highlights some of the signalling effects of NO. The scheme was adapted from Bogdan *et al.* (2001) [53].

1.1.4. Nitric Oxide homeostasis

It is evident that NO plays a vital role in a variety of biological systems. Homeostasis of this molecule is therefore critical for normal biological function [57, 58]. There are mechanisms which produce and reduce NO *de novo* to maintain the essential balance required for normal biological function [58].

Nitric oxide is generated *de novo* from L-arginine and molecular oxygen by nitric oxide synthase (a dioxygenase, EC 1.14.13.39) producing L-citrulline as a by-product [11]. The reaction is aided by tetrahydrobiopterin (BH_4), nicotinamide adenine dinucleotide phosphate (NADPH) and flavin containing cofactors, such as FAD, FMN and cytochrome P450, to transfer the electron from NADPH to the oxygen molecule [11, 58]. To date, three nitric oxide synthase (NOS) isoforms have been identified and are named according to their activity [16, 59, 60, 61, 62]. Neural NOS (nNOS) is located in the central and peripheral neurons, while endothelial NOS (eNOS) has been identified in the vascular endothelium, platelets and the heart [16]. The third type, or inducible NOS (iNOS), is expressed in macrophages, hepatocytes and keratinocytes [36]. The enzymes can share up to 60% protein homology and form a part of the cytochrome P450 reductase-like family [36]. Nitric oxide synthases, nNOS and eNOS, contribute to the nitric oxide homeostasis of the body, while iNOS is primarily involved in immune response [60].

It is essential that effective systems exist to remove cytotoxic NO from biological systems due to the potential detrimental effects of this free radical [16, 45, 51, 63]. Several mechanisms for the removal of NO have been identified [64]. NO spontaneously reacts with superoxide to form peroxynitrite and is associated with pathogenesis [17, 44, 65]. Dioxygenase activity of globins, such as haemoglobin and myoglobin, are able to decompose NO to nitrates [66, 67, 68, 69] and the recently discovered globins, neuroglobin and cytoglobin, might further have NO scavenging functions [70, 71]. The NO oxidase, ceruloplasmin, has been shown to contribute to the endocrine NO homeostasis in plasma by oxidising NO to NO^+ which is subsequently hydrated to nitrite [72, 73]. Pearce and colleagues (2002) [74] suggested that cytochrome *c* oxidase is more likely to remove NO from mitochondria-rich cells under physiological conditions to form a nitrite ion rather than

nitrate. Other enzymes, such as lipoxygenase [75], prostaglandin H synthase [40, 76], peroxidase [77, 78], catalase [79] and nitrite reductases [80], have the capacity to remove NO from the environment by forming nitrite [65]. A study conducted by Igamberdiev and colleagues (2004) [81], identified that dihydrolipoamide dehyrogenase has the capacity to scavenge NO and may act as a methemoglobin reductase using NADPH as an electron donor. A flavohemoglobin-like NO dioxygenase that forms nitrate has further been identified to reduce NO in tissues [57]. NO is recycled from its nitrite and nitrate products via nitrate reduction involving either xanthine oxidoreductase [82], deoxyhaemoglobin [83] or cytochrome bc_1 complex in the mitochondria [80, 84, 85]. This completes the NO cycle as depicted in Scheme 1.4.

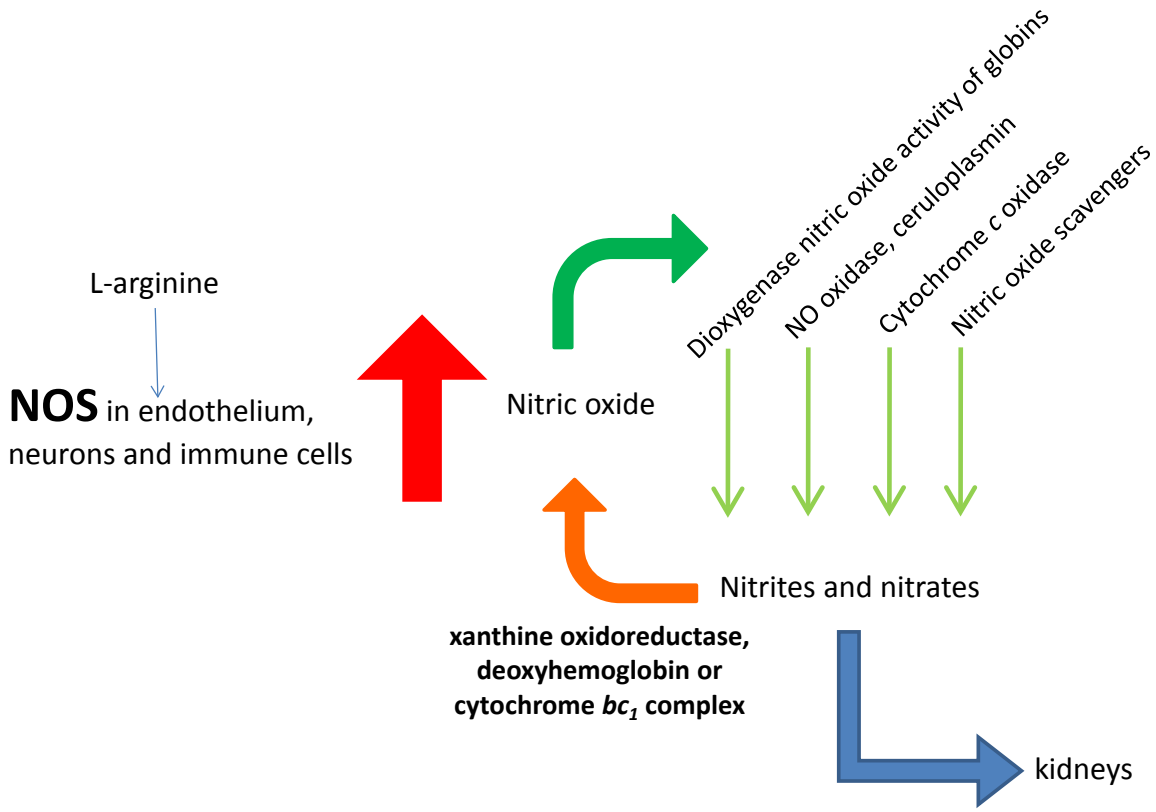

Scheme 1.4. The NO cycle in the body. NO is synthesised by NOS in various cells and oxidised to nitrates or nitrates by globins and other enzymes. Some of the nitrates are excreted by the kidneys. Enzymes generating NO from the nitrates and nitrites are further involved in NO homeostasis. Scheme was adopted from Reutov *et al.* (2002) [58].

1.1.5. Role of Nitric oxide in disease

Many studies have shown that NO plays a crucial role in several pathological conditions [13, 15, 34]. Heart diseases, diseases of the blood vessels, diabetes, neurodegenerative diseases [16], rheumatoid arthritis, systemic lupus erythematosus (SLE), [36, 86] and cerebral malaria [87] are just a few examples in which NO contributes to the disease progression. Nitric oxide contributes to pathogenesis in two ways: too little NO (where its physiological regulation properties are absent or very low) affects mechanisms of cell survival [16, 33] or alternatively high NO levels which results in the spontaneous formation of peroxynitrite causing tissue injury via protein oxidation and nitrosative stress [16, 17, 45, 88, 89]. Low levels of NO in cardiac tissue increases blood pressure which can result in hypertension and angina pectoris [12]. To rectify the balance of NO, patients with high blood pressure, are often treated with nitro-donors [13, 24]. In contrast; high levels of NO are observed in the inflammatory response to combat pathogens [33]. The inflammatory cells (macrophages and neutrophils) secrete NO in micro-molar concentrations which can result in tissue injury through nitrosative stress [63, 88].

Under normal conditions, the inflammatory response ceases after a short period and the wound healing mechanism results in repair of injured tissues [34, 51]. However, in some pathologies (e.g. diabetes type I, rheumatoid arthritis, multiple sclerosis, experimental autoimmune encephalomyelitis, autoimmune diseases) an imbalance of pro-inflammatory cytokines (IL-2, TNFα, IFN-γ) and immuno-suppressive cytokines (IL-4, IL-10, TGFβ; [34]) could result in a cycle of chronic inflammation and ultimately self-destruction [12]. This is a direct result of high levels of reactive oxygen species (ROS) such as nitric oxide and superoxide [15].

1.1.6. Current research methodology to understand biological of NO

The current best practice to study the role of NO in disease is the inhibition of NOS with L-arginine analogs [13]. These studies have contributed valuable information on the physiological role of NO as a regulatory agent. However, limitations of this method are that L-arginine analogs interfere with cardiovascular physiology, cellular integrity and neurotransmission [11, 90, 91, 92, 93, 94]. Furthermore, studies have

observed that a residual NO is essential for the control and down regulation of the local cellular immune system [34]. Complete inhibition of NO synthesis by L-arginine analogs has unfavourable side effects [32]. NOS inhibitors as pharmacological agents are therefore unacceptable [34]. So far, no physiological agents, except for hormones, such as glucocorticoids [95] and cytokines [53], have been identified for the inhibition of NOS [95] and there is therefore a need to identify and develop new tools and alternative mechanisms to study the role of NO as a physiological regulator and causative agent in several pathologies. To address this shortcoming the development of a system to reduce NO to nitrous oxide is proposed.

1.2. Nitric Oxide Redution System

1.2.1. Bi-enzymatic cofactor recycling system

Enzymes are biological catalysts found in all living cells. Their substrate specificity has made them an attractive alternative to chemical synthesis for the production of valuable compounds such as pharmaceutical intermediates and for industrial applications [96, 97, 98, 99, 100, 101, 102].

The main principle for the novel ReSyn™ microspheres immobilised NO reduction system is the recycling of nucleotide cofactor, nicotinamide adenine dinucleotide (NAD) and its reduced form, nicotinamide adenine dinucleotide hydrogen (NADH). This can be achieved by using a two enzyme system [103]. The enzyme reaction and stoichometry of the system is indicated in Scheme 1.4. Briefly, nitric oxide reductase (EC 1.7.99.7), oxidises two NO molecules with conversion of NADH to NAD^+, nitrous oxide and water [104]. The second enzyme, glucose dehydrogenase (EC 1.1.1.47), recycles NAD^+ back to NADH using glucose to form gluconolactone [105, 106, 107] as indicated in Scheme 1.5, allowing for its recycling to oxidise a further two molecules of NO.

The co-immobilisation of enzymes allows for the potential development of multi-enzymatic bio-catalytic processes [108, 109, 110, 111]. It often entails an enzyme of bio-catalytic value in combination with an enzyme performing a co-enzymatic

function, such as the recycling of a cofactor or coenzyme, for example oxidoreductases [112, 113]. For the development of the proposed enzymatic nitric oxide reducing system, the two enzymes are from two different biological sources, and are brought into close proximity. With the co-immobilisation of a fungal nitric oxide reductase (NOR) and a bacterial glucose dehydrogenase (GDH), two chemical reactions could thus be catalysed in close proximity, allowing for near simultaneous kinetics for substrate conversion, and regeneration of the cofactor.

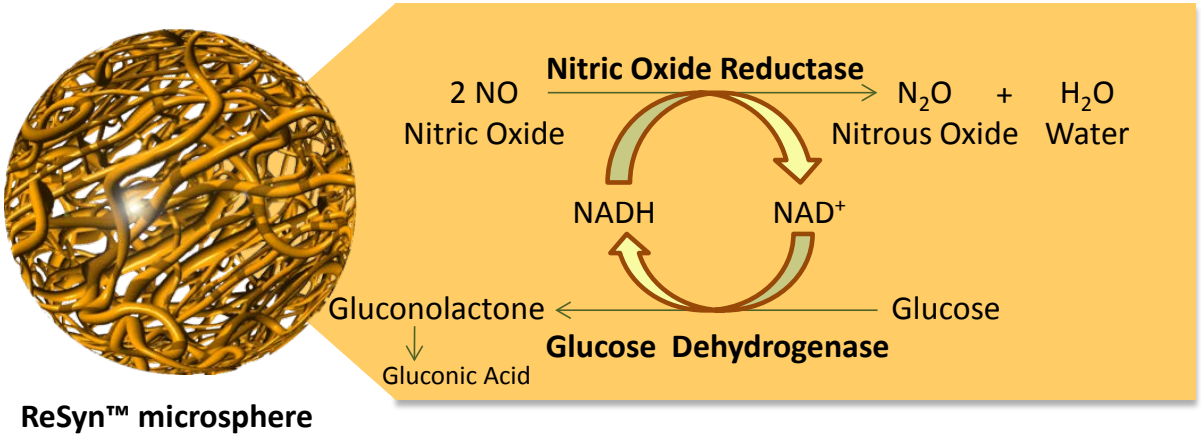

Scheme 1.5. The ReSyn™ microspheres immobilised Nitric Oxide Reduction system. A depiction of the reaction mechanism of the novel Nitric Oxide Reduction system with nitric oxide reductase and cofactor recycling enzyme glucose dehydrogenase. Nitric oxide (2 molecules) is oxidised to nitrous oxide and water in the above reaction with conversion of NADH to NAD^+. The cofactor recycling reaction involves the reduction of glucose to gluonolactone using NAD^+. ReSyn™ microspheres have a high protein binding capacity providing for efficient co-immobilisation of the enzymes.

1.2.2. Microsphere supports

A plethora of enzyme immobilisation techniques have been reported and are available for immobilisation [115, 116, 117, 118, 119]. Several comprehensive reports outline the variety of techniques and the suitability to immobilise a variety of enzyme classes have been published [120, 121, 122, 123]. The available methods of immobilisation, include encapsulation, self-immobilisation (random and crystalline interactions) and solid support (chemical and ionic interactions) (refer to Scheme 1.6.), the latter was selected for the immobilisation of NOR and GDH. Solid supports for enzyme immobilisation have been reported to provide enhanced enzyme stability and high immobilisation yields [124, 125, 126, 127].

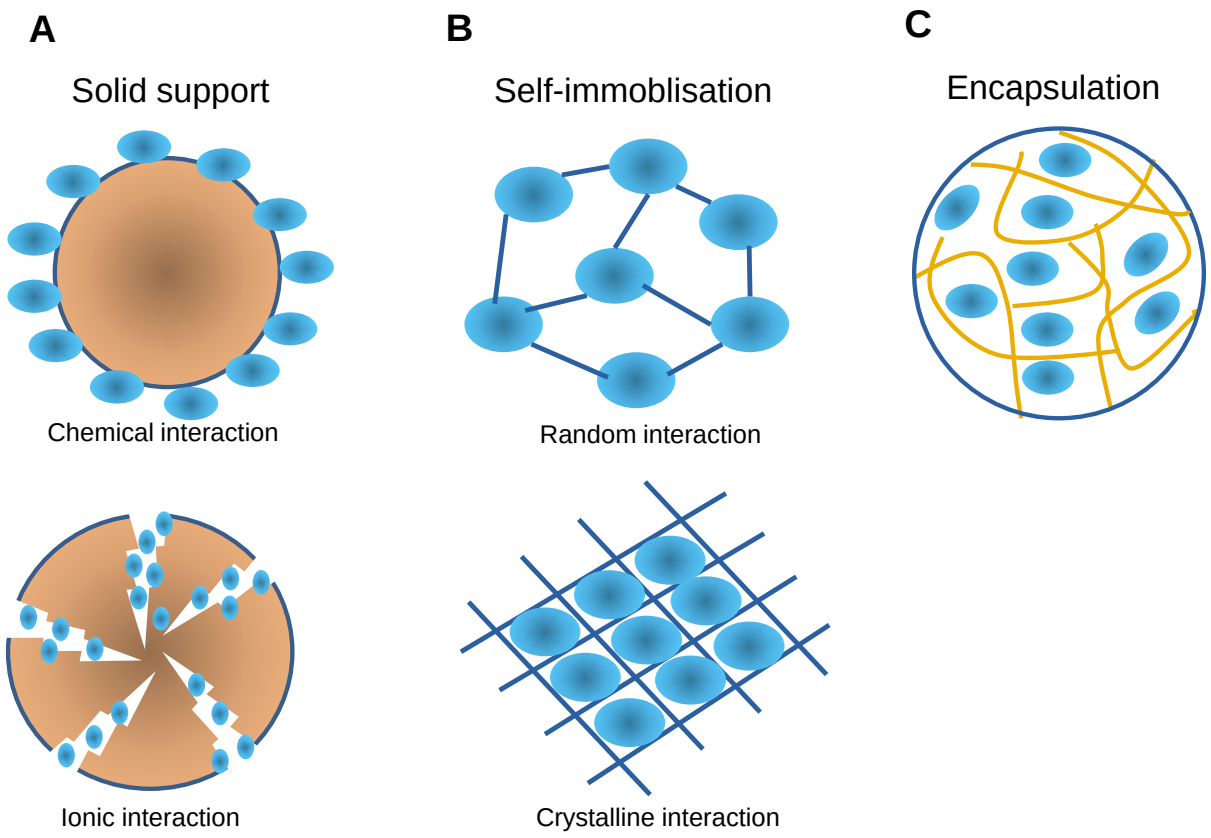

Scheme 1.6. Various enzyme immobilisation techniques. In (A), physical interactions of enzyme with a solid support, e.g. a spherical bead and (B) self-immobilisation strategies with multiple covalent bond formation at random or in crystalline interactions. Enzyme encapsulation is shown in (C), which encapsulates enzymes by physical barrier, e.g. a lipid miscelle. Enzymes are represented as blue spheres and immobilisation carrier in brown. Chemical interactions are represented in straight blue lines [128].

The vast array of possible immobilisation carriers flows from the multiple possible chemical functionalities and variety of materials they can be prepared from and include for instance: carbon nanotubes [129], epoxy activated synthetic supports such as Eupergit®C [123, 130], and activated bio-derived polymer supports such as glyoxyl-agarose [127, 131, 132]. An alternate to using a carrier or support are carrier free self-immobilisation techniques such as Spherezymes™ [133]. ReSyn™ microspheres are a relatively new immobilisation carrier with comparatively high binding capacity and high functional group densities (www.resynbio.com). These features, as well as the proposed structure of the polymer beads, make it ideally suited for the immobilisation. In consideration of the possible immobilisation carriers available, ReSyn™ microspheres were used for this study based on the aspetical manufacture required for *in vitro* cell culture environment (refer to Scheme 5.4) and that this immobilisation technology provides a loosely linked polymer network that

offers exceptionally high surface area for the binding of enzymes which translates to high volumetric activity. Furthermore, it's suitability for the efficient immobilisation of the multimeric enzyme GDH has been demonstrated before [114].

1.2.3. Nitric Oxide Reductase

Nitric oxide reductase (NOR) is an enzyme that plays an essential role in denitrification in bacteria [134, 135, 136] and some fungi [135, 137, 138, 139, 139]. Enzymatic reduction of NO to nitrous oxide with NOR is essential, as NO is toxic to cells during denitrification [139, 140, 141]. In bacteria, NORs are part of a large enzyme family which includes cytochrome oxidases [134, 136, 142, 142], whereas in certain fungi, NOR is a member of the cytochrome P450 family [139, 143, 144, 145]. This study will focus on the fungal NORs due to their single domain structure and sole requirements for NAD(P)H as a cofactor [104, 146, 147]. The cytochrome P450s with NO reducing capacities (P450nor) have been identified in several fungal species [137, 140, 148, 149, 150, 151, 152]. This study will focus on an isoform identified in *Aspergillus oryzae,* Anor [152].

1.2.4. Glucose dehydrogenase recycling mechanism

Glucose dehydrogenase (GDH) is involved in the first step of the non-phosphorylating Entner-Doudoroff pathway [153, 154, 155] oxidising glucose to gluconolactone [155], which is further processed to pyruvate that feeds into the citric acid cycle [156]. GDH has shown to be a useful catalyst to convert glucose to gluconolactone and simultaneously regenerate NADH [110, 157]. Glucose, an abundant molecule in all living organisms, is the substrate for GDH, which will power the continuous reduction of NAD^+ to NADH. The GDH (GDH 102 from Codexis Inc.) applied in this study is a recombinant isozyme from *Bacillus megaterium* which was expressed in *E. coli* [106, 107, 158]. The Codexis GDH has been engineered for improved catalytic activity as well as thermostability [158].

1.2.5. The cofactor: NADH

NAD(H) is the commonly used abbreviation for nicotinamide adenine dinucleotide which is found in living cells, and serves as a redox agent in reactions catalysed by oxidoreductases [159]. It occurs in an oxidised form (NAD^+) that accepts electrons or a reduced form that donates electrons to the reaction, denoted as NADH. In the NO reduction system, NADH donates two electrons to nitric oxide reductase to catalyse the reaction which reduces NO to generate nitrous acid and water [104, 160]. Glucose dehydrogenase can subsequently use glucose to reduce NAD^+ to NADH for subsequent reuse by NOR. Due to the relative abundance of glucose (in e.g. cell culture media), the system will remove NO continuously and ensure the catalytic nature of the proposed system (Scheme 1.4), assisting in the evaluation of the system.

Cofactor recycling systems have previously been reported [103, 108, 109, 110, 112, 161, 162], through either the attachment of the cofactor to a solid surface e.g. membrane reactor, hollow-fibre or packed bead reactors [103, 108, 109, 112, 162]. For this study, a novel enzyme immobilisation technology has been applied to sustain a good proximity between the enzymes and the cofactor, which may potentially improve substrate availability and reaction catalysis. Furthermore, immobilised enzyme can be removed from the biological system and can be regenerated for cost saving [117]. Twala *et al.* (2012) [114], have previously demonstrated that enzymes can be immobilised with high efficiency on the proprietary polymer support ReSyn™. The authors' further demonstrated encapsulation of an enlarged cofactor (as yet unpublished). Although the cofactor encapsulation would present a suitable approach for the development of the NOR system, the PEG'ylated NADH presents structural obstruction to the binding site of the nitric oxide reductase (NOR). However, the addition of NADH is sufficient for demonstrating and evaluating the proposed cofactor recycling system using the two enzymes.

1.2.6. Value proposal of the NOR system

Enzymes often require the assistance of cofactors to catalyse oxidation-reduction reactions [159]. It is proposed that the cofactor recycling by a second enzyme will ensure continuous reduction of NO by the first enzyme. This system may have an application in the investigation of the role of NO in for instance a model of inflammatory response. The continuous reduction of NO in a biological environment, with potentially benign (or reduced toxicity) secondary effects, is the purpose of the proposed synthetic biological system. It differs from alternate methods to achieve the same, including NOS inhibitors to prevent nitrosative tissue injury and may reduce an inflammatory response (similar to glucocorticoid treatment) as observed in acute inflammation and other pathologies [95, 163, 164].

An advantage of this novel bi-enzymatic nitric oxide reduction system would be its high substrate selectivity, thus avoiding limitations of NOS inhibitors such as arginine-analogues which can interfere with arginine metabolism [12, 93, 165] and should not alter the physiological functions, which is a concerning side effect of glucocorticoids [163]. Nitric oxide reductase is specific for nitric oxide and to a lesser degree to other small molecules, such as carbon monoxide [31, 32, 95, 163]. It is therefore proposed, that the bi-enzymatic nitric oxide reduction system may have a potential application as a research reagent for the investigation of NO's role in an *in vitro* inflammatory model. This knowledge may facilitate to comprehend the biology of NO and determine its role in a variety of pathologies such as chronic inflammation, autoimmune diseases, septicaemia, and organ rejection. Furthermore, the NO reduction system could further assist in investigating the functions of NO in tissues and living organisms, without the undesired side effects of current NOS inhibitors mentioned above, further improving our fundamental understanding of this important biological molecule.

The nitric oxide reduction system will be unique and, to the best of the authors' knowledge, the first of its kind prepared. Its preparation and evaluation is the focus of this doctoral study.

1.3. Development of NOR System

1.3.1. Optimisation of the NOR activity assay

For the development of the NOR system, an assay which would be able to quantify the enzymatic reduction of NO was required. In the first experimental chapter (Chapter 2), the optimisation of the NOR activity assay is outlined. Previously, the enzymatic reduction of NO was determined by gas chromatography [104] which was not considered suitable for the extensive NOR activity quantification required for the development of the NOR system. Hence a more convenient micro-titre assay was developed. This assay involved the addition of the substrate via a NO donor, NOC-5, and the indirect measurement of cofactor consumption, NADH. This assay allowed for high through-put screening of Anor transformants, characterisation of recombinant Anor, and the quantification of residual NOR activity after immobilisation on the microspheres.

1.3.2. Isolation of Nitric Oxide Reductase

Kaya and his colleagues (2004) [152] have studied the expression of the cytochrome P450nor gene from *Aspergillus oryzae*. The gene was denoted as *nicA* (CYP55A5) and deposited into Gene bank (No. AB055659) and the isoform of this enzyme family was named Anor. The coding region of this gene was synthesised and cloned into two expression plasmids. Initially, the plasmid was introduced into a protease-deficient *A. niger* strain D15 and subsequently transformed into *E. coli* BL21 (DE3). The aim was to express and purify sufficient functional Anor for the development of the NOR system. The isolation and characterisation of Anor from *A. niger* D15 is discussed in Chapter 3 and the expression of Anor in *E. coli* BL21 (DE3) in Chapter 4. Both studies outline the transformation of *nicA* into the host, the screening for transformant with the highest NOR activity and the characterisation of the recombinant Anor.

1.3.3. Immobilisation of enzymes

Previous studies have shown that enzyme immobilisation may alter enzyme activity and hence it was necessary to investigate several immobilisation variables. At first the most suitable immobilisation buffer and reaction conditions were determined. Thereafter, the pH profile and temperature stability at 37˚C were investigated in an effort to identify the most suitable immobilisation chemistry for the co-immobilisation of the enzymes for preparation of the system. The third step of the immobilisation studies was the synchronisation of both enzymatic reactions and the determination of concomitant substrate consumption. This is outlined in Chapter 5.

1.3.4. Evaluation of NOR system

For the evaluation of the NOR system, an *in vitro* inflammation model with human macrophage-like cells was developed and the cytokine response was analysed to determine the potential anti-inflammatory properties of the NOR system. Chapter 6 presents these studies. An outline for the development of the NOR system is presented in Scheme 1.7.

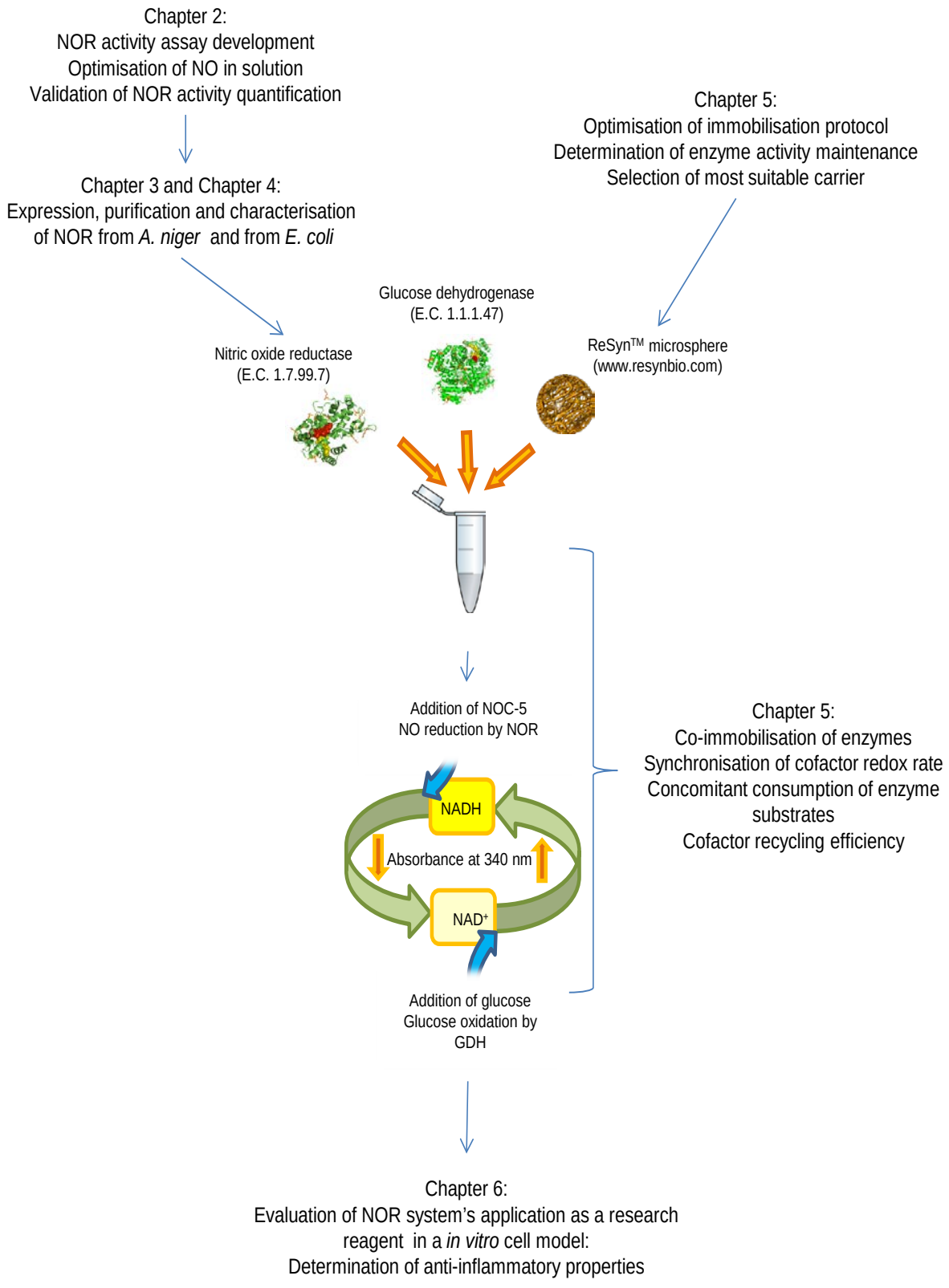

Scheme 1.7. An overview of the NOR system development. The development commenced with the development of an NOR activity assay (Chapter 2) followed by the expression and characterisation of Anor (Chapter 3 and 4). The assembly of the NOR system is described in Chapter 5 and its evaluation in Chapter 6.

1.4. Outputs: Publication and conference proceedings

S. Garny, J. Verschoor, N. Gardiner and J. Jordaan. Spectrophotometric activity micro-assay for pure and recombinant cytochrome P450-type nitric oxide reductase. Analytical Biochemistry Nov 2013 (Epub pii: S0003-2697(13)00531-9. doi: 10.1016/j.ab.2013.11.005, ahead of print).

S. Garny, N. Gardiner, J. Verschoor and J. Jordaan. A novel nitric oxide reduction system presents protection against the cytotoxic effect of nitric oxide. Keystone Symposium on Molecular and Cellular Biology: Metabolic Control of Inflammation and Immunity, Colorado, USA, 2013 (poster).

S. Garny, D. Gardiner, J. Verschoor and J. Jordaan. Optimisation of spectrophotometric micro-assay for the quantification of Nitric Oxide Reductase activity, SASBMB, Champange Sports Resort, Dakensberg, 2012 (poster).

S. Garny, S.H. Rose, W.H. van Zyl, I. Gerber and J. Jordaan. Expression and Screening of Nitric Oxide Reductase in *Aspergillus niger.* SASBMB, Bloemfontein, 2010 (poster).

S. Garny, I. Gerber and J. Jordaan. Biocompatibility of ReSyn™, BioMatSAS, Johannesburg, 2009 (poster).

Chapter 2
Development of a spectrophotometric micro-assay for the quantification of Nitric Oxide Reductase activity

2.1. Introduction

As outlined in Chapter 1, the development of the Nitric Oxide Reduction (NOR) system required the development of a facile, fast and reliable nitric oxide reductase activity assay. NOR activity is currently determined by gas chromatography (GC) [137, 140, 148, 149, 151, 152, 166, 167, 168], amperometric assays [141, 169, 170, 171], stopped-flow rapid scan spectroscopy [104] and conventional UV spectrophotometry [160, 168, 172].

The determination of NOR activity by GC involves the purging of NO into the reaction flask devoid of oxygen [104]. The product of the enzyme reaction (N_2O) is quantified by sampling the head space of the reaction flask at regular intervals. This method represents an end-point enzyme reaction assay, not suitable for real-time kinetic monitoring of enzyme. Turnover rates (T/O) for NO have previously been reported, ranging from 5000 to 32000 min^{-1} with K_m values ranging from 0.08 mM to 0.8 mM NO or NADH as listed in Table 2.1.

The amperometric assays concerns are real-time determination of NO reduction with electrical charge generation [141, 169, 170, 171, 172, 173, 174]. Also in these studies, NO gas was added to the reaction mixture. The decrease in electrical signal was correlated to the NOR activity. The electrical signal was converted into concentrations of NO, which required the titration of NO against reduced myoglobin, i.e. the involvement of another assay for the determination of NO in solution [169]. However, this NO quantification methodology is a direct determination of NO in solution which can be related to NOR activity provided that no other non-enzymatic NO consumption takes place in that solution [170]. Furthermore, this NO

quantification is most suitable for NORs with numerous domains involved in the NOR reaction as observed with bacterial NORs [134, 175].

Table 2.1. NO reduction activity determined in fungi and bacteria.

Source	Enzyme	Gene	Enzyme kinetics	Reference
Fusarium oxysporum	Fnor	*CYP55A1*	K_m= 0.113 mM NADH; T/O= 31500 min^{-1}	[104, 140, 176]
Cylindrocarpon tonkinese	Cnor1	*CYP55A2*	K_m = 0.320 mM NADH; T/O = 32000 NO.min^{-1}	[137]
Cylindrocarpon tonkinese	Cnor2	*CYP55A3*	K_m = 0.71 mM NADH T/O =24000 NADH.min^{-1}	[137]
Trichosporon cutaneum; T. montevideense	Tnor	*CYP55A4*	12700 N_2O per min^{-1}	[151, 167, 177]
Aspergillus oryzae	Anor	*CYP55A5*	K_m = 0.179 mM NO T/O = 10000 NO.min^{-1}	[152]
Histoplasma capsulatum	Nor1p	*NOR1*	K_m =0.080 mM NO T/O = 5000 NO.min^{-1}	[168]
Pseudomonas stutzeri	Cyt *cbb3*	*norO*	K_m = 0.012 mM NO	[170]
Escherichia coli	Cyto *bo3*		T/O = 0.3 mM NO.min^{-1}	[171]
Escherichia coli	FlavoRb	*NorRVW*	K_m = 0.4 mM NO	[141]

However, the determination of NO reduction by stopped-flow rapid scan spectroscopy was correlated to NADH oxidation by the decrease in absorbance at 340 nm [160]. The decrease of absorbance at 340 nm has the potential for real-time quantification of NO reduction. However, this methodology was mainly applied for the investigation of NO reduction mechanisms [160, 178] instead of NOR activity quantification and kinetic characterisation. This methodology requires a stopped-flow instrument (a rapid mixing device) linked to a spectrophotometer. It is a fast and reliable procedure for the determination of NOR activity by measuring indirect NADH consumption.

All three NOR activity assays described above were performed with the addition of NO gas to the reaction flask and are not considered suitable for the development of a fast and reliable micro-assay. NO is a small diatomic gaseous molecule with a very short half-life and fast rate of diffusion, challenging the estimation of NO in solution [9, 179, 180]. Thus, it was the objective of this study to develop a simple miniaturised micro-spectroscopic assay for the quantification of NOR activity with addition of a NO donor, NOC-5. The development of NO releasing reagents or zwitterionic polyamine/NO adducts such as NOC-5 ([3-(2-hydroxy-1-(methylethyl)-2-

nitrosohydrazino)-1-propanamine]), allowed for the development of a kinetic assay that follows the reduction of NO through spectrophotometric quantification of NADH. Kaya *et al.* (2004) [152] demonstrated the linearly proportional relationship between the oxidation of NADH to NAD^+, with the release of NO from NOC-5 with the intention to quantify NO in solution with NOR. However, this study set out to apply this principle to establish and optimise the assay conditions for the development of a NOR activity assay rather than for the quantification of NO in solution. Nakahara *et al.* (1993) [104] determined the stoichiometry of NO reduction by NOR as 2:1:1 for NO:NADH:N_2O. Therefore, for each NADH oxidized to NAD^+, two molecules of NO are converted to N_2O (refer Equation 1).

$$2\ NO + NADH + H^+ \rightarrow\ N_2O + H_2O + NAD^+ \quad \text{(Equation 1)}$$

For the development of the nitric oxide reduction system, a robust and reliable kinetic assay was required to asses the NO reduction. This chapter describes the development of a fast, reliable and convenient method for the quantification and kinetic characterization of NOR that utilizes the monitoring of NADH as a suitable substrate for real-time kinetic measurements. Due to the magnitude of requirements for the development of the NOR system (including the screening for NOR activity, establishing enzyme yields after purification, kinetic enzyme characterisation and the determination of enzyme activity maintenance after immobilisation), the assay was further miniaturised to a 384 well format.

2.2. Materials

A NOR solution from *Aspergillus oryzae* was purchased from Wako Chemical GmbH (Germany). Reactions were performed in flat bottom 96 well micro-titre plates from Greiner Bio One (Germany) and 384 well micro-titre plates from Genetix (now Molecular Devices, England). Assay reagents including NADH and buffer components were purchased from Sigma-Aldrich (Germany) and NOC-5 was purchased from Merck-Millipore (Germany). Greiner Bio One UV plates were used for the spectrophotometric quantification of NOC-5 at 250 nm. The optical density was measured in a BioTek Powerwave HT UV VIS micro-titre plate reader (USA).

2.3. Methods

2.3.1. Assay development

With the intent of creating a robust and reliable method for the quantification of NO reducing enzymes, the assay parameters were established starting with the NADH concentration and the determination of the light path in the micro-titre plates (96 and 384 wells). Optimum pH, temperature and buffer were determined and then the substrate concentration range that could be obtained from the NO-donor reagent, NOC-5. Finally, the dynamic enzyme concentration range was determined under these optimal conditions for enzyme activity determination. For the validation, and as an example of an application of this assay, the kinetic parameters of a commercial preparation of NOR were determined.

2.3.1.1. NADH concentration

NADH has an absorption maximum of 340 nm with a molar extinction coefficient, ϵ, of 6.22 $mM^{-1}.cm^{-1}$ [181, 182]. The detection limit of the BioTek Powerwave HT micro-titre plate reader at 340 nm was determined by measuring optical density at increasing NADH concentrations. The length of the light path in a 96 well plate and in a 386 well micro-titre plate, with 150 µl and 70 µl total reaction volume respectively, was calculated using standard concentrations of NADH and the Beer-Lambert relationship between the extinction coefficient and path length.

2.3.1.2. Reaction temperature and pH

It is well known that enzyme activity is affected by temperature and pH [183]. Thus, it was important to characterise NOR activity at various pH (4.2 to 8.6) and temperature values. For the purpose of this study, the enzyme activity was determined at room temperature and 37˚C.

The substrate for NOR, NO, was obtained from the decomposition of NOC-5, which is pH dependent [184]. Therefore, the NOC-5 decomposition rate at various pH values was determined first. NOC-5 was observed to be stable at high pH and thus a 200 mM NOC-5 stock solution was prepared in 50 mM NaOH and diluted to 0.05 mM NaOH concentration. This had a minimal effect on the pH of the reaction solution. To

obtain the maximum rate of NO release, NOC-5 was allowed to decompose in Britton-Robinson buffer (50 mM sodium phosphate dibasic, 50 mM boric acid, 33 mM citric acid and 50 mM TRIS; with pH adjustment using potassium hydroxide) within a pH range of 4.2 to 8.6 with increments of 1 pH unit. The decomposition of 1 mM NOC-5 was monitored at 37˚C for 30 minutes in a UV transparent micro-titre plate at 250 nm.

Thereafter, an activity profile of the commercial NOR over the pH range 4.2 to 8.6 in Britton-Robinson buffer was established. To eliminate the NO release rate from NOC-5 decomposition as a determinant of NOR activity at different pH values, a 20 mM NOC-5 solution was pre-incubated in Britton-Robinson buffer pH 5 for 1 minute at 37˚C, before it was added to the buffered enzyme solution for the activity determination at a particular pH. This was done to ensure that each sample contained the same initial amount of NO.

2.3.1.3. Assay buffer

Although sodium phosphate buffer at pH 7.2 is frequently used for NO reduction assays [104, 152, 160, 169], there is no report of the evaluation of various buffering agents that could be found for the assay. Due to this lack of comparison the authors evaluated a variety of potentially suitable buffers for assay at pH 6. In consideration of the addition of base stabilised NOC-5, a relatively high buffer concentration of 200 mM was chosen for the assay to prevent a pH shift. The following buffering agents were chosen for evaluation: sodium phosphate; MES (2-(*N*-morpholino)ethanesulfonic acid); HEPES (4-(2-hydroxyethyl)-1-piperazineethanesulfonic acid); TRIS (tris(hydroxymethyl)aminomethane); and TEA (triethanolamine).

2.3.1.4. Estimation of solution phase NO

The introduction of solution phase NO has previously been conducted by bubbling of NO gas into the enzyme reaction mix, but this approach is too cumbersome for high throughput assays and may undergo autoxidation resulting in an unknown NO concentration. The release of this volatile substrate into solution phase is preferred through the use of a solid NO donor, in this case NOC-5. NO concentration in solution is affected by several factors, including the pH dependent release of NO

from NOC-5, oxidation of NO with oxygen, as well as the rate of diffusion of the volatile NO [185, 186]. Due to these variables, the determination of NO concentration from NOC-5 decomposition required more sophisticated analysis. The relationship of NO formation and consumption was previously described as a six order polynomial equation [186, 187]:

NO in solution = NO release rate – NO/O_2 oxidation – NO diffusion

$$d[NO]/dt = e_{NO}k_1[NOC\text{-}5]_0^{(-kt)} - 4k^*[NO]^2[O_2] - (k_La/V)[NO] \quad \text{(Equation 2)}$$

The first term of equation 2 describes the rate of release of NO from the NO donor, which was characterised as first order release kinetics in deoxygenated solution. The NO release rate = e_{NO} k_1 $[NOC\text{-}5]_0^{(-kt)}$, where k_1 (min^{-1}) is the first-order decomposition constant obtained by the decrease in absorbance of the chromophore NOC-5 at 250 nm as it spontaneously releases NO [184, 186] and $[NOC\text{-}5]_0$ the initial NOC-5 concentration. The rate of release of NO is further dependent on the stoichiometric ratio of NOC-5 decomposition defined by e_{NO}. Based on the proposed stoichiometric release of NO from NOC-5, e_{NO} would theoretically be two [188]. However, this ratio is dependent on the reaction mix and other factors that as yet have not been established [187, 189]. The time taken for the NOC-5 decomposition is assigned as t (min).

The oxidation kinetics of NO in aqueous solutions are represented by the second term in equation 2, which further contributes to the uncertainty of the exact concentration of NO in solution. This factor accounts for the reaction of NO with oxygen in solution to form nitrite ions. The stoichiometry of this reaction is generally expressed as: $4NO + O_2 + 2H_2O \rightarrow 4H^+ + 4NO_2^-$ [190, 191, 192]. The rate of nitrite formation is described by the rate constant, k*, of 2.4×10^6 $M^{-2}.s^{-1}$ between 35 to 37˚C [179, 185].

The third component in equation (2) is the volumetric mass transfer coefficient that describes the diffusion of NO from the liquid phase into the gas phase. Lewis & Deen (1994) proposed that the NO diffusion from liquid into gas was the main process in which NO was removed from the reaction mixture [185].

Method *(A)* involved the calculation of NO in solution by solving only the first term of equation 2, i.e. the rate of release of NO (mM NO.min^{-1}): d[NO]/dt = $e_{NO}k_1[NOC\text{-}5]_0^{(-kt)}$, where e_{NO} was assumed to be 2 or less, where k_1 was the average of the rate constants determined and NOC-5 concentration at time t=0. This equation does not include the potential loss of NO by oxidation or diffusion, which was assumed to be negligible due to NO consumption by NOR as soon as the NO is produced. For the determination of the rate constant of NOC-5 decomposition, k_1, the rate of decomposition for NOC-5 (concentrations between 0.016 and 2 mM) in 200 mM TEA buffer (pH 6) was recorded at 250 nm for 30 minutes at 37˚C in a 96 well UV micro-titre plate as described before [184, 186]. The first-order decomposition rate constant, k_1, was calculated from the gradient (-m) generated by a plot of ln (A_0-A∞) with time, where A_0 is absorbance at t=0 and A∞ is the absorbance at the time when no further decrease in absorbance is observed [184, 186]. The average of all the rate constants was applied to calculate the rate of NO release.

For method *(B)*, the enzymatic determination of NO (as demonstrated by Kaya *et al.*, 2004; [152]), a constant concentration of NOR (0.285 µM) was allowed to reduce NO generated from varying concentrations of NOC-5 (0 to 8.6 mM) in 200 mM TEA buffer pH 6 at 37˚C. The rate of reduction was estimated by the following the rate of NADH consumption monitored by the decrease in absorbance at 340 nm for 5 minutes in a 384 well plate.

2.3.1.5. Lower limit of detection and dynamic range

On completion of the optimisation of the various assay parameters, an evaluation of assay linearity, lower limit of detection (sensitivity) and dynamic range was undertaken. NOR activity was measured by a decrease in absorbance at 340 nm (NADH) over 5 minutes in a 384 well micro-titre plate with increasing concentrations of a commercial NOR preparation (0.02 to 0.9 µM) to establish the dynamic range of the NOR activity assay. NOC-5 concentration was added in excess to the reaction mixture to ensure that NOC-5 did not limit the NADH consumption. Thus, the enzyme reaction contained 2 mM NOC-5 and 1 mM NADH in 200 mM TEA pH 6 buffer at 37˚C.

2.3.1.6. Assay reproducibility

The reproducibility of the NOR activity assay was established by repeating the assay on three consecutive days with reagents prepared on each day with the optimal reaction condition (2 mM NOC-5 and 1 mM NADH in 200 mM TEA pH 6). A 20 mM NOC-5 stock solution (in 50 mM NaOH) was allowed to release NO for one minute at 37˚C in Britton-Robinson buffer pH 5 before it was added to the reaction mixture. The intention of this pre-incubation of NOC-5, was to pre-empt the oxidation of NADH by NOC-5 and to ensure excess NO in solution. A NOR dilution series was prepared from the commercial NOR stock solution and the NO reduction was initiated by the addition of the assay reagents. The NADH consumption was monitored for 5 minutes at 37˚C.

2.3.2. Kinetic characterisation of NOR in micro-assay

In the past numerous P450-type enzymes with NOR activity have been isolated from various sources [139, 140, 144, 145, 148, 149, 151, 152, 193, 194]. This indicates the general interest in the NO reducing enzymatic reaction. For the characterisation of new isoforms of NO reducing enzymes, a fast and reliable assay is required to determine the kinetic constants. The Michaelis-Menten constant (K_m) and the maximum velocity (V_{max}) were calculated using a 0.14 mM NOR enzyme solution with varying NOC-5 concentrations. A non-linear regression analysis for single ligand binding (SigmaPlot 10.0, Systat Software Inc. Germany) and Lineweaver-Burk analysis (reciprocal of initial velocity (v_0) and substrate concentration [S]), were used to calculate the enzyme's kinetic parameters.

2.4. Results

2.4.1. Assay development

2.4.1.1. NADH concentration

The optical measurement of NADH at 340 nm was used to monitor NOR activity. The stoichiometry of 2:1 was used for enzyme activity calculations considering one NADH molecule is required for the reduction of two NO molecules [104]. A linear increase in

absorbance at 340 nm for 0 to 0.5 mM NADH was observed for 96 well plates and from 0 to 1 mM NADH for 384 well plates (Fig. 2.1). Using the Beer Lambert Law, the light path for the 150 µl volume in a 96 well micro-titre plate was 0.35 cm and for the 70 µl volume in the 384 well micro-titre plate was calculated to be 0.47 cm from the equations y= 2.222x (R^2=1) and y= 2.917x (R^2=0.99) for the for the 96 well and 384 well micro-titre plate (respectively).

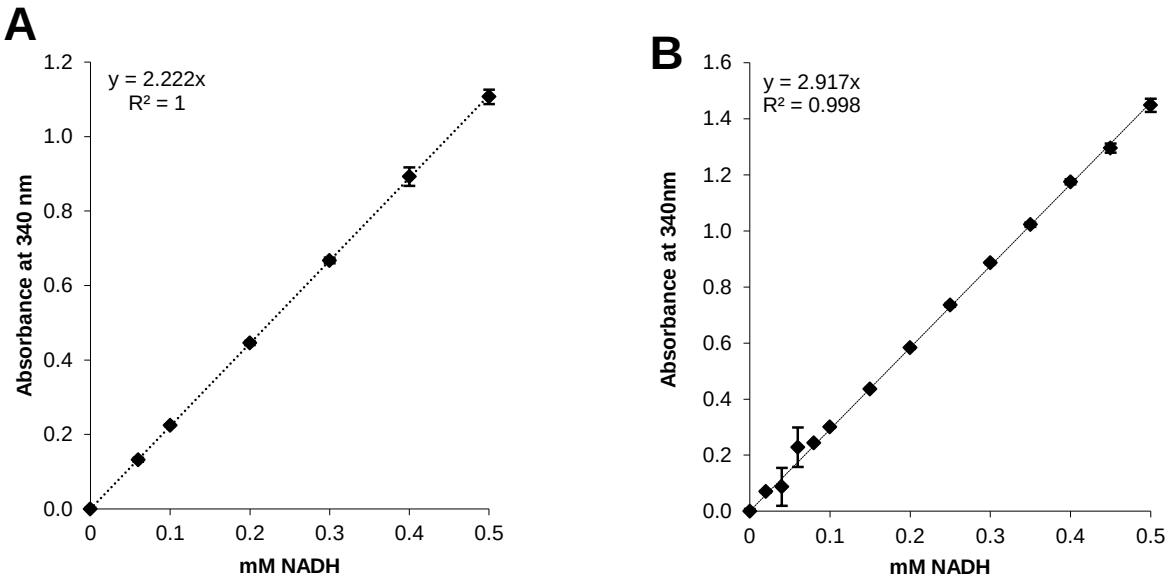

Figure 2.1. Quantification of NADH at 340 nm. In (A), the standard curve for NADH in a 96 well micro-titre plate and (B) for a 384 well micro-titre plate. The gradient and the extinction coefficient of NADH was used to calculate the light path to 0.35 cm for the 96 well micro-titre plate (A) and 0.47 cm in the 384 well micro-titre plate (B).

2.4.1.2. Optimum conditions for NOR activity assay

The optimum conditions for the quantification of NOR were established as 2 mM NOC-5 and 1 mM NADH in 200 mM TEA buffer (pH 6) at 37˚C. The NOR activity at 37˚C was 24.4 µM NO.min^{-1} which was approximately double that at 28˚C (12.3 µM NO.min^{-1}), therefore all subsequent assays were performed at 37˚C.

The pH dependent NOC-5 decomposition is shown in Figure 2.2. The most suitable NOC-5 decomposition rate was observed at pH 5. Neither low (pH 4) or high pH (8 to 9) was suitable for NOC-5 decomposition. At low pH (pH 4), NO was released at an extremely fast rate and NO gas formation (in the form of bubble formation) interfered in the spectrophotometric assay, whereas at pH 5, the NOC-5 decomposition rate was completed after 90 seconds without interference. The NOC-5 decomposition

was more gradual in Britton-Robinson buffer pH 6 with a maximum rate after 5 minutes. No apparent NOC-5 decomposition took place at pH 8 or 9.

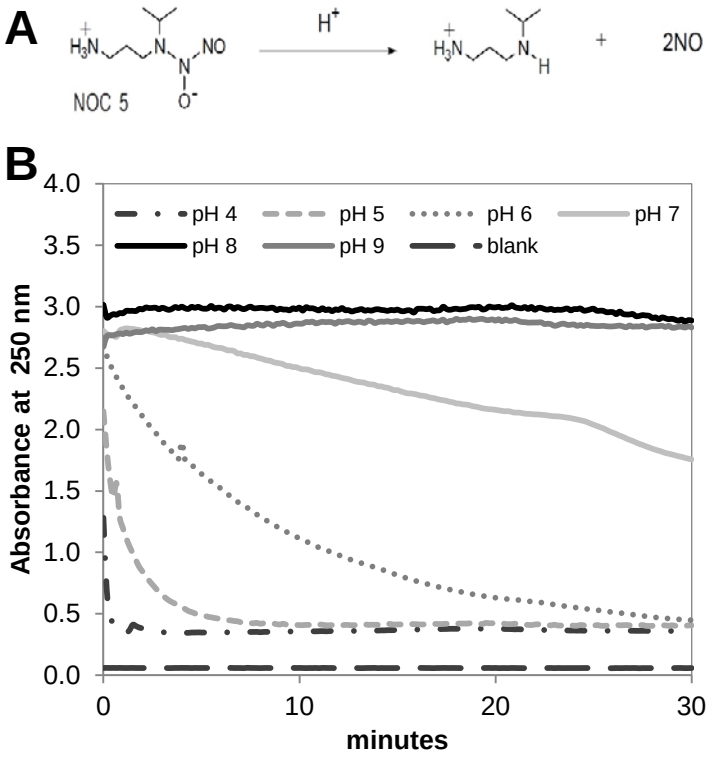

Figure 2.2. The pH profile of NOC-5 decomposition. A) The chemical structure of NOC-5 decomposition to an amine adduct and 2 NO molecules in the presence of hydrogen ions. B) The NOC-5 decomposition with increasing pH. A stock solution of 5 mM NOC-5 was prepared in 50 mM NaOH and added to Britton-Robinson buffer for a final concentration of 1 mM. NOC-5 decomposition was monitored at 250 nm in a UV micro-titre plate at 37˚C for 30 minutes. The blank sample contained only Britton-Robinson buffer. NOC-5 chemical structure was copied from http://www.dojindo.com.

The pH profile of NOR demonstrated maximum enzyme activity at pH 6.2, with high activity also detected at pH 6.6 (Fig. 2.3). A variety of buffers at pH 6 and 200 mM concentration were subsequently evaluated for their effect on the enzyme assay. Although the choice of buffer had little effect on the activity, increased activity was observed in TEA and HEPES buffer (Table 2.2).

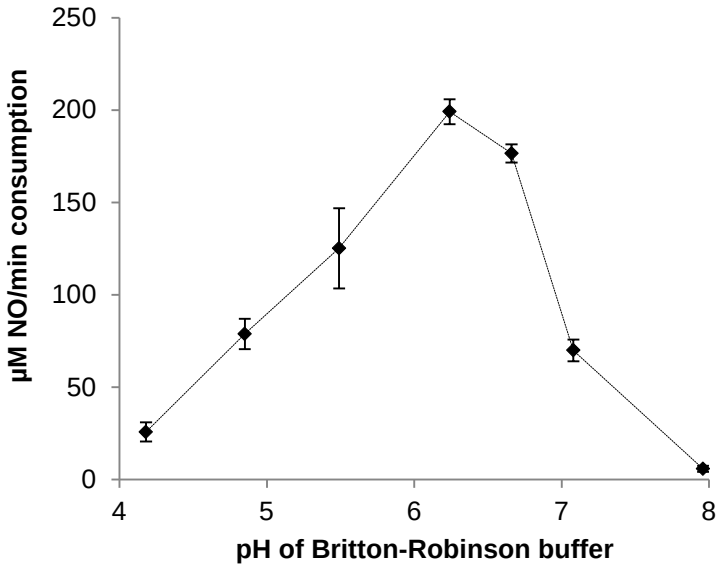

Figure 2.3. pH profile of NOR activity. The enzyme reaction contained 0.07 µM NOR solution, 1.7 mM NOC-5 and 1 mM NADH in Britton-Robinson buffer with various pHs. The reaction was monitored for 5 minutes at 37˚C. The decrease in absorbance at 340 nm was correlated to NADH consumption which was converted to µM $NO.min^{-1}$ consumption.

Table 2.2. NO reduction rate by 0.07 µM NOR at 37˚C in various buffers (200 mM).

Buffer	µM $NO.min^{-1}$	SD[a]
$NaPO_4$	182.9	11.1
MES	191.4	11.3
TRIS-HCl	210.4	14.7
TEA	250.9	4.3
HEPES	289.8	9.5

[a] standard deviation of triplicates

2.4.1.3. Substrate concentration and availability

The accurate quantification of NO concentration in solution is essential to determine the kinetic parameters of nitric oxide reducing enzymes. Due to several variables influencing the effective concentration of NO in solution after its release from NOC-5 decomposition, accurate estimation of NO concentration presented a challenge. This study attempted to determine the NO concentration by (A) a mathematical calculation of NO release from NOC-5 which was compared to (B) from enzymatic NO reduction by NOR.

A) Mathematical calculation of substrate concentration

The decomposition of NOC-5 was determined by spectrophotometric measurement at 250 nm from which the decomposition rate constant, k_1, was calculated as described by Maragos *et al.* (1991) [184]. The calculated NO release did not include the NO oxidation reaction, or the volumetric mass-transfer coefficient. This method for NO concentration only applies for a closed system, and was chosen since it best simulated the enzymatic consumption of NO after its formation. For this mathematical computational method, the equation was solved by applying the variables as indicated in Table 2.3. The initial NOC-5 concentration, $[NOC\text{-}5]_0$, and the calculated NO release rate (µM $NO.min^{-1}$) generated a direct linear correlation with an equation where y= 0.147x (R^2= 1). The average of the decomposition rate constant, k_1, was used in the subsequent determinations for rate of release of NO. The knowledge of the NOC-5 decomposition rates was essential for the substrate optimisation studies as it allowed for the estimation of NO concentrations.

Table 2.3. Kinetic parameters for mathematical NO estimation in solution.

$[NOC\text{-}5]_0$	k_1 (per min)[a]	µM $NO.min^{-1}$ [b]
2	0.202	294.3
1	0.174	145.7
0.5	0.235	72.6
0.25	0.242	36.1
0.125	0.250	17.9
0.064	0.254	9.1
0.031	0.272	4.3
0.016	0.102	2.0
average	0.216	

$[NOC\text{-}5]_0$ in mM

[a] k_1= gradient (-m) which was determined from ln (A_0-A_{30}) [182, 184]

[b] NO release rate=e_{NO} k_1 $[NOC\text{-}5]_0$ $^{e\text{-}kt}$, where e_{NO}= 2, t= 5 min [186]

B) Enzymatic quantification of substrate

Kaya *et al.* (2004) [152] have indicated that NOR isolated from *Aspergillus oryzae* was suitable for the quantification of NO in solution. The rate of enzymatic reduction of NO is dependent on the available NO in solution. In this study, an objective was to investigate whether the decrease in absorbance of NADH presents a direct correlation to NO concentration. A non-linear regression was observed with increasing NOC-5 concentration vs. NO reduction (Fig. 2.4 A) at concentrations up to 10 mM. A linear increase of NO reduction rate was however observed between 0 and

1.5 mM NOC-5 of where y= 86.2x (R^2= 0.977) and 88.8x (R^2= 0.982) from two experimental repeats (Fig. 2.4 B). These results support the findings of Kaya *et al.* (2004) [152] that NOR could be used to quantify NO in solution. The average of the gradients (87.5) determined, was used to extrapolate the NO concentration.

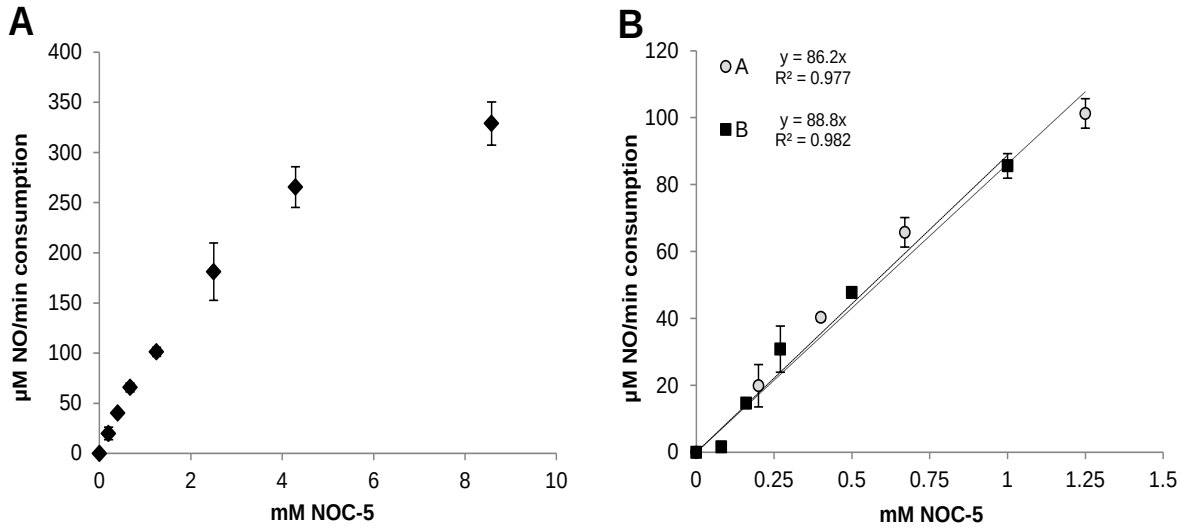

Figure 2.4. NO estimation from NO reduction by NOR. A) Determination of limitations for NO reductions from excess NOC-5 concentration with 0.3 µM NOR. B) The plot of A was zoomed into NOC-5 concentrations below 2 mM to indicate linear relationship between NO reduction and NOC-5 concentration. The square markers (■) in plot B, trace an experimental repeat of A in plot (B: ○). The decrease of 1 mM NADH at 37˚C for all reactions was used to calculate the NO reduction by NOR.

The close correlation between the two methods of NO estimation indicated that the release rate of NO from NOC-5 can be determined by either the enzymatic quantification (y= 87.5x; R^2= 1; Table 2.4) or by applying the decomposition rate constant ($e_{NO}\ k_1\ [NOC\text{-}5]_0\ e^{-kt}$ (y= 87.3x; R^2= 1; Table 2.4). This close correlation indicates that the non-enzymatic reduction of NO by oxidation and diffusion is likely to be negligible. The decomposition stoichiometry of NOC-5 is theoretically 2 moles of NO [188]. However, it has been noted that this may be less in different reaction conditions [184]. In this study, this decompostion stoichiometry was calculated to~1.19 moles of NO.

Table 2.4. The calculated NO release rate from enzymatic NO quantification and mathematical estimation.

	µM NO.min^{-1}	
	y=87.5x	y= 87.3x
mM NOC-5	Enzymatic NO reduction rate	NO release rate*
8.58	750.8	748.9
4.29	375.4	374.5
2.5	218.8	218.2
1.25	109.4	109.1
0.67	58.6	58.5
0.4	35.0	34.9
0.2	17.5	17.5
0	0.0	0.0

*e_{NO}=1.19

2.4.1.4. Lower limit of detection and dynamic range for NOR activity quantification

At first, the NOR activity was determined with increasing concentrations of a commercial NOR solution to verify ratios of enzyme concentration to NOR activity and to establish the lower limit of detection. A linear range from 0.04 to 0.9 mM of the commercial NOR was determined with an assay sensitivity ranging from 1.5 to 160 µM NO.min^{-1} (y= 0.238x; R^2= 0.991) as shown in Figure 2.5 A. The assay was repeated with a recombinant NOR in two plate formats, 96 wells or 384 wells with reaction volumes of 150 µl and 70 µl (Fig. 2.5 B). Here, the aim was to establish the linear dynamic range for different reaction volumes and plate formats. For the 384 well plate, a linear increase in NO reduction rate from 14 to 308 µM NO.min^{-1} (y= 2.269x; R^2= 0.991) was observed, whereas the 96 well plate presented a linear dynamic range from 10 to 282 µM NO.min^{-1} (y= 3.378x; R^2= 0.981) as shown in Figure 2.4 B. Overall, a linear dynamic range of one order of magnitude was noted for the enzymatic assay of NOR.

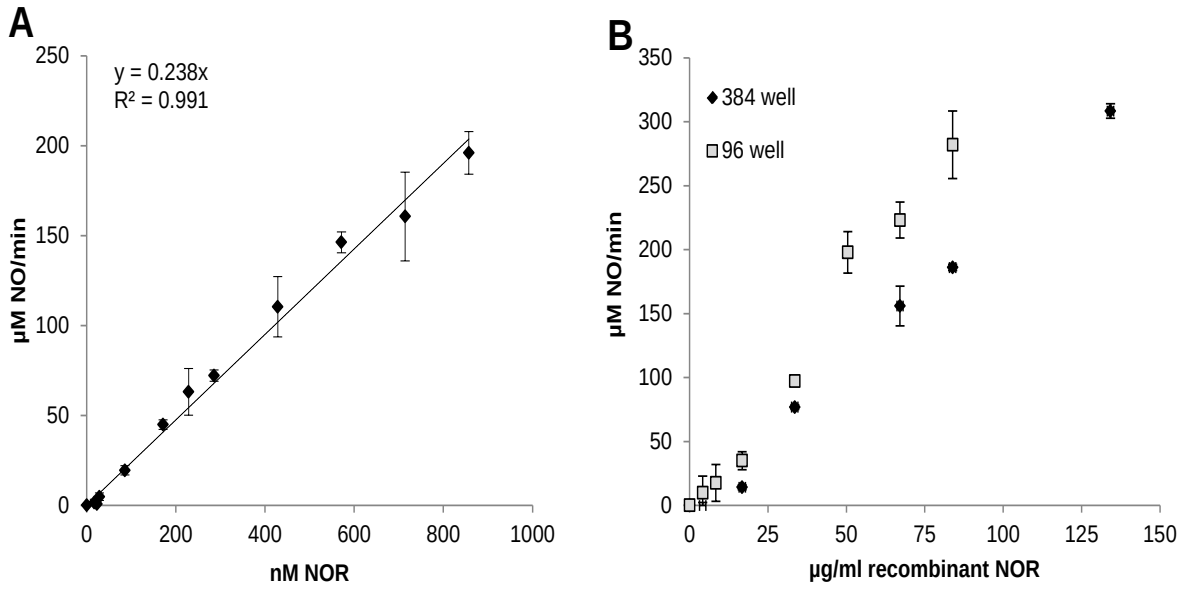

Figure 2.5. Linear dynamic range of NOR activity assay. In (A), the NO reduction rate was determined with increasing concentrations of the commercial NOR in a 384 well plate. In (B), the NO reduction rate was determined with increasing enzyme concentrations of recombinant NOR protein content in [♦] 384 well plate and [□] in 96 well plate. The reaction mixture contained 2 mM NOC-5, 1 mM NADH and 200 mM TEA buffer (pH 6) and was performed at 37˚C for 5 minutes. The enzyme activity (µM $NO.min^{-1}$) was calculated from the NADH consumption rate.

2.4.1.5. Assay reproducibility

In order to determine assay reproducibility, the assay was repeated over several days. Inter-well variability and day to day variability were less than 10% within the dynamic range of the assay (Fig. 2.6). Higher variability was observed at the higher NOR concentrations. The experimental set confirms the assay is reliable (R^2 equal to 0.964).

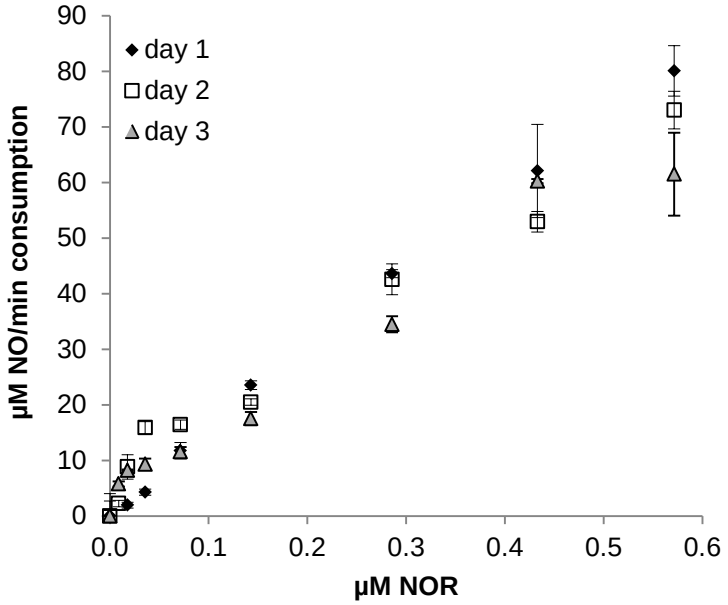

Figure 2.6. Reproducibility of a NOR activity assay. The linear relationship of NOR concentration and NO reduction was measured on three consecutive days. The reaction mixture contained 5 µl commercial NOR at various concentrations, 2 mM NOC-5 and 1mM NADH in 200 mM TEA pH 6. The NADH consumption rate was monitored for 5 minutes at 37˚C from which the enzyme activity (µM NO.min^{-1}) was calculated.

2.4.2. Kinetic characterisation of NOR

The kinetic characterization of NOR solution (NOR from *A. oryzae*) aimed to establish the affinity of NO for NOR under the described assay conditions and the versatility of the assay for the enzymatic kinetic parameter determination. Kinetic constants for Anor have been reported before [152], but it was considered useful to compare the kinetic characteristics of the commercial NOR obtained in this assay to these existing values. For the determination of kinetic constants of any enzyme, data relating to the initial velocity with increasing substrate concentration was obtained. Lineweaver-Burk double reciprocal plot and non-linear regression analyis , were employed to calculate the kinetic constants (Table 2.5).

Table 2.5. Kinetic constants of 0.14 µM NOR from *A. oryzae*.

NO quantification method	LB[a] plot		N-L[b]	
	K_m	V_{max}	K_m	V_{max}
enzymatic	209	632	222	658
equation	208	632	221	658

[a] Lineweaver-Burk plot
[b] Non-linear regression analysis
K_m and V_{max} in µM NO and µM NO.min^{-1}, respectively

The K_m calculated in this study is slighlty higher at an average of 215 µM NO than the previously reported value of 179 µM NO [152], while the V_{max} is nearly double (645 µM NO.min^{-1}) in this study than the reported value of 352 µM NO.min^{-1} [152]. The faster NO reduction (V_{max}) highlights the optimal reaction conditions developed in this study. Therefore it was concluded that this method provides a suitable way to characterise NOR activity in sample solutions.

2.5. Discussion and Conclusions

This study set out to develop a simple kinetic assay to quantify NOR activity from a P450-type NOR. To achieve this, various assay variables were investigated. The oxidation of NADH was chosen as a colorimetric "readout" for the quantification of NO reduction. NADH has a strong extinction coefficient and a wide dynamic range with suitable sensitivity. The optimal reaction mixture and conditions were 1 mM NADH, 2 mM NOC-5 in 200 mM TEA buffer pH 6 at 37˚C. NOR activity was evaluated in several types of buffers with little variation in enzyme activity, indicating the potential versatility of this enzyme assay.

The optimisation of substrate concentration and estimation of solution phase NO required a more in depth analysis. The NO concentration in solution derived from the decomposition of NOC-5 has previously been described as a six order polynomial (Equation 2) [186, 187]. However, it was demonstrated here that in the presence of enzyme, the rate of NO release is the major variable determining NO concentration, and that alternate factors influencing NO concentration are negligible. To the author's knowledge this is the first study that presents the relationship between the quantification of NO with NOR and its correlation to a mathematical estimation of NO. It was proposed that this approach may be suitable for the development of other assays utilising rate dependent substrate release agents.

This NOR activity assay demonstrated a linear dynamic range in excess of one order of magnitude which can be accounted to the small reaction volumes, i.e.micro-liters. This is in contrast to the other studies which assayed NO reduction in milli-liters and over a longer assay duration [104, 169]. The assay demonstrated high inter-well reproducibility and low day to day variability. This assay does not require laborious

techniques of saturation the reaction mixture with NO [104] or expensive equipment like GC [104] or Clark-type platinum electrode [169], and is therefore proposed as a reliable method for the quantification of NOR activity and suitable for kinetic characterisation of a commercial Anor preparation with comparable kinetic constants to previously reported values.

In this study, the assay was shown to be suitable for quantification of NOR activity, however, the lack of sensitivity indicates that the commercial NOR is unlikely to be suitable for potential application in the quantification of NO in biological solutions. Furthermore, the use of NADH based assays may be complicated by the presence of alternate NADH reducing enzymes in crude samples.

This assay was used for the high throughput screening of Anor secreting *A. niger* D15 transformants (Chapter 3), and the quantification and characterisation of NOR expressed in *E. coli* (Chapter 4). Furthermore, this assay was applied for the determination of NOR activity maintenance after its immobilisation and the synchronisation of cofactor recycling (Chapter 5).

Chapter 3

Expression and Purification of Nitric Oxide Reductase from *Aspergillus niger*

3.1. Introduction

For the construction of the nitric oxide reductase system, the fungal nitric oxide reductase, P450nor [NOR; EC 1.7.99.7; changed to E.C. 1.7.2.5 Brenda; E.C. 1.7.1.14 (KEGG)], was chosen as the prefered enzyme to reduce nitric oxide (NO) to nitrous oxide (N_2O) and water (H_2O) [104, 195]. As indicated by the enzyme's name, P450nor, it belongs to the P450 superfamily of haem containing enzymes which are found in almost all living organisms, and responsible for catalysing a vast range of chemical reactions [196, 197, 198, 199, 200]. P450s were first identified in the 1950s and in 1964 the distinctive Soret peak at 450 nm upon carbon monoxide binding with the pre-treatment of a reducing agent of the Fe-protoporhyrin IX pigment, resulted in the name allocation cytochrome P450 [201, 202]. The cytochrome P450s, generally abbreviated by CYP, can be divided in four classes based on the mechanism of electron delivery to the active site from the cofactor, NAD(P)H [198, 203]. In general, P450s catalyse monooxygenation reactions in which a redox partner is required for the transfer of electrons from the reduced pyridine nucleotides to the reaction centre [200, 204, 205, 206]. The transferred electrons facilitate the binding and activation of the iron-bound molecular oxygen [203]. P450nor has been allocated into the fourth class as it receives its electron directly from NAD(P) [104]. P450s in this class are unique to fungi and function as nitric oxide reductases during denitrification [140, 150] and so far, only one member for this class has been described, CYP55, containing five isoforms: Fnor1 (CYP55A1) from *Fusarium oxysporum* [176, 193], Cnor (CYP55A2 and CYP55A3) from *Cylindrocarpon tonkinese* [137, 148], Tnor (CYP55A4) from *Trichosporum cutaneum* [151] and Anor (CYP55A5) from *Aspergillus oryzae* [152], exhibiting higher homologies to bacterial P450s than to eukaryotic P450s [139].

Despite the diversity in origin of P450s and variations in the catalytic mechanisms, secondary structures are highly conserved [207]. P450nor, like the other CYPs, has an I-helix which forms part of the proton transfer groove on the distal side of the haem where the conserved threonine 243 forms part of the oxygen-binding pocket [206, 208, 209], and is believed to play a role in the NADH consumption rate, N_2O release and the formation of reaction intermediates [195]. In all P450s, the haem-binding loop lies in the N-terminal to the L-helix and is confined to the inner core between the I-helix and the proximal L-helix (refer to Scheme 3.1. below). The cysteine 352 residue places the haem group within the proximal haem-binding loop [160, 210]. Unlike the other P450s, the F,G-loops are placed just above the I-helix due to hydrophylic regions of the I-helix deflecting the hydrophilic regions of the F,-G helices and thus opening up the haem pocket to a greater extent than in other P450s [211]. A unique accumulation of positively charged amino acids beneath the B'-helix in the haem distal pocket, have been proposed as the NADH binding site as no classical NADH binding motif has been identified [146, 211]. A hydrogen bonding network formed by Ser296, Thr243, Asp393 and a water molecule on the protein surface of the distal pocket is proposed to be essential in the proton delivery during NO reduction which requires charge compensation of the transferred NADH-hydride [178]. When an NO radical binds to the haem Fe(III), two electrons are donated from NADH and subsequently the nitrogen of the radical is protonated with two hydrogen ions to form an intermediate Fe(III)-NHOH. A second NO molecule binds to this complex and forms an unstable Fe(III)-$N_2O_2H_2$, which is stabilized by the transfer of a proton from the nitrogen atom to the second NO, creating a tautomer. The dissociation of the N_2O and H_2O as well as the formation of the coordinated haem Fe(III) complex completes the catalytic cycle [212].

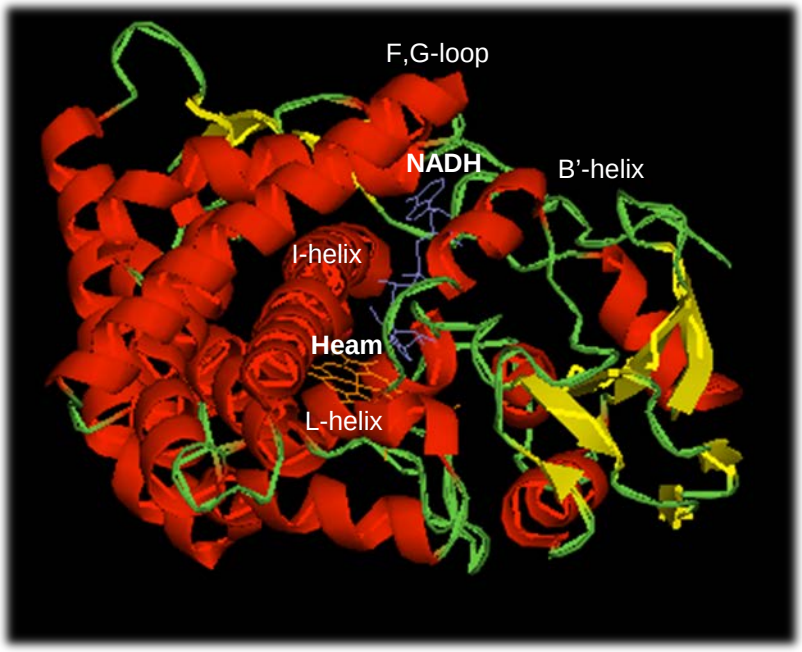

Scheme 3.1. A ribbon structure of P450nor (Fnor) derived from crystallography. Amino acid residues forming helical loops are shown as red ribbons and beta pleated sheets in yellow arrows. NADH (purple) groove is between the F,G-loop and B'-helix and the heam (orange) is nestled between the I and L-helices. The structure was rendered from protein database file "1ROM" using PyMol Molecular Graphics System (version 0.99) from DeLano Scientific LLC (Carolina, USA). The crystal structure was determined by Park *et al.* (1997) [213].

The P450nor isoform of interest for this study, abbreviated Anor, was first isolated from *Aspergillus oryzae* by Kaya and colleagues in 2004 [152], and the gene was denoted the abbreviation *nicA* (*CYP55A5*). The Anor protein is encoded by 3785 nucleotides which translate into 408 amino acid residues, consequently the protein molecular mass is estimated at 45.7 kDa. Amino acid sequence alignment studies have shown that Anor shares 60% homology with the other isolated P450nors such as Fnor, Cnor and Tnor [152]. A major and minor expression pattern was identified for this gene which is under the control of two expression factors nirA and Rox1 [152] which has been associated with responsiveness to nitrate [214] and suppression of gene expression under aerobic conditions [215, 216, 216]. This gene has been entered in the NCBI database with GenBank accession number: AB055659 [152].

Aspergillus niger, a closely related species, has been of interest to the protein biotechnology industry as an expression system due to its ability to produce a diverse range of heterologous enzymes and the associated benefit of its secretory pathway, secreting proteins in large quantities [217]. Several *A. niger* expression

systems were developed to maximise protein production and secretion, of particular interest for the expression of recombinant fungal proteins that are not routinely expressed in bacteria [218, 219, 220, 221]. For example, Wiebe *et al.* (2001) [222] and Gordon *et al.* (2000) [223] developed a recipient strain for recombination and secretion of heterologous proteins, *A. niger* D15, a protease deficient strain (*prtT*), non-acidifying (*phmA*) and an uridine auxotrophic (*pyrG*) mutant [222, 223]. The uridine auxotroph facilitates the selection of transformants when a $pyrG^{+}$ expression plasmid has been integrated into its genome. For these reasons, *A. niger* D15 was chosen as a suitable expression system for Anor in this study.

Rose and van Zyl (2002) [224] have developed a plasmid (pGTP) with a constitutive expression cassette for the synthesis and secretion of heterologous proteins [224]. A secretion signal from the Xyn2 beta-xylanase, *xyn2,* from *Trichoderma reesei* [225] and the gene of interest are placed under the transcriptional control of a glyceraldehyde-3-phosphate dehydrogenase promoter (pgd_p) from *A. niger* [226]. Transcription is terminated by glucosamylase terminator ($glaA_T$) from *Aspergillus awamori* [226]. This expression cassette ensures high level constitutive expression of the gene as well as its extra-cellular secretion which pre-empts the protein degradation by intra-cellular proteases and the disruption of the host's metabolism [227]. A proteolytic cleavage site (KR) for the endoprotease KEX2 was placed between the signal sequence and the gene of interest. This serves to remove the signal sequence during the protein's translocation through the endoplasmic recticulum into the cytoplasm [225]. This further ensures transport to the endoplasmic reticulum for post-translational modification. This plasmid vector was used in this study to facilitate the expression and purification of the recombinant Anor.

In addition to the genetic manipulation of host strains and expression cassettes, optimisation of culture media is another strategy to maximise heterologously expressed protein production, with an emphasis on increasing protein secreting mycelia. Wang *et al.* (2003) observed that bioprocessing parameters such as initial glucose concentration and the intensity of agitation affected heterologous protein production [228]. With the consumption of glucose and the increase of biomass, an increase in protease activity was observed accompanied by a decrease of

heterologous protein production [229]. The effect of high agitation on protein production was attributed to the increase of mechanical stress resulting in the breakage of mycelia with the resultant release of intracellular protease and consequent degradation of heterologous proteins [230]. Xu and his colleagues (2000) observed that the spore inoculum contributes to the pellet size of filamentous fungi in submerged cultures in which 4 million spores per millilitre produced a pellet size of 1.6 mm with the highest heterologous protein production and lowest protease degradation [231]. Papagianni and colleagues (2004) also described a relationship between low spore inoculums to a larger pellet diameter and lower protease activity in the culture medium [232]. In the present study, the bioprocess parameters such as glucose concentration, agitation and spore inoculum and their respective effects on the production of Anor were investigated.

The preparation of the nitric oxide reduction system in this study required the expression and purification of Anor. Two distinct approaches were followed to achieve this expression in fungal (*Aspergillus niger*) and bacterial (*Escherichia coli*) host organisms. Chapter 3 describes the expression and purification of Anor in *A. niger*, while Chapter 4 covers bacterial expression. The purified enzyme was subsequently used for immobilisation and characterisation of the enzyme. The three main objectives of this chapter were the expression of Anor and its secretion into the culture medium; the optimisation of growth conditions for maximum Anor production; and the subsequent purification of Anor from the culture medium.

3.2. Materials

3.2.1. Genes, vectors and host strain

The *nicA* gene (*CYP55A5*) from *Aspergillus orzyzae* on plasmids pMA and pMK with optimised codon usage for *A. niger* and *xyn2* secretion signal peptide as well as a KEX2 cleavage site were synthesised by GeneArt (Germany). The expression plasmid pGTP (plasmid map in Appendix to Chapter 3, Section A.3.1.3) and the mutant *A. niger* D15 (*pyrG prtT phmA*) were kindly provided by Prof. W.H. van Zyl (University of Stellenbosch). The approximate 1 kbp sized DNA fragments identified

on agarose gel electrophoresis were purified with a Zymoclean™ Gel DNA Recovery kit, which was purchased from ZymoResearch. Restriction enzymes were purchased either from Roche (BamHI, HindIII, EcoRI and XhoI) and from New England BioLabs Inc. (Not1). T4 ligase and the High Pure Plasmid Isolation kit were purchased from Roche and the Ex Taq polymerase was purchased from TaKaRa (Thermo Scientific, USA). The pGTP primers were kindly provided by Dr. Shaunita Rose (University of Stellenbosch).

3.2.2. NOR activity assay and protein quantification assay

NOC-5 (3-[2-Hydroxy-1-(1-methylethyl)-2-nitrosohydrazino]-1-propanamine) was purchased from Calbiochem (Merck Millipore, Germany). NADH and NaOH were purchased from Sigma-Aldrich (Germany). Nitric oxide reductase solution (Anor from *A. oryzae*) was purchased from Wako Chemical GmbH (Germany). The reagents for protein quantification, 1× Bradford dye and the protein standard bovine gamma globulin were purchased from Bio-Rad (USA). The 384 well micro-titre plates were purchased from Genetix (Molecular Devices, USA). A PowerWave HT micro-titre plate reader was used for assays (BioTek Instruments, USA). An EpMotion 5075 automated pipetting station was used for automated pipetting of assay reagents (Eppendorf, Germany).

3.2.3. Purification of Anor

Calbiochem Miracloth and 1.2 µm in-line Milligard Opticap Filters were purchased from Merck Millipore (Germany). Filtration through optical filters utilised a miniplus 3 peristaltic pump (model M312 - Gilson, France). A FreeZone® Triad™ freeze drying system (Labconco, USA) fitted with a Pascal Adixen (2015 SD) vacuum pump (Alcatel, France) was used for sample preservation. Sephacryl 300 HR size exclusion resin was purchased from Sigma-Aldrich (Germany). The ion exchange resin, Toyopearl Super Q 650M, was purchased from Tosoh Bioscience (Germany). Columns, XK 26 and XK 16, were purchased from GE Healthcare (Sweden). An ÄktaExplorer System was used for protein purification (GE Healthcare, Sweden). The gel filtration standards for calibration of the size exclusion column were purchased from Bio-Rad (USA).

3.2.4. SDS-PAGE reagents

Electrophoresis was performed in the Invitrogen gel tank system and powered by and the PowerPac™ Universal from Bio-Rad (USA). NuPage® Bis-Tris 4-12% gradient gels together with the accompanying electrophoresis chambers from Invitrogen (USA) were used. The molecular weight markers were purchased from Fermentas Life Science (USA). Colloidal Coomassie Brilliant Blue stain was prepared according to a method outlined in Appendix to Chapter 3, Section A.3.3.2. Gel Images were photographed using GeneSnap software and analysed with Gene Tools version 3.08 (SynGene, UK).

3.2.5. Other reagents and buffers

Ampicillin, kanamycin and bovine haemoglobin were purchased from Sigma-Aldrich (Germany). Aurin tricarboxylic acid ammonium salt GF, yeast extract sorbitol, Cas-amino acids (Difco Bacto), polyethylene glycol 4000 (BDH), bacteriological agar, neopeptone (trypticase BBL) and Novozyme 234 were purchased from Merck Millipore (Germany). Oxoid agar (Oxoid LP0011) was purchased from Basingstoke (England). Ultra-filtration membranes (10 kDa PVC) were purchased from Omega and the Amicon stirred ultra-filtration cell (Merck Millipore, Germany) was used for the ultra-filtration process. Components for stock reagent solutions of AspA trace element (TE) solution (Appendix to Chapter 3, Section A.3.3.2) were purchased from Sigma-Aldrich (Germany). A CentriVap Benchtop Vacuum Concentrator (Labconco, USA) was used for sample desiccation in preparation of amino acid analysis with MS-MS spectrophotometry. The reagents (NH_4HCO_3/ 50% MeOH; DTT, iodoacetamide, trypsin, methanol, acetonitrile and formic acid) required for this procedure were purchased from Sigma-Aldrich (Germany).

3.3. Methods

3.3.1. Design of recombinant Anor genes: *nicA*1 and *nicA*2

To facilitate the purification process, a signal peptide, *xyn2*, was placed upstream of the start codon of *nicA*, by replacing its start codon with that from *xyn2*, which redirects the intra-cellular enzyme to the extracellular environment, while the KEX2 (KR) cutting site was included for cleavage of the signal peptide from Anor post the secretion process (Scheme 3.2). An intron splicing site was identified in the gene sequence between the 3rd and 4th amino acid of the encoded protein [152]. Due to the uncertainty of *Aspergillus niger*'s ability to splice this codon, two gene variants of *nicA* were synthesised, *nicA*1 and *nicA*2. The one variant (*nicA*1) lacked the wild type initiation codon and the amino acids upstream of the splicing site, whereas the second gene variant (*nicA*2) encoded only the amino acid sequence correlating to the reported protein sequence. The *nicA*1 variant lacked 9 amino acids C-terminal to the KEX2 cleavage site at the N-terminus (Scheme 3.2). The genes *nicA*1 and *nicA*2 were synthesised by GeneArt with codon optimisation for expression in *A. niger*.

```
nicA1  MVSFTSLLAGVAAISGVLAAPAAEVESVAVEKR                FPFARPSG
nicA2  MVSFTSLLAGVAAISGVLAAPAAEVESVAVEKRMNSEPVYPRFPFARPSG
nicA   ----------------------------------------------------MNSEPVYPRFPFARPSG
```

Scheme 3.2. Amino acid sequence alignment of recombinant Anor. Gene variants, *nicA*1 and *nicA*2, were dervided from the wild-type *nicA* in *A. oryzae* (*nicA*). The amino acids in grey represent the *xyn2* signal peptide and the double underlined (KR) the KEX2 restriction site. The intron splicing site is indicated in italics (*SE*). The transcription initiation for *nicA*1 and *nicA*2 are at the methionine **(green)** of the *xyn2*. The alignment was done with BioEdit 7.0.9 (Ibis Bioscience, CA). The full sequence is presented in Fig. A.3.1 (Appendix to Chapter 3, Section A.3.1.1).

3.3.2. Expression plasmids of *nicA*1 *and nicA*2

GeneArt provided the gene *nicA*1 on a pMA (AmpR) vector and *nicA*2 on a pMK (KanR) vector backbone. The genes were excised from the pMA and pMK vectors using restriction enzyme digestion with *Not*I and were ligated to pGTP (*bla* gpd_p-gla_T *pyrG*) with a T4 ligase at room temperature for 4 hours. Use of this plasmid placed transcriptional control under the plasmid's glyceraldehyde-3-phosphate

dehydrogenase (*gpd)* promoter, with termination of transcription under the control of the *gla* terminator from *A. awamori* (Scheme 3.3). The pGTP-*nicA*1 and pGTP-*nicA*2 (plasmid maps and nucleotide sequence are presented in Appendix to Chapter 3, Section A.3.1.2 to 3.1.4) were transformed into *E. coli* DH5α according to Sambrook *et al.* (1989) [233]. The *E. coli DH5α transformants* with the correct gene orientation determined by restriction enzyme digests (NotI, XhoI, BamHI and BlgII), were selected and cultured in LB agar (3 days). The plasmid DNA was extracted with the High Pure Plasmid Isolation kit and stored at -20˚C for the *Aspergillus* transformation experiments. A polymerase chain reaction with pGTP primers (Appendix to Chapter 3, Section A.3.2.4.) was used to confirm the presence of *nicA* in recombinant plasmids.

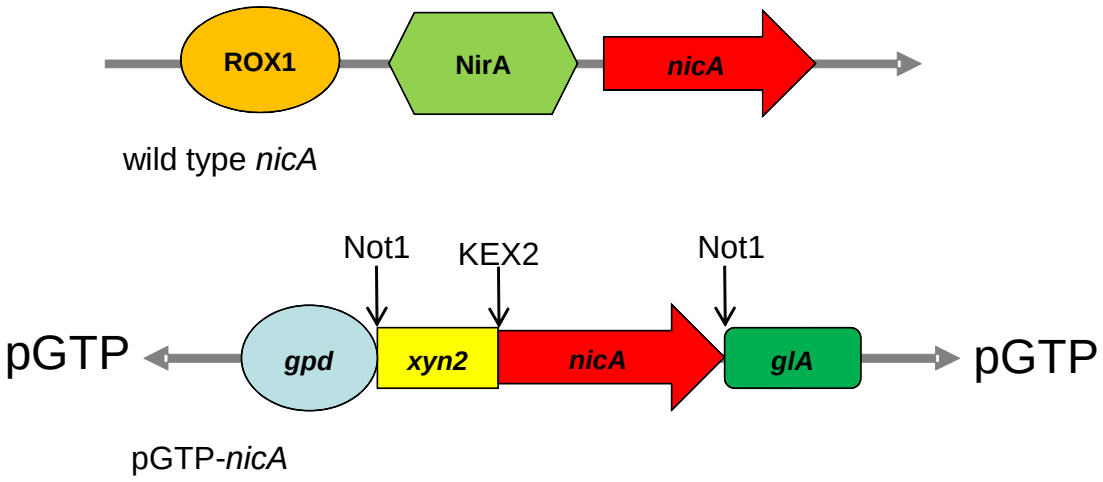

Scheme 3.3. Genetic environment of *nicA* in *A. oryzae* and on the pGTP plasmid. ROX1 and NirA are transcription regulation elements upstream of the start codon of the *nicA* gene (red). The Anor gene, *nicA* (red), on the pGTP plasmid is downstream of a constitutive promoter, *gpd* (blue), and signal peptide, *xyn2* (yellow), separated by the KEX2 restriction site and terminated with a *glA* terminator (green). The enzyme restriction and hydrolysis sites are indicated by arrows.

3.3.3. Transforming *A. niger* D15 with pGTP-*nicA*1 or pGTP-*nicA*2

The protocol described by van den Hondel *et al.* (1992) [218] was followed for the transformation of *A. niger* D15 (*PyrG prtT phmA*) with pGTP-*nicA*1 or pGTP-*nicA*2 plasmids. Briefly, *A. niger* D15 spores (1.0×10^6 spores.ml^{-1}) were added into minimal medium (MM, Table A.3.1, Appendix to Chapter 3, Section A.3.3.1) which was enriched with 0.01 M uridine and trace elements as described previously [219, 224]. The culture was allowed to grow overnight at 30˚C with orbital agitation of 80

rotations per minute (rpm). The mycelia were harvested and rinsed with a 0.6 M NaCl/$CaCl_2$ solution (Appendix to Chapter 3, Section A.3.3.2). The mycelia were drained, and four grams of mycelia were added to 100 ml NaCl/$CaCl_2$ solution in an Erlenmeyer flask. Protoplasts were generated by adding 240 mg of Novozyme 234 to the 4 grams of mycelia in 100 ml NaCl/$CaCl_2$ solution and allowed to digest the mycelial cell walls for 2 hours at 30˚C. The protoplasts were transformed with between 3 and 6 µg plasmid DNA in the presence of 1 volume STC1700 solution (Appendix to Chapter 3, Section A.3.3.2) together with 0.1 M Aurin tricarboxylic acid ammonium salt GR and 60% (v/v) polyethylene glycol 4000. Thereafter, protoplasts were seeded onto transformation plates (Table A.3.1, Appendix to Chapter 3, Section A.3.3.1) and incubated for 3 days at 30˚C. Mycelia from the transformation plates were transferred to transformation plates without oxoid agar and sorbitol. After three days at 30˚C, the spores were harvested and transferred to spore plates (Refer to Table A.3.1, Appendix to Chapter 3, Section A.3.3.1). Spores were harvested after three days at 30˚C with a 0.9% (w/v) NaCl solution. The spores were stored at 4˚C for further experimentation or stored in 40% (v/v) sterile glycerol at -80˚C. Genomic DNA was isolated from transformants cultured for 4 days in minimal medium (Appendix to Chapter 3, Section A.3.2.5). The genomic DNA was subjected to polymerase chain reaction with pGTP primers (Appendix to Chapter 3, Section A.3.2.4) to confirm the presence of the expression plasmid. Transformants with a 1.4 kbp insert were selected for further investigation. For the identification of Anor secreting transformants, the culture medium was tested for nitric oxide reductase (NOR) activity using the assay described in Chapter 2.

3.3.4. Quantification of Nitric Oxide Reductase activity and protein concentratrion determination

For the determination of NOR activity, the NADH oxidation rate was monitored at 340 nm in the presence of a nitric oxide donor, NOC-5 as described in Chapter 2. In brief, the NOR activity assay reagent contained 0.3 mM of NOC-5 dissolved in 50 mM NaOH which was added to 1 mM NADH in 200 mM sodium phosphate buffer (pH 6). The NADH consumption rate was measured for 10 minutes at 37˚C in a 384 well plate at 340 nm. Protein concentration was determined as described by Bradford (1976), where the the dye Comassie Brilliant Blue G-250 binds to protein

and results in a colour change from red to blue with an absorbance at 595 nm [406]. The absorbance was measurued from the colour reaction obtained when 35 ul of the 1× Bradford dye was added to 35 µl of sample in a 384 well plate. The protein concentration was extrapolated from a bovine gamma globulin standard curve. The linear assay range for protein quantification was 0-25 µg.ml^{-1}.

3.3.5. Screening for Anor secreting transformants

Upon successful introduction of pGTP-*nicA*1 or pGTP-*nicA*2 into *A. niger* D15 and its integration into the genome, prototrophic *A. niger* D15[*nicA*1] PyrG^{+} and *A. niger* D15[*nicA*2] PyrG^{+} transformants that were able to grow on agar plates without uridine supplementation were picked for further analysis. The prototrophic *A. niger* D15 that produced 1.4 kbp PCR products were cultured in 5 ml of minimal medium (MM) for 4 to 7 days at 30˚C with 100 rpm orbital agitation. The culture medium was analysed for NOR activity with the NOR activity assay (Section 3.3.4). The screen was repeated after culturing the same transformants in double strength medium (2MM, Table A.3.1, Appendix to Chapter 3, Section A.3.3.1). Transformants having medium to high NOR activity were selected and cultured in 20 ml of MM or 2MM for 7 days at 100 rpm and 30˚C. NOR activity was monitored on day 4 and 7 of growth. Transformants with the highest NOR activity in the culture media were selected for growth optimisation studies in an attempt to increase Anor production.

3.3.6. Optimisation of growth conditions for increased NOR activity

The growth of mycelia is affected by several environmental conditions [234, 235, 236] and therefore several culture variables and their effect on NOR activity were investigated. Transformants were cultured at two agitation intensities and at three different strengths of medium (increasing in glucose concentration and yeast content – media compositions are listed in Table A.3.1, Appendix to Chapter 3, Section A.3.3.1). Several studies have shown that protease activity increases with decreasing glucose concentration [220, 237] which may negatively impact the amount of protein produced. A simulated fed-batch culture strategy was further investigated to reduce or prevent protease degradation of Anor and to increase the rate of enzyme production and reduce the time required to achieve optimal biomass.

Spent medium was replaced with fresh medium upon glucose exhaustion at day 4 and again at day 9 after inoculation.

Previously, studies have shown that the spore inoculums also contribute to mycelia morphology [232, 235], which in turn has been shown to affect protein synthesis and secretion. El-Enshasy and colleagues (1999) [235] have associated a high spore inoculum with smaller mycelial aggregates and higher protein expression. Similarly in this study, media were inoculated with spores ranging from 0.5×10^6 to 13.5×10^6 spores per millilitre.

Anor is a P450 cytochrome with haem in its active site [152]. Haem synthesis follows a tightly controlled metabolic pathway [238] and may present a bottleneck in the expression of P450nor. To improve the secretion of holoprotein (active Anor), the culture media were supplemented with filtered bovine haemoglobin [400]. To monitor the enzyme activity, the culture medium in each flask containing MM or MM with haemoglobin, was measured every 24 hours. To facilitate the processing of numerous samples automated pipetting was used for assaying the culture supernatants.

3.3.7. Protein sample preparation: Concentration and desalting

For the purification process, *A. niger* D15[*nicA*1] or *A. niger* D15[*nicA*2], were cultured in 6× 200 ml culture medium in Erlenmeyer flasks. At first, the mycelia were separated from the culture medium by filtration through Miracloth, and then the media were pooled and filtered through a 1.2 µm Milligard Opticap Filter with a peristaltic pump to remove spores and other cell debris. To ensure ionic interaction of the proteins in the culture media with the ion exchange resin, the culture media were concentrated by ultra-filtration in an Amicon stirred cell ultra-filtration device over a 10 kDa PVDF exclusion filter at 400 kPa nitrogen pressure at room temperature. The concentrated culture media were diafiltered against 20 mM TRIS-HCl buffer pH 7.8 to below 2 mS/cm conductivity using ultra-filtration.

For the purpose of sample preservation – enzyme samples were snap frozen in liquid nitrogen, and lyophilized in a FreeZone® Triad™ freeze drying system and stored at -80˚C for further analysis.

3.3.8. Purification of Anor: anion exchange chromatography

The desalted and concentrated culture media were applied to Super Q 650M anion exchange chromatography resin, pre-equilibrated in 20 mM TRIS-HCl buffer (pH 7.8) in a XK 26 column (26 mm diameter, 40 mm in length) using the sample loading function of the Äkta*Explorer* 10S System. The unbound protein (flow through) was collected for further analysis. The bound protein was washed with three column volumes of 20 mM TRIS-HCl buffer pH 7.8 and eluted with a linear salt gradient (0 to 500 mM NaCl) in 20 mM TRIS buffer (pH 7.8) at a flow rate of 10 ml.min^{-1}. The eluted proteins were monitored at 280 and 254 nm (proteins tracking) and 410 nm (haem monitoring in Anor). Fractions of 5 ml were collected and assayed for NOR activity. Samples containing NOR activity above 0.1 Units.ml^{-1} were pooled, concentrated and lyophilised as indicated (Section 3.3.7).

3.3.9. Purification of Anor: size exclusion chromatography

Preserved samples containing at least 0.1 Units. ml^{-1} Anor were re-suspended in 0.5 ml 50 mM phosphate buffer (pH 7.3) and applied to size exclusion chromatography using Sephacryl HR 300 packed in a XK 16 column (16 mm diameter, 70 mm length). Protein separation and migration at 0.5 ml.min^{-1} was monitored at 260, 254 and 410 nm. The protein sizes were estimated by comparison to gel filtration standards run on the same column. Fractions of 2 ml were collected and analysed for NOR activity and protein content. Fractions with at least 0.1 Units. ml^{-1} NOR activity were pooled and concentrated.

3.3.10. SDS-PAGE analysis of proteins

SDS-PAGE analysis was performed according to the protocol described by Laemmli (1970) [ref], with improvments of the commercially available pre-cast gel systems [407]. At each purification step, proteins in the samples were analysed for molecular size and purity using denaturing SDS-PAGE with a 4-12% gradient Bis-TRIS pre-cast polyacrylamide gel. Aliquots of sample proteins were precipitated according to the 2D protein clean up protocol available from Bio-Rad (Appendix to Chapter 3, Section A.3.3.2) prior to SDS-PAGE electrophoresis. Approximately, 10 µg of protein was loaded into the wells and visualized with colloidal Coomassie Blue stain. The molecular weight of protein subunits was estimated against molecular weight markers, Promega (MW 116, 66, 45, 35, 25, 18.7 and 14.2 kDa). The proteins which migrated to the expected molecular size, 45.7 kDa, of Anor were excised and the identity confirmed by MS-MS spectrometry.

3.3.11. Protein verification by mass spectrometry

The sample preparation and mass spectrometry were performed as a service by Dr. Stoyan Stoychev (CSIR Biosciences, South Africa). Protein bands of interest were trypsin digested (in-gel) as per the protocol described by Shevenko *et al.* (2006) [239]. Briefly, gel bands were destained using 50 mM NH_4HCO_3/ 50% MeOH followed by in-gel protein reduction (50 mM DTT in 25 mM NH_4HCO_3) and alkylation (55 mM iodoacetamide in 25 mM NH_4HCO_3). Proteins were digested overnight at 37 °C using 5 – 50 µl, 10 $ng.\mu l^{-1}$ trypsin, sufficient to cover the gel fragment. Peptides were extracted using 50% acetonitrile (ACN)/ 5% formic acid (FA) and dried using vacuum centrifugation with a CentriVap Benchtop Vacuum Concentrator (Labconco, USA).

Samples were re-suspended in 35 µl 2% (v/v) ACN/ 0.2% (v/v) FA and separated using a Dionex UltiMate 3000 RSLC system coupled to a QSTAR Elite mass spectrometer (AB SCIEX, USA). Peptides were first de-salted on an Acclaim PepMap C18 trap (75 µm × 2 cm) for 8 min at 5 $\mu l.min^{-1}$ using 2% (v/v) ACN/0.2% (v/v) FA, then separated on an Acclaim® PepMap C18 RSLC column (75 µm × 15 cm, 2 µm particle size) that was connected to the trap column via a 10-port switching

valve. Peptide elution was achieved using a flow-rate of 500 nl.min^{-1} with a gradient: 4-60% B in 30 min (A: 0.1 % FA; B: 80% ACN/0.1% FA). Nano-spray was achieved using a MicroIonSpray head assembled with a New Objective, PicoTip® nanospray Emitter (USA). An electrospray voltage of 2.0 - 2.8 kV was applied to the emitter. The QSTAR ELITE mass spectrometer was operated in Information Dependent Acquisition (IDA) using an Exit Factor of 2.0 and Maximum Accumulation Time of 2.5 sec. MS scans were acquired from m/z 400 to m/z 1500. The three most abundant ions were automatically fragmented in Q2 collision cells using nitrogen as the collision gas. Collision energies were chosen automatically as function of m/z and charge.

Protein identification was performed using NCBI's msdb database and PEAKS version 6.1 proteomics software. A false discovery rate of 0.1% was used for peptide identification. Only protein entries with at least one unique peptide were reported. The false discovery rate refers to the number (as a percentage) of false positives based on a reversed or scrambled protein data base, from which peptides of low confidence will present a false hit. Due to the redundancy in databases, there is a need to exclude homologous entries by selecting more than one unique peptide and thus removing or excluding repetitive entries [240].

3.4. Results

3.4.1. Screening transformants for NOR activity

Transformants with a 1.4 kbp PCR product were selected and cultured to determine their capacity to secrete active Anor into the culture medium. From the transformation experiments, 116 transformants were obtained with the correct orientation of the 1.4 kbp insert. Less than 1% of pGTP-*nicA*1 transformed *A. niger* D15 [*nicA*1] and 2.7% of pGTP-*nicA*2 (*A. niger* D15[*nicA*2]) screened transformants presented detectable NOR activity (Table A.3.2, Appendix to Chapter 3, Section A.3.3.4). The screening process was extended to minimal (MM) and double strength (2MM) culture media at two different shaking intensities (100 rpm and 200 rpm) and the activity detected at two different time points (3 days and 7 days after inoculation).

However, these variations offered little to no increase in the yield obtained in the culture medium of the transformants. The data is summarized in Table A.3.3 and Table A.3.4 in Appendix to Chapter 3, Section A.3.3.5.

3.4.2. Optimisation of NOR activity in culture media

The search for the highest Anor producing transformant was extended by investigating various culture conditions. Culture conditions of *A. niger* are known to affect mycelium and biomass development. Glucose concentration, rate of agitation (Fig. A.3.3 and Fig. A.3.4, Appendix to Chapter 3, Section *A.3.3.6.1*), size of spore inoculum (Fig. A.3.5, Appendix to Chapter 3, Section *A.3.3.6.2*) and supplementation with haemoglobin (Fig. A.3.6, Appendix to Chapter 3, Section *A.3.3.6.3*) were investigated in this study in an attempt to improve the yield of active Anor in the culture media. The use of a simulated fed batch culture protocol was also investigated.

From each gene variant, one transformant, which demonstrated the highest NOR activity identified during the optimisation of the culture media described above, was selected for the growth optimisation studies. The highest NOR activity was measured after 12 to 14 days of simulated fed-batch culturing of *A. niger* D15[*nicA*1] in minimal medium supplemented with filtered bovine haemoglobin at an agitation rate of 100 rpm (Fig. 3.1). A spore inoculum of 14×10^6 spores.ml^{-1} and agitation of 100 rpm resulted in compact mycelia pellets. The mycelia at higher orbital agitation appeared as mesh, which could have been due to mycelia breakage and thus potentially releasing intracellular proteins, including proteases. *A. niger* D15 is a protease deficient strain, but it may express low quantities of intracellular protease which could result in reduced yield of active Anor [226]. NOR activity from *A. niger* D15[*nicA*2] did not increase with extended duration of culturing or with haemoglobin supplementation. *A. niger* D15[*nicA*1] was thus used for NOR production using 21 day fed-batch culturing regime and subsequently used for the purification of Anor (Fig. A.3.7, Appendix to Chapter 3, Section *A.3.3.6.4*).

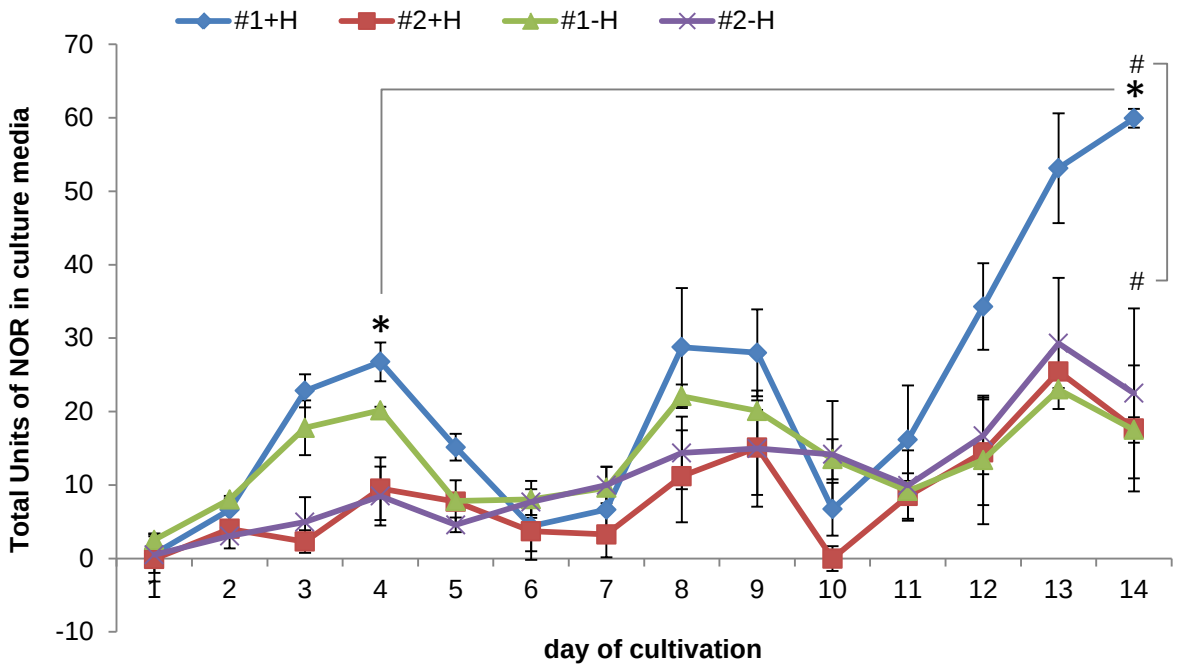

Figure 3.1. NOR activity in culture media from simulated fed-batch of *A. niger* D15[*nicA*1] and *A. niger* D15[*nicA*2]. *A. niger* was cultured either in 200 ml minimal medium (#1-H, #2-H) or with medium supplemented with bovine haemoglobin (#1+H, #2+H; 1 $g.L^{-1}$). Each flask was inoculated with 14 × 10^6 spores per millilitre and incubated at 30˚C with agitation of 100 rpm. NOR activity was monitored every 24 hours. Each data point is a representation of triplicate culture flasks from which each enzyme activity was assayed in triplicate. Error bars are representative of standard deviations. Spent media was replaced with fresh media on day 4 and day 9. Statistical difference is indicated by * and #. The *P* value is smalller than 0.0001 (Unpaired *t* test, GraphPad Software, Inc.).

NOR activity was improved by a 2.4 fold increase from day 4 to day 14 in media supplemented with haemoglobin for *A. niger* D15[*nicA*1] which is indicated by * (refer to Fig. 3.1). A 3.4 fold higher NOR activity was measured in the *A. niger* D15[*nicA*1] culture supplemented with haemoglobin when compared to the other cultures (indicated by # in Fig. 3.1).

3.4.3. Purification of Anor

3.4.3.1. Ion exchange chromatography of Anor

Anor has an isoelectric point between pH 5 and 6 and is therefore negatively charged above these pH values. This property was exploited to separate Anor by anion exchange chromatography. Super Q 650M was chosen for its comparatively high protein binding capacity and potential to achieve a high degree of resolution.

Since *A. niger* D15[*nicA*1] presented higher NOR activity from the growth optimisation studies (Section 3.4.2), it was used as a source of Anor for the chromatographic purification process. *A. niger* D15[*nicA*1] was cultured in MM or in MM+H at 100 rpm for several days. On day 4, 8 and 16, culture media were harvested and prepared for the purification process as described in Section 3.3.7. Concentrated culture medium from *A. niger* D15[*nicA*1] was applied to a Super Q 650M anion exchange column. The NOR activity was measured in fractions presenting enzyme activity, and a protein with corresponding 410 nm (heam) peak which occurred from 300 to 400 ml elution volume. The elution profiles from the Anor containing supernatant (Fig. 3.2) harvested on day 16 was used as representative example of the ion exchange purification process. The active fractions were pooled and concentrated and preserved for size exclusion chromatography as indicated above (refer to Section 3.3.7).

From the elution profile, an interesting observation was made. Namely, that second protein peak (280 nm in blue) presented high NOR activity [a] without a distinct 410 nm (pink) peak, in contrast to the third protein peak that corresponded to a 410 nm peak that also presented NOR activity [b] (Fig. 3.2 A [a] and [b], respectively). Here it seems, that this protein species [a] has much higher specific NOR activity when compared to the second protein species [b]. It is important to note that protein species [a] eluates around 300 ml, whereas the protein species [b] eluates around 340 ml. Fractions from both NOR activity peaks were collected and prepared for size exclusion chromatography.

The elution profiles of culture media supplemented with haemoglobin (Fig. 3.2 B), shows a small NOR activity peak that corresponded to a 280 and 410 nm peak. A major 410 nm peak was eluted thereafter, which likely correlates to the unused haemoglobin in the culture medium. The next protein peak (blue) corresponded to a NOR activity peak (green) as well as a 410 nm peaks (pink). Only the fractions associated with the major NOR activity peak were collected and prepared for size exclusion chromatography. It is interesting to note that the fractions with the highest NOR activity eluted at the same volume, i.e. around 300 ml as the protein species [a] in Figure 3.2 A.

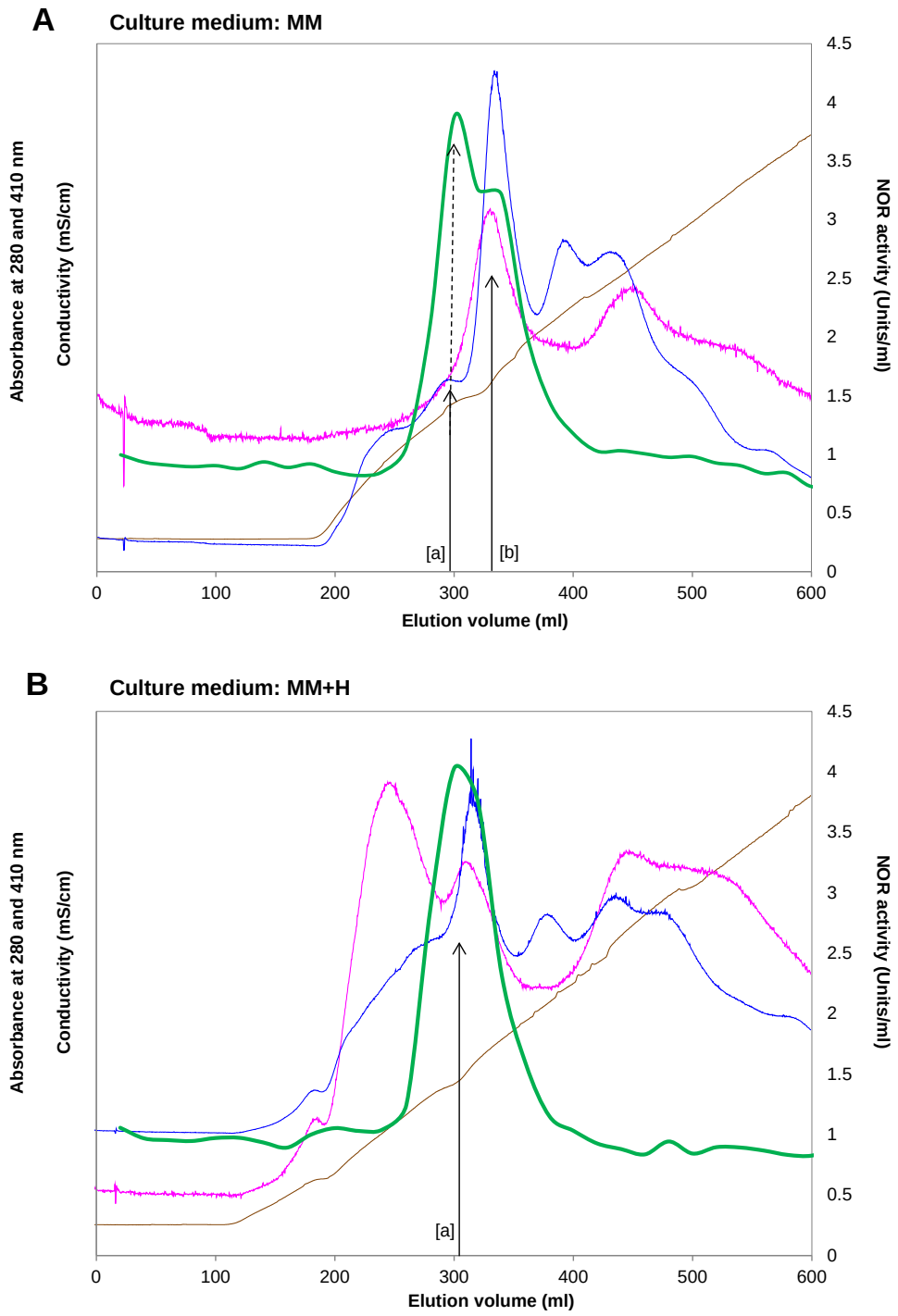

Figure 3.2. Anion exchange chromatograph of spend culture medium from *A. niger* D15[*nicA*1]. *A. niger* D15[*nicA*1] was cultured in MM and MM+H for 16 days at 30˚C with agitation of 100 rpm. In (A), the chromatograph shows the proteins secreted from *A. niger* D15[*nicA*1] when cultured in MM and in (B), when cultured in MM+H. Protein content was monitored at 280 nm (blue). Haem content was monitored with 410 nm (pink). Absorbance was measured in mAU. Conductivity (mS/cm) is indicated with brown line and NOR activity (Units.ml^{-1}) is presented by the green line. The activity profile is superimposed onto the chromatograph. The proteins (280 nm) with corresponding haem peak (410 nm) and NOR activity (green peaks) are indicated by arrows (solid and dashed lines). In MM (A), two protein species with 280 nm and 410 nm as well NOR activity was observed and is annotated by [a] and [b]. The elution profile of MM+H (B) presented one protein species with the three indicators for Anor (280 nm, 410 nm and NOR activity) and was annotated with [a].

3.4.3.2. Size exclusion purification process of Anor

For separation of Anor from other negatively charged proteins with different sizes, molecular exclusion chromatography with Sephacryl 300 HR (molecular weight separation range from 10 to 1500 kDa) was used. The elution profile from the size exclusion chromatography (SEC) corresponds to the IEC elution profile shown in Figure 3.2 and is shown in Figure 3.3. The elution profile of the sample cultured in MM is shown in Figure 3.3 A. Here two distinct protein peaks, [a] and [b], were observed both having NOR activity, however, only the first elution peak [b] had a distinct 410 nm peak. The low-haem containing protein, [a], presents lower NOR activity in contrast to peak [b].

In Figure 3.3 B, two major protein peaks were observed of which only the larger protein, [b], presented NOR activity and a corresponding 410 nm absorption. The protein denoted as [a], elutes approximately at the same volume as the protein species in Fig. 3.3 A [a], indicating that this is likely the same protein.

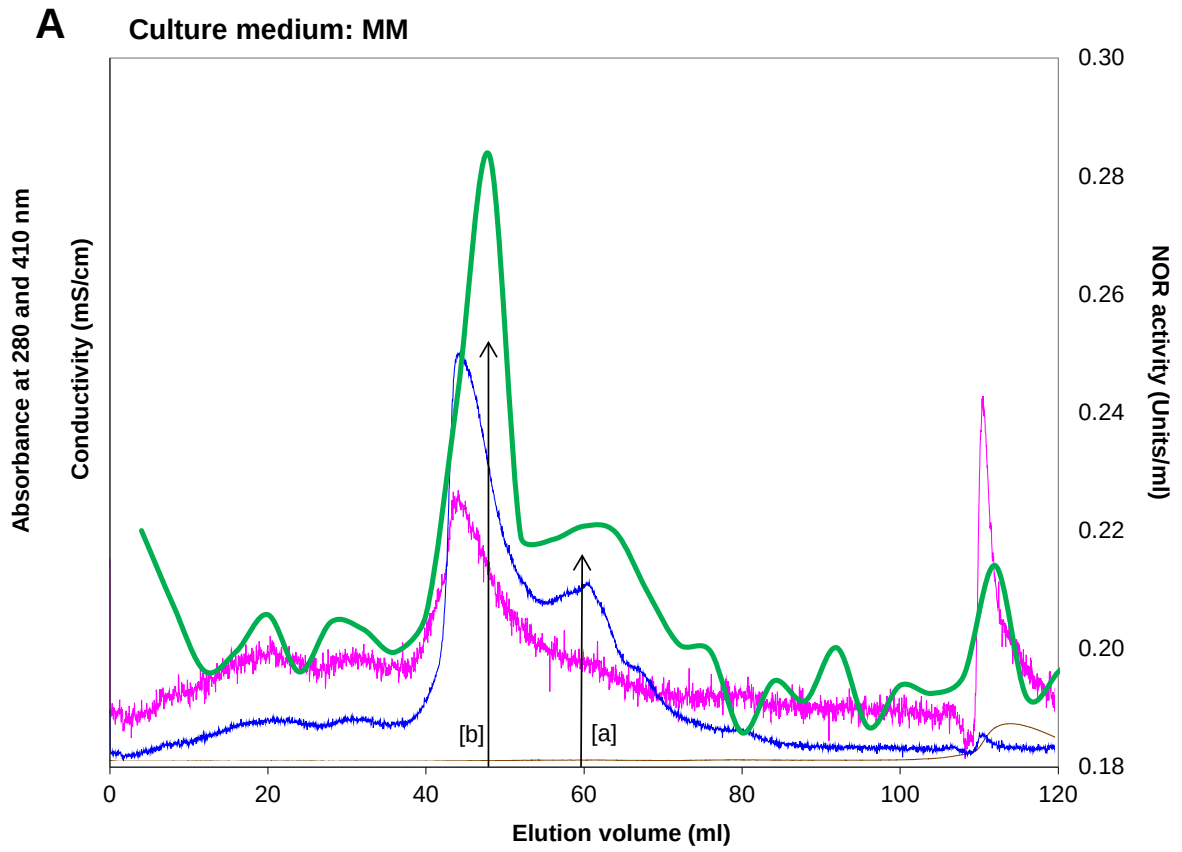

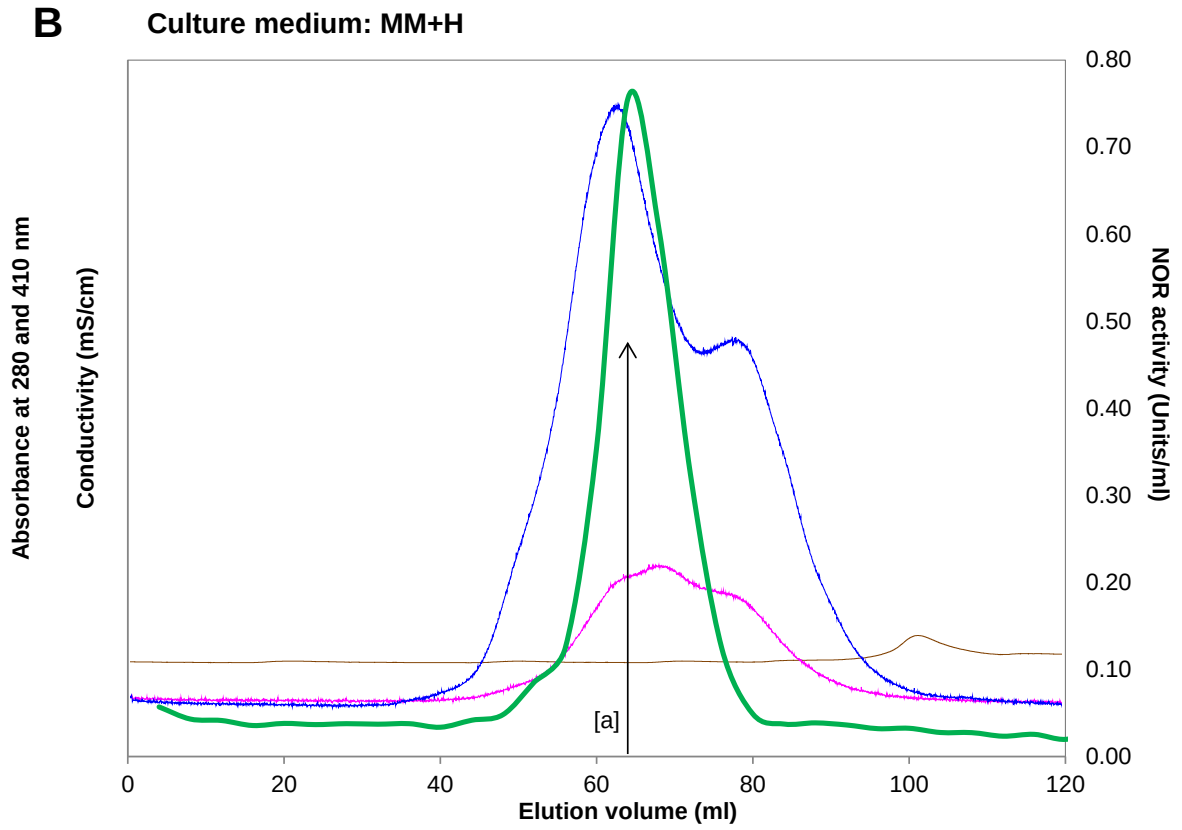

C

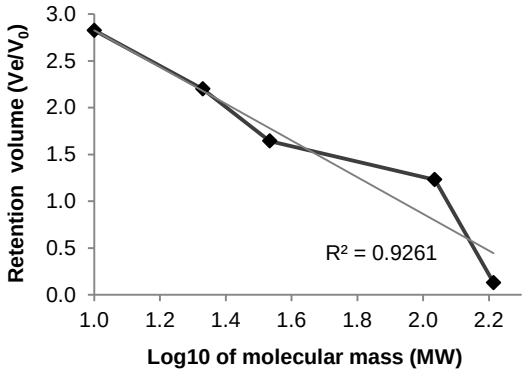

D

Sample	kDa	ml
vitamin B12	1.35	124
equine myoglobin	17	114
chicken ovalbumin	44	86
bovine gamma globulin	158	75
thyroglobulin (V_o)	670	56
Protein [b]	108	45
Protein [a]	72-79	64-60

Figure 3.3. Size exclusion chromatography of the IEC-purified NOR active fractions from *A. niger* D15[*nicA*1]. *A. niger* D15[*nicA*1] was cultured either in (A) MM and (B) MM+H for 16 days at 30˚C with agitation of 100 rpm. Protein eluted according to size differences in 25 mM TRIS buffer (pH 7.8). Protein content was monitored at 280 nm (blue). Haem content was monitored with 410 nm (pink). Absorbance was measured in mAU. Anor activity (Units.ml^{-1}) is represented in green and conductivity (mS/cm) is indicated with a brown line. The activity profile is superimposed onto the chromatograph. The proteins (280 nm) with corresponding haem peak (410 nm) and NOR activity (green peaks) are indicated by arrows. In MM (A), two protein species with 280 nm and 410 nm as well NOR activity was observed and is annotated by [a] and [b]. The elution profile of MM+H presented only one protein species with the three indicators for Anor (280 nm, 410 nm and NOR activity) and was annotated with [a]. In (C), Calibration curve for size exclusion chromatography and in (D), the corresponding molecular weights estimated from (C) are shown for [a] and [b] together with those fore calibration proteins.

The NOR active fractions from size exclusion chromatography correlated to a molecular weight of 72.3 and 101 kDa for protein fractions [a] and [b] shown in Fig. 3.3 A respectively, and 78.6 kDa for protein denoted [a] in Figure 3.3. B when compared to the gel filtration standards (Fig. 3.3 C and D). The molecular weight of the protein [a] in both the haem and non-haem containing culture batches is similar (72. 3 vs. 78.6 kDa) as observed in the two purification batches. The molecular weight observed for this native protein species was larger than the previously reported molecular weight of Anor at 45.7 kDa by Kaya *et al.* (2004) [152]. Here, it may be speculated that protein aggregation or potential dimerization could have resulted in the increased molecular weight [241].

The NOR active fractions were pooled and prepared for SDS-PAGE to assess the purity of the protein samples after chromatography. After SEC, multiple protein bands were still present in the protein sample (Fig. 3.4, lane 4 in A and B, respectively). The major protein band with mobility of 55 kDa in the haem containing

culture medium (Fig. 3.4 B, lane 4) was excised and a tryptic digest fingerprint conducted to determine its identity. The resultant 54% sequence coverage to cytochrome P450nor from *Aspergillus oryzae* (Accession number Q8NKB4_ASPOR) confirmed its identity. An example of the results is presented in Figure A.3.8 (Appendix 3, Section A.3.4.1).

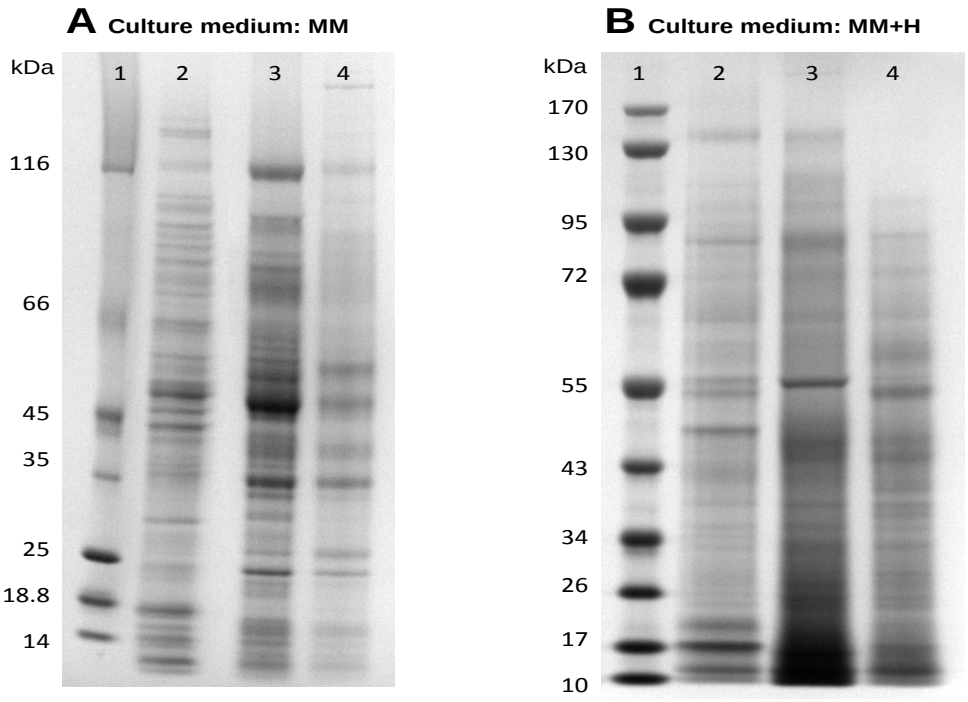

Figure 3.4. Reducing gradient SDS-PAGE analysis of Anor purification. *A. niger* was either cultured in MM (A) or in MM+H (B). The molecular weight marker was applied to lane 1, in (A) Fermentas Page Ruler SM0431 and in panel (B) Fermentas Page Ruler SM0671. Lanes from 2 to 4 contained samples after the following purification process:2 - ultra-filtrated crude; 3 - after Super Q 650M; 4 - after Sephacryl 300HR. The samples for electrophoresis were prepared according to the protocol provided by NuPAGE® Invitrogen. For qualitative assessment, approximately 10 µg protein of sample was loaded into each well. The gel was stained with Coomassie Brilliant Blue and the image was taken with GeneSnap version 7.01 (SynGene, UK).

The purification of Anor is outlined in the purification table below. The tables illustrate the purification yields of Anor from *A. niger* after culturing for 16 days in minimal medium (MM – Table 3.1) and in medium supplemented with haemoglobin (MM+H – Table 3.2). The medium supplementation with haemoglobin contributed to the total protein in the crude extract and therefore presents an apparent lower specific activity (5.5 $U.mg^{-1}$, Table 3.2) when compared to the 13.5 $U.mg^{-1}$ specific activity in the crude extract from the *A. niger* D15[*nicA*1] cultured in MM (Table 3.1). However, an approximate 1.5 fold higher enzyme activity was determined from *A. niger*

D15[*nicA*1] cultures supplemented with haemoglobin after Super Q 650M purification. This implies that haemoglobin supplementation was favourable for the expression of Anor. Most of the enzyme activity was lost after size exclusion chromatography, which is most likely to due protein aggregation as mentioned above.

Table 3.1. Purification of recombinant Anor from *A. niger* D15[*nicA*1] cultured in MM

Purification process	Total protein	Specific Activity	Total Activity	Yield	Fold purification
	mg	$U.mg^{-1}$	Units	%	×
Crude extract	3.293	13.5	44.5	100.0	1.0
Ultra-filtration	1.569	23.1	36.4	81.8	1.7
Super Q 650M	0.425	22.9	9.8	21.9	1.7
Sephacryl 300HR*	0.004	6.9	0.03	na	na

* 48% of the Super Q650M was loaded onto the Sephacryl 300HR column
na- not applicable

Table 3.2. Purification of recombinant Anor from *A. niger* D15[*nicA*1] cultured in MM+H.

Purification process	Total protein	Specific Activity	Total Activity	Yield	Fold purification
	mg	$U.mg^{-1}$	Units	%	×
Crude extract	9.013	5.5	49.2	100.0	1.0
Ultra-filtration	1.453	22.5	32.6	66.4	4.1
Super Q 650M	0.465	31.3	14.6	29.6	5.7
Sephacryl 300HR*	0.015	4.4	0.07	na	na

NOR activity units were determined by the NOR activity assay as described in Methods. One unit of enzyme was defined as the amount of protein that can reduce one µmole of NO per minute [152].

* 28% of the Super Q 650M was loaded onto the Sephacryl 300HR column
na- not applicable

3.5. Discussion and Conclusions

From a total of 116 *A. niger* D15 transformed colonies the highest producer of the two constructs pGTP[*nicA*1] or pGTP[*nicA*2] were selected for further study. Low transformation efficiencies were achieved but this is not unusual for eukaryotic expression systems due to tougher cell walls which may be re-enforced with chitin or melanin [217, 242]. The entry of DNA is artificially facilitated by enzymatic digestion of mycelia and treatment of the protoplasts with $CaCl_2$/PEG [242]. Unlike in prokaryotic expression systems where the plasmid remains as circular DNA, in

eukaryotic expression systems the heterologous DNA integrates into the host's genome through recombination [242].

In an effort to maximize Anor yield and to prevent its degradation by proteases, a protease deficient strain of *A. niger,* termed D15, was used as an expression host. Furthermore, culture conditions were optimised for increased biomass and Anor production. Although previous studies have shown that an increased glucose concentration can positively increase the protein production [228]; in this study, a 1% (w/v) glucose resulted in the highest NOR activity, as opposed to 10 and 20% (w/v) glucose containing media. The preferred agitation rate of 100 rpm produced compact fungal pellets, but did not significantly affect NOR activity in the culture media. Spore inoculums have been shown to affect mycelia morphology which was linked to protein production and secretion [231, 232]. In this study, the size of the spore inoculum did not significantly increase NOR activity in the culture media over 7 days. In an effort to increase mycelia biomass for increased protein production, *A. niger* D15 transformants (*A. niger* D15[*nicA*1] and *A. niger* D15[*nicA*2]) were cultured in a simulated fed-batch culture that involved removing spent medium and replacement with fresh medium. This strategy increased the production rate of NOR and assisted in producing sufficient quantities of the protein for purification.

The nitric oxide reductase, P450nor, from *A. oryzae* (Anor) belongs to the P450 superfamily which has a haem in its active site [104, 140]. The synthesis of haem is a complex process [238] and could potentially pose limitations to the synthesis of Anor in *A. niger* D15. Both *A. niger* transformants were further cultured in a simulated fed-batch culture which was supplemented with 1 $g.L^{-1}$ of bovine haemoglobin. NOR activity increased with time for *A. niger* D15[*nicA*1] supplemented with haemoglobin when compared to the other cultures. The low NOR activity on day 5 and day 10 is linked to the addition of fresh media on day 4 and 9. The extended growth period allowed for an accumulation of biomass, and consequently an increased protein yield.

A. niger D15[*nicA*2] did not show improved NOR activity. The encoding of *nicA*1 commences at the start codon of the signal sequence, *xyn2*, and presents no other alternative, whereas *nicA*2 possess two potential start codons. Bearing this in mind, it may be speculated that *nicA*2 might have presented two expression patterns: one

from the start codon from the signal sequence, *xyn*2, and the other from the start codon just after the KEX2 cutting site (wild type start codon). Therefore, it may be suggested that Anor encoded from the signal sequence start codon resulted in its secretion whereas the expression of Anor from the wild type start codon might have resulted in an intracellular protein.

From the purification studies, it was observed that the haemoglobin supplemented cultures favoured a single peak with NOR activity which correlated to high haem and protein absorbance (410 nm and 280 nm absorbance peak, respectively). After IEC, the proteins with 55 kDa mobility on a SDS-PAGE gel were moderately enriched instead not an anticipated 45.7 kDa protein. The size increase could have resulted from protein glycosylation which readily occurs in fungi [225, 243, 244, 245]. No further enrichment was achieved by subsequent SEC, which was also associated with a concomitant loss of NOR activity. A substantial amount of protein in the SEC was found to have a molecular weight ~75 kDa, while the denaturing SDS-PAGE gel revealed a more accurate size estimation of 55 kDa. Potential protein aggregation may have been observed in the SEC elution profile, which is potentially due to protein carbonylation as described by Karuzina and colleagues (1999) [246]. They have demonstrated that cytochrome P450s exposed to oxygen (which reacts with the Fe^{3+} to form hydroxyl radicals known as the Fenton reaction) could have resulted in an increase of carbonyl content, this manifested as native dimerisation in SEC 250 chromatography; 50 kDa protein was observed as a 100 kDa species [246].

Protein aggregation and denaturation by carbonylation may facilitate to rationalise the observation that only one protein species was observed in the presence of haemoglobin, where the introduction of haemoglobin could potentially scavenge oxygen thereby reducing the Fenton reaction [247]. The reduction in dissolved oxygen in the culture media could potentially reduce the iron catalysed oxidation of amino acids of P450nor and thus pre-empted apoprotein modifications which are followed by aggregation, SH-group oxidation, carbonyl production and intermolecular cross linking [246].

As mentioned before, the synthesis of haem is strictly regulated and its absence may result in apoprotein synthesis. The absence or loss of haem from cytochrome P450s,

introduces conformational changes and alters its hydrophobicity resulting in protein denaturation and aggregation [246, 248, 249]. It may be concluded that two observed protein species from the elution profiles might be a reflection of native and aggregated Anor.

In conclusion, two objectives were achieved in this chapter. Firstly, Anor was successfully expressed as an extracellular protein and NOR activity was measured in the culture media. To our knowledge, this is the first report of an intracellular fungal recombinant P450nor being expressed and secreted into a culture medium. Secondly, the growth conditions were optimised to increase the yield of active Anor. Unfortunately, purification resulted in insufficient quantities of pure Anor for the intended immobilisation and characterisation. The parallel investigation of the production of this enzyme in *E. coli* resulted in higher yields suitable for protein immobilisation and characterisation (Chapter 4).

Chapter 4
Expression, Purification and Characterization of Nitric Oxide Reductase in *Escherichia coli*

4.1. Introduction

In the previous chapter it was established that NOR is a member of the P450 family. The synthesis of P450s and other haem proteins [197], require a biosynthetic pathway to produce protohaem [250, 251, 252, 253, 254]. Such a haem biosynthesis pathway has been identified and characterised in *Escherichia coli* [255]. Briefly, the process involves nine enzymatic reactions to achieve the final product, protoporphyrin IX [254, 256, 257]. Ferrochelatase is the final enzyme in this process, and catalyses the insertion of ferrous iron into the protoporphyrin IX [258].

Haem biosynthesis is strictly regulated and this can prove problematic for the heterologous expression of recombinant haemoproteins in *E. coli* [259, 259, 260, 260, 261, 262]. The expression of haem proteins using strong promoters such as T7 polymerase results in a protein population without the haem cofactor (apo-protein), as protein production and folding outpaces haem insertion [259, 260, 262]. Several strategies have been developed to improve haem incorporation for increased yield of functional holo-proteins. A limiting factor in production of haem proteins was shown to be at the point of synthesis of 5-aminolevulinic acid [263, 264, 265, 266, 267]. Several studies have observed a greater yield of the haem-containing protein by the addition of 5-aminolevulinic acid to the culture medium [263, 267, 268, 269, 270, 271, 272, 273]. However, it was shown that the expression of recombinant proteins did not all benefit from this approach [259, 262]. External supplementation of haem, e.g. in the growth media, is challenged by the dependency of uptake on transport across the cell membrane, which is not an efficient process in common laboratory strains of *E. coli* [250, 251, 272, 273, 274, 275]. Therefore, studies were conducted to co-express haem transport genes from enteropathogenic bacteria [276, 277, 278, 279] and haem receptors [272, 273]. A more recent strategy to improve haem

incorporation into recombinant haem-protein, was the co-expression of the terminal enzyme of the haem biosynthesis pathway, ferrochelatase, together with the augmentation of 5-aminolevulinic acid [262]. This current study will not pursue such an extensive haem-protein expression optimisation, but will rely on the supplementation of the culture medium with 5-aminolevulinic acid and haemoglobin to overcome the bottleneck in the haem biosynthesis pathway and pre-empt holo-protein production.

Besides the challenges in holo-protein production of haemoproteins, the heterologous expression of an eukaryotic protein in a prokaryotic system presents its own set of challenges. This includes the transcriptional and translational aspects of protein production which can be addressed by the choice of expression vector, promoter, terminator, codon usage, location of protein expression and genetic engineering of the host strain [280]. Incorrect protein folding and aberrant post-translational modifications are notorious challenges faced with eukaryotic protein expression in *E. coli* [245]. Furthermore, the recombinant protein might become enclosed in inclusion bodies which can result in insoluble and aggregated protein intermediates, potentially presenting advantages in purification when applying this strategy, but are difficult to solubilise and subsequently retain activity of the expression target [280, 281]. Proteolysis of the heterologous protein presents another major challenge which has largely been addressed by genetic engineering of the host strain, e.g. *E. coli* BL21 (DE3) which lacks the ompT outer membrane protease [282]. Despite these challenges, fungal nitric oxide reductase, P450nor, has been expressed in several different *E. coli* strains (HB101, XL-1 Blue, JM105, Y1090) using the pUC19 expression plasmid [283]. Nevertheless, the specific nitric oxide reductase activity was disappointingly low, ranging from 0.32-1.34 $pmol.mg^{-1}$ [283]. In the pursuit of P450nor structural characterization, P450nor (Fnor and Tnor) was expressed in *E. coli* JM109 using a T7 polymerase-driven expression vector [146, 147, 148, 178, 213]. To the best of the author's knowledge, the expression of a recombinant P450nor isoform, Anor, has not yet been reported.

The aim of the work reporte in this chapter was to obtain sufficient functional Anor for the development of the nitric oxide reduction system. Previous attempts to express Anor in an eukaryotic expression system and the purification of this secreted protein

from the extracellular environment resulted in disappointingly low yields. Consequently, the strategy reported in this chapter was to express histidine tagged Anor in an intracellular environment and then to extract it using a single purification step.

For this purpose, the first objective entailed the expression of Anor from a pET-28a vector in *E. coli* BL21 (DE3). The second objective was the characterisation of the recombinant Anor purified from *E. coli*. It was essential to ensure that the purified protein was indeed the protein of interest and that it was largely similar to the wild-type fungal Anor. Characterisation included comparison of the Soret peak of Anor and the kinetic constants for Anor. The third objective was to evaluate the potential to increase yields through the supplementation of the expression medium with 5-aminolevulinic acid and haemoglobin.

4.2. Materials

4.2.1. Genes, vectors, host strain and culture media

The gene variants encoding nitric oxide reductase, Anor, were synthesised by GeneArt (Germany) as described in Section 3.3.1. For the expression of Anor in *E. coli*, the pET-28a vector purchased from Novagen (USA) and *E. coli* BL21 (DE3) (F^- ,*dcm, ompT*$^-$*, hsd*S(r_B^-,m_B^-), *gal*, λ(DE3) was purchased from Stratagene (USA). For the gene amplification reaction, the Ex Taq polymerase and its supplementary reagents were purchased from TaKaRa Bio Inc. (Japan). Primers were synthesised by Inqaba Biotec (South Africa). The PCR reaction was performed in a G-Storm thermocycler (Gene Technologies, UK). The Zymoclean Gel DNA Recovery Kit and the Zyppy Plasmid Miniprep Kit were purchased from Zymo Research Corporation (USA). The Fast-Link DNA Ligation Kit was purchased from Epicentre Biotechnologies (USA). The restriction enzymes, NcoI and SalI, reaction buffer, DNA loading dye, TopVision agarose and isopropyl β-D-thiogalactopyranoside (IPTG) was purchased from Thermo Scientific (USA). The Aurum Plasmid Mini Kit was purchased from Bio-Rad (USA). The DNA molecular weight marker was purchased from Promega (USA) and the ethidium bromide was purchased from Sigma-Aldrich

(Germany). A NanoDrop 1000 (ND-1000 spectrophotometer, USA) was used for plasmid DNA quantification and the sequence analysis was done with ABI 3130XL sequencer by Inqaba Biotech (South Africa). The electroporation procedure was carried out with a Bio-Rad Gene Pulser® electroporator (USA). The reagents for the super optimal catabolite repression (SOC) media were purchased from Sigma-Aldrich and prepared according to current protocols [233]. Luria broth, 5-aminolevulinic acid, haemoglobin and kanamycin were purchased from Sigma-Aldrich. *E. coli* culturing was performed in a Zhicheng orbital shaking incubator (China) and an Avanti J-30I from Beckman Coulter (USA) was used for centrifugation.

4.2.2. Reagents and instruments used for biophysical analysis

The reagents for the nitric oxide reductase activity assay and for protein quantification were the same as those described in Section 3.3.4. For the quantification of P450 content, a Shimadzu spectrophotometer (Japan) was used, while the carbon monoxide required for the experimentation was purchased from Speciality Gases (South Africa). The sodium dithionite and the reagents for the sodium phosphate buffer were purchased from Sigma-Aldrich (Germany).

4.2.3. Purification of Anor

E. coli cell lysis was carried out using detergent based YPER solution (Thermo Scientific, USA) and DNase I (Bio-Rad, USA). The protease inhibitor cocktail was purchased from Sigma-Aldrich (Catalogue no. S8830). The nickel affinity resin, MagReSyn™ NTA, was a gift from ReSyn Biosciences (South Africa). The magnetic separator was purchased from Invitrogen (Life Technologies, USA). For the end-over-end mixing an Elmi Intelli mixer (USA) was used.

4.2.4. SDS-PAGE reagents

The PowerPac Universal was from Bio-Rad (USA). The Bis-Tris NuPAGE® precast acrylamide 4-12% gradient gels were purchased from Invitrogen (USA). The molecular weight marker was purchased from Fermentas. Colloidal Coomassie

Brilliant Blue stain was prepared in this laboratory (Appendix to Chapter 3, Section A.3.3.2). The destained gel was imaged using a Syngene Genebox using GeneSnap software and analysed with GeneTools version 3.08 (Syngene, UK).

4.3. Methods

4.3.1. Design of recombinant Anor genes: *nicA*1 and *nicA*2

The cloning strategy entailed the amplification of the coding sequence of Anor, termed *nicA*, from the plasmid DNA using a forward primer containing a start codon and a *Nco*I restriction site, and a reverse primer containing a *Sal*I restriction site. These restriction sites were included to facilitate directional cloning into a prokaryotic expression plasmid, pET-28a, with a C-terminal His-tag sequence configuration. With successful ligation of the amplicons into the expression plasmid backbone, *nicA* would be placed under the expression control of a T7 promoter and terminator. The pET-28a vector also encodes for kanamycin resistance to facilitate selection of transformed *E. coli* clones. The genetic environment of the recombinant *nicA* gene is shown in Scheme 4.1.

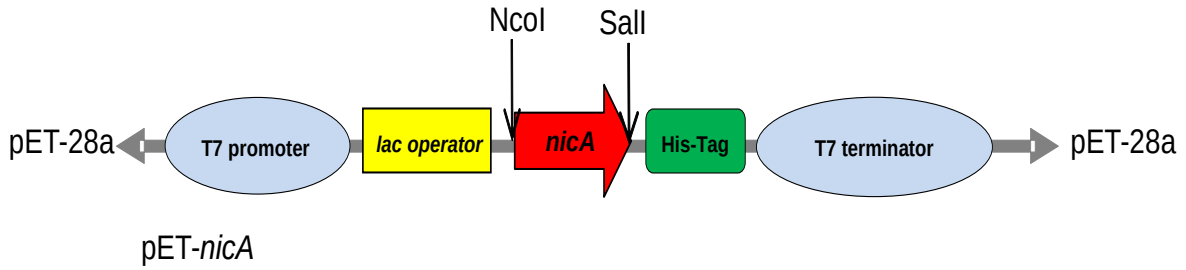

Scheme 4.1. Genetic environment of *nicA* in *E. coli* on the pET-28a plasmid. The gene *nicA* is under the transcriptional control of the T7 promoter and terminator. The lac operator facilitates IPTG gene induction, while the poly-histidine tail facilitates the affinity purification of Anor. The enzyme restriction sites are indicated by vertical arrows. The wild type genetic environment of Anor was described in Chapter 3, Scheme 3.3.

4.3.2. Transforming *E. coli* with pET-*nicA*1 or pET-*nicA*2

For the transformation experiments, the plasmid DNA from pMA-*nicA*1 and pMK-*nicA*2 was extracted from *E. coli* DH10B (Chapter 3, Section 3.3.2) using an Aurum mini plasmid extraction kit. This DNA was then used as a template for amplification of the coding sequence of *nicA* using primers FnicA1 or FnicA2, respectively, together with RnicA (Appendix to Chapter 4, Section A.4.1.1). A PCR product of 1.4 kbp size was excised from the agarose gel after electrophoresis and the DNA was recovered using a Zymoclean DNA recovery kit. The PCR product as well as pET-28a were digested with *Nco*I and *Sal*I (reaction details in Appendix to Chapter 4, Section A.4.1.1) and the digested DNA was separated by 0.8% (w/v) agarose gel electrophoresis. The DNA band corresponding to 1.4 kbp and 5.3 kbp were excised and recovered from the agarose as before. The restriction enzyme-digested PCR product was ligated into the pET-28a vector in a ligation reaction containing 1.5 Units DNA ligase, 1.5 µl vector DNA and PCR DNA, 7.5 mM ATP, 0.75 µl 10× Fast-Link buffer and 2.5 µl of dd H_2O for a total reaction volume of 7.5 µl. The reaction was allowed to proceed for one hour at room temperature and was subsequently heat-inactivated at 70˚C for 10 min. The ligation product was electroporated into 100 µl competent *E. coli* BL21 (DE3) cells using 25 µFD and 200 Ω settings on a Bio-Rad Gene Pulser®. The electroporated *E. coli* cells were allowed to incubate in 1 ml SOC medium for 1 hr at 37˚C at 175 rpm. Thereafter, the cells were plated onto Luria broth agar plates containing 50 $\mu g.ml^{-1}$ kanamycin. The plates were incubated overnight at 37˚C.

4.3.3. Screening for pET-*nicA*1 and pET-*nicA*2 containing *E. coli*

Several sets of ten colonies were picked from the overnight agar plates and subjected to colony PCR in search for *nicA*-positive *E. coli*. Each set of 10 colonies was mixed and suspended in a PCR tube containing 50 µl filtered dd H_2O and incubated at 100˚C for 30 minutes. The cellular particulates were removed by centrifugation and 2 µl of the supernatant was used as a template for colony PCR (reaction mixture and conditions described in Appendix to Chapter 4, Section A.4.1.1). Colony pools presenting a ~1.4 kbp product upon agarose gel electrophoresis were selected and a PCR of each of the 10 substituent colonies was

performed. Each positive colony was then cultured in 5 ml Luria broth containing 50 $\mu g.ml^{-1}$ kanamycin overnight at 190 rpm.

4.3.4. Screening for NOR activity from *E. coli* containing pET-*nicA*1 and pET-*nicA*2

For the expression of Anor from pET-*nicA*1 or pET-*nicA*2-transformed *E. coli* cells, 10 ml of Luria broth containing 50 $\mu g.ml^{-1}$ kanamycin was inoculated with 100 µl of overnight culture described in Section 4.3.3. The cultures were allowed to grow for 4 hours at 37˚C at 190 rpm, at which point IPTG (0.5 mM final concentration) was added to the culture to induce *nicA* expression via the *lac* operon complementation system of *E. coli* [284]. At this point, the temperature was reduced to 30˚C. The *E. coli* cells were harvested the next day by centrifugation at 3500 ×*g* for 15 minutes at 4˚C. The cell pellet was washed twice with 0.2 mM phosphate buffer at pH 7.2. The cells were lysed with a lysis buffer comprising of 2 ml of YPER per 1 g of pellet, 4.4 K units DNase I in its reaction buffer (10 mM TRIS-HCl pH 8 and 2.5 mM $MgCl_2$) and Sigma-Aldrich protease inhibitor cocktail. The cells were mixed with this lysis buffer and incubated at room temperature with gentle agitation for 15 minutes. The cell debris was separated from the cell lysate by centrifugation (14000 ×*g* for 10 minutes). The supernatant was analysed for NOR activity according to the NOR activity assay described in Section 3.3.4. This overnight culture was used to isolate the plasmid for sequencing analysis and to prepare glycerol stocks of the expressing organism.

4.3.5. Purification of Anor with MagReSyn™ NTA

To purify and characterise Anor, one of each construct (pET-*nicA*1 and pET-*nicA*2) containing *E. coli* colony with the highest NOR activity, was selected (Section 4.3.4). An overnight starter culture of *E. coli* BL21[*nicA*2] was used to inoculate 500 ml Luria broth containing 50 $\mu g.ml^{-1}$ kanamycin and the culture was grown at 37˚C and 190 rpm orbital shaking to a final cellular density correlating to an optical density around 0.4 at 600 nm. At this point, IPTG was added to a final concentration of 0.5 mM for induction of gene expression. The temperature was then reduced to 30˚C. The cells were harvested after 18 hours of growth.

The cells were harvested by centrifugation at 6000 ×*g*, 4˚C for 15 minutes and washed twice with 100 ml, 20 mM sodium phosphate buffer (pH 7.2). *E. coli* cells were lysed using lysis buffer (same as above with adjusted volumes) and were incubated for 15 minutes at room temperature with gentle end-over-end mixing (15 rpm). The lysed cells were centrifuged at 14000 ×*g* for 20 minutes at 4˚C. The supernatant was pooled and an equal volume of double strength binding buffer was added to obtain a final concentration of 20 mM imidazole, 500 mM NaCl in 80 mM sodium phosphate buffer (pH 7.2). The histidine tagged protein was recovered by magnetic bead purification. MagReSyn™ NTA was equilibrated by washing the resin with three times its volume of single strength binding buffer. The cell lysate was added to the equilibrated resin. The protein was allowed to interact with the resin for 3 minutes on ice, after which the unbound protein was removed using a magnet and stored at 4˚C for further analysis. The resin was washed three times its volume with binding buffer containing 20 mM imidazole and 500 mM NaCl in 80 mM sodium phosphate buffer (pH 7.2). Anor protein was then eluted using a $1/10^{th}$ of the resin's volume with elutation buffer containing 500 mM imidizole in 80 mM sodium phosphate buffer (pH 7.2).

4.3.6. Spectroscopic analysis of Anor: direct difference spectroscopy

The P450 concentration was determined using a Shimadzu spectrophotometer according to the method of Gruengerich *et al.* 2009 [285]. All spectra were obtained by three repeated scans of the samples from 250 nm to 700 nm. A 10 fold dilution of the affinity purified protein was prepared in 200 mM TEA buffer (pH 6), and scanned accordingly. The sample was then reduced by adding 50 mM sodium dithionite ($Na_2S_2O_4$) final concentration, to a sample volume of 2 ml with subsequent wavelength scan. Carbon monoxide (CO) was bubbled through the reduced sample for 20 seconds with a continuous stream of bubbles to saturate the solution, followed by immediate scanning of the sample. The cuvette chamber was kept at 25˚C for the duration of the experiment. The haemoprotein content was calculated from the difference between the reduced protein sample spectra and the CO-bound reduced protein spectra using an extinction coefficient of 91000 $M^{-1}.cm^{-1}$ at 450 nm [285]. To establish whether NO, the substrate of Anor, would produce a similar Soret peak, the

procedure was repeated. Here, the sample was reduced with 1.2 mM NADH and the wavelength was recorded. Thereafter, NO from 2 mM NOC-5 was added to the sample and the wavelength was recorded as with the CO binding.

4.3.7. Quantification of Nitric Oxide Reductase activity and protein concentration

Nitric oxide reductase (NOR) activity was assayed by measuring the reduction of NADH at 340 nm in a 384 well plate as described previously (refer to Chapter 2 and Chapter 3). Intracellular NADH utilising *E. coli* enzymes would also be present in the cell lysate and could potentially interfere with the enzymatic reduction of Anor. It was therefore necessary to monitor the rate of NADH reduction in the absence of NOC-5. The observed activity was subtracted from the activity in the presence of NOC-5 to correct for any competing activities. The protein concentration of all samples was determined using the Bradford reagent as previously described by Bradford (1976) [406] and the optical density assayed in a 384 well micro-titre plate. Here, 35 µl of the sample was mixed with 35 µl of the Bradford reagent and the colour was allowed to develop for 5 min at room temperature. The absorbance was measured at 595 nm. The protein concentration was extrapolated from a bovine gamma globulin standard (BGG) curve. The linear assay range for protein quantification was 0-25 $\mu g.ml^{-1}$.

4.3.8. SDS-PAGE analysis of proteins

All purified Anor protein samples were analysed by SDS-PAGE to estimate their purity [407]. Here, the cell lysate, unbound protein, eluates and the microspheres (to estimate the tagged protein not released from the beads) were denatured with reducing agent (500 mM DTT) and NuPAGE® Anti-oxidant (provided in the precast NuPAGE® gel kits) at 70˚C for 10 minutes. An approximate total of 13 µg of protein was loaded into each well of a Bis-Tris NuPAGE® precast 4-12% gradient gel and visualized with Colloidal Coomassie brilliant blue stain (Appendix to Chapter 3, Section A. 3.3.2). The molecular weight of the proteins was estimated using molecular weight markers.

4.3.9. Amino acid sequence analysis by mass spectrometry

To confirm identity, the proteins that migrated according to the expected molecular size of Anor were excised and the identity confirmed by tryptic digest fingerprinting using MS-MS spectrometry as described in Chapter 3 section 3.3.11. The sample preparation and amino acid analysis were performed by Dr. Stoyan Stoychev (CSIR, Biosciences, South Africa).

4.3.10. Nucleotide sequence analysis of pET-*nicA*1 and pET-*nicA*2

From an overnight culture (18 hours), plasmids from *E. coli* BL21*[nicA*1] and *E. coli* BL21[*nicA*2] were extracted with Zyppy Plasmid Miniprep Kit. The plasmid concentration was determined with a NanoDrop 1000 (ND-1000 spectrophotometer, USA) and the sequence analysis was done with an ABI 3130XL sequencer Inqaba Biotech (South Africa). Sequence files were viewed and edited with BioEdit Sequence Alignment Editor version 5.0.9 (USA). Sequence alignments and plasmid maps were constructed with DNAMAN version 5.2.9 (Lynnon BioSoft, Canada).

4.3.11. Optimisation of growth conditions for increased NOR activity

E. coli maintains low levels of free haem and haem intermediates, because higher concentrations of these compounds can prove toxic for the cells [275, 286]. With the T7 polymerase driving high expression rates, the synthesis of large quantities of P450 apo-proteins is an inevitable risk. For this reason, it has become common practice to supplement the culture medium with 5-aminolevulinic acid to overcome the bottleneck of haem synthesis and to increase holo-protein yields [264, 265, 287]. However, this strategy alone is not always sufficient [267]. We therefore tested supplementation with 5-aminolevulinic acid, haemoglobin, and a combination thereof, to determine which method would provide the highest holo-protein yield.

In brief, an overnight starter culture of *E. coli* BL21[*nicA*2] was used to inoculate either 4 × 250 ml Luria broth containing 50 µg.ml^{-1} kanamycin alone, and similar media supplemented with filtered haemoglobin to a final concentration of 0.2 g.L^{-1} which was added to the culture media before inoculation. The haem precursor, 5-

aminolevulinic acid, was added to the culture media to a final concentration of 0.5 mM one hour before IPTG induction. The third supplementation strategy entailed the addition of both reagents at the indicated time points and concentrations. The culture was grown at 37˚C and 190 rpm orbital shaking to a final cellular density with an optical density around 0.4 at 600 nm. At this point, IPTG was added to achieve a final concentration of 0.5 mM for induction of gene expression. The temperature was then reduced to 30˚C. The cells were harvested after 18 hours of growth. The expressed Anor protein was harvested and purified as described in Section 4.3.5. Protein concentration, enzyme activity and P450 content were determined for each culture (refer to Section 4.3.7 and 4.3.6, respectively).

4.4. Results

4.4.1. Expression and identification of Anor in *E. coli*

E. coli was transformed with pET-28a vector carrying either *nicA*1 or *nicA*2 with the intention of expressing Anor at sufficient yield to continue with the development of the nitric oxide reductase system. Firstly, the *E. coli* transformants carrying a *nicA* vector were identified, and following expression, the enzyme activity of the crude cell lysates were determined (Appendix to Chapter 4, Section A.4.1). Since an adequate yield of activity was essential, the *E. coli* transformant representing the highest enzyme activity was selected for further study.

The *E. coli* cultures with the highest NOR activity were selected (one of each construct) for purification and Anor characterisation studies. The two selected colonies were cultured for protein purification and characterisation. Table 4.1 presents the NOR activity from *E. coli* BL21 (DE3) transformants carrying either pET-*nicA*1 or pET-*nicA*2. In consideration of NADH oxidation in the cell lysate (L), the NADH consumption rated determined in the absence of NOC-5 was subtracted from the NOR activity. Furthermore, the lysate of *E. coli* BL21 (DE3) without a pET-28a vector was included to quantify other nitric oxide related redox activity naturally present in *E. coli*, such as nitric oxide reductases [135] and nitric oxide dioxygenases [67]. This background NO reducing activity accounted for between 20% and 24%

(pET-*nicA*1 and pET-*nicA*2, respectively, refer to Table 4.1) when compared to total NOR activity in a cell lysate (L), indicating that an estimated 97% and 19% of Anor (pET-*nicA*1 and pET-*nicA*2, respectively) was found in the unbound fraction (UB). NOR activity from cell lysates and unbound fraction indicated the possible contribution of NADH-NO catalysing enzymes to the observed NOR activity (Table 4.1). The NOR activity in pET-*nicA*1 eluate (21%) was four times lower than with pET-*nicA*2 (93%). Another possible contribution to the NOR activity observed in the unbound fraction (UB*, Table 4.1) could have been due the calculated quantitative recovery and the dilution of inhibitory compounds in the lysis buffer. This apparently resulted in the observed amplified NOR activity.

Table 4.1. NOR activity purified from *E. coli* BL21[*nicA*1] and *E. coli* BL21[*nicA*2].

plasmid construct		Total protein^	Total activity	Specific activity	Yield	Fold purification
	Sample	mg	Units	Units.mg^{-1}	%	×
pET-*nicA*1	L	2.3	48.1	21.2	100	1.0
	UB*	2.5	56.1	22.3	117	1.1
	E	0.3	10.2	38.2	21	1.8
pET-*nicA*2	L	4.2	38.7	9.3	100	1.0
	UB*	3.0	16.5	5.6	43	0.6
	E	1.0	36.1	35.2	93	3.8
Negative control	L	3.5	9.4	2.7		

L-lysate, UB- unbound, E-eluate

* Protein and enzyme activity determination tendered towards quantitative recovery that could have resulted in amplified values due to dilution or sample volume as well as endogenous NADH-NO activity.

The differences in Anor expression were also observed after the SDS-PAGE analysis (Fig. 4.1, lanes comparison of 3 and 2). The affinity purification process has enriched a 45 to 55 kDa protein species from *nicA*2 expression, whereas only a minor protein migration band was visible in the eluate of *E. coli* BL21[*nicA*1]. The protein migration profile of *nicA*1 expressing *E. coli* BL21 was very similar to the protein migration profile of the negative control (Fig. 4.1, lane 1). Most the NOR activity was measured in the unbound fraction of *E. coli* BL21[*nicA*1], indicating that this activity may be due to endogenous NADH-NO reducing enzymes, rather than the expression of Anor. The highest NOR activity expressing insert, *nicA*2, was chosen for further studies.

Lane	samples	
1	negative control	
2	Eluate	*nicA* 2
3		*nicA* 1
4	Unbound	*nicA* 2
5		*nicA* 1
6	Lysate	*nicA* 2
7		*nicA* 1
8	MwM	

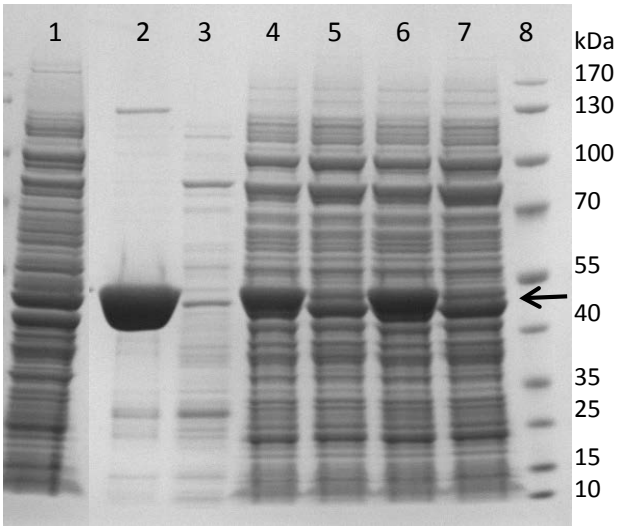

Figure 4.1. Denaturing and reducing SDS-PAGE gradient analysis of proteins from *E. coli* BL21[*nicA*1] and *E. coli* BL21[*nicA*2]. The affinity tagged protein was purified with the MagReSyn™ NTA beads. For qualitative analysis, an approximately 13 µg of the denatured and reduced protein was loaded onto a 4-12% gradient NuPAGE gel. The arrow guides to the anticipated 45.7 kDa sized protein. The gel was stained with Colloidal Coomassie Brilliant Blue stain overnight with gentle agitation. The gel was destained in double distilled water and the image photographed with GeneSnap version 7.01 (SynGene, UK). MwM-protein molecular weight marker in kDa.

Nucleotide sequence analysis (refer to Appendix to Chapter 4, Section A.4.1.4) of pET-*nicA*1 supported the findings that the NOR activity was not from Anor expression by *E. coli* BL21[*nicA*1], but endogenous NO reduction may have contributed to the NADH consumption. The lower NOR activity may be due to lower Anor expression. The nucleotide sequence of pET-*nicA*1 lacks the *nicA* start codon as well as 303 bps (Fig. A.4.5, Appendix to Chapter 4, Section A.4.1.4). This nucleotide loss was likely due to an NcoI cutting site. However, *nicA*2 on pET-*nicA*2 did contain the wild-type start codon with the insertion of three random nucleotides placing the start codon in an optimal reading frame for *nicA*2 expression (Fig. A.4.5, Appendix to Chapter 4, Section A.4.1.4). These findings were further confirmed by tryptic digest finger printing of the protein corresponding to the BL21[*nicA*2] 45 kDa eluate in lane 2 (Fig. 4.1) where a 78.4% coverage of cytochrome P450nor (Q8NKB4_ASPOR) confirmed its identity (Appendix to Chapter 4, Section A.4.1.5). Thus active expression of the fungal NOR in *E. coli* was successfully demonstrated and the first objective was achieved.

4.4.2. Characterisation of Anor

P450 enzymes present a characteristic absorbance at 450 nm upon the binding of carbon monoxide to its reduced haem centre; this is termed the Soret peak [201, 202]. This characteristic spectrophotometric property provides a means to demonstrate and quantify the P450 properties of a sample [201]. The Soret peak of Anor at 450 nm in the presence of carbon monoxide was compared to that in the presence of nitric oxide. The results and implications of the findings are elaborated below.

4.2.2.1. Spectroscopic analysis of the Soret peak

The objective was to determine whether purified protein would produce the characteristic P450 Soret peak at 450 nm in an effort to illustrate the structural integrity of the heterologously expressed P450nor (Anor). The characteristic Soret peak of Anor was first demonstrated using the conventional method as described by Gruengerich *et al.* (2009) [285]. Here, the substrate-free Anor in its resting state (Fe^{3+}) was reduced with sodium dithionite to Fe^{2+}, and the expected shift from 410 nm to 450 nm was observed after CO binding as shown in Figure 4.2 A. As for all published P450nor absorption spectra, this recombinant Anor also presented a prominent 418 nm peak with other minor peaks of ~535 and 568 nm in its oxidative state (blue arrows in Fig. 4.2), indicating that the haem was in an oxidised form [151, 152]. No peaks were observed after sodium dithionite reduction, but after saturating the sample cuvette with CO, a peak-shift was observed at 370 nm as well as a characteristic Soret peak at 450 nm. As expected, the formation of the characteristic Soret peak confirmed that the recombinant NOR was indeed a P450. Furthermore, from this Soret peak shift, the percentage of apo to holo-protein was calculated to 94% (the ratio percentage absorbance from the 450 nm peak and peak in the 410 nm peak) indicating that most Anor were holo-proteins.

It was further of interest to determine whether this P450nor-like enzyme would produce the Soret peak after NADH reduction and subsequent NO binding. In Figure 4.2 B, the characteristic Soret peak at 450 nm was also observed in the presence of NO, albeit with a reduced peak height. This may be accounted to lower NO concentration of NO in solution from 2 mM NOC-5. This experiment was repeated

with higher NOC-5 concentrations and the Soret peak was measured at regular intervals for an hour. With time, an increase in amplitude of a 420 nm peak was observed (data not shown) which may indicate that the characteristic thiol ligand from the cysteine 352 was denatured [160, 210, 285]. These results indicate that Anor purified from *E. coli* BL21[*nicA*2] is not only a P450 but that it also produces the characteristic Soret peak in response to NO binding to its heam reactive centre.

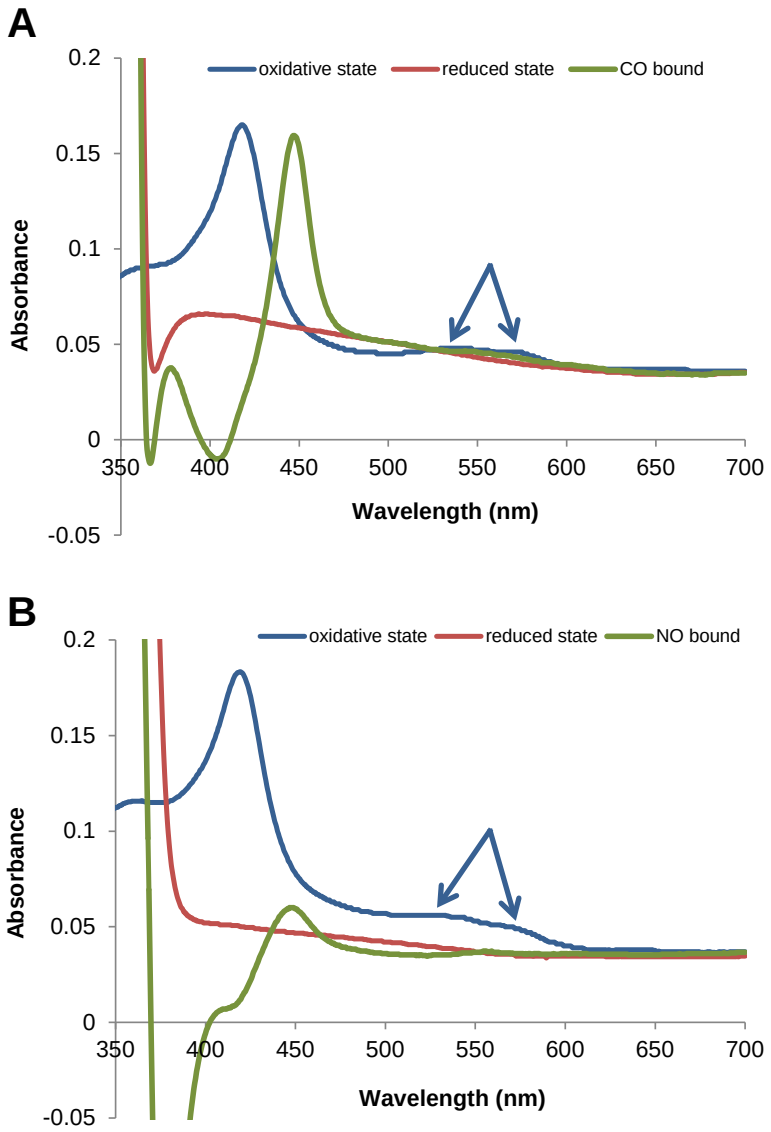

Figure 4.2. Spectroscopic properties of Anor purified from *E. coli*. The spectroscopic scan is an average of three scans with one minute intervals. The blue line represents Anor in its oxidative state; red: reduced state and green line when either CO (A) or NO (B) bound to the reactive centre. In (A) the characteristic Soret peak at 450 nm of the haem is depicted when bound to CO after reduction with 50 mM sodium dithionite ($Na_2S_2O_4$). The P450 yield was calculated at 71 nmol P450.mg^{-1}. In (B) the Soret peak in the presence of NO after reduction with 1.2 mM NADH is shown. The P450 yield was 22 nmol.mg^{-1}. For both reactions, 0.1 mg of the same Anor batch was prepared in 200 mM TEA buffer pH 6. The reaction chamber was kept at 25˚C. Minor peaks are indicated by blue arrows.

4.2.2.2. Kinetic constants of Anor

The affinity of the substrate for its active site (indicated by K_m), the maximal velocity of an enzyme (V_{max}) and the enzyme's turnover number (k_{cat}) are important parameters for kinetic characterisation of an enzyme [288, 289]. In an effort to characterise recombinant Anor, these parameters were determined and compared to kinetic constants of a commercial preparation of Anor isolated form *A. oryzae* [152].

The kinetic constants (K_m) and maximal velocities (V_{max}) reported by Kaya and his colleagues (Anor^A) [152], the wild-type Anor (commercial Anor preparation, Anor^B, Chapter 2) as well as two different recombinant enzyme preparations (Anor^C and Anor^D) are shown in Table 4.2. The kinetic constant, K_m, from the wild-type Anor determined by the NOR activity assay (Anor^B) deviated only by a marginal 11% from the K_m determined by gas chromatography (Anor^A). Anor^B presented a slower catalytic rate (4700 NO.min^{-1}) which might be due to compromised enzyme integrity caused by extended storage. The kinetic characterisation described for the commercial preparation was repeated for the recombinant Anor. A higher substrate affinity (lower K_m) was measured for Anor^C and Anor^D which were expressed in and purified from *E. coli* BL21[*nicA*2]. The maximum velocity (V_{max}) for Anor^D deviated only by a marginal 3% from the wild-type Anor^A. Similarly for the catalytic turnover (k_{cat}) of the recombinant enzymes were within the same order of magnitude when compared to the wild-type Anor^A. The determination of enzyme efficiency, K_m/k_{cat}, [290, 291] and specificity constant (V_{max}/K_m) [291, 292, 293] were included for a more comprehensive characterisation of the recombinant Anor. The higher specificity constant (V_{max}/K_m) as well as the improved enzyme efficiency (k_{cat}/K_m) [294] highlights that Anor expression in *E. coli* might have altered NOR's interaction with its substrate. The NOR activity presents sufficient sensitivity for the detection of changes in enzyme kinetics which may be attributed to the direct determination of enzyme rates with the new NOR activity assay (as described in Chapter 2). The close similarity of the kinetic characteristics of the recombinant enzymes to the wild-type Anor indicates that the enzyme of interest was indeed expressed and purified by *E. coli* BL21[*nicA*2].

Table 4.2. Kinetic characterisation of Anor purified from *E. coli* BL21[*nicA*2].

NOR	µM NOR	K_m µM NO	V_{max} µM NO.min^{-1}	k_{cat} NO.min^{-1}	k_{cat}/K_m min^{-1}.µM^{-1}	V_{max}/K_m
Anor^{A}	0.028	197	352	12571	64	1.8
Anor^{B}	0.140	222	658	4700	21	2.9
Anor^{C}	0.026	97	269	10567	109	2.8
Anor^{D}	0.037	117	342	9364	80	2.9

Anor^{A}: reported values of wild-type Anor [152]
Anor^{B}: commercially acquired wild-type Anor solution
Anor^{C} and Anor^{D}: recombinant Anor

4.4.3. Optimisation of NOR activity in culture media

As indicated previously, the yield of Anor apo-protein is subject to the synthesis of haem within the host organism which is strictly regulated in *E. coli* [254]. It has therefore become common practice to supplement culture media with a haem precursor, 5-aminolevulinic acid [263, 268, 269, 270, 272, 273]. As shown in the previous chapter, it was reasoned that the addition of haemoglobin to the culture medium might assist by increasing the yield of expressed Anor in *E. coli*. Various culture medium optimisation strategies were explored (Appendix to Chapter 4, Section A.4.2), however, only the supplementation of 5-aminolevulinic acid and haemoglobin to the medium is described here. The yield of Anor was compared to the yield with the addition of 5-aminolevulinic acid (I, A) one hour before induction, or the addition of haemoglobin (I, H) to the culture medium before inoculation, or the addition of both combined (I, A, H). In all the cultures, gene expression was induced with 0.5 mM IPTG as before. Anor was purified as previously described but the culture volume was increased to 4× 250 ml. As observed in Chapter 3, supplementation of culture media with haemoglobin (I, H) or in combination with 5-aminolevulinic acid (I, A, H) increased the Anor yield two to four fold (Table 4.3). Since the supplementation of the growth media with haemoglobin and 5-aminolevulinic acid resulted in the highest total enzyme activity and total P450 content, this growth strategy was applied to all subsequent culturing procedures.

Table 4.3. Purification yields from 1 L culture (4× 250 ml) from *E. coli* BL21 [*nicA*2]

Media supplementation	Total protein	Total activity	Specific activity	specific P450
	mg	Units	Units.mg-1	nmol.mg^{-1}
I, A	2.9	132	45	2.8
I, H	3.2	547	170	27.7
I, A, H	4.1	363	89	19.1

I-IPTG, A- 5-aminolevulinic acid, H- haemoglobin
The purification yields *E. coli* BL 21[*nicA*2] for IPTG induced culture is shown in Table A.4.3 (Appendix to Chapter 4, Section A.4.2.3).

The yield of recombinant Anor was compared to the purification yields from other P450nor isoforms (Table 4.4). The specific activity and P450 content obtained from this study was comparable to the yields obtained from the wild-type Fnor [104] and Anor [152]. The comparison in yields obtained in this study to the recombinant Fnor [194, 283] was difficult as the available data was incomplete. Nonetheless, the Anor yields obtained in this study were considered sufficient for subsequent immobilisation and development of the NOR system.

Table 4.4. Purification yields of P450nors

Source	P450nor isoform	Specific activity	Specific P450	Reference
		Units.mg^{-1}	nmol.mg^{-1}	
F. oxysporum	Fnor	289	18.3	[104]
A. oryzae	Anor	75	3.3^	[152]
E. coli HB101 and XL1-Blue	Fnor		0.32 & 1.34*	[283]
E.coli	Fnor		600$^{\#}$	[194]
E. coli BL21(DE3)	Anor	129	23.4	this study

^ estimated value from Kaya *et al.* (2004) [152]
* pmol.mg^{-1}
$^{\#}$ nmol.L^{-1}

4.5. Discussion and Conclusions

The nitric oxide reductase for the development of a nitric oxide reduction system was successfully expressed and purified in *E. coli* BL21 (DE3). The *nicA1* and *nicA2* gene variants of Anor were slightly different in their start codon and it appeared that functional expression of the protein only occurred in *nicA*2. Both gene variants from GeneArt (Chapter 3) were prepared for expression in *E. coli* on the pET-28a plasmid. In contrast to the expression of *nicA*1 in *A. niger*, *nicA*2 appeared to provide

functional expression in *E. coli*. The low Anor yield from *E. coli* BL21[*nicA*1] could potentially be attributed to the NcoI cutting site downstream of the PCR generated start codon compromising gene expression (Appendix to Chapter 4, Section A.4.1.4). The enzyme activity observed from *E. coli* BL21[*nicA*1] could have resulted from endogenous NO reducing activity. Therefore, *E. coli* BL21[*nicA*2] was chosen as the source of Anor for further studies. DNA sequence analysis of the plasmid as well tryptic digest fingerprinting successfully confirmed the identity of the gene coding for the 45 kDa protein as well as its expression as Anor, which concludes the first objective of this chapter and it may also be the first report on the expression of Anor in *E. coli*.

The second objective was to characterise the recombinant Anor as a member of the P450 family as well as the kinetic characterisation to ensure its effective catalysis of NO. Recombinant Anor presented the characteristic Soret peak after reduction and the binding of CO or NO to the haem, verifiying P450 function. The comparative K_m for recombinant Anor indicated it had a slightly improved affinity for its substrate, but an overall lower V_{max}. However, the catalytic constant from *E. coli* BL21[*nicA*2] deviated only between 18 to 25% from Anor purified from *A. oryzae* [152]. The kinetic characteristics of recombinant Anor were similar to that of the wild-type Anor^A indicating its suitability for subsequent immobilisation and preparation of the NOR system.

The third objective involved attempting to increase the enzyme yield through culture medium supplementation. The addition of haemoglobin or in combination with 5-aminolevulinic acid did increase specific enzyme activity, total enzyme activity as well as specific P450 content. This is an interesting observation since the *E. coli* cell wall is generally impermeable to haem or haem proteins [262, 272, 287]. The uptake of haem or haem proteins requires haem receptor, haem binding proteins and the Ton system, which are energy-requiring transport mechanisms described mostly for enteric/pathological bacteria [250, 295, 296, 297, 298, 299]. The mechanism in which haemoglobin contributes to a higher nitric oxide reductase activity is unknown and since elucidation of this mechanism extends beyond the scope of this study, it was not further investigated. Nonetheless, the supplementation with haemoglobin or in combination with 5-aminolevulinic acid might have contributed to an increased

Anor yield and thus this culturing strategy was used for all subsequent expressions. The protein yield from supplemented cultures was higher overall, and thus some part of the contribution may have been as a nutrient that resulted in protein expression.

The aim and objectives set out for this part of the study was successfully completed, namely the expression and purification of Anor with sufficient yield for its subsequent immobilisation. The recombinant Anor presented similar characteristics to the wild-type Anor and this enzyme preparation was therefore considered suitable for the immobilisation for the preparation of a bi-enzymatic cofactor recycling system.

Chapter 5
Development and Evaluation of a Nitric Oxide Reduction System

5.1. Introduction

The substrate specificity of enzymes has made them an attractive alternative for the production of valuable compounds such as pharmaceutical intermediates as well as for industrial applications [96, 97, 98, 99, 100, 101, 102]. Enzyme technologists have applied enzymes for the development of "green technology" and "white biotechnology" which focuses on cleaner chemical production processes, with fewer by-products and milder reaction conditions, built on the utilisation of renewable resources [97, 300]. Among protein engineering techniques, immobilisation, i.e. the attachment of enzymes to an insoluble carrier, has improved enzyme stability and reduced the cost of these biological catalysts by making them recoverable and thereby re-usable for application in bio-catalytic processes [101].

The co-immobilisation of enzymes allows for the potential development of multi-enzymatic bio-catalytic processes [108, 109, 110, 111]. It often entails an enzyme of bio-catalytic value in combination with an enzyme performing a co-enzymatic function, such as the recycling of a cofactor or coenzyme, for example oxidoreductases [112, 113]. With the co-immobilisation of a fungal nitric oxide reductase (NOR) and a bacterial glucose dehydrogenase (GDH), two chemical reactions would be catalysed in close proximity, allowing for near simultaneous kinetics for substrate conversion and cofactor regeneration. The proposed system is illustrated in Scheme 5.1.

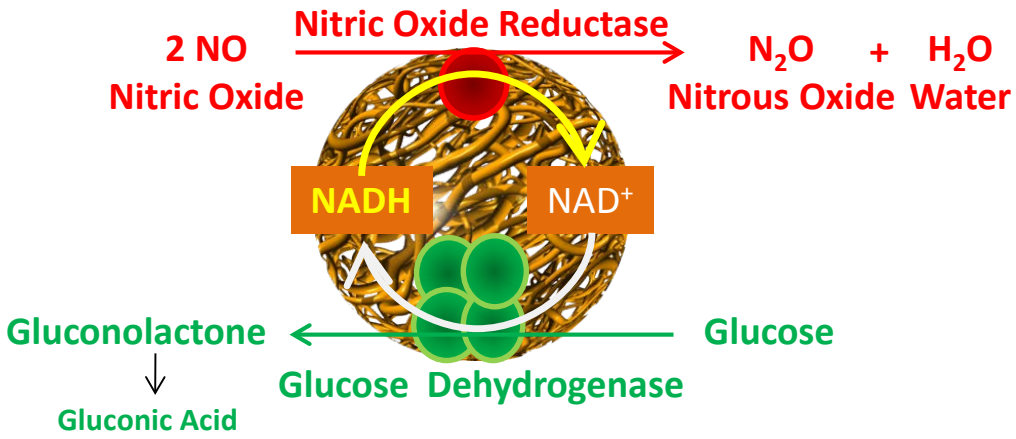

Scheme 5.1. Cofactor recycling by the NOR system with concomitant reduction of NO and oxidation of glucose. The simultaneous consumption of the NO and glucose is catalysed by NOR and GDH, respectively. Refer also to Scheme 1.5 in Chapter 1.

ReSyn™ microspheres constitute a relatively new immobilisation carrier platform with comparatively high binding capacity and high functional group densities (www.resynbio.com). These features, as well as the proposed structure of the polymer beads, make these ideally suited for the immobilisation of multimeric enzymes such as glucose dehydrogenase [114]. The interaction of the enzyme with the immobilisation carrier consists of several components, each of which may contribute to the maintenance of enzyme activity, and thereby contribute to the efficiency of the system under development. Scheme 5.2 illustrates the components contributing to enzyme-carrier interaction [128]. The polymer backbone is the anchor for the chemical interactions to which the functional groups and non-functinal groups are attaced, which affect the micro-environment [128]. The functional groups react with the amino acid residues on the enzyme, which can influence the orientation of the enzyme, access to the active site and conformational flexibility of the enzymes for catalytic processes [124, 128, 301, 302, 303, 304].

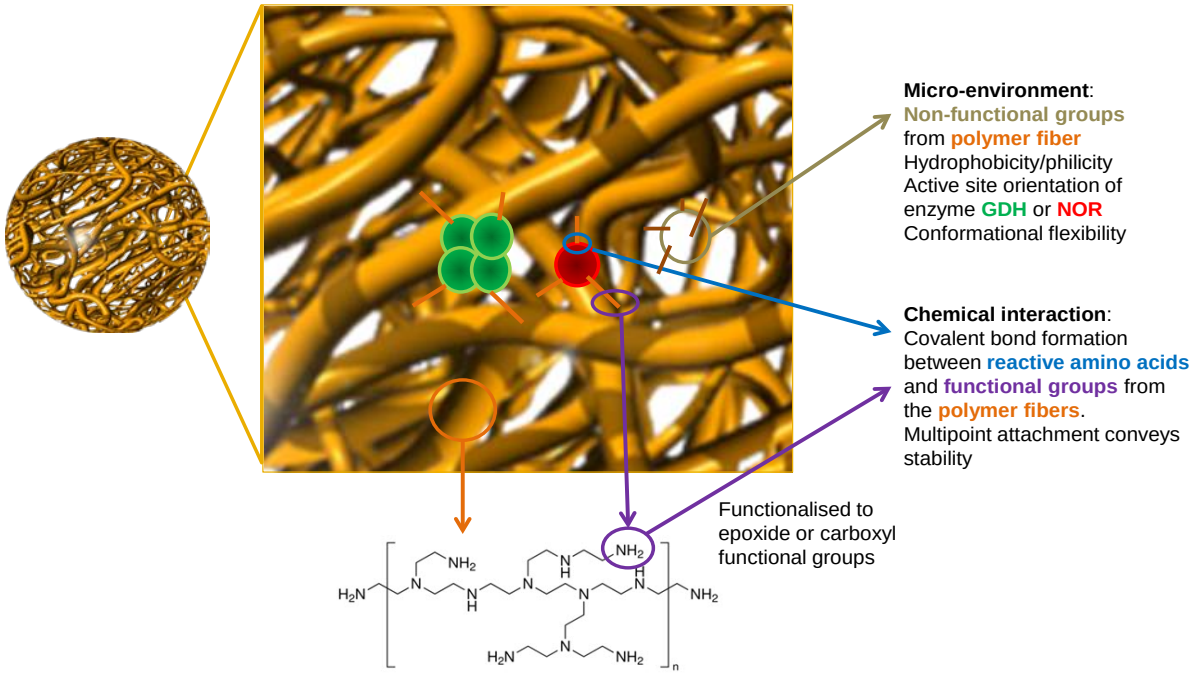

Scheme 5.2. Essential components for covalent immobilisation of enzymes. The polymer fibres of ReSyn™ microsphere (orange ring) are the backbone for the functional groups (purple ring) and non-functional groups (brown ring). The reactive amino acids such as lysine residues (blue ring) on the enzymes (green and red spheres) react with the functional groups to form a covalent bond between immobilisation carrier and the enzyme. Scheme adapted from Cao (2005) [128].

The functional groups, such as aldehydes, epoxides and carboxyl (which are routinely activated for coupling), interact with reactive amino acid residues on the surface of the protein to form covalent bonds. The multipoint attachment of the enzyme to the functional groups of the carrier, as well as the micro-environment of the carrier, have been shown to improve overall enzyme stability [114]. Multipoint attachment can promote rigidity and prevent dissociation of multimeric enzymes [305, 306, 307, 308].

From the methods available, including self-immobilisation, encapsulation, and chemical coupling onto solid supports, the latter was selected for the immobilisation of NOR and GDH. Chemical coupling has been reported to provide enhanced stability and high immobilisation yields [124, 125, 126, 127]. The vast array of possible immobilisation carriers flows from the multiple possible chemical functionalities and variety of materials from which they can be prepared.

An alternate to using a carrier, are carrier-free self-immobilisation techniques such as Spherezymes™ [133]. All possibilities considered, ReSyn™ microspheres were

used for this study. The technology provides a loosely linked polymer network that offers exceptionally high surface area for the binding of enzymes which translates to high binding capacities, and has demonstrated suitability for the efficient immobilisation of the multimeric enzyme GDH [114].

The immobilisation process entails incubation of the protein with the carrier under desirable conditions to allow chemical reactions to take place between the functional groups from the polymer support and the reactive amino acid residues from the enzyme [128]. There are numerous reports on the alteration of enzymes which have observed enhanced enzyme performance, including increased temperature stability [116, 127, 131, 132, 302, 309, 310, 311] and shifting of the enzyme pH profiles (attributed to the micro-environment) for immobilised enzymes [114, 120, 310, 312, 313], albeit with a reduction in the overall activity of the enzyme. Enzyme activity maintenance (also referred to as residual activity) is a key consideration for immobilisation of an enzyme onto a solid carrier [115]. Structural attributes, such as distribution of amino acid residues of the enzyme, are important considerations that can contribute to the activity maintenance after immobilisation. It is therefore important to consider this aspect of the enzyme's physical properties before immobilisation [116, 128]. The amino acid residues may further provide information on suitable carrier chemistry to achieve immobilisation of the enzyme [128].

NOR is a comparatively smaller enzyme (45 kDa; [152]) than the 120 kDa sized GDH, and has a different distribution of reactive amino acids such as lysine and serine (reactive with epoxide functional groups) on its surface (refer to Scheme 5.3). The active site of NOR is situated near the core of the enzyme (red for haem and yellow for NADH in Scheme 5.3 A; [213], whereas glucose oxidation takes place in a cavity termed the 'Rossmann' fold close to the subunit C of the tetrameric GDH (red for glucose and yellow for NAD^+ in Scheme 5.3 B; [314]. The tetrameric structure of GDH has been shown to disassociate under alkaline conditions [314, 315, 316, 317] indicating a high degree of instability. NOR is a member of the P450 family and has a haem in its active site (red in Scheme 5.3 A) which is prone to oxidation and inactivation [246]. Considering the potential effect of the immobilisation chemistry on the activity of the enzymes, two immobilisation chemistries were used in this study, namely epoxide (reactive with multiple residues including lysine and serine) and *N*-

hydroxysuccinimide (NHS) activated carboxyl chemistries, only reactive with lysine residues.

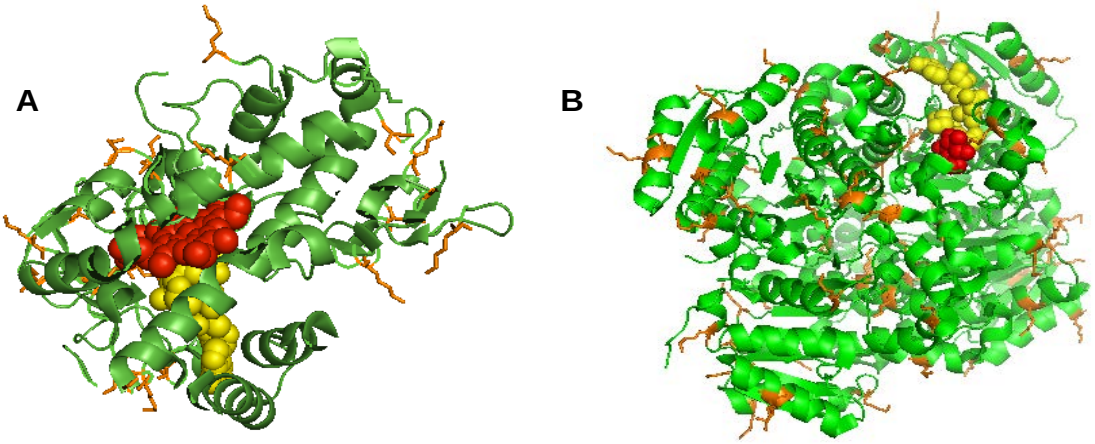

Scheme 5.3. The structural representations of NOR and GDH. The lysine residues are presented as orange sticks on NOR (A) and GDH (B). The position of the active site of NOR (haem) and GDH (glucose) are indicated by the red spheres and the cofactor position by the yellow spheres. The structures were generated from the PDB data base using PyMOL™ software (DeLano Scientific LLC. 2006).

The efficient and continuous reduction of nitric oxide with concomitant regeneration of NADH by glucose oxidation is the primary aim of the current study. Achieving this aim consists of the following objectives: the selection of a suitable carrier for the immobilisation of the enzymes, optimisation of the immobilisation and the characterisation of the NOR system. This was initiated by determining the protein binding capacity of the microspheres and the optimal immobilisation conditions for the enzymes. The immobilised enzymes were subsequently evaluated for enzyme activity maintenance at 37˚C in a neutrally buffered environment (tissue culture medium), and the activities synchronised for reduction of their substrates. Scheme 5.4 illustrates the key considerations for the development of the NOR system.

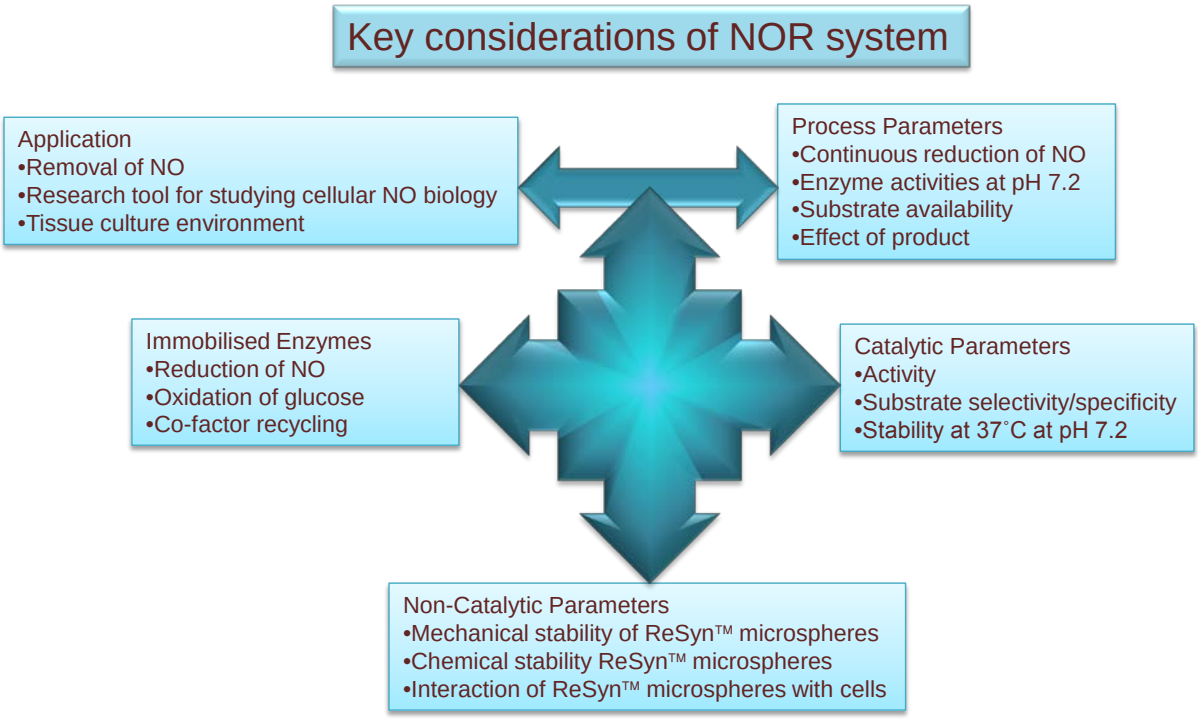

Scheme 5.4. The key considerations for the development of a bi-enzymatic NOR system. The application for the NOR system was the primary consideration for the system requirements, followed by the process parameters, enzyme functionality, catalytic parameters and non-catalytic parameters. Achieving all the aforementioned parameters contributes to the overall success of the NOR system and its potential application in cell biology. Adopted from Cao (2005) [128].

5.2. Materials

5.2.1. ReSyn™ microspheres and functionalisation

Epoxide and carboxylate functional microspheres were supplied by ReSyn Biosciences (Pty) Ltd (South Africa) as listed in Table 5.1. The reagents required for the functionalisation of the microspheres were purchased from Sigma-Aldrich, which included 1-ethyl-3-(3-dimethylaminopropyl)carbodiimide (EDC), *N*-hydroxysuccinimide (NHS), aminocaproic acid and aspartic acid. A Beckman Allegra X-22 R centrifuge and a Beckman Microfuge 18 centrifuge was used for recovery of the microspheres while a CaptAir® Bio PCR workstation from Erlab group (China) was used to ensure sterility of the microspheres during use.

Table 5.1. ReSyn™ microspheres supplied by ReSyn Biosciences (South Africa).

ReSyn™ microsphere Acronym	Functional group	Functional group density (µmoles.g^{-1})	concentration (mg.ml^{-1})	BSA binding capacity* (mg BSA.mg^{-1} microsphere)
E3500	Epoxide	3500	5.0	2.1
E1200	Epoxide	1200	6.6	1.8
E300	Epoxide	300	6.6	1.3
C2400	Carboxyl	2400	6.3	2.4^
C1200	Carboxyl	1200	4.9	2.8^

* BSA binding done in dd H_2O
^ BSA binding capacity determined for NHS EDC activated microspheres in 20 mM TEA pH 8.

5.2.2. Immobilisation of protein or enzymes onto ReSyn™ microspheres

Bovine serum albumin (BSA) for the determination of protein binding capacity was purchased from Roth Chemicals (USA). The immobilisation buffer, TEA, was purchased from Sigma-Aldrich. An ELMI Intelli-Mixer (USA) was used for the end-over-end mixing. Low protein binding Eppendorf tubes were purchased from Sigma-Aldrich (Germany).

5.2.3. Enzyme assays and protein quantification

The reagents for the nitric oxide reductase activity assay and for protein quantification were the same as those described in Chapter 3, Section 3.3.4. GDH 102 (*Bacillus megaterium*) was purchased from Codexis (USA). Glucose was purchased from Sigma-Aldrich (Germany). For the desalting of GDH a PD-10 gel filtration column was used (GE Healthcare, Sweden). A PowerWave HT Microplate reader (BioTek, USA) was used for spectrophotometric measurements. Acrodisk syringe filters (0.8/0.2 µm pore size) were purchased from Pall Cooperation (USA). The cofactors, NAD and NADH, were purchased from Sigma-Aldrich and NOC-5 (3-(Aminopropyl)-1-(hydroxy-3-isopropyl-2-oxo-1-triazine) as well as the glucose assay kit were purchased from Calbiochem (Merck Millipore, Germany). The DAF-FM (4-amino-5-methylamino-2',7'-difluorescein) was purchased from Molecular Probes (Invitrogen). The relative fluorescence units (RFU) from excitation and emission at 485/530 nm were measured using an FL*x*800 fluorescence micro-titre plate reader (BioTek, USA).

5.3. Methods

5.3.1. Functionalisation of Microspheres

The epoxide functionalised microspheres were supplied by ReSyn Biosciences (refer to A in Scheme 5.5), whereas the carboxyl functionalised microspheres were functionalised for coupling immediately prior to immobilisation. This was achieved by using 1-ethyl-3-(3-dimethylaminopropyl)carbodiimide (EDC) in the presence of *N*-hydroxysuccinimide (NHS) resulting in the formation of an intermediate NHS ester derivative. The amine group of proteins displace the NHS ester to form an amide bond with the ReSyn™ microspheres as shown in Scheme 5.5 B. The activation of the microspheres via the carbodiimide-mediated process, was performed using filter-sterilised activation solution containing 20 mM EDC, 50 mM NHS in 100 mM MES (pH 6) and 500 mM NaCl for 15 minutes at room temperature with gentle end-over-end mixing (10 rpm on ELMI Intelli-Mixer).

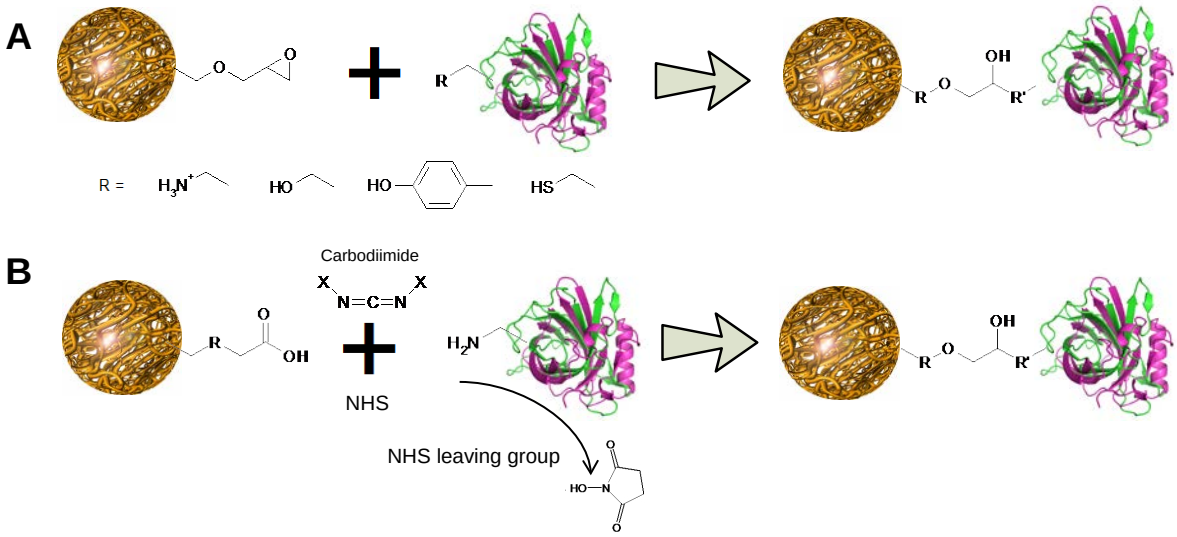

Scheme 5.5. Reactivity and functionalisation of ReSyn™ microspheres. The polymer backbone of ReSyn™ microspheres containing epoxide functional groups (A), where R on the protein are the various reactive amino acid residues capable of coupling to the epoxide group to form covalent bonds. In (B), the carboxyl functional group ReSyn™ microspheres are treated with carbodiimide and NHS to generate a reactive intermediate to which the amino acid residues bind covalently to form a stable amide bond by displacing the NHS intermediate [318]. Chemical drawings were supplied by ReSyn Biosciences (www.resynbio.com).

5.3.2. Immobilisation of BSA onto ReSyn™ microspheres

BSA was chosen as a model protein to test the initial capacity for immobilisation of proteins on to the microspheres. To estimate the binding capacity of the various ReSyn™ microspheres, a 10 $mg.ml^{-1}$ BSA solution was prepared in 20 mM triethanolamine buffer (TEA, pH 8.0) and filter-sterilized using a 0.2 µm Acrodisk syringe filter for sterile storage. The microspheres (0.5 ml suspensions) were washed three times with 1 ml autoclaved dd H_2O or filter sterilized immobilisation buffer during the evaluation of immobilisation buffers. To determine the capacity of the microspheres, 1 ml of the BSA solution was added to the 0.5 ml ReSyn™ microspheres (refer to Table 5.1 for ReSyn™ microsphere concentrations). The carboxyl microspheres were treated with the activation solution as described in Section 5.3.1 and washed three times to remove excess activation solution. The BSA solution was subsequently added to the functionalised ReSyn™ microsphere suspension. The binding was performed by end–over-end mixing of the protein solution and microspheres at 25 rpm and 4˚C for 18 hours.

5.3.3. Determination of protein binding capacity

The binding capacity was calculated as the difference between the starting protein concentration and the residual protein left in solution. The unbound BSA in the supernatant (after recovery of the microspheres by centrifugation at 3000 ×*g* for 10 minutes) was pooled with 3× 1 ml 4 M NaCl washes (to remove non-covalently bound BSA). This was compared to a suitably diluted BSA solution. The absorbance of 200 µl of a ten-fold dilution of the unbound fractions were compared to an equivalent dilution of the starting material and quantified in a 96 well UV micro-titre plate with optical density measurement at 280 nm. This methodology was applied for the determination of BSA binding capacity of the epoxide functionalised ReSyn™ microspheres. The BSA binding capacity for the carboxyl functionalised ReSyn™ microspheres was determined with the Quick Start™ 1× Bradford reagent (Bio-Rad, USA) since the NHS ester displaced by immobilisation (refer to Scheme 5.5) interferes with optical density measurements in the UV spectrum. For this method of protein quantification, a fifty fold dilution of the standard protein and unbound fractions was required due to the sensitivity of this assay. A total volume of 35 µl of

diluted sample was mixed with 35 µl of the Quick Start™ 1× Bradford reagent in a 384 well plate. After a 5 minute reaction, the absorbance was measured at 595 nm. The protein concentration was determined as described above. For determination of the specific protein binding capacity, the protein bound was divided by the weight of the microspheres. For dry weight determination, 1 ml of microsphere suspension was lyophilised for 18 hours and weighed. The binding capacity was calculated using the equations below:

BSA binding capacity= total starting protein (10 mg) – total unbound protein (mg)
Specific binding= binding capacity ÷ particle dry weight (for 0.5 ml suspension)

5.3.4. Immobilisation of NOR and GDH

For the enzyme immobilisation studies, a reduced quantity of ReSyn™ microspheres was used (300 µl with an average dry weight of 1.4 mg). It was washed three times with the respective immobilisation buffers and re-suspended to its original volume. The enzyme, either GDH or NOR, was added to the microspheres and mixed for 18 hours at 4˚C on an ELMI Intelli-Mixer (25 rpm) in Eppendorf™ low protein binding tubes.

The initial protein concentration of each enzyme was determined with the Quick Start™ 1× Bradford reagent and extrapolated from a standard curve of bovine gamma globulin (BGG). This value was used for the determination of the unbound protein by difference as described in Section 5.3.3.

The enzyme activity maintenance for NOR and GDH was calculated as a percentage of the immobilised enzyme activity in relation to the activity of the free enzyme in solution. For the optimisation of the immobilisation procedure, the enzyme activity maintenance was determined after 18 hours in 20 mM TEA buffer at pH 6, 7 and 8 at 4˚C with agitation. Thereafter, the enzyme activity maintenance upon immobilisation onto the various carriers was established. For the selection of the most suitable carrier for the NOR system's application in an *in vitro* cell model, the temperature stability at 37˚C in PBS was established as well as the pH profile was determined in Briton-Robinson buffer.

5.3.5. Co-immobilisation of NOR and GDH

For co-immobilisation of the enzymes onto the selected functionalised ReSyn™ microspheres, the initial enzyme activity was determined for both enzymes and used to determine the ratio of enzymes (NOR: GDH) required for synchronised cofactor utilisation after immobilisation onto the microspheres, i.e. so that the forward reaction (NADH oxidation by NOR) proceeds at a similar reaction rate as the reverse reaction (NAD reduction by GDH). This synchronisation of cofactor utilisation rate involved the determination of the enzyme activity in solution, the enzyme activity maintenance after immobilisation, also considering the enzyme activity maintenance at pH 7.2 (determined as described in Section 5.3.4). GDH presented an approximate 100 fold higher comparative specific enzyme activity and thus only a 1/100th of GDH was added to the enzyme mixture (i.e. NOR: GDH was 1: 1/100) which was added to 300 µl ReSyn™ microspheres. The enzymes were immobilised by allowing them to interact with ReSyn™ microspheres for 18 hours with gentle agitation at 4˚C. The excess enzyme was removed by washing the particles three times with immobilisation buffer and the particles were re-suspended in sterile dd H_2O.

5.3.6. Quantification of cofactor redox reaction

The oxidation and reduction of the cofactor NADH by NOR and GDH were assayed by measuring the decrease or increase (respectively) of absorbance at 340 nm. The oxidation reaction of NADH measured the NOR activity, whereas the GDH activity was measured by the increase of absorbance. The NOR activity assay was performed as described previously (Chapter 2, Section *2.6.1.1*). The regeneration of NADH from NAD was monitored in a reaction mixture containing 50 mM glucose, 1 mM NAD in 200 mM TEA pH 8. For evaluation of the NOR system (co-immobilised enzymes), the pH of the reaction buffer was adjusted to neutral pH, due to the proposed application and evaluation in tissue culture.

5.3.7. Cofactor recycling assay

To demonstrate that the system was indeed recycling the cofactor, the two half reactions were assayed independently. A 50 fold dilution of the NOR system from

the original stock solution (0.56 mg.ml^{-1}) was prepared in 200 mM TEA buffer pH 7 containing 0.5 mM NADH. To commence the enzyme reaction, NOC-5 was added to a final concentration of 2 mM. The reaction mixture (70 µl) was transferred into a 384 well micro-titre plate. The reaction was monitored at 340 nm for 30 minutes at 37˚C for the duration of the reaction. Thereafter, the removed aliquot was returned to the reaction tube and 8.3 mM glucose (final concentration) was added to the reaction tube. The suspension was subsequently mixed by gentle agitation and 70 µl was pipetted into a 384 well micro-titre plate and the reaction monitored for a further 30 minutes at 37˚C. This was repeated for at least three cycles. The assays were run in triplicate for three separate preparations of the co-immobilised enzyme system. Scheme 5.6 outlines the experimental design for the cofactor recycling.

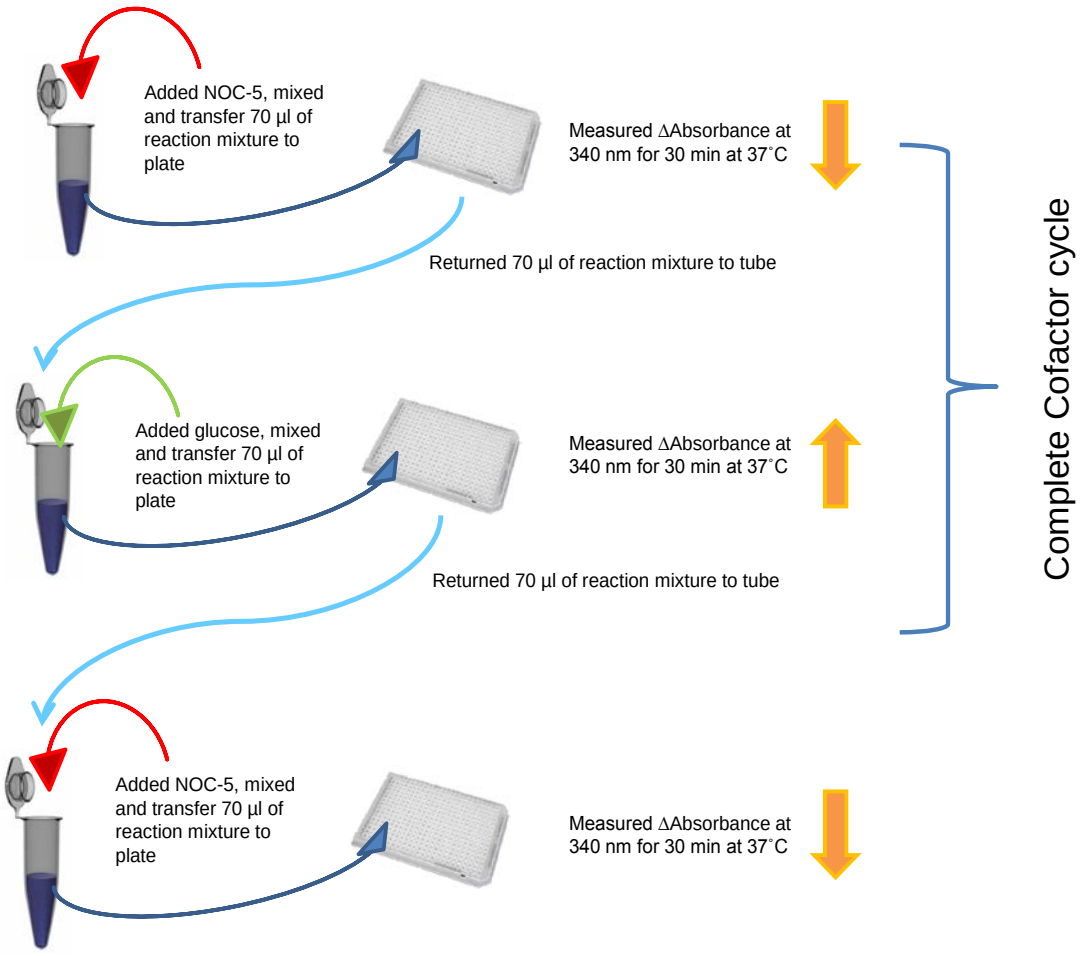

Scheme 5.6. Experimental procedure for the two half-reactions from the NOR system. The reaction mixture contained the NOR system and 0.5 mM NADH in 200 mM TEA pH 7. With the addition of NOC-5 (red arrow), the NOR system would reduce NADH to NAD$^+$, which would be recycled to NADH by GDH with the additions of glucose (green arrow). The half-reactions were measured in a 384 well micro-titre plate at 37˚C. The reaction mixture in the plate was returned to the reaction tube. This experimental procedure was designed to demonstrate the cofactor recycling of NADH.

5.3.8. Quantification of substrate consumption by NOR system

For the purposes of testing the efficiency of the system in tissue culture, the system was evaluated in RPMI supplemented with 1 mM NADH. To demonstrate the ability to reduce NO in RPMI solution, the NOC-5 was added to the reaction mixture to a final concentration of 2 mM. The reaction was allowed to proceed for 30 minutes at 37˚C. After the 30 minutes reaction time, 90 µl (triplicate samples) was transferred to a black 96 well micro-titre plate to which 1 µM DAF-FM (4-amino-5-methylamino-2',7'-difluorescein) final concentration was added. The residual NO in solution from NOC-5 was quantified from the excitation of the fluorescent dye (DAF-FM) which developed after 30 minutes incubation at 37˚C. The fluorescence determined in the sample containing NOR system, NOC-5 and NADH in RPMI (NORsys) was compared to a sample containing NOC-5, NADH in RPMI (N+N). The background control (negative control) was the sample containing only RPMI and NADH (RPMI). The sample N+N was considered as the positive control for NO reduction and thus 100% of residual NO in solution. The sample RPMI was the negative control for NO in solution.

The quantification of glucose was determined at the end of this experiment. Here, a 100 fold dilution was prepared for each sample and 25 µl thereof was transferred to a 384 well micro-titre plate to which 25 µl of the glucose assay reagent from the glucose detection kit was added. The reaction was incubated for 30 minutes at room temperature. The glucose concentration was extrapolated from a standard curve prepared for this assay. RPMI and N+N were used as negative and positive controls for gluclose (100% glucose) in which the glucose concentration was anticipated to remain unchanged. Glucose reduction was only anticipated in the sample containing the NOR system (NORsys). Scheme 5.7 is a representation of these experiment.

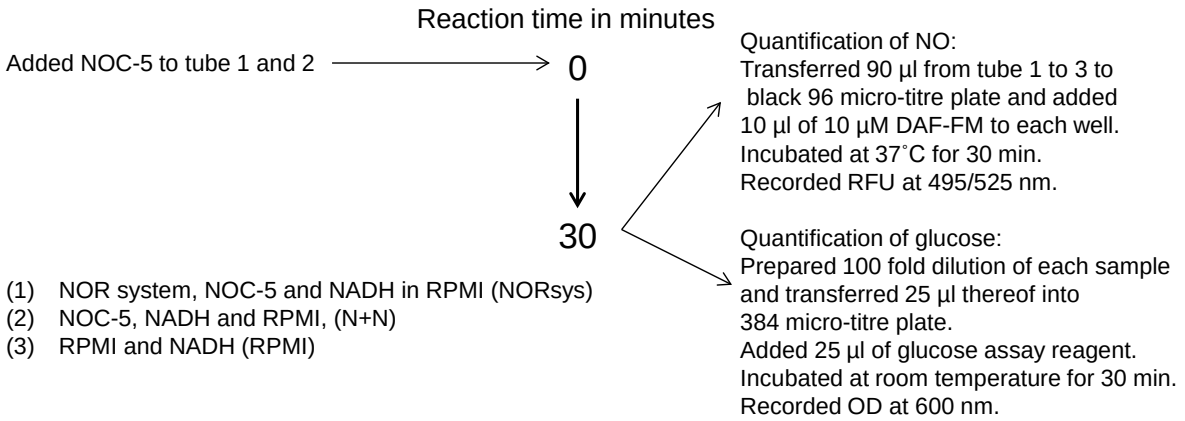

Scheme 5.7. Experimental procedure for the quantification of the simultaneous substrate consumption by the NOR system. The reaction was performed in RPMI supplemented with 1 mM NADH. To the first reaction tube the NOR system and NOC-5 was added (1), to the second reaction tube only NOC-5 was added (2) and the third tube only contained the reaction mixture (3). The reaction was initiated by the addition of NOC-5 to tube 1 and 2. The absorbance at 340 nm, the fluorescence and the glucose concentration were determined after 30 minutes incubation at 37˚C.

5.4. Results

5.4.1. BSA binding capacity

The protein binding capacity of the five different variants of ReSyn™ microspheres (custom preparations provided by ReSyn Biosciences; refer to Table 5.1) was determined using bovine serum albumin (BSA) as a standard. The objective was to identify the one microsphere that would fulfil the requirements as outlined in Scheme 5.4, since these factors contribute to the outcome of enzyme immobilisation (refer to Scheme 5.2). The first step in the selection of the optimal carrier was the consideration of the protein binding capacity of the various preparations. Two different functional group chemistries (epoxide and carboxyl) were evaluated for the immobilisation, further varying in functional group density (300, 1200, 2400 and 3500 µmoles.g^{-1}). The two different functional chemistries resulted in different protein interactions (refer Scheme 5.5), while differences in functional group density potentially allow for increased coupling efficiency and variations in the multipoint attachment to the proteins.

Figure 5.1 is a microscopic image of the microspheres provided by ReSyn™ Biosciences, photographed on a Neubauer Haemocytometer for estimation of microsphere size.

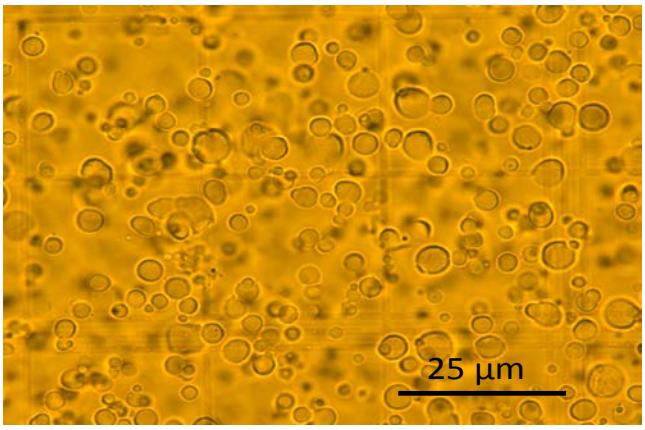

Figure 5.1. Light micrograph of ReSyn™ microspheres. ReSyn™ microspheres size estimation of 3 to 10 µm with Neubauer Haemocytometer with 50× magnification of E1200 ReSyn™ microspheres. An Olympus BX41TF light microscope (Japan) was used. The micrograph was captured with a CC12 camera.

The BSA binding capacity of the microspheres presented in Table 5.1 were determined in water as an immobilisation solution, which is not considered ideal for immobilisation of enzymes. Triethanolamine (TEA) buffering agent was therefore used to immobilise BSA onto the microspheres to determine its effect on the BSA binding capacity of the various ReSyn™ microspheres. Other buffering agents such as MES and HEPES were also investigated, however these and other tertiary amine-based buffer components (Good's buffers) have been shown to generate radicals and it has been suggested that these buffers are not suitable for redox processes in biochemistry [319, 320].

TEA as an immobilisation compatible buffering reagent did not alter the BSA binding capacity (Table 5.2) when compared to the BSA binding capacity illustrated in Table 5.1. The duration and temperature of BSA binding to the carrier was done for 24 hours at 4˚C, respectively, as a routine protocol for all immobilisation procedures. Although, the reaction between the activated carboxyl functional groups and amine residues of the proteins can occur more rapidly, the time was set as a constant to ensure sufficient reaction time [318].

Table 5.2. ReSyn™ microspheres BSA binding capacity in 20 mM TEA pH 8.

ReSyn™ microsphere Acronym	Functional group	Functional group density (µmoles.g^{-1})	concentration (mg.ml^{-1})	BSA binding capacity (mg BSA.mg^{-1} microsphere)
E3500	Epoxide	3500	5.0	2.6
E1200	Epoxide	1200	6.6	1.7
E300	Epoxide	300	6.6	2.4
C2400	Carboxyl	2400	6.3	2.4
C1200	Carboxyl	1200	4.9	2.8

Functional group density do not necessarily relate to binding capacity. However, an increase in functional group density may result in an increased number of covalent protein attachments that can improve protein stability [116, 128].

5.4.2. Selection of conditions for enzyme immobilisation

The second step considered in the determination of the optimal carrier for the development of the co-immobilised enzyme system was to maximise the enzyme activity maintenance for the two different chemistries (epoxide and carboxyl) and functional group densities (3500, 1200 and 300 µmoles.g^{-1}). The immobilisation conditions evaluated are shown in Figure 5.2, for NOR (red bar) and for GDH (blue bar). The enzyme stability at three pH-values was determined over a period of 24 hours at 4˚C. Enzyme activity appeared to be suitably maintained for all three pH-values evaluated, however, 20 mM TEA buffer at pH 8 was chosen for all the subsequent immobilisation reactions due to the more favourable interaction of the reactive amino acid resides (e.g. lysine) with the functional groups of the carrier at this pH [124].

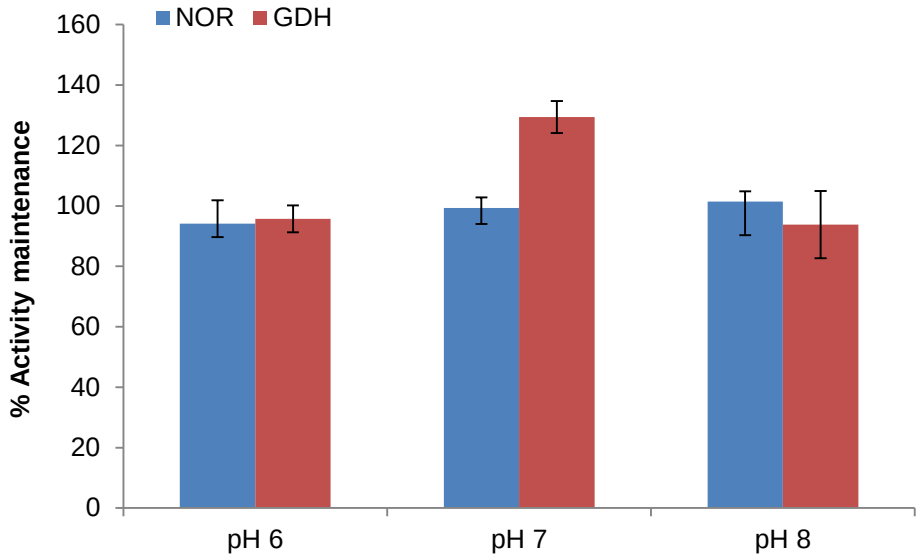

Figure 5.2. Enzyme stability in 20 mM TEA buffer with a pH of 6, 7 and 8. The enzymes were incubated at 4˚C for 24 hours with agitation (15 rpm on Intelli Mixer). The % of activity maintenance of NOR is presented by the red bars and the % activity maintenance for GDH is shown by the blue bars. The enzyme activity was determined by monitoring the increase or decrease in absorbance at 340 nm in a 384 well micro-titre plate at 37˚C for 5 minutes. Error bars represent the standard deviation from triplicate assays.

5.4.3. Activity maintenance of immobilised enzymes

For the determination of enzyme activity maintenance on various ReSyn™ microspheres, NOR and GDH, were immobilised onto the carrier with the immobilisation conditions described in Section 5.4.2. The enzymes were immobilised to each carrier for the selection of the most suitable carrier.

Immobilised NOR activity maximally maintained on carboxyl functionalised carriers at 44 and 113% calculated activity yield for carrier with 2400 and 1200 µmoles.g^{-1} functional group densities (C2400 and C1200, respectively) as shown in Table 5.3. A 15 fold higher specific enzyme activity on the C1200 carrier was observed when compared to E1200 carrier and confirmed in three different immobilisations. To our knowledge, this is the first report of NOR immobilisation onto a microsphere carrier.

Table 5.3. NOR activity maintenance on ReSyn™ microspheres.

NOR	Total mg NOR immobilised onto carrier	Enzyme activity (µmoles NADH.min^{-1})	% Activity maintenance	Specific activity*/mg carrier
E3500	0.136	0.024	5.1	0.361
E1200	0.123	0.024	5.0	0.443
E300	0.144	0.013	2.7	0.174
C2400	0.138	0.201	43.9	2.188
C1200	0.138	0.528	112.9	6.978
Free Enzyme	0.273	0.468	100.0	

* Specific activity in µmoles NADH.min^{-1}, which was calculate from enzyme activity divided by total mg of GDH immobilised onto carrier

GDH is a homo-tetramer consisting of four glucose oxidising units of 30 kDa each, and is considered notoriously difficult to immobilise [311, 314, 321]. The ReSyn™ microspheres were selected for this study, since they had demonstrated suitability for the efficient immobilisation of this enzyme [114]. Table 5.4 shows that the functionalised carboxyl microspheres exhibited a twofold higher specific enzyme activity per mg of carrier than epoxide functional microspheres for the same functional group densities (1200 µmoles.g^{-1}; refer to Table 5.2). Similar to NOR activity maintenance, GDH activity maintenance was higher on the carboxyl functionalised carriers. A summary of the results for GDH are presented in Table 5.4.

Table 5.4. GDH activity maintenance on ReSyn™ microspheres.

GDH	Total mg GDH immobilised onto carrier	Enzyme activity (µmoles NAD.min^{-1})	% Activity maintenance	Specific activity*/mg carrier
E3500	0.147	0.014	0.2	0.198
E1200	0.139	0.043	0.6	0.713
E300	0.160	0.013	0.2	0.162
C2400	0.185	0.176	2.3	1.424
C1200	0.151	0.315	4.2	3.804
Free Enzyme	0.302	7.581	100.0	

* Specific activity in µmoles NAD.min^{-1}, which was calculate from enzyme activity divided by total mg of GDH immobilised onto carrier

The carboxyl carrier with a 1200 µmoles.g^{-1} (refer to Table 5.2) functional group density presented the highest enzyme activity maintenance according to the cofactor redox rates established in 200 mM TEA buffer. These results present an indication which carrier would be suitable for the development of the NOR system. But further

analysis was required to establish which carrier would be most suitable for the application of the NOR system, i.e. its functionality in an *in vitro* cell model. Therefore, the enzyme activity of the immobilised enzymes on the five carriers was investigated at 37˚C and at various Britton-Robinson buffer pH-values.

5.4.4. Temperature stability of NOR and GDH on ReSyn™ microspheres

For selecting the most suitable carrier for co-immobilisation of NOR and GDH, due consideration must be given to the intended application of the system. For application in physiological conditions, enzyme stability at 37˚C in phosphate buffered saline (PBS) and activity at pH 7.2 were minimum requirements for evaluation of the NOR system.

For the determination of the enzyme stability at 37˚C, the enzyme activity of immobilised GDH and NOR was measured over 5 days. The NOR activity was reduced to ~30% within 60 hours of incubation, but appeared to stabilise after this period on the carboxyl functional microspheres (Fig. 5.3 A). Furthermore, NO reduction by NOR on carrier C1200 was detectable after three months storage at 4˚C in 20 mM TEA pH 8. GDH activity was maintained at 37˚C in PBS over the five days at >80% for the C1200 carrier (Fig. 5.3 B). The observed GDH stability over several months correlates to findings from Pauly & Pfleiderer (1977) [316]. These findings highlight the suitablility of the NOR system for its application *in vitro* studies with the potential to invesitage the continuous reduction of NO for up to 5 days. Furthermore, it also presents the suitablility of the NOR system as a research reagent with a self-life of three months.

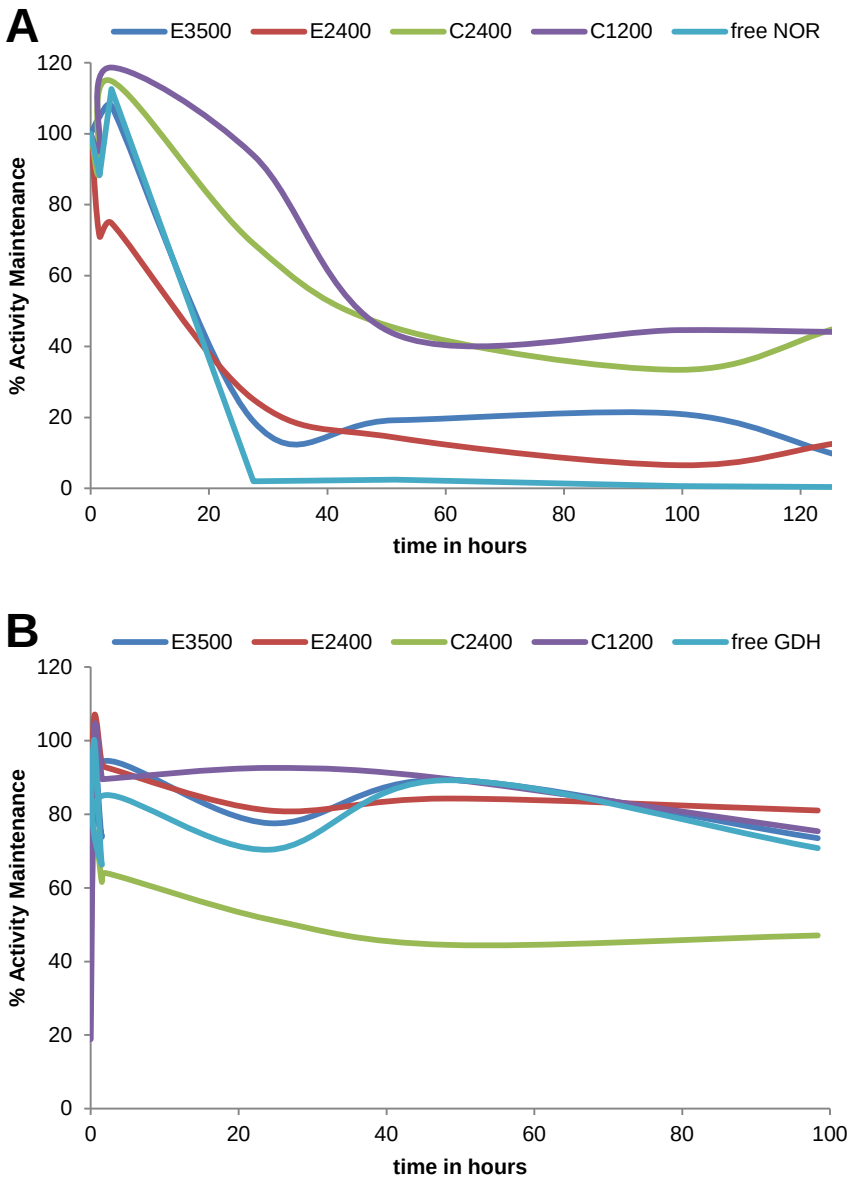

Figure 5.3. Enzyme activity maintenance at 37˚C in PBS pH 7.2. Immobilised enzymes were incubated at 37˚C with 15 rpm agitation over 5 days. Enzyme activity was determined by enzyme activity assay (Section 5.3.6). NOR activity is presented in (A) and GDH activity in (B). Enzyme activity is presented as percentage residual activity where the activity at time point zero was considered 100%.

5.4.5. pH profile of immobilised NOR and GDH

The final step in the carrier selection process was the determination of the % activity maintenance of both enzymes at physiological pH of 7.2. This was essential for the synchronisation of enzyme activity and the development of the NOR system, which entails the co-immobilisation of both NOR and GDH. Therefore, enzyme activity profiles were established for free NOR and GDH (enzyme in solution), as well as the

immobilised enzymes. Britton-Robinson buffer, adjusted to various pH values, was used as a replacement to the standard reaction buffers and the assays were performed at 37˚C. The optimal enzyme activity for NOR was around pH 6 for the free and immobilised forms of the enzyme (Fig. 5.4 A). The pH profile of GDH activity did not show much deviation from the enzyme in solution; with optimal activity between pH 7 to 8 (refer to Fig. 5.4 B). The enzyme activity profiles for both enzymes are presented in Figure 5.4 C. The dotted line represents the physiological pH of 7.2, demonstrating significant activity of both enzymes at this pH, albeit that NOR activity was reduced to ~35% whereas GDH activity was nearly optimal.

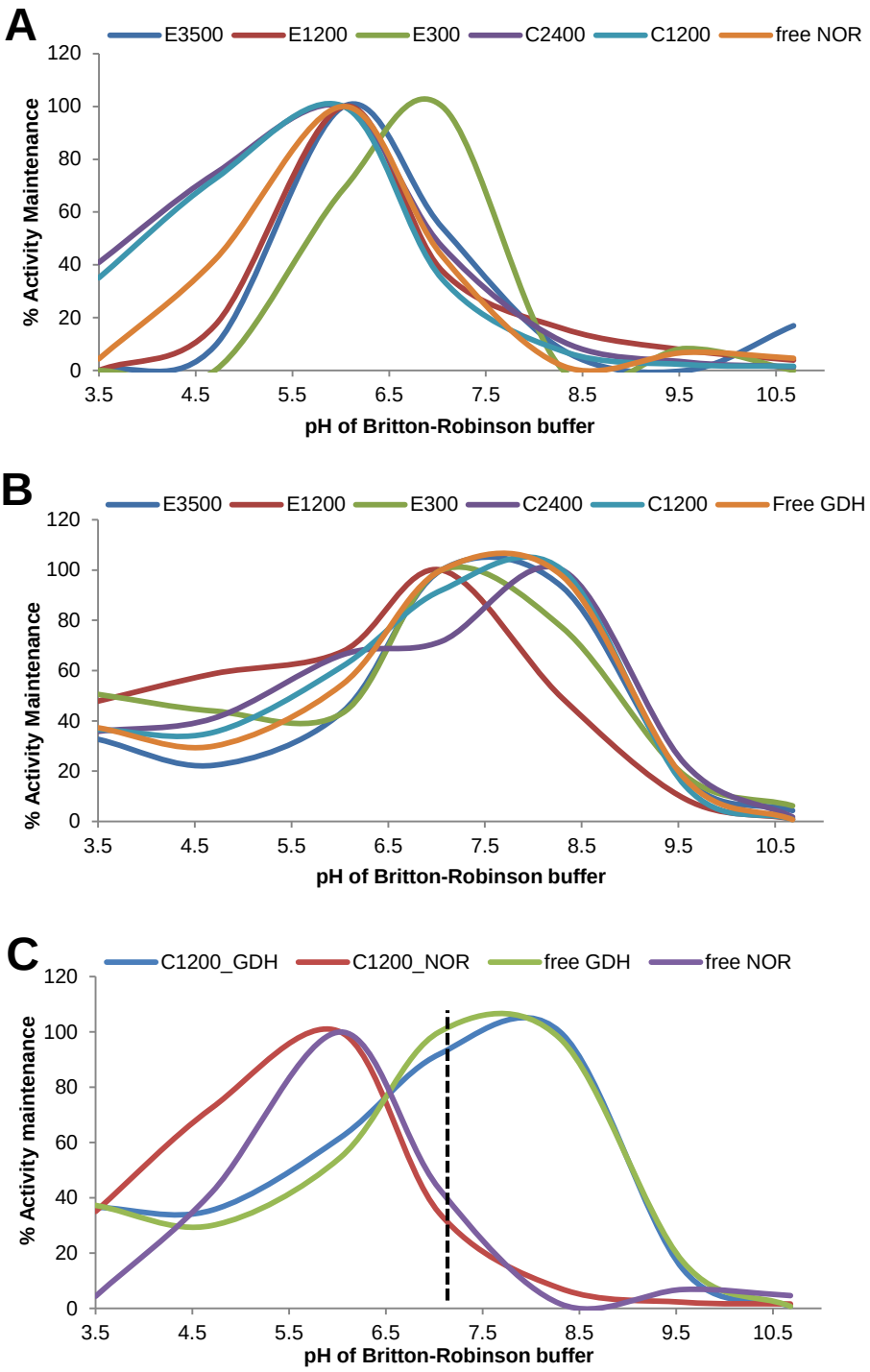

Figure 5.4. The pH profiles of immobilised and free NOR and GDH. The pH profile of NOR is shown and in (A) and GDH in (B). The activity at the physiological pH (pH 7.2) of both enzymes is indicated by the dotted line in (C). The enzymes were immobilised in 20 mM TEA pH 8, washed before the enzyme activity was measured in Britton-Robinson buffer at 37˚C.

In summary, the carboxyl functional group carrier, C1200, was found to be the most suitable immobilisation carrier for the development of the NOR system. This functional group and its density allowed the retention of the highest enzyme activity

of NOR and GDH upon immobilisation on ReSyn™ carrier and that could be conserved at 37˚C in PBS over at least 5 days. There was ample overlap of the pH stability profiles of the enzymes' activity at physiological pH, allowing 35% and 92% activity for NOR and GDH, respectively.

5.4.6. Co-immobilisation of enzymes

For the construction of the NOR system, both enzymes were co-immobilised onto the carrier identified in Section 5.4.5. The immobilisation rate of the enzymes was not determined and thus the carrier was not loaded to capacity to ensure sufficient binding sites for both enzymes. The activity maintenance and cofactor oxidation or reduction rate were different for each enzyme and thus it was necessary to synchronise the cofactor oxidation and reduction rates at pH 7.2. GDH had a much higher cofactor reduction rate (379.1 µmoles $NAD.min^{-1}$) than the oxidation rate of NADH by NOR (0.469 µmoles $NADH.min^{-1}$). However, NOR activity was conserved quantitatively (a calculated 113%) after immobilisation onto C1200 (Table 5.3), whereas GDH activity after immobilisation was reduced to 4.2% (Table 5.4). Enzyme activity was affected by the pH of thereaction buffer and at the physiological pH of 7.2 (refer to Section 5.4.5). GDH activity was conserved at 92% at pH 7.2. In contrast to NOR activity which was reduced to 35% at this pH when compared to NOR's optimal enzyme activity is at pH 6 From the above information, comparative activities for NOR activity was 0.147 µmoles $NADH.min^{-1}$ and GDH activity was 11.4 µmoles $NAD.min^{-1}$ (Table 5.5). The enzyme concentrations were therefore adjusted to obtain an equal cofactor rate for both half-reactions (Table 5.5). The average cofactor redox rate from three individual preparations was shown to be 0.077/0.082 µmoles $NAD/H.min^{-1}$ (Table 5.5). This confirms the suitability of the calculation methodology to synchronise the two half-reactions.

Table 5.5. Synchronisation of redox rates for the co-immobilisation of NOR and GDH.

Enzyme	Initial activity* (enzyme in solution)	Residual activity* (immobilised enzyme)	% Activity maintenance	% Activity maintenance at pH 7.2	Theoretical total activity*	Measured enzyme activity[#]
NOR	0.468	0.528	113	35	0.182	0.082 (±0.03)
GDH	379.1	15.75	4.2	92	14.49	0.077 (±0.01)

* Enzyme activity measured in µmoles NAD/H.min^{-1}.
[#] Average of 3 enzyme immobilisation events determined in 200 mM TEA buffer pH 7.2
Theoretical total activity was calculated as follows:
((% Activity maintenance at pH 7.2/ 100) × % Activity maintenance)/100 × Initial activity
GDH Initial activity and Residual activity from Table 5.4 was multiplied by its dilution factor of 50.

5.4.7. Demonstration of cofactor recycling

To demonstrate beyond doubt that the cofactor was indeed being recycled, we devised an experimental procedure outlined in Section 5.4.8 (Scheme 5.6). In this experiment, the cofactor recycling was monitored for 30 minutes, and the substrates required for each half-reaction were alternated. The experiment commenced with the addition of NOC-5 and the NO reduction with NADH oxidation was monitored for 30 minutes at 37˚C. Thereafter, glucose was added to the reaction and the increase of absorbance was monitored for 30 minutes. In this reaction the NAD was recycled back to NADH. The oxidation of NADH to NAD and back to NADH was monitored for six cycles; the free enzymes were monitored as a positive control (Fig. 5.5). The negative control indicated that the cofactor was oxidised in the presence of NOC-5 during the experimental period. The total NADH turnover appeared to reduce with each cycle. This is most likely due to the dilution of the system by addition of the substrates in accordance with the experimental design.

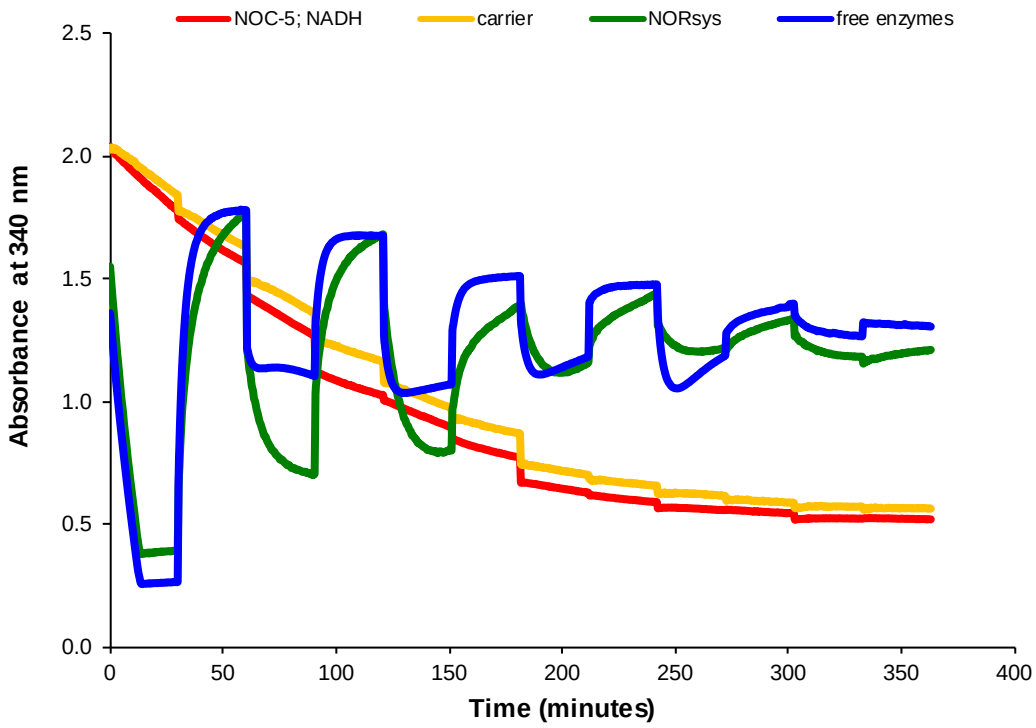

Reagent	NOC-5 NADH	carrier	NORsys	Free enzymes
NADH	✓	✓	✓	✓
NOC-5	✓	✓	✓	✓
carrier		✓		
NORsys			✓	
Free enzymes				✓

Figure 5.5. Cofactor recycling by NOR system. The reduction and oxidation of the cofactor, NAD/H, by the NOR system was compared to the NADH recycling of free NOR and GDH (in solution). The bi-enzymatic reaction NADH absorbance was monitored at 340 nm for 30 minutes (37˚C). For the NOR system, NOR and GDH were co-immobilised onto C1200 microspheres. No NADH degradation (NADH in reaction buffer) was observed during incubation duration (data not shown).

5.4.8. Consumption of substrates by NOR system

The primary requirement of a functional NO reducing system is the ability for the system to efficiently recycle the cofactor for continuous reduction of solution phase NO. To demonstrate the substrate consumption by the NOR system, the disappearance of both substrates, NO and glucose, were monitored and quantified. In the NADH oxidation reaction, NOR reduces NO from NOC-5 which was quantified by relative fluorescence units (RFU) generated by the interaction of residual NO in

solution with DAF-FM. Similarly, for the NAD^+ reduction reaction by GDH and the oxidation of glucose, residual glucose was quantified using a glucose assay kit.

The relative fluorescence units (RFU) relating to the comparative NO concentration in the samples indicated little to no fluorescence in the sample containing the system (NORsys). The negative control containing only RPMI and the NADH resulted in a similar RFU. The positive assay control containing NOC-5 and NADH in RPMI illustrated a high fluorescence. This successfully demonstrates the system is capable of reducing NO in culture medium (Fig. 5.6 A). Concomitant determination of the residual glucose concentration, (in combination with the assays demonstrating the recycling of NADH) indicates that the reduction half-reaction was operational. In comparison to the negative control (RPMI), the sample containing NOC-5 and the NOR sytem presented a quantifiable glucose reduction (Fig. 5.6 B). There was a lower glucose concentration in the sample containing NOC-5 and NADH (N+N) when compared to the sample containing only RPMI. This reduced glucose concentration could have been attributed to the oxidation NADH to NAD^+ by NOC-5 (Fig. 5.5). This cofactor oxidation by NOC-5 became apparent in the glucose assay and resulted in an apparent glucose reduction.

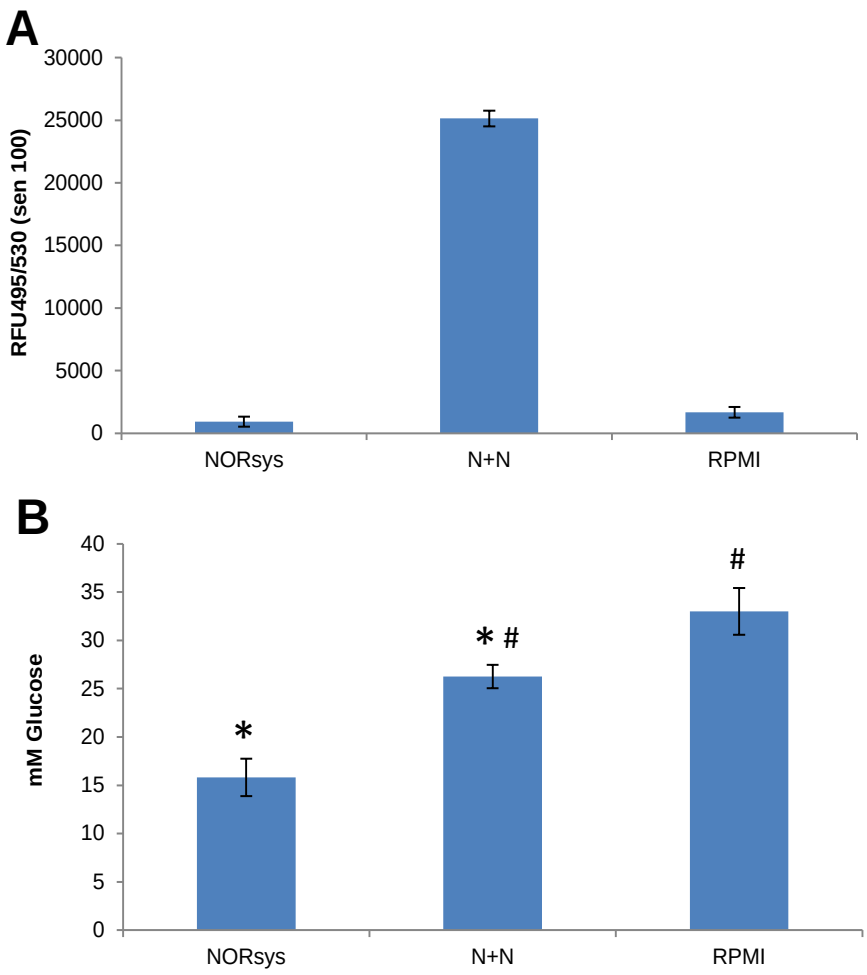

Reagent	NORsys	N+N	RPMI
NORsys	✓		
NOC-5	✓	✓	
NADH	✓	✓	✓
RPMI	✓	✓	✓

Figure 5.6. Concomitant substrate consumption by NOR system. The residual NO was quantified with DAF-FM (RFU) and is presented in (A). The residual glucose in solution was quantified with the glucose assay kit and is shown in (B). The reactions were performed at 37˚C for 30 minutes. Statistical significance was determined from triplicate samples where $P<0.001$ is indicated by * and $P<0.01$ by $^{\#}$ (Unpaired *t* test, GraphPad Software, Inc.).

5.5. Discussion and Conclusions

This study was set out to develop a system consisting of a co-immobilised enzyme system capable of reducing nitric oxide with the concomitant recycling of NADH from NAD^+ using glucose. The enzyme activity maintenance of the enzymes after immobilisation was used as the primary criterion to select the carrier as well as the relative enzyme concentrations for the co-immobilisation. The NOR system was evaluated for its capacity to simultaneously reduce both substrates and the concomitant ability to recycle the cofactor. These results clearly demonstrate the reduction of NO with cofactor recycling, and are considered suitable for application testing.

From the immobilisation studies, NOR and GDH activity was highest on the C1200 carrier with improved enzyme stability in solution and little to no alteration of the pH profile. Interestingly epoxide functionalised carriers have previously been considered ideal for protein immobilisation [127, 130, 302, 302, 322, 323, 324]. However, in this study, we found EDC NHS functionalised carboxyl supports the most optimal for high enzyme activity maintenance.

NOR in solution was unstable and lost activity within 24 hours. The immobilisation of NOR onto the carboxyl activated carriers conveyed enzyme stability at 37˚C in PBS for several days making it suitable for evaluation in culture conditions. In contrast to NOR, hardly any GDH activity was lost during its incubation in PBS at 37˚C, which lines up with previous reports on GDH's stability in solution [316, 321, 325].

For the co-immobilisation of NOR and GDH, the enzyme activity was synchronised by adjusting the enzyme concentrations in accordance with the ratios calculated from the theoretical maintenance in activity. The average from three NOR system preparations presented near synchronous redox rates (0.082:0.077 µmoles $NAD/H.min^{-1}$; refer to Table 5.5). Simultaneous consumption of the substrates, NO and glucose, together with the recycling of the cofactor was clearly demonstrated, indicating successful preparation of the NOR system.

Chapter 6
Evaluation of an applications for the Nitric Oxide Reduction System

6.1. Introduction

In an acute inflammatory response, typical of a host-pathogen interaction, particulate matter from the pathogen induces a cascade of events commencing with its binding to receptors on the host cell surface [326, 327, 328]. A vast diversity of mechanisms of cellular defense and the resolution of inflammation exist, depending on the type of pathogen and on the type of host cell [328]. Many studies of the inflammatory response induced by bacterial lipopolysaccharides (LPS) have established a close interaction of pro-inflammatory cytokines and nitric oxide [329, 330, 331, 332, 333]. An uncontrolled progression of acute inflammation in response to bacterial infection may progress to critical and life threating disease conditions such as sepsis [50, 333, 334, 335, 336].

The inflammatory response has been studied extensively with the intention to elucidate the mechanism of progression to a life-compromising disease condition [335, 337, 338, 339, 340]. For this, many *in vitro* models were developed. This study will use a similar approach for its evaluation of the NOR system as a potential anti-inflammatory reagent. The NOR system might have an anti-inflammatory properties by reducing the NO from the cell environment which might alter the secretion of pro-inflammatory cytokines such as IL-6 and TNFα [385]. Previous studies have observe that IL-8 [331, 372] and TNFa [336] were affected by NO produced by macrophages [331]. A common approach for the investigation of anti-inflammatory properties of a reagent entails the stimulation of commercially available macrophage-like cells with LPS together with the reagent of interest. The quantification of pro-inflammatory cytokines serves as an indicator whether the reagent presents anti-inflammatory properties [329, 341, 342, 343, 344, 345, 346, 347]. A well-established cellular response to LPS, is the synthesis of NO by inducible nitric oxide synthase (iNOS)

mediated by the binding of LPS to Toll-like receptors [19, 326, 329]. The receptors propagate the signal via NFκB to the nucleus and induce the transcription and activation of iNOS [43, 61, 348, 349, 350]. Simultaneously, LPS activates the secretion of pro-inflammatory cytokines such as Interleukin 1β and 6 (IL-1β and IL-6) as well as chemokine 8 (IL-8) and tumour necrosis factor alpha (TNFα) [329, 341, 345]. Each cytokine has its own unique role in the progression of inflammation and defense against the invading pathogen [351, 352, 353, 354]. Pro-inflammatory cytokines initiate the defense response with the recruitment of other immune cells such as neutrophils and macrophages [47, 48, 49, 50]. Only the initial inflammatory response that facilitates the production of NO will be investigated, i.e. the LPS-induced NO production by iNOS, together with the synergistic secretion of pro-inflammatory cytokines [19, 35, 43, 355, 356, 357]. Therefore, this study focused only on the inflammatory response of macrophages in isolation of other immune cells [346, 358].

The human myeloid cell line, monocyte-like U937, has been shown to differentiate into macrophage-like cells with phorbol 12-myristate 13-acetate (PMA) and dimeythyl sulfoxide (DMSO) [346, 358]. As macrophages, U937 cells have been shown to respond to LPS from various micro-organisms [329, 345]. The acute inflammatory response progresses in stages where the cytokine secretion appears within 6 hours of exposure to the immunogen and may linger for 24 hours after its initiation [329, 345, 350].

The human myeloid cell line U937 was selected because of the potential applications of the NOR system as an anti-inflammatory reagent. An *in vitro* acute inflammation model with LPS-induced cytokine synthesis was developed. The determination of the anti-inflammatory properties of the NOR system was assessed by measuring the LPS-induced cytokine secretion in the presence or absence of Dexamethasone, the anti-inflammatory reagent [359, 360] that is also an iNOS suppressing reagent [95, 163, 164], or the removal of NO by a NO scavenger, such as cPTIO [377].

6.2. Materials

6.2.1. Tissue culture materials: preparation of reagents

For the *in vitro* cell culture model, the RPMI cell culture medium, fetal bovine serum (FBS) and human recombinant Interferon gamma (IFNγ) from Gibco (Life Technologies, USA) were used. The intracellular NO detecting dye Diaminofluorescein-FM diacetate (4-Amino-5-methylamino-2′,7′-difluorescein diacetate), NO scavenger (2-(4-Carboxyphenyl)-4,4,5,5-tetramethylimidazoline-1-oxyl-3-oxide potassium salt, cPTIO) and NO donor (S-nitroso-N-acetylpenicillamine, SNAP) from Molecular Probes (Invitrogen, USA) were used for the *in vitro* inflammation experiments. The phosphate buffered saline (PBS) was purchased from Lonza (BioWhittaker, Belgium). NOC-5 was obtained from Calbiochem (Merck Millipore, Germany). DMSO (tissue culture grade), nicotinamide adenine nucleotide (NADH), phorbol 12-myristate-13-acetate (PMA), Dexamethasone (Dex), U937 cells (European Cell Culture collection, Public Health of England) and the *Escherichia coli* 0111:B4 lipopolysaccharides (LPS) were purchased from Sigma-Aldrich (Germany). The NOR system and the carrier were prepared as described in Chapter 5, Section 5.3.

A HeraCell150 Heraeus incubator (Thermo Electron Corporation, Germany) was used for incubation of the cell cultures and the Labconco Class 2 Type A2 Biosafety cabinet (USA) was used for cell manipulations. Filtered pipette tips from BioPointe Scientific (Mexico) were used for all procedures. Tissue culture flasks and micro-titre plates for culturing were from TPP (Switzerland). Visual inspection of the cell cultures was done with an Olympus CKX41 inverted microscope (Philippines) and cell concentration was determined with the TC™ 10 automated cell counter from Bio-Rad (Singapore). Acrodisc® Syringe filters from PALL Corporation (UK) were used to filter-sterilize solutions.

6.2.2. Assays: Cell titre, Cytotox assay and NO quantification

For the biochemical assays, the CellTitre 96® AQueous One Solution cell (Promega, USA) proliferation assay and the CytoTox 96® Non-radioactive Cytotoxicity assay

(Promega, USA) were used to determine cell viability. The Pierce® LAL Chromogenic Endotoxin Quantification kit was used to determine endotoxin content in tissue culture reagents. Absorbance measurements were conducted using a HT Powerwave spectrophotometer (BioTek, USA). Fluorescence measurements were performed in black 96 well micro-titre plates (Greiner bio-one, USA) using an FL*x*800 micro-titre plate reader (BioTek, USA). The BD Cytometric Bead Array (CBA) Human inflammation Cytokines kit, the BD FACSArray bioanalyzer and the software FCAP Array version 1.0 are all products from Becton, Dickenson & Company (USA). The samples for this assay were prepared and analysed in round bottom 96 well micro-titre paltes (Greiner bio-one, USA).

6.3. Methods

6.3.1. Cell culture maintenance

The human myeloid cell line, U937, was cultured in 10 ml culture medium containing RPMI and 10% foetal bovine serum (FBS) at 100% humidity and 5% CO_2. The cells were collected by centrifugation (300 ×*g* for 3 minutes) and diluted one third into fresh culture medium every third to fourth day to maintain a growing cell culture stock for the development and evaluation of the LPS-induced inflammation model.

6.3.2. U937 monocyte differentiation to macrophage-like cells

Daigneault *et al.*, have described the differentiation of monocyte-like THP-1 cells with PMA [408] and a similar protocol was followed for this study. Monocyte-like U937 cells were differentiated to macrophage-like cells with 10 $ng.ml^{-1}$ PMA for 4 days. In this process, PMA was added to a cell suspension containing approximately 100 000 $cells.ml^{-1}$ in RPMI and 10% FBS. The suspension was gently mixed by swirling and subsequently pipetted into a 96 well cell culture micro-titre plate to a final volume of 100 µl. The micro-titre plate with the cells was incubated at 5% CO_2 and 37˚C. After 48 hours, 50 µl of the spent medium was removed from each well and replaced with fresh culture medium. The cells were allowed to grow for another 48 hours before

the experimental procedures commenced. The culture medium for all the experimental procedures only contained RPMI and no FBS.

6.3.3. Preparation of reagents for cell culture studies

Great care was taken in the preparation of reagents used for the inflammation model of U937 cells. A stock solution of LPS (5 $mg.ml^{-1}$), Dex (1 $mg.ml^{-1}$), PMA (10 $mg.ml^{-1}$) and SNAP (20 mM) were prepared in tissue culture grade DMSO which was tested for endotoxins with the Pierce® LAL Chromogenic Endotoxin Quantification kit (refer to Section 6.3.4.4). All reagent vials were opened and prepared in a class 2 biosafety cabinet. The NOR system and the NHS activated ReSyn™ microspheres (carrier) were washed three times in RPMI before their addition to the cell cultures. The endotoxin concentration of this preparation was also determined (refer to Section 6.3.4.4). Serial dilutions of the reagents were prepared in RPMI. The cofactor, NADH was prepared in a tenfold stock solution in double distilled H_2O. This solution was filter-sterilised before its addition to the cell culture.

6.3.4. Biochemical assays

6.3.4.1. Cell viability assay

Cell viability was determined with the CellTitre-96® AQueous One Solution according to the manufacturer's instructions. The metabolising cells were quantified by addition of 20 µl of AQueous One Solution to 100 µl of culture media. The NADH produced by the cells reacts with the [3-(4,5-dimethylthiazol-2-yl-)-5-(3-carboxymethoxyphenyl)-2-(4-2sulfophenyl)-2 H-tetrazolium to form a brown formazan product [361, 362, 363]. This reaction was allowed to proceed for 1 hour at 37˚C and the absorbance was measured at 490 nm with the Powerwave HT micro-titre reader (Bio-Tek, USA). A serial dilution of cells was prepared to generate a standard curve to extrapolate viable cell number from measured absorbance.

6.3.4.2. Cytotoxicity assay

For the determination of cellular cytotoxicity, the lactose dehydrogenase (LDH) activity in the culture medium was quantified. LDH is an intracellular enzyme and its presence in the spent culture medium serves as an indicator for compromised cell

integrity and thus cellular cytotoxicity and cell lysis [364, 365, 366]. For the determination of cellular cytotoxicity, the lactose dehydrogenase (LDH) activity in the culture media was quantified with the CytoTox96® Non-Radioactive Cytotoxicity Assay (Promega, USA).

6.3.4.3. NO quantification with DAF-FM DA

Nitric oxide was quantified by fluorescence emission from its reaction with 5 µM Diaminofluorescein-FM diacetate (DAF-FM DA). For this assay, 100 µl of culture media was transferred to a black 96 well micro-titre plate to which 10 µl fluorescence dye (10× stock solutions) was added and incubated for 1 hour at 37˚C. The relative fluorescence units (RFU) from NO-DAF-FM (DA) was recorded at an emission wavelength of 528 (±20 nm) after excitation at 485 (±20 nm) with a FL*x*800 fluorescence micro-titre reader (BioTeck, USA). The sensitivity of the instrument was adjusted to obtain the optimal RFU recordings.

6.3.4.4. Endotoxin quantification assay

The endotoxin concentrations were determined with the Pierce® LAL Chromogenic Endotoxin Quantification kit for the tissue culture reagents, such as the carrier, the NOR system, monocyte cells, DMSO, PBS and *E. coli* 0111:B4 LPS as a positive control. For this assay, a sterile 96 well micro-titre plate was equilibrated to 37˚C for 10 minutes on a heating block (AccuBlock™ Digital Dry Bath, Labnet International, USA). The sample (50 µl) was pipetted into the plate and incubated for 5 minutes at 37˚C. Thereafter, 50 µl of the Limulus Amebocyte Lysate (LAL) reagent was added to the sample and mixed by gentle shaking of the plate for 10 seconds. The bacterial endotoxins were allowed to activate the proenzyme of the modified LAL assay for 10 minutes at 37˚C. To the activated proenzyme, 100 µl of the colourless substrate, p-Nitroaniline, were added and the enzymatic conversion of the colourless substrate into a yellow coloured product was allowed to proceed for 6 minutes at 37˚C. The reaction was stopped by the addition of 50 µl of stop reagent and the absorbance recorded at 405 nm. The endotoxin units ($EU.ml^{-1}$) were calculated from the *Escherichia coli* (0111:B4) endotoxin standard curve.

6.3.4.5. Cytokine analysis

The LPS-induced cytokine secretion by the PMA treated U937 cells was quantified by the BD™ Cytometric Bead Array Human Inflammation kit (USA) and detected with the BD FACS Array Bioanalyser with a 488 nm laser. The data was analysed with the FCAP Array™ v 1.0 (Soft Flow Inc., USA). The spent cell culture media were stored at -80˚C and thawed on the day of analysis, from which 50 µl was added to 50 µl of cytokine capture bead mixture (10 µl of IL-1β, IL-6, IL-10, IL-12p70 and TNFα). For the cytokine IL-8, the sample was diluted tenfold of which 50 µl was added to the 10 µl IL-8 capture beads. To all samples, 50 µl of the phycoerythrin (PE) detection reagent was added. The tube was mixed by gentle mixing and incubated for 3 hours at room temperature. The samples were washed to remove unbound cytokines and phycoerythrin detection reagent. Then, 1 ml of wash buffer was added to each sample, briefly vortexed and centrifuged at 200 ×*g* for 5 minutes. The supernatant was aspirated and discarded. The bead pellet was re-suspended in 300 µl wash buffer. The samples were transferred to a round bottom 96 well micro-titre plate for cytokine detection by the BD FACS Array Bioanalyzer. The instrument settings were adjusted to the following voltage settings: Forward scatter: 250; side scatter: 234; Far red: 373; Yellow: 473; NIR: 355; and Red: 460. For each sample, 10000 events were recorded.

6.3.5. Development of U937 inflammation model

Macrophages have been observed to produce NO in response to several external stimuli, such as LPS and IFNγ [62, 329, 343, 345, 348]. Therefore, the PMA differentiated U937 cells were stimulated with increasing concentrations of iNOS inducing stimulants with the objective to quantify NO in solution. The PMA differentiated cells were also exposed to increasing concentrations of dexamethasone (0, 0.1, 1 and 10 $\mu g.ml^{-1}$), DMSO, LPS and NOR system to determine whether any of these reagents would contribute to the baseline fluorescence of the DAF-FM DA detection agent. The NO was quantified by the addition of 5 µM DAF-FM DA to the stimulated cells and the RFU was recorded after 30 minutes incubation at 37˚C.

6.3.6. Evaluation of anti-inflammatory properties of NOR system: cytokine analysis

For the LPS-induced inflammation model, the PMA differentiated U937 cells were challenged with 50 µg.ml^{-1} LPS together with the various treatment regimens for 6 hours. All treatments were prepared in triplicate wells for each assay, i.e. cell viability assay, cytotoxicity assay, NO fluorescence and cytokine analysis. In an effort to determine whether the NOR system (concentration) exhibited anti-inflammatory properties via the reduction of NO, cells sensitised with LPS were treated with the NOR system and the cytokine response was compared to that of 0.25 mM cPTIO (NO scavenger) and 10 ng.ml^{-1} dexamethasone treated cells. An NO donor, 0.2 mM SNAP, was used as positive control for the NO related cytokine response. The addition of NHS activated ReSyn™ microspheres [i.e. carrier without immobilised enzymes (1% v/v)] to the cells, served as negative control for the NOR system. The cytokine secretion of non-LPS stimulated monocyte-like cells and the PMA differentiated cells served as negative control for LPS challenged cells. The cytokine response of LPS stimulated PMA differentiated U937 cells was used as a positive control for the inflammation-related cytokine response.

6.4. Results

6.4.1. Development of *in vitro* inflammation model

For the development of the *in vitro* inflammation model, various reagents were investigated for their effect on cell viability and their capacity in stimulate NO production. The effect of various agents such as dexamethasone (Dex), *E. coli* lipopolysaccharides (LPS) and the reagent vehicle (DMSO), on cell viability was investigated. NO and pro-inflammatory cytokine synthesis have been reported for U937 cells in response to LPS [329, 341, 345] and therefore the NO production was quantified under these conditions.

Stock solutions of Dex and LPS were prepared in DMSO (refer to Section 6.3.). Considering that DMSO may lead to compromised cell viability [367], the effect of

DMSO as well as Dex and LPS on cell viability was investigated. The monocyte-like U937 cells were differentiated to macrophage-like cells for four days after stimulation with PMA. The spent culture media was replaced with fresh RPMI medium and treated with either DMSO or with Dex or LPS dissolved in DMSO at increasing concentrations. As a polar agent and organic solvent, DMSO at high concentrations such 1% (v/v), did result in compromised cell viability (Fig. 6.1. A). Therefore, Dex and LPS concentrations were introduced at a maximum of 0.1% (v/v) DMSO. Cells viability was unaffected by the exposure to dexamethasone (Fig. 6.1 B), however, LPS in DMSO did affect cell viability (Fig. 6.1 C).

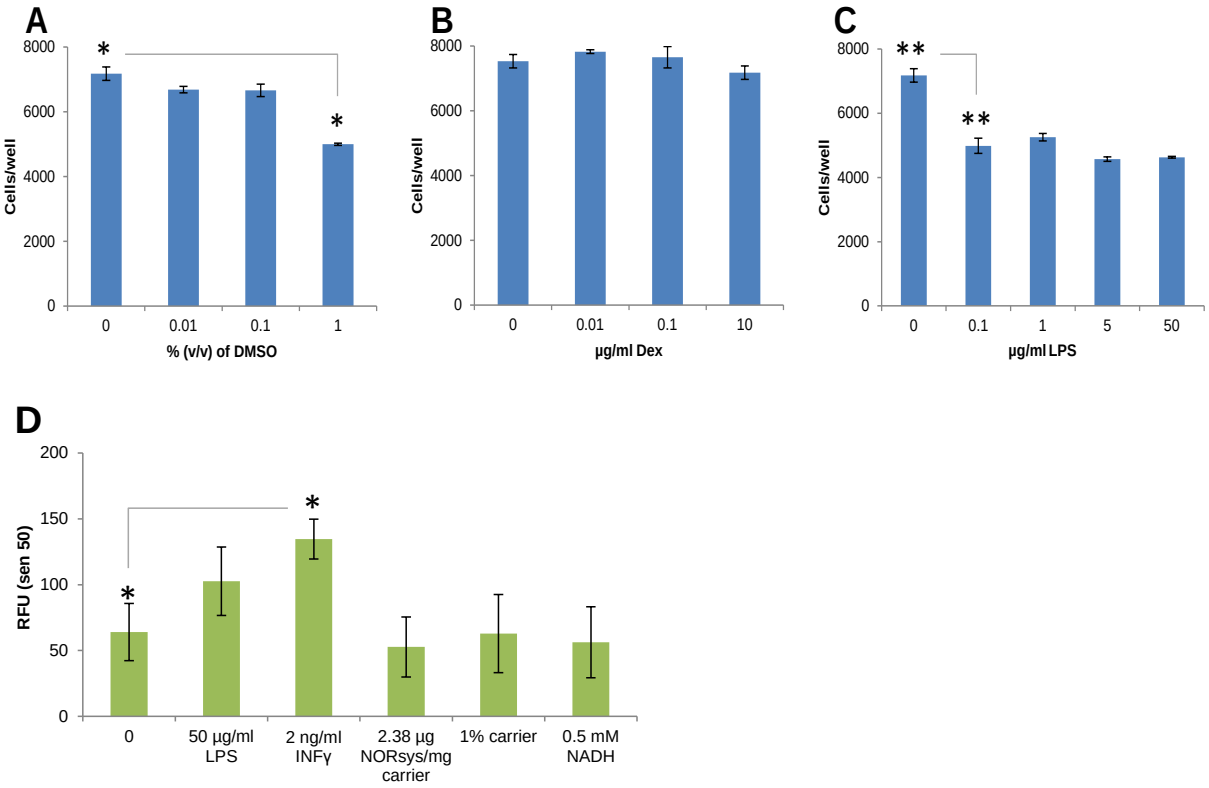

Figure 6.1. Cell viability and dissolved NO levels in solution from PMA differentiated U937 cells. U937 cells were differentiated to macrophage-like cells with 10 ng.ml^{-1} PMA for four days. Cell viability (Cells/well) was determined after 24 hour exposure to (A) DMSO, (B) Dex and LPS (C). in (D) PMA treated cells were treated with 50 µg.ml^{-1} LPS, 2 ng.ml^{-1} INFγ, 2.38 µg NORsys.mg^{-1} carrier, 1% (v/v) carrier and 0.5 mM NADH for 24 hours. The intracellular NO was quantified with 5 µM DAF-FM DA and the fluorescence was recorded after 6 hours incubation. Fluroscence sensitivity was set to 50 units. Error bars are the standard deviation of triplicate samples. Statistical significance with a $P \leq 0.0003$ is indicated by ** and $P \leq 0.02$ by * (Unpaired *t* test, GraphPad Software, Inc.).

LPS may induce the NO synthesis from iNOS, initiated by its binding to the Toll-like receptor 4. This signal is then mediated via the NFκB pathway and initiates the transcription process for iNOS [43]. *E. coli* (0111:B4) LPS was dissolved in DMSO to

prepare a stock solution (5 mg.ml^{-1}) that was further diluted to determine the potency of LPS for the induction of NO production, and subsequent detection with intracellular fluorescence dye DAF-FM DA. The RFU measured after 24 hour LPS stimulation was marginally higher than the RFU determined from the untreated cells (Fig. 6.1 D), however, the difference was not statistically significant to the 95% confidence level.

The experiment was repeated with IFNγ, another iNOS inducing reagent, and compared to LPS. IFNγ activates iNOS transcription via the JAK-STAT pathway [348, 368]. It was hoped that an alternative pathway of iNOS activation would result in detectable NO production. A marginally higher NO signal was determined from IFNγ treated cells compared to untreated cells (P<0.02), indicating that the U937 cells do produce detectable NO upon stimulation (Fig. 6.1 D).

The cells were also treated with the NOR system, the carrier and NADH to determine the biocompatibility of these reagents. The RFU measured from cells exposed to the NOR system, carrier or NADH at the relevant concentrations were similar to untreated cells, indicating that these reagents did not appear to elicit NO production (Fig. 6.1 D).

Although IFNγ treated cells did produce detectable NO, this reagent was not applied further, due to its expense. Instead, LPS was used for all the subsequent studies to stimulate a cytokine response. Thus it was assumed that LPS would suffice in the initiation of an acute inflammatory response in PMA differentiated U937 cells and stimulate the secretion of pro-inflammatory cytokines.

6.4.2. Evaluation of anti-inflammatory properties of the NOR system: cytokine analysis

A synergistic interaction of cytokines and nitric oxide has been attributed to the critical progression of disease, such as in sepsis [335, 336, 337, 369, 370, 371]. Work done with *in vitro* macrophage models suggested that nitric oxide augments the release of cytokines such as IL-8 [331, 372] and TNFα [370, 373, 374], of which the latter has been associated with TNFα shock and cytotoxicity [370]. LPS-

stimulation of PMA differentiated U937 cells was shown to result in secretion of IL-1β, IL-6, IL-10 and TNFα [329, 345, 375]. Therefore, it was hypothesised that reducing NO by the NOR system could potentially alter the cytokine response of PMA differentiated LPS-challenged U937 cells. The altered cytokine response of the NOR system treated cultures was compared to those obtained with the NO scavenger, cPTIO, and the anti-inflammatory reagent, dexamethasone (Dex).

6.4.2.1. Cytokine response from exogenous NO

Relationships between NO and various cytokines have been previously described [19, 33, 53, 331, 372, 376]. Thus, it was hypothesised that the reduction of NO by the NOR system may modulate the cytokine response and provide a method for the evaluation of the system. Since, NO production induced with LPS or IFNγ stimulation was lower than expected (Fig. 6.1 B), exogenous NO was added to the PMA differentiated LPS challenged cells. Here the intention was to augment the cytokine response specific to exogenous NO as observed by Turpaev *et al.* (2003, 2004) [376, 377]. In this way, the hypothesis was tested that the reduction of NO by the NOR system would alter the cytokine response and thus provide evidence for the anti-inflammatory properties of the NOR system.

For this experiment, U937 cells were differentiated to macrophage-like cells with 10 $ng.ml^{-1}$ PMA for four days. Then the cells were challenged with 21 $\mu g.ml^{-1}$ LPS together with 0.2 mM SNAP for 6 hours. The cell viability was not compromised by the various treatments (SNAP, NOR system, Dex and cPTIO), which was confirmed by the cytotoxicity assay (blue and red bar, respectively in Fig. 6.2 A). However, cells treated with the carrier did show reduced cell per wells and increased cytotoxicity (Fig. 6.2 A). As for the NO in solution from the NO donor, SNAP, cells treated with the carrier and dex had high RFU, whereas in the presence of the NOR system (0.37 $\mu g.ml^{-1}$) and the NO scavenger (0.25 mM cPTIO), NO reduced (green bar in Fig. 6.2 A).

The cytokine profiles of monocyte-like cells (undifferentiated U937, Mo), differentiated cells (Mø) and treated cells (SNAP, NORsys, carrier, Dex and cPTIO) were established (Fig. 6.2 B to G). As expected, very low concentrations of cytokines were produced by the monocyte-like cells (Mo) and the untreated differentiated

macrophage-like cells (Mø). These were considered as the negative controls for inflammatory response. The differentiated macrophage-like cells treated with LPS were considered as the positive controls for the pro-inflammation cytokine profile. These LPS treated cells registered the highest levels of cytokines (IL-1β, IL-6. IL-10 and TNFα), indicating that LPS indeed stimulated an inflammatory response (Fig. 6.2 B, C, D and G).

The increase in the chemokine IL-8 after PMA mediated differentiation might indicate oxidative stress in the cell culture [377]. Earlier studies suggested that IL-8 production was a response to ROS and reactive nitrogen intermediates [377]. The higher IL-8 concentration from cells treated with the exogenous NO (SNAP, carrier, NOR sys, dex and cPTIO) supports the notion that IL-8 was secreted due to oxidative stress (Fig. 6.2 E). The treatment of the LPS stimulated macrophage-like cells with SNAP resulted in a very similar depressed cytokine profile for IL-1β, IL-6 and IL-10 (Fig. 6.2 B, C and D) even in the presence of the NOR system, carrier, Dex and cPTIO, showing that the inflammation model was overwhelmed with this non-physiological NO intervention. This was not the case with TNFα which, although somewhat reduced by the presence of exogenous NO (Fig. 6.2 G), could be abolished by treatment with Dex. Although the excess NO provided externally did not affect the viability of the cells for the duration of the experiment and allowed for secretion and determination of cytokines such as IL-8, IL-12 and TNFα, it could not be applied validly as an *in vitro* model to assess the efficiency of the NOR system. It did, however, demonstrate the potency of the NOR system to lower the NO concentrations (Fig. 6.2 A) under conditions of excessive production that still allowed IL-8, IL-12 and reversible TNFα secretion (Fig. 6.2 E, F and G). A different approach was therefore undertaken to elucidate the potential anti-inflammatory properties of the NOR system with a broad range of inflammatory cytokines.

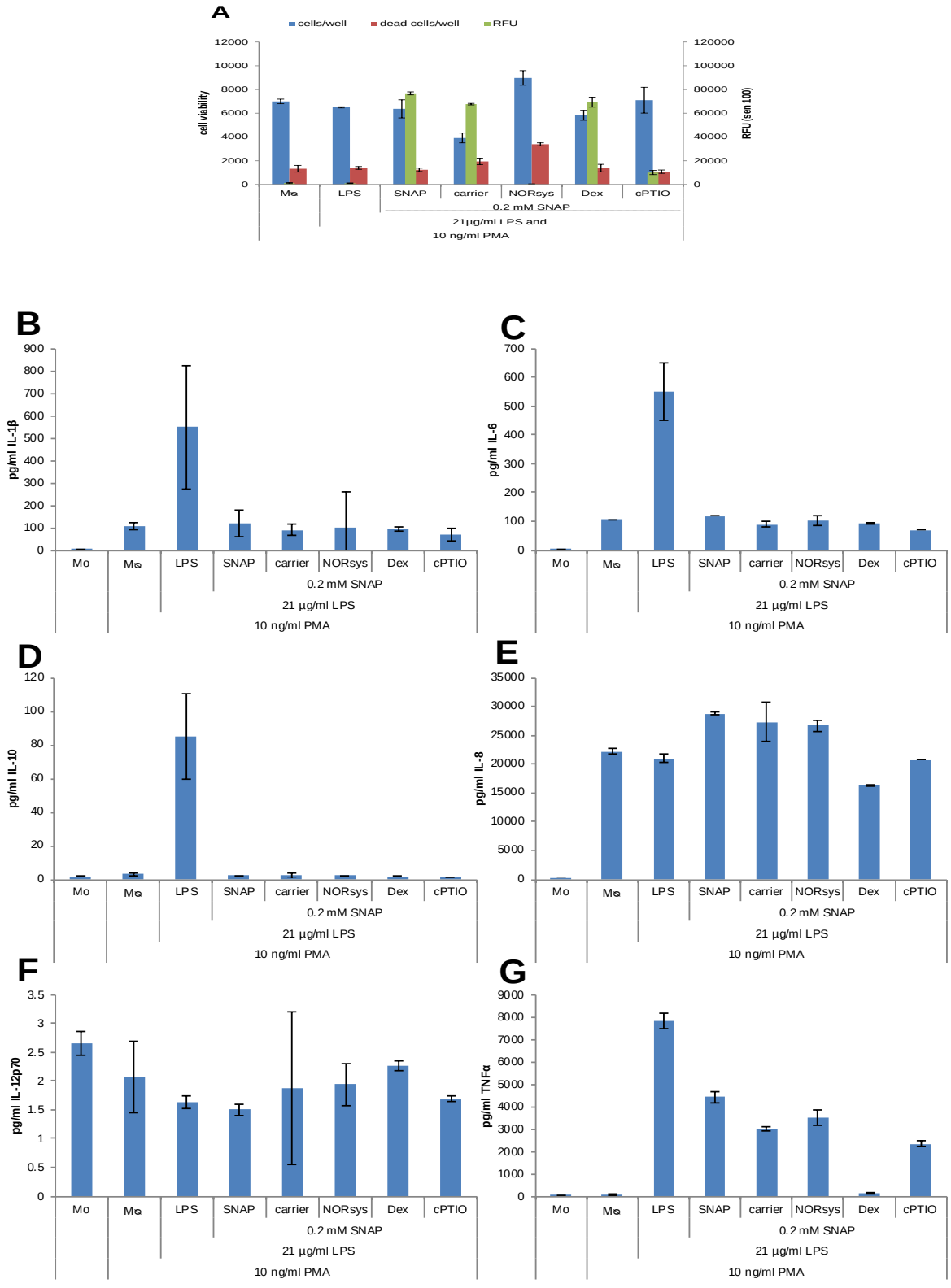

Figure 6.2. Assessment of the NOR system on exogenous NO induced cytokine response in an *in vitro* inflammation cell model. The PMA differentiated and LPS-stimulated U937 cells were exposed to exogenous NO from 0.2 mM SNAP for 6 hours. The LPS-stimulated U937 cells were treated with 1% (v/v) carrier, 0.37 µg.ml^{-1} NOR system, 10 ng.ml^{-1} Dex and 0.25 mM cPTIO. Cell viability (cells/well) and cytotoxicity (dead cells/well) as well as the RFU, representing residual NO concentration are presented in (A). The cytokine concentration of IL-1β (B), IL-6 (C), IL-10 (D), IL-8 (E), IL-12p70 (F) and TNFα (G) are shown. The standard deviations of triplicates are indicated by the error bars.

6.4.2.2. Cytokine response from U937 cells after 6 hours and 24 hours of treatment

Since the exogenous NO overwhelmed the cytokine response (Fig. 6.2), the anti-inflammatory properties of the NOR system could not be elucidated. Although, IFNγ stimulation resulted in higher NO production than LPS stimulation (Fig. 6.1 B), this reagent was not considered, due to its expense. Therefore, the cytokine analysis was repeated by treating PMA differentiated cells with 50 $\mu g.ml^{-1}$ LPS. Here, it was thought that LPS would induce an inflammatory response resulting in the secretion of cytokines and low levels of NO. Although NO levels produced by LPS might be below the detection limit, the NOR system was expected to reduce NO and thus may alter the cytokine response. The cytokine response was monitored at two different time intervals, namely after 6 hours and 24 hours after LPS stimulation and treatment, to cover the different mechanisms by which the anti-inflammatory properties could potentially only become evident within 24 hours of incubation [49, 359].

The cytokine response by the U937 monocytic cells (Mo) registered low quantities of cytokines in comparison to the PMA differentiated cells and PMA differentiated LPS treated cells (Fig. 6.3), except for IL-12, which was high only for the undifferentiated monocytes. The very low IL-12p70 signals that were detected in the differentiated and stimulated cell cultures confirmed that only LPS was the pro-inflammatory cytokine stimulant and no other factors such as non-specific phagocytosis, which is known to stimulate IL-12p70 production [378, 379]. Furthermore, the anti-inflammatory reagent, Dex, did reduce cytokine responses when compared to the LPS stimulated cells in all cases, testifying to the validity of the test to assess anti-inflammatory reagents or systems. Combined, the evidence indicated that the inflammation cell model was suitable for the evaluation of anti-inflammatory properties of the NOR system. The treatment with cPTIO compromised cell viability. Therefore the cytokine profiles of these cells are not shown in Figure 6.3.

Interleukin 1β, together with LPS, have been shown to induce iNOS transcription and the production of NO was determined [329]. Although our NO detection method appeared not to be sensitive enough to detect the *in vitro* concentration of NO, the cytokine profile indicated an NO induced response. The amounts of pro-inflammatory

IL-1β, IL-6 and IL-8 did increase upon LPS stimulation after 24 hour incubation, but could not be brought down with the NOR system treatment. Notably, the carrier alone seemed to induce stimulation of IL-1β, IL-6, IL-10 and IL-8, implying that the particle platform is immunologically active. Because it was suspected that endotoxin could have contributed to this immunogenic response, the endotoxin units (EU) were determined for the carrier, the NOR system, cell culture and cell culture reagents. The carrier solution contained 0.08 $EU.ml^{-1}$, which was lower than the endotoxin content for the NOR system and the cell culture (0.99 and 0.65 $EU.ml^{-1}$, respectively). The cell culture reagents such as RPMI, DMSO and PMA did contain less than 0.03 $EU.ml^{-1}$. In other words, the immunogenic response observed in the carrier treated cells, was most likely not due to endotoxins in the carrier solution.

A possible plausible cause of the immunogenic properties of the carrier may be due to the chemical nature of this particle. The ReSyn™ microsphere has a high density of positively charged reactive groups (refer to Chapter 5) which is to the benefit of the high protein binding capacity. However, in its application in the *in vitro* cell culture model this property seems to be a disadvantage. Here it may be speculated that the charged reactive groups on the surface of the particle may have interacted with the cell surface which is generally negatively charged [380], resulting in an immunogenic response [381]. This unforeseen property of the carrier may have affected the anticipated outcome of the anti-inflammatory properties of the NOR system. For all cytokines measured except IL-12p70, the NOR system was capable of at least returning the inflammatory cytokine response back to that of the untreated cells after 24 hours, and in the case of IL-6 to even lower than the untreated cell control (Fig. 6.3 C).

Interleukin 6 (IL-6) is a marker of inflammation but it has also been implicated in the resolution of inflammation and tissue repair depending on its cellular context [382]. IL-6 has been observed in the acute phase of inflammation with dual activity, either as pro- or anti-inflammatory cytokine [351] in which anti-inflammatory properties have been observed [351, 383]. However, in combination with other chemokines such as TNFα, IL-6 was observed to contribute to cellular cytotoxicity with dependence on the concentration of NO [384, 385]. Another bifunctional effect of NO was observed in connection with IL-6: low NO increased IL-6 and high NO reduced

IL-6 mRNA expression and IL-6 protein levels [386, 387]. IL-6 in LPS stimulated cells increased over time for all samples (6 vs. 24 hours, Fig. 6.3 D), while inclusion of the NOR system showed reduced IL-6 after 24 hours when compared to the LPS treated cells (P<0.04, Fig. 6.3 D*), supporting the notion that NO may modulate IL-6 levels and that the NOR system can reduce the effect by removing the NO.

IL-10 is another cytokine known to be involved in counter-acting the inflammatory response by the down regulation of TNFα [353, 354] and other cytokines [337]. In the presence of the NOR system, a decrease in IL-10 was observed after 24 hours (P=0.02; Fig. 6.3 E*). This might be an indication of the potential anti-inflammatory activity of the NOR system in that it reduced the IL-10 secretion after 24 hours compared to the LPS stimulated cells.

Together with IL-1β and TNFα, the chemokine IL-8 plays a role in the neutrophil recruitment to inflamed tissue [337]. Nitric oxide has been implicated in the regulation of IL-8 via p38 MAPK activation in LPS-stimulated macrophages [331]. An increase in IL-8 was observed after 24 hours when untreated cells were compared to LPS treated cells (except for Dex treated cells, refer to Fig. 6.3 F), but could not be recovered back to normal by the NOR system. IL-8 may have been induced by TNFα via the NFκB pathway [388] together with other oxidative related stress signals suggesting that compounded signalling may have resulted in the relatively high IL-8 concentrations observed in the LPS-stimulated PMA differentiated U937 cells. However, this effect could not be neutralised by the NOR system.

The sixth pro-inflammatory cytokine measured in the cell cultures was TNFα. TNFα is a cytokine involved in many diseases [389, 390] but for the purpose of this study, the focus shall remain with the role of TNFα in acute inflammation in response to LPS in macrophages. The synergy of TNFα and NO relates strongly to refractory hypotension observed in septic shock [370]. The inhibition of iNOS by specific inhibitors such as L-NAME revealed that mere abolishment of NO synthesis does not resolve haemodynamic collapse [336, 370], as small amounts of NO seem to be vital for the subsidence of inflammation [35]. Thus, the NOR system was evaluated for its capacity to reduce TNFα concentrations via the reduction of NO. The TNFα concentrations which were determined in cells treated with the NOR system were

lower when compared to LPS stimulated cells, however, not statistically significant; thus the NOR system did not present a TNFα tempering effect (Fig. 6.3 G).

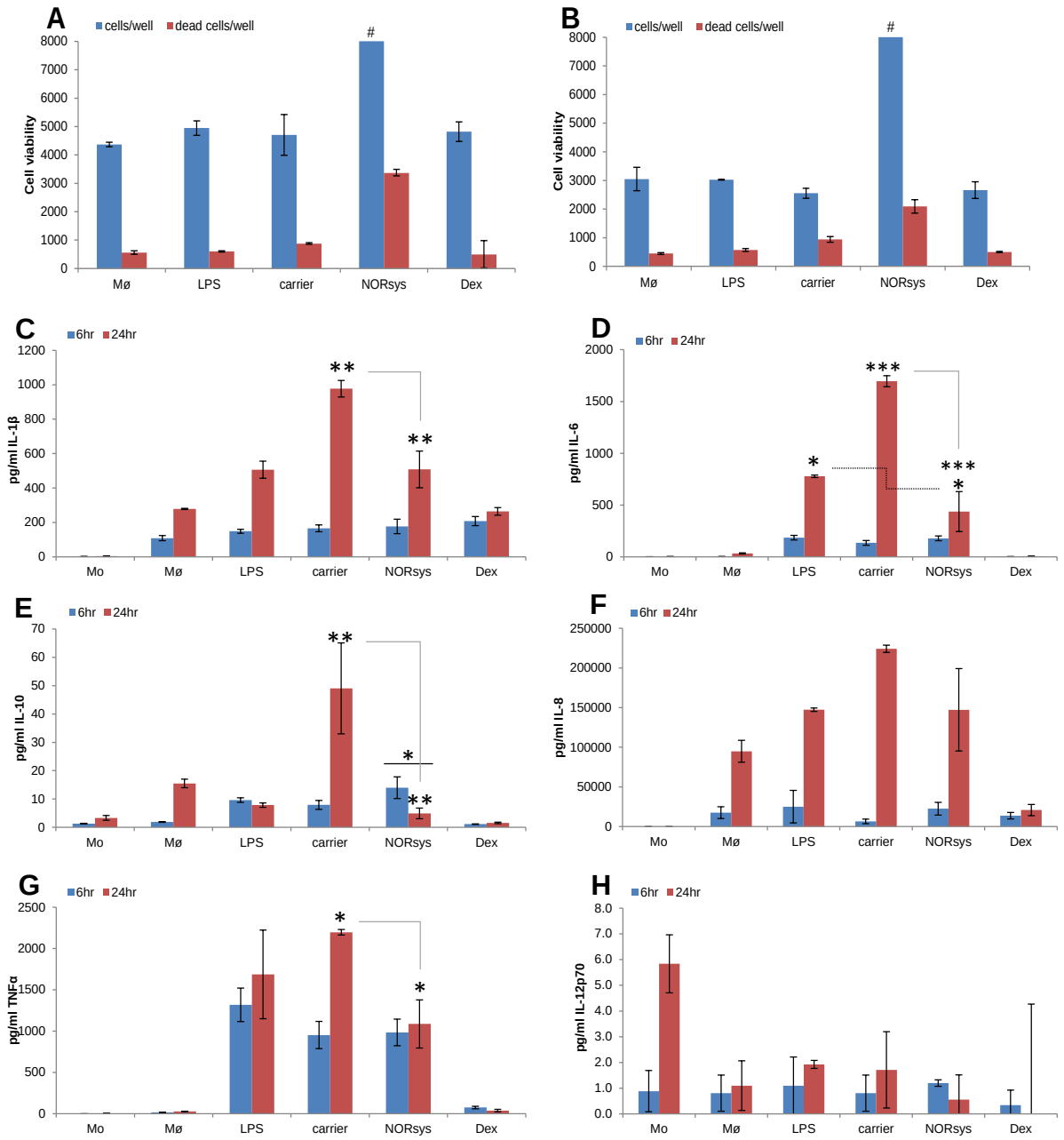

Figure 6.3. Assessment of the NOR system in an *in vitro* inflammation cell model. Monocyte-like U937 cells were differentiated to macrophage-like cells with 10 ng.ml^{-1} PMA. The macrophage-like cells were stimulated with 50 µg.ml^{-1} LPS and treated with 1% (v/v) carrier, 0.37 µg.ml^{-1} NOR system or 10 ng.ml^{-1} dexamethasone. The cell viability (cells/well) and cytotoxicity (dead cells/well) are presented in (A) (6 hours after treatment) and in (B) (24 hours after treatment). NADH (0.05 mM) was added to the NOR system, but interacts with the assay reagents. This artefact is indicated by # in (A) and (B). The cytokine concentrations (pg.ml^{-1}) are represented in (C) IL-1β, (D) IL-6, (E) IL-10, (F) IL-8, (G) TNFα and (H) IL-12p70. The error bars represent the standard deviations of triplicate assays. The statistical significance of $P \leq 0.02$ is presented either by *, ** or *** determined with the Unpaired *t* test (GraphPad Software, Inc.).

In summary, cells treated with the NOR system displayed an altered cytokine profile, particularly for IL-6 and IL-10 when compared to LPS stimulated cells and the control with the carrier only. Although several of the observations may be interpreted as an anti-inflammatory activity, the inflammatory response induced by the carrier only makes the study inconclusive. The biological validation of the NOR system therefore remains inconclusive. In particular, the carrier system must be modified or replaced, such that it provides an inflammatory neutral particle platform for enzyme immobilisation.

6.5. Discussion and Conclusion

Nitric oxide has been shown to modulate the cytokine response to immunogens such as LPS [33, 35, 87, 347, 357, 369, 372, 386]. This study pursued the hypothesis as to whether an enzymatic system capable of reducing NO (NOR system) would have anti-inflammatory properties. For the evaluation of this hypothesis, an *in vitro* inflammation model was developed.

Human monocyte-like U937 cells were differentiated to macrophage-like cells and stimulated with immunogens such as LPS and IFNγ. Although, IFNγ stimulation of differentiated U937 cells resulted in higher NO output than LPS, LPS was used as the more affordable stimulator of inflammation. Cytokines that are associated with acute inflammation were detected in PMA differentiated and LPS stimulated U937 cells, when compared to unstimulated cells. LPS stimulated cells treated with the anti-inflammatory reagent dexamethasone, resulted in low cytokine response similar to untreated cells not exposed to LPS. This indicated that the *in vitro* inflammation model was suitable for the evaluation of the anti-inflammatory properties of the NOR system.

From the cytokine analysis, it was evident that the carrier system without its immobilised enzymes (NOR and GDH) induced inflammatory cytokines. Cytokine response from LPS stimulated cells treated with the NOR system was similar to the cytokine response from LPS stimulated cells after 24 hours, suggesting that the immunogenic response to the carrier was neutralised by the NOR system.

The hypothesis that the NOR system may lower the NO-induced inflammatory response of LPS exposure should therefore be supported by experiments using a non-immunogenic carrier. The NOR system in its current composition is unable to lower the inflammatory effect of NO under *in vitro* conditions simulating the physiological concentrations of NO. The NOR system does, however, lower the concentration of non-physiological concentrations (high) of NO, which may occur under extreme conditions of immune challenge.

Chapter 7
Summary, Conclusion and Future Work

7.1. Summary and Conclusion

The intricate role of nitric oxide in biological processes is extensive [1, 11], and ranges from a signalling molecule [3, 10, 12] to an agent that can be responsible for the progression of disease [13, 15,, 16, 17]. The concentration and availability of NO determines whether it is beneficiary or detrimental in these biological processes [10, 25, 27 28, 31]. High NO concentrations have been implicated in various disease states and their progression [32, 34, 44]. The synergistic and complex relationships in inflammation make this an interesting biological molecule [33, 35.

The initial role of NO as an effector molecule was elucidated using inhibitors of NO synthesis including arginine analogues, such as L-NAME [56]. These analogues did facilitate an appreciation of NO's role in the cellular environment; but a full understanding of its role was compromised when it became apparent that these reagents interfered with arginine metabolism and other physiological systems [91, 92, 93]. Similary, the application of immune suppressing reagents such as glucocorticoids revealed the role of NO in inflammation and the cytokine response, but the full understanding of this is masked by the fact that glucocorticoids are known to non-specifically suppress cytokine responses [39, 95]. These challenges in the study of NO identified the need for new approaches for the understanding of NO's role in biology. The development of a tailorable nitric oxide reduction system is a novel approach to the study of NO to assist in the understanding of acute inflammation and ways to manage it.

The development of the NOR system required the establishment of a NOR activity assay as well as the production and assembly of various system components. The NOR system is a bi-enzymatic cofactor recycling system which involved the reduction of NO by NOR and the oxidation of glucose by GDH for recycling of the

cofactor. These two enzymes were co-immobilised onto NHS-EDC functionalised ReSyn™ carboxyl microspheres.

The first step necessitated by the proposed development of the NOR system, was the development of a fast and reliable NOR activity assay, which is described in Chapter 2. The NOR activity assay was applied in the screening, purification and kinetic characterisation of recombinant NOR (Chapter 3 and 4). The kinetic characterisation of NOR required a more in depth analysis for the estimation of NO concentration in solution. The enzymatic estimation of NO in solution (excess enzyme) was compared to a well-established mathematical computational method and an excellent correlation was obtained. This method of NO estimation was subsequently applied for the determination of kinetic constants of a commercial NOR solution (wild-type Anor) as well as a recombinant NOR preparation (expressed in *E. coli*). From these studies, it became evident that the kinetic constansts (K_m and k_{cat}) were comparable to the values determined by gas chromatography [152], but with improved convenience and cost efficiency. These findings have been accepted for publication in Analytical Biochemistry. After the evaluation of the NOR activity assay for its suitability to determine NOR activity, this assay was applied to quantify the enzyme activity after immobilisation and to synchronise NO reduction with glucose oxidation for cofactor recycling, described in Chapter 5.

The second step in the NOR system developmental process required the purification of NOR, because the commercial source was discontinued. The NOR from *A. oryzae* (Anor) was initially expressed in and purified from *A. niger* (Chapter 3) and subsequently in *E. coli* (Chapter 4). The latter expression system resulted in sufficient enzyme for the immobilisation studies, the assembly of the NOR system (Chapter 5) and its subsequent evaluation in *in vitro* studies (Chapter 6). A variant of GDH, engineered for stability, was readily available commercially from Codexis and thus recombinant expression was not pursued. From the purification studies, it was observed that the addition of bovine haemoglobin was beneficial for Anor synthesis in *A. niger* and *E. coli*. The underlying mechanism for the improved yields were beyond the scope of this study. The Anor yield from *E. coli* was comparable to the yields from purification processes reported on wild-type Fnor [104] and Anor [152].

To the authors knowledge, this is the first investigation in which Anor has been expressed heterologously with a histidine affinity tag.

The assembly of the NOR system entailed co-immobilisation of NOR and GDH. This process entailed the selection of the carrier fulfilling the key requirements of the applications of the NOR system, the synchronisation of cofactor redox rates, the concomitant consumption of both enzymes substrates, and the determination of cofactor recycling efficiency (Chapter 5). In carrier selection, it was observed that the carboxyl functionalised carrier was preferable for the immobilisation of NOR and GDH with regard to enzyme activity maintenance and enhanced temperature stability at 37˚C. While the immobilisation of GDH has previously been reported, the immobilisation of Anor represents, to the best of the author's knowledge, novel work. There are reports on GDH's use in cofactor recycling applications such as biocatalysis, but its application for the continuous reduction of NO by NOR presents a unique application. In this study, it was shown that the NOR system consumes both substrates with subsequent cofactor recycling. This approach was potentially beneficial for the study of NO biology, which was demonstrated in Chapter 6.

The final step in the development of the NOR system was the evaluation of its suitability as a reagent to determine the effect of NO reduction in an *in vitro* inflammatory cell model (Chapter 6). Human monocyte-like cells (U937) were differentiated into macrophage-like cells and stimulated with *E. coli* LPS to induce NO synthesis and pro-inflammatory cytokine synthesis. Despite various efforts, NO in solution was not detected after LPS stimulation. Therefore it was concluded that NO concentration was below the sensitivity of the NO specific fluorescent dye. Nonetheless, an anti-inflammatory response was observed from cells which were differentiated to macrophage-like cells and stimulated with LPS. As anticipated, macrophage-like cells stimulated with LPS and treated with dexamethasone (immune suppressing reagent) showed a low pro-inflammatory cytokine response. This confirmed the indications from the literature that glucocorticoids are efficient immune suppressing reagents [359, 372, 391, 392], that do not distinguish synergistic relationship of NO and cytokines [95, 360]. These findings highlight the significance and suitability of the NOR system as a reagent to study the role of NO in an inflammatory response. However, an unforeseen immunogenic response was

observed in LPS stimulated cells treated with the carrier only. The NOR system in all cases did reduce the immunogenic response induced by the carrier. However, one cannot at this stage distinguish whether this was due to masking of the inflammatory surface of the carrier with the NOR enzyme, or whether it is due to removal of NO by the NOR enzyme of the system. This observation hinders the prediction of potential anti-inflammatory applications for the NOR system.

7.2. Future Work

The evaluation of the NOR system as an anti-inflammatory reagent was inconclusive, and this provides opportunity for further study. The immunogenicity of the carrier could be addressed by reducing the particles' surface charge through chemical finishing with a neutral compound. An alternative strategy would be the determination of the anti-inflammatory properties of the NOR system in a trans-well *in vitro* cell model. Trans-well culturing systems would prevent direct interaction of the NOR system with the cells and would be able to reduce the fast diffusing NO in solution mimicking an *in vitro* model for studying the inflammation across the blood brain barrier. This cell model could elucidate the interaction of NO and inflammatory response observed in cerebral malaria. The inclusion of the bi-enzymatic NO reducing system in haemofiltration could present another application of the NOR system as a potential anti-inflammatory reagent or for research in severe sepsis and haemodynamic shock. The NOR system may complement cytokine traps in haemofilters that are currentlybeing investigated in an effort to improve the outcome of septic shock and other inflammation syndromes [393, 394].

The authors propose that the diagnostic application of this system should be investigated. This detection method might be developed into a suitable technology for the diagnosis of e.g. asthma. In this diagnostic application the nitric oxide in the breath would condensate onto a membrane strip which would contain the NOR system. In the presence of NO, NADH is reduced to a faster rate than its interaction with a colour reagent such as water-soluble formazans. Only the NADH recycled by GDH would react with formazan and the colour would be an indicator of NO in the breath. Such NO detection system would be much smaller and could be developed

into a point of care device. The current detection of asthma is determined from NO in the breath of patients, which is directed into a chamber containing ozone [395]. In this chamber, the light emission from the reaction of NO and ozone is used as an output for NO in the breath. This instrument is relatively large and not generally available for patients.

The reduction of NO and the formation of NADH by GDH of the NOR system may be exploited in the development of a biosensor for the continuous monitoring of NO, as an important diagnostic molecule. Further, the system may have applications as a bio-research tool to assist in the understanding of NO and its implications in biology.

Appendix to Chapter 3: Anor from *A. oryzae*

A.3.1. Amino acid and nucleotide alignments

A.3.1.1. Amino acid alignment of Anor from *A. oryzae*

The coding sequence determined by Kaya *et al.* (2004) [152] was used to express Anor, the nitric oxide reductase of interest for this study. This wild-type Anor expression gene, nicA, has two expression patterns from the starting codon of *nicA*, a major and minor [152], of which the major expression pattern was used as a template to design the *nicA* gene for this study. In an attempt to exclude the wild type signalling peptide sequence, which guides the protein to its intracellular destination, two gene variants were designed. The two variants of the *nicA* gene have a 9 amino acid difference at the N-terminus, where *nicA*1 excludes the wild type initiation codon and intron splicing amino acids and *nicA*2 is identical to the wild type. A signal peptide sequence (*xyn2*) and a KEX2 cutting site (KR) were inserted upstream of the *nicA* gene to ensure that the protein product of the *nicA*, Anor, gene is secreted to the extracellular environment. Figure A.3.1 shows the amino acid alignments of *nicA* in *A. oryzae*, *nicA*1 and *nicA*2. The genes *nicA*1 and *nicA*2 were synthesised by GeneArt (Germany) with codon optimisation for *Aspergillus niger*. The nucleotide sequence and the amino acid translations received from GeneArt on plasmids pMA or pMK are presented in Appendix to Chapter 3, Section A. 3.1.4.

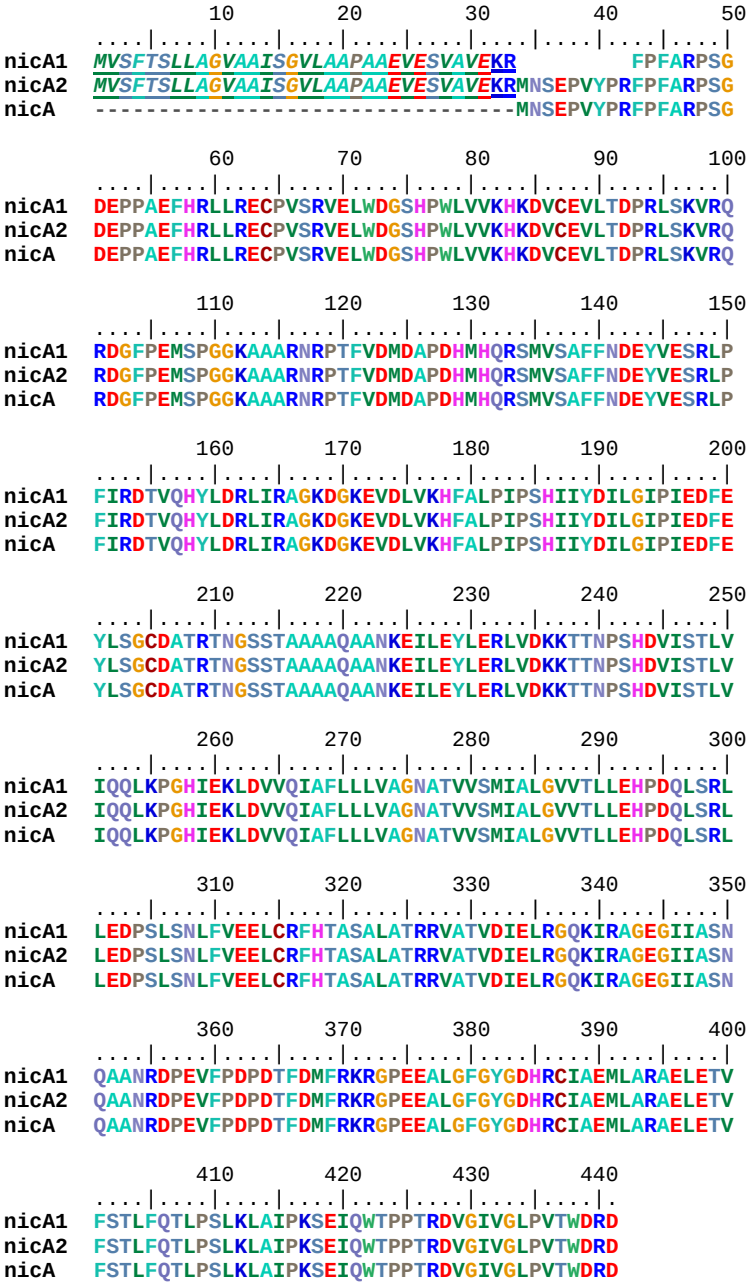

Figure A.3.1. Amino acid sequence alignment of *nicA* gene product. The underlined sequence is the inserted signal peptide sequence (*xyn2*) and the KEX2 cutting site (KR). The gene *nicA*1 codes for has nine amino acids (MNSEPVYPR) less than *nicA*2 and *nicA*. The amino acids sequences coded by *nicA*1 are continuous. The space between the KEX2 site and first *nicA*1 coded amino sequences acids is a result of the alignment algorithms from BioEdit Sequence Alignment Editor version 5.0.9 (USA).

A.3.1.2. Plasmid map for pGTP-*nicA*1 and pGTP-*nicA*2

The *nicA* gene was ligated to the pGTP plasmid at a *Not*1 restriction site and denoted as either pGTP-*nicA*1 or pGTP-*nicA*2. The *nicA* gene is placed under the control of the *gpd* promoter and its termination by the *gla* terminator. Plasmid pGTP has the backbone of plasmid pGTP1/pGTP, a derivative from pSPORT plasmid. Figure A.3.2 presents the plasmid maps of pGTP-*nicA*1 or pGTP-*nicA*2.

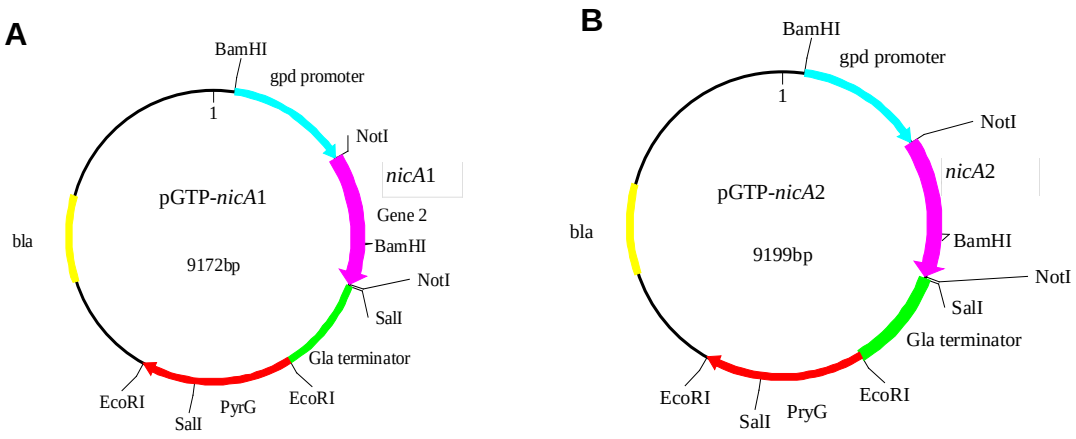

Figure A.3.2. Plasmid map of pGTP-*nicA*1 and pGTP-*nicA*2 of either 9172 (A) or 9199 (B) base pairs. The nucleotides code for numerous restriction digest enzyme sites (BamHI, NotI, SalI, EcoRI), the constitutive promoter *pgd* from *A. niger* and the *gla* terminator from *A. awamori*, a *PyrG* gene and a beta lactamase resistance gene, *bla*, as an antibiotic selection marker. Plasmid maps were generated with DNAMAN (Lynnon BioSoft, Canada).

A.3.1.3. pGTP plasmid map and restriction enzymes sites

pGTP1/pGTP: a pSPORT derivative containing *A. niger* gpd promoter (BamH1-Not1) and *A. awamor*i glucoamylase terminator (Sal1-EcoR1) is named pGTP1. The *PyrG* marker was inserted into the *Eco*RI site. The plasmid was kindly provided by Prof. W.H. van Zyl, University of Stellenbosch.

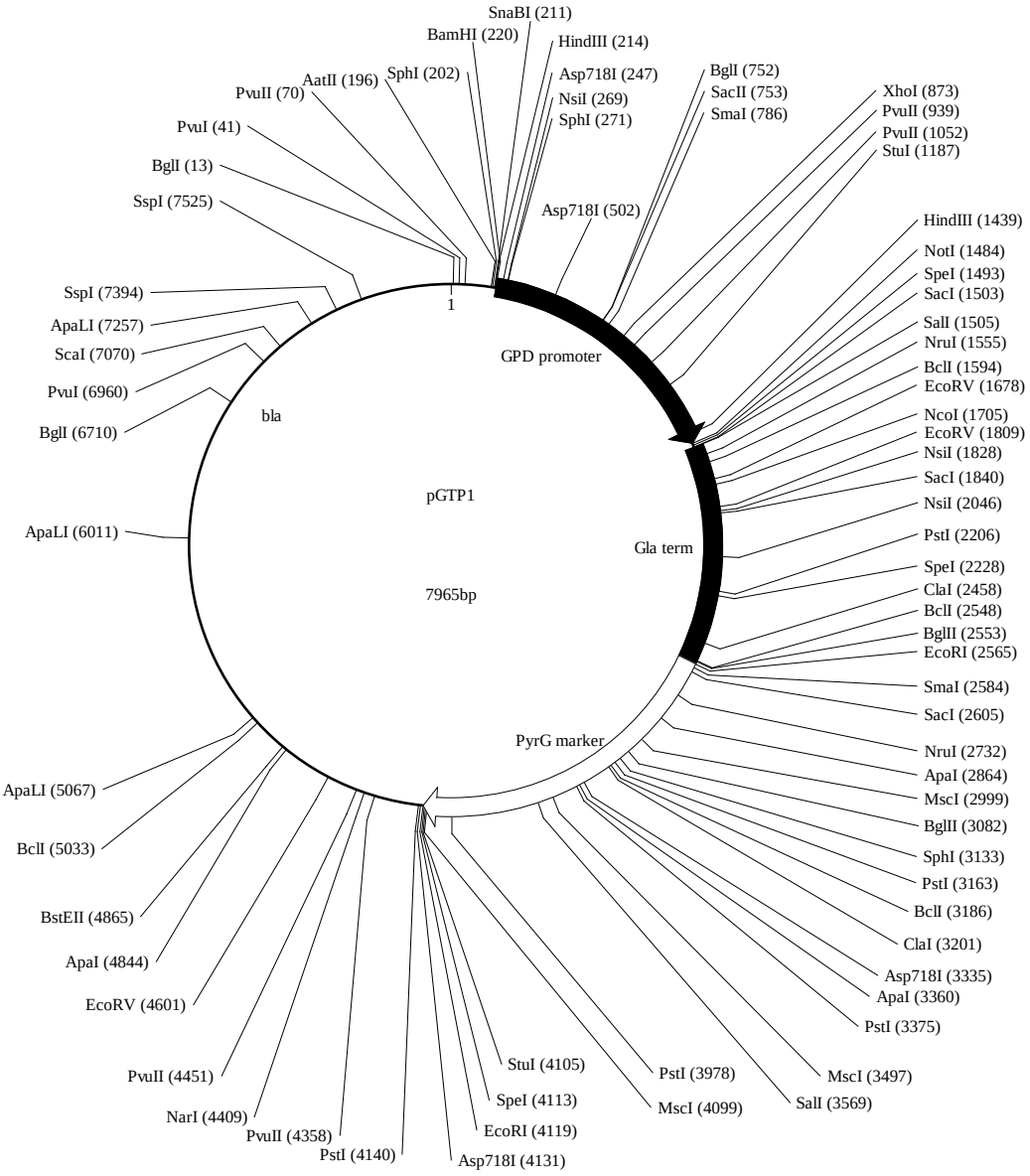

Figure A.3.3. Plasmid map of pGTP1. The plasmid sequence codes for *gdp* promotor, *gla* terminator and the auxotrophic marker (*PyrG*). The restriction enzyme digesting sites are listed. The plasmid map was provided by Dr S. Rose (University of Stellenbosch).

A.3.1.4. Sequences as received from GeneArt (Germany)

Gene 0915924 gene 2 (also *nicA*1)

```
GGTACCGCGGCCGCATGGTGTCCTTCACCTCCCTGCTCGCCGGCGTCGCCGCCATCTCTGGCGTCCTCGCTGCTC
CTGCCGCCGAGGTCGAGTCCGTCGCCGTCGAGAAGCGCTTCCCCTTCGCTCGCCCTTCCGGCGACGAGCCCCCTG
CCGAGTTCCACCGCCTCCTCCGCGAGTGCCCCGTGTCCCGCGTCGAGCTGTGGGATGGCTCCCACCCCTGGCTCG
TCGTCAAGCACAAGGATGTCTGCGAGGTCCTCACCGATCCCCGCCTCTCCAAGGTCCGCCAGCGCGACGGCTTCC
CCGAGATGTCCCCTGGCGGCAAGGCCGCTGCCCGCAACCGCCCCACCTTCGTCGATATGGATGCCCCCGATCACA
TGCACCAGCGCTCCATGGTGTCCGCTTTCTTCAACGATGAGTACGTCGAGTCCCGCCTCCCCTTCATCCGCGATA
CCGTCCAGCACTACCTCGATCGCCTCATCCGCGCTGGCAAGGACGGCAAAGAAGTCGATCTCGTCAAGCACTTCG
CCCTCCCCATCCCTTCCCACATCATCTACGATATCCTCGGCATCCCCATCGAGGATTTCGAGTACCTCTCCGGCT
GCGACGCCACCCGCACCAACGGCTCCTCCACCGCCGCTGCTGCCCAGGCCGCCAACAAAGAAATCCTCGAGTACC
TCGAGCGCCTCGTCGATAAGAAAACCACCAACCCCTCCCACGATGTCATCTCCACCCTCGTCATCCAGCAGCTCA
AGCCCGGCCACATCGAGAAGCTCGATGTCGTCCAGATCGCCTTCCTCCTCCTCGTCGCCGGCAACGCCACTGTCG
TGTCCATGATCGCTCTCGGCGTCGTCACCCTCCTCGAGCACCCCGATCAGCTCTCCCGCCTCCTCGAGGATCCCT
CCCTCTCCAACCTCTTCGTCGAGGAACTCTGCCGCTTCCACACCGCCTCCGCCTTGGCTACCCGTCGCGTCGCTA
CCGTCGATATCGAGCTGCGTGGCCAGAAGATCCGGGCTGGCGAGGGCATCATCGCCTCCAACCAGGCCGCTAACC
GTGATCCTGAGGTGTTCCCCGATCCCGATACCTTCGACATGTTCCGCAAGCGCGGTCCCGAGGAAGCCCTCGGCT
TCGGCTACGGCGATCATCGCTGTATTGCCGAGATGCTCGCTCGCGCCGAGCTGGAAACCGTGTTCTCCACTCTCT
TCCAGACCCTGCCCTCCCTGAAGCTCGCCATCCCCAAGTCCGAGATCCAGTGGACCCCCCCCACCCGTGACGTCG
GCATCGTCGGCCTCCCCGTCACTTGGGATCGTGATTGAGCGGCCGCGAGCTC
```

Pink: P450NOR F2 and P450NOR R1 primers (F1 only on Gene 3)
Yellow: P450NOR F1 (primer for Gene 2 and 3).
Green: *xyn2* and KEX site

```
1          GGTACCGCGGCCGCATGGTGTCCTTCACCTCCCTGCTCGCCGGCGTCGCCGCCATCTCTG
1             Y  R  G  R  M  V  S  F  T  S  L  L  A  G  V  A  A  I  S

61         GCGTCCTCGCTGCTCCTGCCGCCGAGGTCGAGTCCGTCGCCGTCGAGAAGCGCTTCCCCT
20         G  V  L  A  A  P  A  A  E  V  E  S  V  A  V  E  K  R  F  P

121        TCGCTCGCCCTTCCGGCGACGAGCCCCCTGCCGAGTTCCACCGCCTCCTCCGCGAGTGCC
40         F  A  R  P  S  G  D  E  P  P  A  E  F  H  R  L  L  R  E  C

181        CCGTGTCCCGCGTCGAGCTGTGGGATGGCTCCCACCCCTGGCTCGTCGTCAAGCACAAGG
60         P  V  S  R  V  E  L  W  D  G  S  H  P  W  L  V  V  K  H  K

241        ATGTCTGCGAGGTCCTCACCGATCCCCGCCTCTCCAAGGTCCGCCAGCGCGACGGCTTCC
80         D  V  C  E  V  L  T  D  P  R  L  S  K  V  R  Q  R  D  G  F

301        CCGAGATGTCCCCTGGCGGCAAGGCCGCTGCCCGCAACCGCCCCACCTTCGTCGATATGG
100        P  E  M  S  P  G  G  K  A  A  A  R  N  R  P  T  F  V  D  M

361        ATGCCCCCGATCACATGCACCAGCGCTCCATGGTGTCCGCTTTCTTCAACGATGAGTACG
120        D  A  P  D  H  M  H  Q  R  S  M  V  S  A  F  F  N  D  E  Y

421        TCGAGTCCCGCCTCCCCTTCATCCGCGATACCGTCCAGCACTACCTCGATCGCCTCATCC
140        V  E  S  R  L  P  F  I  R  D  T  V  Q  H  Y  L  D  R  L  I

481        GCGCTGGCAAGGACGGCAAAGAAGTCGATCTCGTCAAGCACTTCGCCCTCCCCATCCCTT
160        R  A  G  K  D  G  K  E  V  D  L  V  K  H  F  A  L  P  I  P

541        CCCACATCATCTACGATATCCTCGGCATCCCCATCGAGGATTTCGAGTACCTCTCCGGCT
```

```
180       S  H  I  I  Y  D  I  L  G  I  P  I  E  D  F  E  Y  L  S  G

601       GCGACGCCACCCGCACCAACGGCTCCTCCACCGCCGCTGCTGCCCAGGCCGCCAACAAAG
200       C  D  A  T  R  T  N  G  S  S  T  A  A  A  A  Q  A  A  N  K

661       AAATCCTCGAGTACCTCGAGCGCCTCGTCGATAAGAAAACCACCAACCCCTCCCACGATG
220       E  I  L  E  Y  L  E  R  L  V  D  K  K  T  T  N  P  S  H  D

721       TCATCTCCACCCTCGTCATCCAGCAGCTCAAGCCCGGCCACATCGAGAAGCTCGATGTCG
240       V  I  S  T  L  V  I  Q  Q  L  K  P  G  H  I  E  K  L  D  V

781       TCCAGATCGCCTTCCTCCTCCTCGTCGCCGGCAACGCCACTGTCGTGTCCATGATCGCTC
260       V  Q  I  A  F  L  L  L  V  A  G  N  A  T  V  V  S  M  I  A

841       TCGGCGTCGTCACCCTCCTCGAGCACCCCGATCAGCTCTCCCGCCTCCTCGAGGATCCCT
280       L  G  V  V  T  L  L  E  H  P  D  Q  L  S  R  L  L  E  D  P

901       CCCTCTCCAACCTCTTCGTCGAGGAACTCTGCCGCTTCCACACCGCCTCCGCCTTGGCTA
300       S  L  S  N  L  F  V  E  E  L  C  R  F  H  T  A  S  A  L  A

961       CCCGTCGCGTCGCTACCGTCGATATCGAGCTGCGTGGCCAGAAGATCCGGGCTGGCGAGG
320       T  R  R  V  A  T  V  D  I  E  L  R  G  Q  K  I  R  A  G  E

1021      GCATCATCGCCTCCAACCAGGCCGCTAACCGTGATCCTGAGGTGTTCCCCGATCCCGATA
340       G  I  I  A  S  N  Q  A  A  N  R  D  P  E  V  F  P  D  P  D

1081      CCTTCGACATGTTCCGCAAGCGCGGTCCCGAGGAAGCCCTCGGCTTCGGCTACGGCGATC
360       T  F  D  M  F  R  K  R  G  P  E  E  A  L  G  F  G  Y  G  D

1141      ATCGCTGTATTGCCGAGATGCTCGCTCGCGCCGAGCTGGAAACCGTGTTCTCCACTCTCT
380       H  R  C  I  A  E  M  L  A  R  A  E  L  E  T  V  F  S  T  L

1201      TCCAGACCCTGCCCTCCCTGAAGCTCGCCATCCCCAAGTCCGAGATCCAGTGGACCCCCC
400       F  Q  T  L  P  S  L  K  L  A  I  P  K  S  E  I  Q  W  T  P

1261      CCACCCGTGACGTCGGCATCGTCGGCCTCCCCGTCACTTGGGATCGTGATTGAGCGGCCG
420       P  T  R  D  V  G  I  V  G  L  P  V  T  W  D  R  D  *  A  A

1321      CGAGCTC
440       A  S
```

Gene 0915923 gene3 (also *nicA*2)

GGTACCGCGGCCGCATGGTGTCCTTCACCTCCCTGCTCGCCGGCGTCGCCGCCATCTCTGGCGTCCTCGCTGCTC
CTGCCGCCGAGGTCGAGTCCGTCGCCGTCGAGAAGCGCATGAACTCCGAGCCCGTCTACCCCCGCTTCCCCTTCG
CTCGCCCTTCCGGCGACGAGCCCCCTGCCGAGTTCCACCGCCTCCTCCGCGAGTGCCCCGTGTCCCGCGTCGAGC
TGTGGGATGGCTCCCACCCCTGGCTCGTCGTCAAGCACAAGGATGTCTGCGAGGTCCTCACCGATCCCCGCCTCT
CCAAGGTCCGCCAGCGCGACGGCTTCCCCGAGATGTCCCCTGGCGGCAAGGCCGCTGCCCGCAACCGCCCCACCT
TCGTCGATATGGATGCCCCCGATCACATGCACCAGCGCTCCATGGTGTCCGCTTTCTTCAACGATGAGTACGTCG
AGTCCCGCCTCCCCTTCATCCGCGATACCGTCCAGCACTACCTCGATCGCCTCATCCGCGCTGGCAAGGACGGCA
AAGAAGTCGATCTCGTCAAGCACTTCGCCCTCCCCATCCCTTCCCACATCATCTACGATATCCTCGGCATCCCCA
TCGAGGATTTCGAGTACCTCTCCGGCTGCGACGCCACCCGCACCAACGGCTCCTCCACCGCCGCTGCTGCCCAGG
CCGCCAACAAAGAAATCCTCGAGTACCTCGAGCGCCTCGTCGATAAGAAAACCACCAACCCCTCCCACGATGTCA
TCTCCACCCTCGTCATCCAGCAGCTCAAGCCCGGCCACATCGAGAAGCTCGATGTCGTCCAGATCGCCTTCCTCC
TCCTCGTCGCCGGCAACGCCACTGTCGTGTCCATGATCGCTCTCGGCGTCGTCACCCTCCTCGAGCACCCCGATC
AGCTCTCCCGCCTCCTCGAGGATCCCTCCCTCTCCAACCTCTTCGTCGAGGAACTCTGCCGCTTCCACACCGCCT
CCGCCTTGGCTACCCGTCGCGTCGCTACCGTCGATATCGAGCTGCGTGGCCAGAAGATCCGGGCTGGCGAGGGCA
TCATCGCCTCCAACCAGGCCGCTAACCGTGATCCTGAGGTGTTCCCCGATCCCGATACCTTCGACATGTTCCGCA
AGCGCGGTCCCGAGGAAGCCCTCGGCTTCGGCTACGGCGATCATCGCTGTATTGCCGAGATGCTCGCTCGCGCCG
AGCTGGAAACCGTGTTCTCCACTCTCTTCCAGACCCTGCCCTCCCTGAAGCTCGCCATCCCCAAGTCCGAGATCC
AGTGGACCCCCCCCACCCGTGACGTCGGCATCGTCGGCCTCCCCGTCACTTGGGATCGTGATTGAGCGGCCGCGA
GCTC

Pink: P450NOR F2 and P450NOR R1 primers (F1 only on Gene 3)
Yellow: P450NOR F1 (primer for Gene 2 and 3).
Green: *xyn2* and KEX site
Blue: Gene 3 start codon and P450nor

```
1          GGTACCGCGGCCGCATGGTGTCCTTCACCTCCCTGCTCGCCGGCGTCGCCGCCATCTCTG
1                        M  V  S  F  T  S  L  L  A  G  V  A  A  I  S

61         GCGTCCTCGCTGCTCCTGCCGCCGAGGTCGAGTCCGTCGCCGTCGAGAAGCGCATGAACT
20         G  V  L  A  A  P  A  A  E  V  E  S  V  A  V  E  K  R  M  N

121        CCGAGCCCGTCTACCCCCGCTTCCCCTTCGCTCGCCCTTCCGGCGACGAGCCCCCTGCCG
40         S  E  P  V  Y  P  R  F  P  F  A  R  P  S  G  D  E  P  P  A

181        AGTTCCACCGCCTCCTCCGCGAGTGCCCCGTGTCCCGCGTCGAGCTGTGGGATGGCTCCC
60         E  F  H  R  L  L  R  E  C  P  V  S  R  V  E  L  W  D  G  S

241        ACCCCTGGCTCGTCGTCAAGCACAAGGATGTCTGCGAGGTCCTCACCGATCCCCGCCTCT
80         H  P  W  L  V  V  K  H  K  D  V  C  E  V  L  T  D  P  R  L

301        CCAAGGTCCGCCAGCGCGACGGCTTCCCCGAGATGTCCCCTGGCGGCAAGGCCGCTGCCC
100        S  K  V  R  Q  R  D  G  F  P  E  M  S  P  G  G  K  A  A  A

361        GCAACCGCCCCACCTTCGTCGATATGGATGCCCCCGATCACATGCACCAGCGCTCCATGG
120        R  N  R  P  T  F  V  D  M  D  A  P  D  H  M  H  Q  R  S  M

421        TGTCCGCTTTCTTCAACGATGAGTACGTCGAGTCCCGCCTCCCCTTCATCCGCGATACCG
140        V  S  A  F  F  N  D  E  Y  V  E  S  R  L  P  F  I  R  D  T

481        TCCAGCACTACCTCGATCGCCTCATCCGCGCTGGCAAGGACGGCAAAGAAGTCGATCTCG
160        V  Q  H  Y  L  D  R  L  I  R  A  G  K  D  G  K  E  V  D  L

541        TCAAGCACTTCGCCCTCCCCATCCCTTCCCACATCATCTACGATATCCTCGGCATCCCCA
180        V  K  H  F  A  L  P  I  P  S  H  I  I  Y  D  I  L  G  I  P

601        TCGAGGATTTCGAGTACCTCTCCGGCTGCGACGCCACCCGCACCAACGGCTCCTCCACCG
200        I  E  D  F  E  Y  L  S  G  C  D  A  T  R  T  N  G  S  S  T
```

```
661       CCGCTGCTGCCCAGGCCGCCAACAAAGAAATCCTCGAGTACCTCGAGCGCCTCGTCGATA
220       A  A  A  A  Q  A  A  N  K  E  I  L  E  Y  L  E  R  L  V  D

721       AGAAAACCACCAACCCCTCCCACGATGTCATCTCCACCCTCGTCATCCAGCAGCTCAAGC
240       K  K  T  T  N  P  S  H  D  V  I  S  T  L  V  I  Q  Q  L  K

781       CCGGCCACATCGAGAAGCTCGATGTCGTCCAGATCGCCTTCCTCCTCCTCGTCGCCGGCA
260       P  G  H  I  E  K  L  D  V  V  Q  I  A  F  L  L  L  V  A  G

841       ACGCCACTGTCGTGTCCATGATCGCTCTCGGCGTCGTCACCCTCCTCGAGCACCCCGATC
280       N  A  T  V  V  S  M  I  A  L  G  V  V  T  L  L  E  H  P  D

901       AGCTCTCCCGCCTCCTCGAGGATCCCTCCCTCTCCAACCTCTTCGTCGAGGAACTCTGCC
300       Q  L  S  R  L  L  E  D  P  S  L  S  N  L  F  V  E  E  L  C

961       GCTTCCACACCGCCTCCGCCTTGGCTACCCGTCGCGTCGCTACCGTCGATATCGAGCTGC
320       R  F  H  T  A  S  A  L  A  T  R  R  V  A  T  V  D  I  E  L

1021      GTGGCCAGAAGATCCGGGCTGGCGAGGGCATCATCGCCTCCAACCAGGCCGCTAACCGTG
340       R  G  Q  K  I  R  A  G  E  G  I  I  A  S  N  Q  A  A  N  R

1081      ATCCTGAGGTGTTCCCCGATCCCGATACCTTCGACATGTTCCGCAAGCGCGGTCCCGAGG
360       D  P  E  V  F  P  D  P  D  T  F  D  M  F  R  K  R  G  P  E

1141      AAGCCCTCGGCTTCGGCTACGGCGATCATCGCTGTATTGCCGAGATGCTCGCTCGCGCCG
380       E  A  L  G  F  G  Y  G  D  H  R  C  I  A  E  M  L  A  R  A

1201      AGCTGGAAACCGTGTTCTCCACTCTCTTCCAGACCCTGCCCTCCCTGAAGCTCGCCATCC
400       E  L  E  T  V  F  S  T  L  F  Q  T  L  P  S  L  K  L  A  I

1261      CCAAGTCCGAGATCCAGTGGACCCCCCCCACCCGTGACGTCGGCATCGTCGGCCTCCCCG
420       P  K  S  E  I  Q  W  T  P  P  T  R  D  V  G  I  V  G  L  P

1321      TCACTTGGGATCGTGATTGAGCGGCCGCGAGCTC
440       V  T  W  D  R  D  *  A  A  A  S
```

A.3.2. DNA manipulation reactions

A.3.2.1. Restriction enzyme digest reaction

For the restriction enzyme digests in a total reaction volume 17 µl, 10 µl DNA, 2 µl 10× restriction enzyme buffer, 2 µl of enzyme, 0.2 µl 1% (w/v) BSA and 2.8 µl dd H_2O were mixed and incubated at 37˚C for 3 hours. Restriction enzyme buffer B contained 10 mM TRIS-HCl, 5 mM $MgCl_2$, 100 mM NaCl, 1 mM 2-Mercaptoethanol with a pH of 8 at 37˚C. The restriction enzyme buffer H contained 50 mM TRIS-HCl, 10 mM $MgCl_2$, 100 mM NaCl, 1 mM Dithioerythritol (DTE), pH 7.5 at 37˚C. Restriction enzyme buffer B was used for BamHI (10 $U.\mu l^{-1}$, Roche) and HindIII (10 $U.\mu l^{-1}$, Roche) digests and restriction buffer H was used with EcoRI (10 $U.\mu l^{-1}$, Roche), XhoI (10 $U.\mu l^{-1}$, Roche) and NotI (10 $U.\mu l^{-1}$, NEB, UK) digests.

A.3.2.2. Nucleotide gel electrophoresis

A 0.8% (w/v) agarose Techcomp gel (LTD, Hong Kong, Cat # 9201) was prepeared in 1× TAE (TRIS acetate EDTA) buffer and 5 µl of ethidium bromide solution (Sigma-Aldrich) was added. A current of 80 volts was applied to the gel for DNA fragments separation over 20 minutes. Restriction enzyme digested λ DNA was used as molecular size markers.

A.3.2.3. Ligation reaction

For the DNA ligation to the plasmid pGTP, 2 µl DNA, 2 µl 10× buffer, 2 µl ligase T4 (5 $U.\mu l^{-1}$, Roche) and dd H_2O in a total reaction volume of 20 µl, were mixed and incubated at room temperature for 4 hours.

A.3.2.4. PCR reaction to identify *E. coli* colonies containing the gene of interest

PCR reaction in 50 µl contained 0.25 µl of 10× Ex Taq (5 U.µl^{-1}, TakaRa), 4 µl NTP, 1 µl DNA, 6 µl pGTP forward primer, 6 µl pGTP reverse primer and 27 µl dd H_2O with thermocycling of: (2" 94˚C, 2" 40˚C) × 1; (1' 30" 72˚C, 1'94˚C, 1' 50˚C) × 25 and (7' 72˚C, 4˚C until stopped) × 1 in a GeneAmp PCR System 9700 (Applied Biosystems).

A 1.4 kbp DNA fragment was anticipated with the pGTP primers (kindly provided by Dr Shaunita Rose (University of Stellenbosch)

pGTP primers:

forward primer (F1): TTCCGCTTCCTCGCTCACT

reverse primer (R1): GGCTGCGGCGAGCGGTATC

A.3.2.5. Genomic DNA extraction from mycelia

Mycelia cultured in minimal medium for 2 days were harvested by filtering through Myra cloth (Calbiochem, Merck Millipore) and rinsed twice with dd H_2O. Excess water was removed by squeezing the mycelia. The mycelia were snap frozen with liquid nitrogen in a porcelain mortar and then crushed to a fine powder. The powder was transferred to a reaction tube and 400 µl of STE buffer (sodium chloride TRIS EDTA buffer, pH 8) together with 400 µl of PCI (phenol: chloroform: isopropanol; 2:1:1) were added to the powder. The mixture was briefly mixed and incubated on ice for 1 hour. The supernatant was transferred to a new tube after centrifugation at 13000 ×*g* for 5 minutes and 400 µl of PCI was added. This was repeated once more. Thereafter, 700 µl of chloroform isopropanol was added to supernatant and subjected to centrifugation (as above). A 1/50 volume of 5 M NaCl and 1 volume 100% ethanol were added to the supernatant. The mixture was gently mixed and centrifuged again for 5 minutes. The pellet was washed once with 1 ml 70% (v/v) ethanol and then dried in an oven. A small volume (50 µl) of dd H_2O was added to the pellet. The pellet was allowed to re-hydrate over night at room temperature. Thereafter, it was stored at 4˚C.

A.3.3. Growing of *A. niger* in culture

A.3.3.1. Culture medium composition and agar plates

Table A.3.1. Media composition for *A. niger* fermentation.

Media (% w/v)	MM	2MM	3MM	MM+H	TF agar	SP agar
Glucose	1.0	10	20	1.0	1.0	1.0
Yeast Extract	0.5	1.0	1.5	0.5		0.1
$MgSO_4.7H_2O$	0.04	0.08	0.16	0.04	0.04	
Cas AA	0.2	0.4	0.6	0.2		0.1
Neopeptone						0.2
Oxoid agar					1.5	
Sorbitol					21.9	
Bacteriological agar						1.8
AspA*	2	4	6	2	2	2
TE*	0.1	0.2	0.3	0.1	0.1	0.1
Bovine haemoglobin#				1		

*(% v/v); # $g.L^{-1}$; Cas AA: cas amino acid (Difco Bacto); TE: trace elements

A.3.3.2. Reagents and preparation of stock solutions

1) 20× AspA solution:

A 20× AspA solution contained 30% $NaNO_3$, 2.6% KCl and 7% KH_2PO_4, all (w/v).

2) 0.6 M $NaCl/CaCl_2$ solution

The 0.6 M $NaCl/CaCl_2$ were solution was prepared as follows: 39.7 g of $CaCl_2.2H_2O$ and 34.8 g NaCl dissolved in 1 L water and autoclaved for 20 minutes.

3) 1000× trace element solution (TE):

The stock solution of trace elements contained the following chemical constituents: 2.2% $ZNSO_4.7H_2O$, 1.1% H_3BO_3, 0.5% $MnCl_2.4H_2O$, 0.5% $FeSO_4.7H_2O$, 0.17% $CoCl_2.6H_2O$, 0.16% $CuSO_4.5H_2O$, 0.15% $Na_2MoO_4.H_2O$ and 5% EDTA (no Na salt), all (w/v).

4) STC 1700 solution:

A STC 1700 solution was prepared with the following reagents: 21.8% sorbitol, 0.74% $CaCl_2.2H_2O$, 0.02% NaCl in (w/v), 0.1% of 1 M TRIS buffer (pH 7.5) in (v/v).

5) PEG 4000 solution:

A PEG 4000 solution contained: 60% PEG 4000, 0.74% $CaCl_2$ in (w/v), 1% 1 M TRIS buffer (pH 7.5) in (v/v).

6) Transformation plates:

The transformation plates were prepared from the following reagents: 0.04% $MgSO_4.7H_2O$, 1% glucose, 1.5% oxoid agar (Oxoid LP0011, Basingstocke, England), 21.86% sorbitol all in (w/v) and were prepared in dd H_2O. This solution was autoclaved and thereafter 2% of 50× AspA and 0.1% of TE solution in (v/v) was added.

7) Spore plates:

Minimal media with nitrate, 1% glucose, 0.2% neopeptone (trypticase BBL), 0.1% yeast extract (Merck Biolab), 0.1% casamino acid all in (w/v) and 0.8% bacterial agarose was prepared in dd H_2O and sterilised by autoclaving the solution for 20 minutes.

8) Bovine haemoglobin solution:

Haemoglobin was dissolved in 50 ml of dd H_2O overnight. The haemoglobin solution was added to sterile MM to a final concentration of 1 $g.L^{-1}$ and mixed. The particulate matter was removed by centrifugation for 20 minutes at 10000 ×*g*. Thereafter the MM+haemoglobin solution was filter sterilized through a 0.22 µm DuraPore PVDF membrane Stericup filter units (Merck Millipore).

9) Colloidal Coomassie brilliant blue stain:

Ammonium sulfate (100 g, $H_8N_2O_4S$) was dissolved in 600 ml dd H_2O, then 1 g of Coomassie G-250 (Sigma-Aldirch, Germany) was added and dissolved. Thereafter, ortho phosphoric acid was added to a final concentration of 30% (v/v) to which 20% (v/v) ethanol was added for final volume of 1 L. Reagents were obtained from Sigma-Aldrich and were of analytical grade. This protocol is an adaptation to the protocol reported by Neuhoff *et al.* (1988) [396].

10) Protein precipitation for SDS-PAGE electrophoresis:

The protocol from Bio-Rad 2D clean up kit (Cat # 163-2130) was followed with the following reagents prepared in the laboratory:

Precipitation reagent 1: 10% trichloroacetic acid, 4 M NaCl

Precipitation reagent 2: 0.1% sodium deoxycholate

Wash reagent 1: 50% acetone (v/v)

Wash reagent 2: 20% acetone (-20˚C) (v/v)

Wash additive: 1.5% starch (v/v)

A.3.3.3. Spore maintenance

Spores from the glycerol stock (which were stored at -80˚C) were used to generate a spore solution. The spores from the glycerol stock were plated onto spore plates and incubated at 37˚C. After 4 days, the spores were harvested with sterile 0.9% (v/v) physiological saline and were counted with a Neubauer haemocytometer (Brand, Germany) to determine the spore concentration. The spore solution was stored at 4˚C for a maximum of three months before it was discarded and fresh spore solution was generated. Sporulation of *A. niger* mycelia was induced on minimal medium agar plates with nitrate, 1% glucose (w/v), 0.2% trypticase (BBL) (w/v), 0.1% yeast extract (w/v) and 0.1% (w/v) casamino acids, 0.04% $MgSO_4$ (w/v), 6% $NaNO_3$ in (w/v) trace elements as well as 0.015M uridine (for *PyrG*$^-$) and without uridine for transformed *A. niger* D 15.

A.3.3.4. Screening for Anor expression by *A. niger* D15

For the screeingin of Anor expressing A. niger D15 transformants, 50 ml culture medium was inoculated with the spores of the 116 transformants (containing a 1.4 kbp insert with correct orientation). The spend culture medium was tested for nitric oxide reductase (NOR) activity. The NADH reduction rate was categoriesd to identify the transformant presenting the highest NOR activity (Table A.3.2).

Table A.3.2. Categorisation of NADH reduction for NOR activity

NADH reduction rate	NOR activity
0 < 19	None
20 < 39	Low
40 < 59	Medium
60 < 79	High
80 < above	Very high

The NOR activity determined by the cultured transformants is presened in Table A.3.3. Only a few of the transformants of the 116 evaluated, presented high to very high NOR activity (0.4% for pGTP-*nicA*1 and 5% for pGTP-*nicA*2).

Table A.3.3. NOR activity from *A. niger* D15 transformants determined after 3 days

	% of total transformants cultured	
NOR activity	pGTP-*nicA*1	pGTP-*nicA*2
None	84.3	75.2
Low	13.6	16.1
Medium	1.6	3.7
High	0.2	2.7
Very High	0.2	2.3

It was observed that the mycelial increased with time and thus it was considered essential to evalualte the NOR activity after 3 days in culture and and after 7 days.

A.3.3.5. Screening of NOR activity from transformants cultured in two different glucose concentrations in culture media after 3 and 7 days

Culture conditions such as glucose concentration and yeast content contribute to the protein expression and production in *A. niger* [228, 397], and therefore the transformants were cultured in two different strengths of minimal medium. NOR activity was determined from 50 ml cultures in minimal medium (MM) and double strength minimal medium (2MM) after 3 days (refer to Table A.3.5). Furthermore, it was observed by Sharma *et al.* (2009), that some proteins were expressed during the exponential phase and others during stationary phase [398]. Therefore, NOR activity was assayed on day 3 and day 7 (refer to Table A.3.6).

Table A.3.4. NOR activity from *A. niger* D15 transformants in two different culture media after 3 days.

	% of total transformants cultured			
	pGTP-*nicA*1		pGTP-*nicA*2	
NOR Activity	MM	2MM	MM	2MM
None	85.3	80.2	90.2	69.3
Low	13.8	12.3	3.3	22.2
Medium	0.9	4.7	0.8	4.6
High	0.0	1.9	3.3	1.3
Very High	0.0	0.9	2.4	2.6

Table A.3.5. NOR activity in culture media from *A. niger* D15 transformants measured after 3 and 7 days.

NOR activity	% of total transformants cultured			
	pGTP-*nicA*1		pGTP-*nicA*2	
%	day 3	day 7	day 3	day 7
None	62.5	64.6	83.5	78.7
Low	30.6	34.2	15.6	11.2
Medium	4.2	1.2	0.9	6.7
High	1.4	0	0	1.1
Very High	1.4	0	0	2.2

From the NOR activity screening process, it was observed that there are slight differences between *A. niger* D15[*nicA*1] (pGTP-*nicA*1) or *A. niger* D15[*nicA*2] (pGTP-*nicA*2) with their NOR activity in MM or 2MM as well as day 3 or day 7. *A. niger* D15[*nicA*1] showed medium to very high NOR activity in 2MM and at day 3, whereas *A. niger* D15[*nicA*2] showed medium to very high NOR activity in MM and 2MM. High to very high NOR activity was observed at day 7. These findings were used to select one transformant from each plasmid construct to investigate the effect of glucose concentration, agitation, inoculum and haemoglobin supplementation in a simulated fed-batch culture on NOR activity.

A.3.3.6. Optimisation of culture conditions for maximal Anor production

A.3.3.6.1. Glucose concentration and agitation

Wang *et al*. (2003) [228] observed that the initial glucose concentration and agitation intensity affected the development of biomass. Therefore, *A. niger* transformants containing either pGTP-*nicA*1 or pGTP-*nicA*2, were cultured in three different strengths of 200 ml minimal medium at two different agitation intensities (100 rpm and 200 rpm). The NOR activity was monitored every 24 hours and the highest NOR activity was observed on day 4 and day 5 with MM at 100 rpm and 200 rpm for *A. niger* D15[*nicA*1] as indicated in Figure A.3.4. At first, *A. niger* D15[*nicA*1] was cultured in medium in which the glucose was autoclaved together with the other medium components resulting in the Maillard reaction (complex glucose). This resulted in low NOR activity, thus this experiment was repeated and the NOR activity was measured from *A. niger* D15[*nicA*1] cultured in medium to which glucose was added aseptically to the hot autoclaved cultured media. Both culturing procedures were repeated for *A. niger* D15[*nicA*2] as shown in Figure A.3.5.

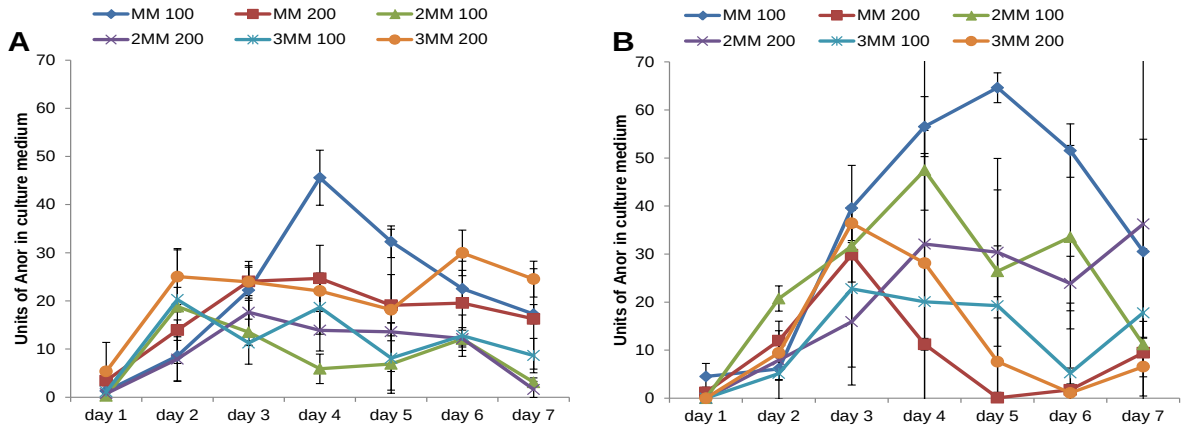

Figure A.3.4. The effect of culture media and agitation on NOR activity from *A. niger* D15[*nicA*1]. Different strengths of 200 ml minimal media (MM, 2MM and 3MM) were inoculated with *A. niger* D15[*nicA*1] spores (0.5×10^6.ml^{-1}) and were cultured with agitation at 100 rpm and 200 rpm at 30˚C. In (A), cultured media contained complex glucose by the Maillard reactions and in (B), the glucose was added aseptically to the culture media. NOR activity was monitored every 24 hours. Each data point is the average from triplicate culture flasks. A high variability was observed and thus no statistical difference is presented here.

For *A. niger* D15[*nicA*2], the highest NOR activity was observed at day 3 under the different culture conditions. Culture media with the highest NOR activity was observed when *A. niger* D15[*nicA*2] was cultured in MM with 100 rpm and 200 rpm

agitation as indicated in Figure A.3.5. It appears that the Maillard reactions did not alter the NOR activity (Fig. A.3.5. A), nor did the increase in medium concentration benefit NOR activity (Fig. A.3.5 B).

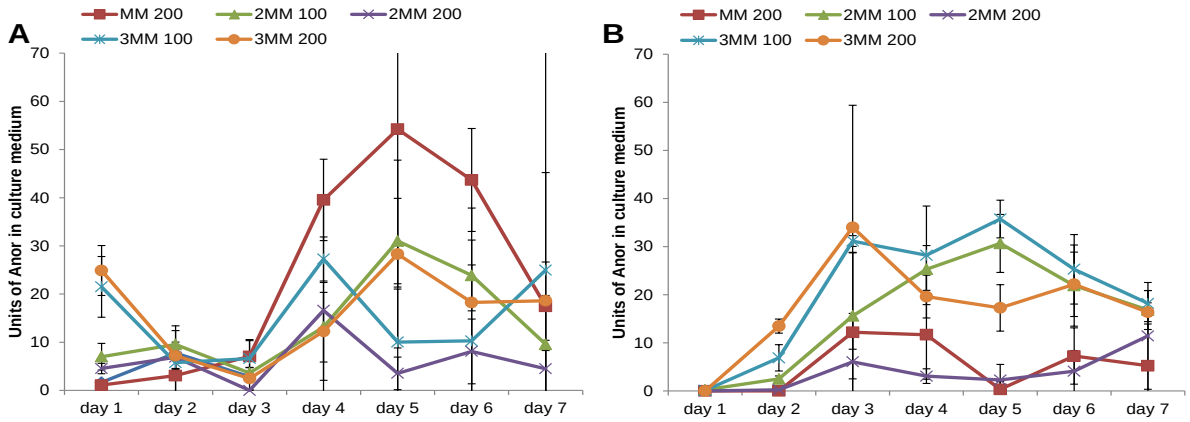

Figure A.3.5. The effect of culture media and agitation on NOR activity from *A. niger* D15[*nicA*2]. Different strengths of 200 ml minimal media (MM, 2MM and 3MM) were with inoculated *A. niger* D15[*nicA*2] spores (0.5×10^6.ml^{-1}) and were cultured with agitation at 100 rpm and 200 rpm at 30˚C. In (A), cultured media contained complex glucose by the Maillard reactions and in (B), the glucose was added aseptically to the culture media. NOR activity was monitored every 24 hours. Each data point is the average from triplicate culture flasks. No statistical difference was observed. MM 100 culture was contaminated on day 3 and excluded from this study.

It was observed that 2MM and 3MM resulted in small mycelial pellets whereas MM favoured the development of larger mycelia pellets (Fig. A.3.6). Gordon *et al.* (2000) [399] proposed that protein secretion takes place at the tips of mycelia, which would translate to more protein sections. Therefore, the larger mycelial pellet may have favoured Anor section which was observed as higher NOR activity in the culture medium.

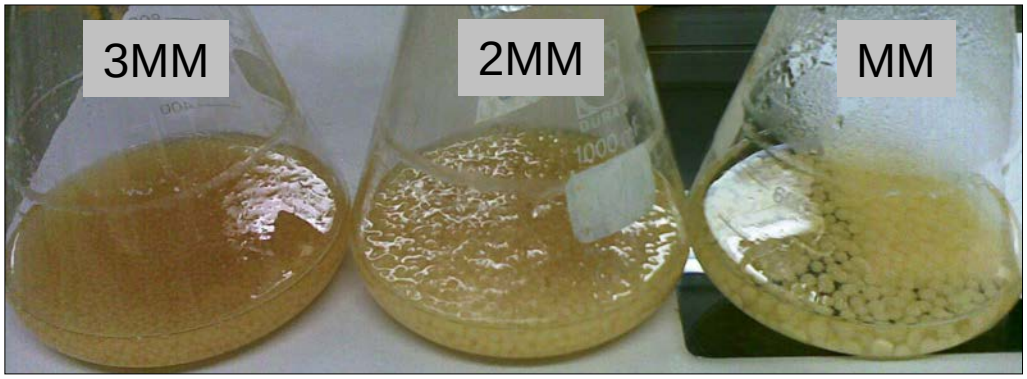

Figure A.3.6. Mycelia of *A. niger* D15[*nicA*2] after 2 days in culture. Culture media composition determined mycelia pellet size and possible NOR activity.

For both, *A. niger* D15[*nicA*1] and *A. niger* D15[*nicA*2], MM showed to be most favourable in yielding high NOR activity. The addition of glucose to autoclaved media resulted a in higher NOR activity for *A. niger* D15[*nicA*1] (Fig. A.3.4 B). Therefore this was followed for all subsequent culturing experiments. Furthermore, the other strengths of the media, 2MM and 3MM did not increase NOR activity and thus further culturing was done only with MM.

A.3.3.6.2. Spore inoculum

Xu and his colleagues (2000) [231] observed that the spore inoculum contributes to the pellet size of filamentous fungi in submerged cultures. Papagianni and colleagues (2004) [232] also described a relationship between inoculums, pellet aggregation and protein secretion. Therefore, four different spore inoculums were investigated for their effect on NOR activity in culture media. Since minimal medium with simple glucose (Fig. A.3.4 B) has shown the highest NOR activity for *A. niger* D15[*nicA*1], MM was also used in this study. As before, 200 ml of MM was inoculated with either 0.5 × 10^6 spores.ml^{-1}, 1.5 × 10^6 spores.ml^{-1}, 4.5 × 10^6 spores.ml^{-1} or 13.5 × 10^6 spores.ml^{-1}. Each inoculum was performed in triplicate. The flasks were incubated for 7 days at 30˚C with 100 rpm agitation. Nitric oxide reductase activity was measured every 24 hours. Neither spore inoculation method showed significant increase of nitric oxide reductase activity (Fig. A.3.7), but a difference in pellet size was observed (data not shown).

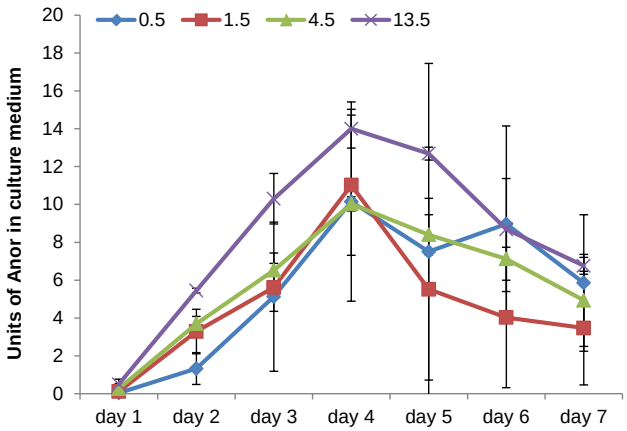

Figure A.3.7. The effect of spore inoculum on *A. niger* D15[*nicA*1]. *A. niger* D15[*nicA*1] was cultured in MM for 7 days at 30˚C with 100 rpm agitation. Four different concentrations of spores were added to 200 ml of MM: 0.5 x 10^6 spores.ml^{-1} (0.5), 1.5 x 10^6 spores.ml^{-1} (1.5), 4.5 x 10^6 spores.ml^{-1} (4.5) or 13.5 x 10^6 spores.ml^{-1} (13.5). The NOR activity was measured every 24 hours. Each data point is the average from triplicate culture flasks for which the NOR assay was also conducted in triplicates. No statistical difference was observed.

A.3.3.6.3. Supplementation with haemoglobin

The nitric oxide reductase, P450nor, from *A. oryzae* (Anor) belongs to the P450 superfamily which has a haem in its active site [104, 140]. The synthesis of haem is complex process [238] and might pose a bottleneck for the synthesis of Anor in *A. niger* D15. The addition of haemoglobin to the culture medium has been shown to increase the activity of haem peroxidase between 7 to 10 fold in comparison to the enzyme activity in non-supplemented media [400]. Both *A. niger* transformants, D15[*nicA*1] and D15[*nicA*2], were cultured in MM supplemented either with autoclaved or filtered bovine haemoglobin solution to determine its effect on the yield of active Anor (Fig. A.3.8). Supplementation with haem increased NOR activity only for *A. niger* D15[*nicA*1] with filtered bovine haemoglobin on day 5 and 6 of culturing duration (Fig. A.3.8 B). It was observed that NOR activity decreased after the 4th day of culturing when haem was supplemented with autoclaved haemoglobin, hence filtered haemoglobin was used for all subsequent experiments. Furthermore, *A. niger* D15[*nicA*1] showed statistically significant higher NOR activity than *A. niger* D15[*nicA*2] on day 5 and 6. Therefore, *A. niger* D15[*nicA*1] was chosen as the preferred transformant for further experiments.

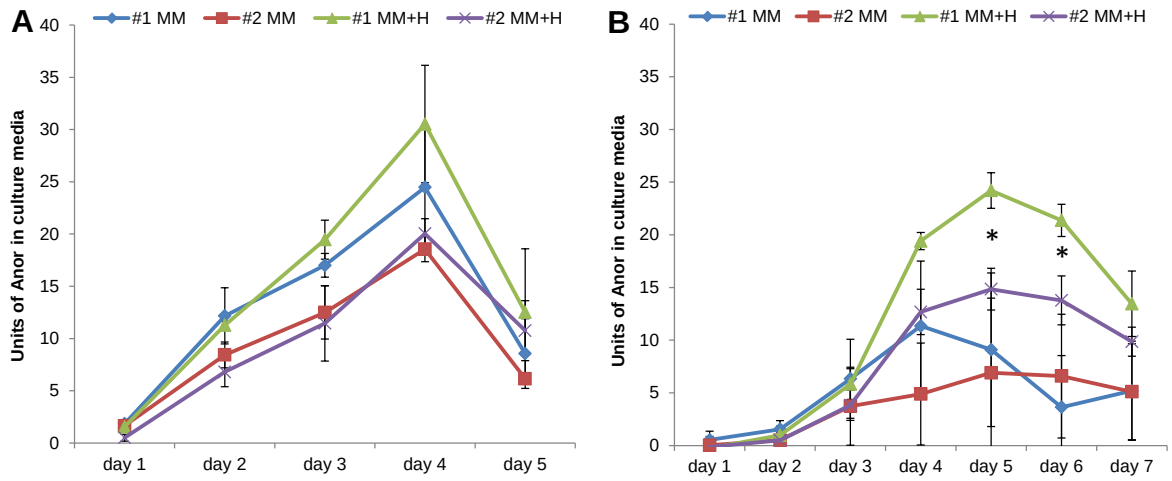

Figure A.3.8. The effect of culture media supplementation with haemoglobin on NOR activity. *A. niger* D15 was cultured at 30˚C with 100 rpm agitation. The minimal medium (MM) was supplemented with 1 g.L^{-1} haemoglobin (MM+H). In (A), the NOR activity of *A. niger* D15[*nicA*1] (#1) and *A. niger* D15[*nicA*2] (#2) when cultured in 200 ml MM or in MM with autoclaved bovine haemoglobin (MM+H). In (B), the NOR activity from *A. niger* D15[*nicA*1] and *A. niger* D15[*nicA*2] when cultured in 200 ml MM or in MM with supplemented with filtred hemoglboin (MM+H). The NOR activity was measured every 24 hours. Each data point is the average from triplicate culture flasks of which the NOR assay was also conducted in triplicates. Statistical significant differences are indicated by * where $P< 0.01$ (Unpaired *t*-test, GraphPad Software, Inc.).

A.3.4. Purification of Anor

A.3.4.1. Amino acid sequence analysis of 55 kDa proteins from SDS-PAGE

The proteins with the anticipated mobility on a SDS-PAGE gel (55 kDa) was excised and identified by tryptic digest fingerprinting. The methods used were adapted from Shevchenko *et al*. (2007) [239] and the analysis was done by Dr Stoyan Stoychev (CSIR Biosciences, South Africa). A Dionex UltiMate 3000 RSLC system coupled to a QSTAR ELITE mass spectrometer was operated in Information Dependant Acquisition (IDA) using an Exit Factor of 2.0 and Maximum Accumulation Time of 2.5 sec. The amino acid sequences were identified with NCBI's msdb database and PEAKS version 6.1 proteomics software. Figure A.3.8 is an example of a peptide sequence analysis of a 55 kDa protein from *A. niger* D15[*nicA*1] cultured in MM+H for 4 days after ion exchange purification. A 53.9% coverage of Cytochrome P450nor (*A. oryzae*) with an accession number of Q8NKB4_ASPOR was obtained (Fig. A.3.9). The Unused ProtScore was 46.08, a measurement of all the peptide evidence for a protein that is not better explained by a higher ranking protein [240].

A

Residue	b	y
S	88.0393	1780.785
M	219.0798	1693.753
V	318.1482	1562.712
S	405.1802	1463.644
A	476.2173	1376.612
F	623.2858	1305.575
F	770.3542	1158.506
N	884.3971	1011.438
D	999.424	897.3949
E	1128.467	782.3679
Y	1291.53	653.3253
V	1390.598	490.262
E	1519.641	391.1936
S	1606.673	262.151
R	1762.774	175.119

B

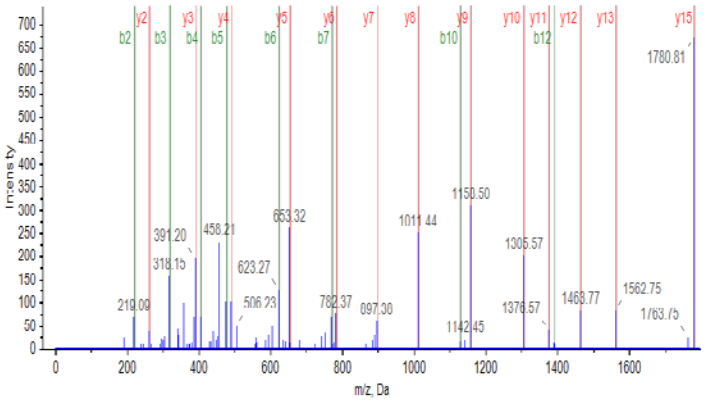

Figure A.3.9. The trytic digest fingerprinting of a 55 kDa purified from *A. niger* D15[*nicA*1]. This protein presented a 53.9% coverage of Cytochrome P450nor from A. *oryzae* (Accession no. Q8NKB4_ASPOR). The table in (A) presents the b and y ions from peptide sequence SMVSAFFNDEYVESR from N-terminal to C-terminal and C-terminal to N-terminal, respectively. The overlapping fragments are highlighted in green. The overlapping MS-MS fragments representative in the mass spec chart (B), where b ions are in green and y-ions in red.

Appendix to Chapter 4: Anor from *E. coli*

A.4.1. Expression of Anor in *E. coli* DH10B and BL21 (DE3)

A.4.1.1. Screening for *nicA* transformants with the polymerase chain reaction

The PCR mixture was used for:

1) the gene construction of pET-*nicA*1 and pET-*nicA*2, and

2) screening of *E. coli* DH10B or BL21 (DE3) containing the pET-*nicA*1 and pET-*nicA*2.

The vector DNA of pMA and pMK (GeneArt, Germany) was used as template for the expression vector construction and total cellular DNA from lysed *E. coli* colonies (incubated for 10 minutes at 100˚C) was used as template for colony PCR screening methodologies. The amplification reaction contained 1.25 Units of Ex Taq polymerase, 5 µl 10× PCR reaction buffer, 0.05 mM of each NTP, 10 µM of each primer (FnicA1 and RnicA for *nicA*1 amplification and FnicA2 and RnicA for *nicA*2 amplification), 2 µl of template DNA and 33.5 µl filtered dd H_2O for a total reaction volume of 50 µl. The amplification process was done in a G-Storm I thermocycler (UK) for 25 cycles, which was preceded by an initial denaturing step for 2 min at 94˚C. The temperature cycle commenced with a DNA denaturing step at 94˚C for 90 seconds, then primer annealing was followed for 1 minute at 60˚C and the DNA elongation was done at 72˚C for 1 minute. This cycle was repeated 25 times and was concluded with an elongation step at 72˚C for 2 minutes. The PCR products were stored at 10˚C for further analysis.

FnicA1: 5’ – GCAGCACCATGGGCTTCCCCTTCGCTCGCCCTTCC – 3’
FnicA2: 5’- GCAGCACCATGGGCAACTCCGAGCCCGTCTAC - 3’
RnicA: 5’- GCAGCAGTCGACATCACGATCCCAAGTGACGGG – 3’

The PCR products were subjected to 0.8% (w/v) agarose gel electrophoresis to identify the PCR reaction in which the primers annealed and amplified the *nicA* gene

of 1.4 kbp as shown in Figure A.4.1. The amplication of pMK-*nicA*1, pMA-*nicA*1, pGTP-*nicA*1 and pGTP-*nicA*2 presented the anticipated 1.4 kbp PCR product (Fig. A.4.1). This PCR product was used for the preparation of the pET-*nicA*1 or pET-*nicA*2 vector for Anor expression in *E. coli* (refer to Chapter 4, Section 4.3.2).

In preparation of the ligation of the 1.4 kbp PCR product in pET-28a, the PCR product was excised from the agarose after gel electrophoresis and the DNA was recovered using a Zymoclean DNA recovery kit. This DNA was digested with NcoI (located in FnicA1 and FnicA2) and SalI (located in RnicA) for directional ligation. The restriction enzyme digest contained either 12 µl pET-28a vector DNA or 20 µl of 1.4 kbp PCR product which was digested with 15 units of enzyme (1.5 µl each) in 3 µl of BamHI buffer [containing 10 mM TRIS-HCl (pH 8.0); 5 mM $MgCl_2$; 100 mM KCl; 0.02% Triton X-100; 0.1 $mg.mL^{-1}$ BSA]. For a final reaction volume of 30 µl, 4 µl of filtered dd H_2O was added to the reaction. The enzymatic digestion was allowed to proceed for 2 hours at 37˚C. The digested PCR product and vector were separated on a 0.8% (w/v) agarose gel. The 1.4 kbp as well as the pET-28a DNA fragments were recovered from the agarose gel. The digested PCR product was ligated to digested pET-28a and electroporated into *E. coli* DH10B as described in Chapter 4, Section 4.3.2.

lane	primer set	template DNA
1	Promega MwM	
2	FnicA2-RnicA	pMK-*nicA2*
3		empty
4		pMK-*nicA2*
5	FnicA1-RnicA	pMA-*nicA*1
6		pMA-*nicA*1
7	FnicA2-RnicA	pGTP-*nicA*2 #3
8		pGTP-*nicA*2 #3
9	FnicA1-RnicA	pGTP-*nicA*1 #4
10		pGTP-*nicA*1 #4

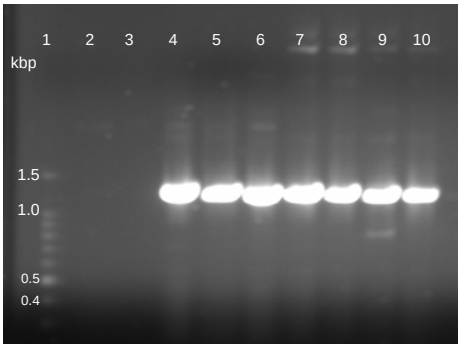

Figure A.4.1. PCR products from vector DNA containing *nicA*1 or *nicA*2. The PCR product (1.4 kbp) was analysed by 0.8% (w/v) agarose gel electrophoresis. The Promega 1 kbp molecular marker (MwM) was used to estimate in kbp of the DNA. The gel was stained with ethidium bromide. The GeneSnap was used to capture the image.

The *E. coli* was allowed to grow in SOC medium for 1 hour and was plated onto Luria agar plates containing 50 $µg.ml^{-1}$ kanamycin. The next day, 50 colonies of each gene vector was selected and screened for *nicA* by colony PCR with primer sets

FnicA1-RnicA or FnicA2-RnicA. The colonies were pooled (10 colonies per reaction) and lysed by boiling for 30 minutes. The total cellular DNA was used as a template in the PCR reactions. Figure A.4.2 A presents the results of the pooled colony PCR reaction. The anticipated ~1.4 kbp product was observed in colonies 21 to 50 (lanes 3, 4 and 5) which were transformed with pET-*nicA*1 and amplified with priner set FnicA1-RnicA. In this PCR reaction a ~1 kbp product was also amplified. The colonies from 41 to 50 were chosen for single colony PCR as the pooled colony PCR reaction showed the least of the ~1 kbp PCR product. In the single PCR reaction only colony 50 presented the ~1.4 kbp PCR product (lane 11 in comparison to the positive control in lane 12; refer to Fig. A.4.2. B). However, colonies 44 and 45 were chosen further investigations.

The same selection process for the colony with the 1.4 kbp PCR product was repeated for *E. coli* transformed with pET-*nicA*2 using the FnicA-RnicA priner set (lanes 7 to 11; Fig. A.4.2. A). The anticipated ~1.4 kbp PCR product was observed in lane 9 and 10 (colonies from 21 to 40), of which colonies from 21 to 30 were subjected to single colony PCR with the primer set FnicA2-RnicA as before. In this PCR reactions, colonies 21, 24, 26 and 27 presented the ~1.4 kbp PCR product (lane 2, 5, 7 and 8, Fig. A.4.2. C). Colony 26 was chosen for further investigations.

A

lane	primer set	Colony pool
1	FnicA1-RnicA	1-10
2		11-20
3		21-30
4		31-40
5		41-50
6	empty	
7	FnicA2-RnicA	1-10
8		11-20
9		21-30
10		31-40
11		41-50
12	no DNA control	
13	Roche MwM II	
14	Roche MwM III	

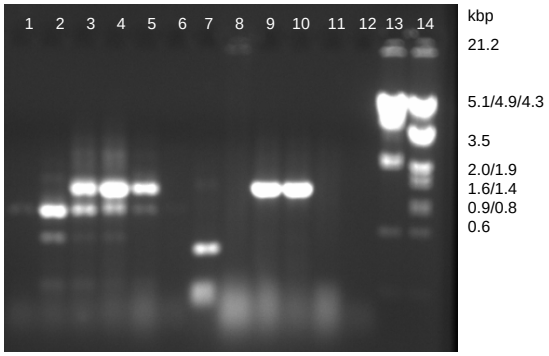

B

lane	priner set: FnicA1-RnicA
1	Roche MwM III
2	41
3	42
4	43
5	44
6	45
7	46
8	47
9	48
10	49
11	50
12	+ve control
13	Roche MwM III

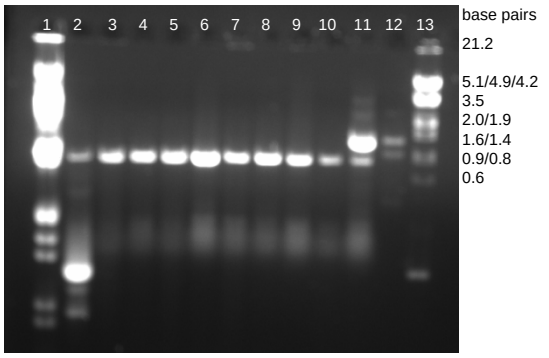

C

lane	priner set: FnicA2-RnicA
1	Roche MwM III
2	21
3	22
4	23
5	24
6	25
7	26
8	27
9	28
10	29
11	30
12	+ve control
13	-ve controll
14	Roche MwM III

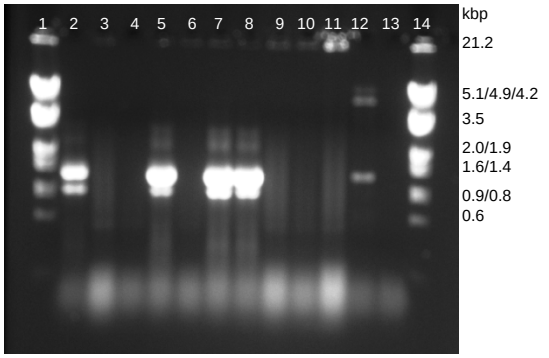

Figure A.4.2. Colony PCR products from pooled *E. coli* DH10B transformants. Transformants contained either pET-*nicA*1 or pET-*nicA*2. The PCR product from genomic DNA templates were separated by 0.8% (v/w) agarose gel electrophoresis. In (A), a ~1.4 kbp PCR product indicates the presence of *nicA*1 (lane 3, 4 and 5) or *nicA*2 (lane 9 and 10). Plasmid DNA of pMA-*nicA*1 or pMK-*nicA*2 were used as a positive control in the PCR reaction. The negative control is a no DNA reaction. For DNA base pair estimation, DNA molecular weight marker II (MwMII) and III (MwMIII) were used (lane 13 and 14). The PCR products of the single colonies which were identified in the pooled PCR reaction (A), are shown for *nicA*1 (B) and *nicA*2 (C). The agarose gel was stained with ethidium bromide. The GeneSnap was used to capture the image.

A.4.1.2. Screening for NOR activity in lysate

A pilot study was conducted to determine whether Anor is expressed in the identified colonies (colony #44 and 45, for *nicA*1 and #26 for *nicA*2, Fig. 2, B and C). As described in Chapter 4 (Section 4.3.4), 10 ml Luria broth with 50 µg.ml^{-1} kanamycin was inoculated with these colonies, gene expression was induced with the addition of 0.5 mM IPTG after 4 hours of incubation at 37˚C. Thereafter, the cells were cultured overnight at 30˚C with agitation at 190 rpm. The culture medium supernatant after harvesting (CM) and the cell lysate (L) were assayed for NOR activity (Fig. A.4.3 A). The proteins molecular sizes were determined on a denaturing gradient SDS-PAGE gel (Fig. A.4.3 B). Transformants harbouring each gene vector showing NOR activity (Fig. A.4.3 A, #26, #44 and #45) were also analysed for the anticipated ~55 kDa protein on SDS-PAGE gel electrophoresis (Fig. A.4.3 B). The presence of this ~55 kDa protein together with NOR activity would indicate the presence of Anor.

Anor is expressed with a poly-histidine tag which has a high affinity for nickel NTA resin. This affinity chromatography was applied to facilitate the purification. In this pilot study, the lysate of colony #45 was applied to the MagReSyn™ NTA to test whether Anor is indeed expressed with a poly-histidine tag. Fig. A.4.3 B, lanes 3 to 7, show that the bulk of a ~55 kDa protein is in the cell lysate after IPTG induction and in lesser quantity in the eluate from the MagReSyn™ NTA.

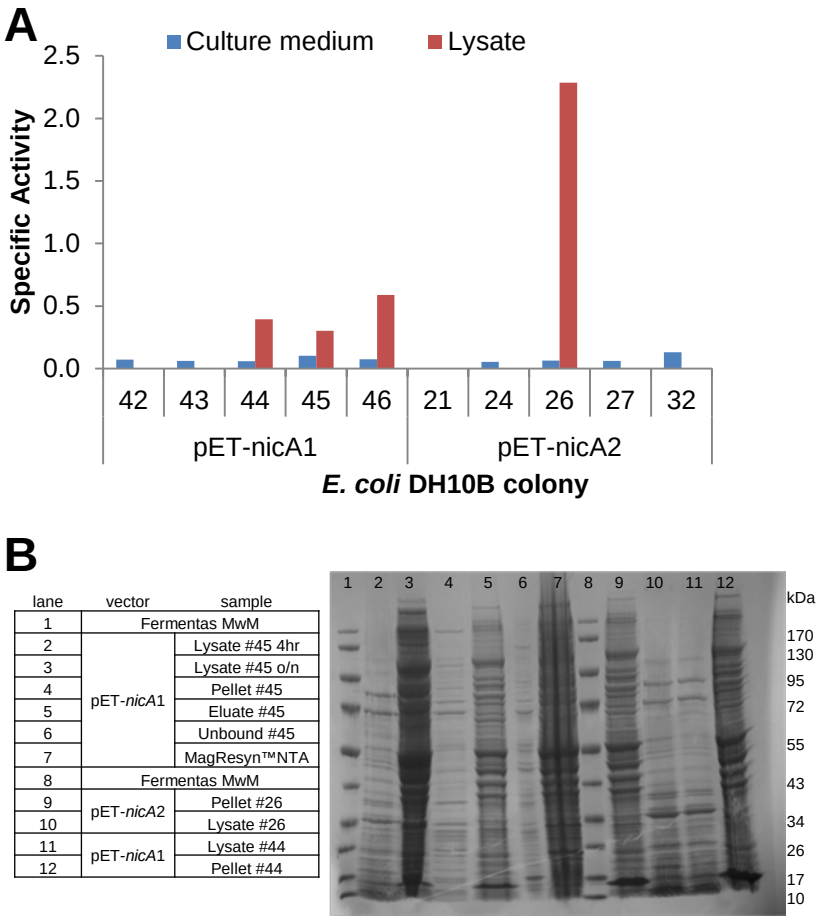

Figure A.4.3. Anor expression in *E. coli* DH10B. The colonies with a ~1.4 kbp PCR product were cultured and analysed for NOR activity (A) and subjected to denaturing 4-12% gradient Bis-Tris NuPage® gel electrophoresis (B). Lysate of colony #45 after 4 hours incubation presents the protein expression before IPTG induction (lane 2) and lysate colony #46 o/n shows the proteins after IPTG induction in stationary growth phase (18 hours culturing, in lane 3). The cells were cultured, lysed and purified as described in Chapter 4, Section 4.3.5. NOR activity, protein concentration and SDS-PAGE gel electrophoresis were determined as described in Chapter 4, Section 4.3.7 and 4.3.8. The gel was stained with Colloidal Comassie brilliant blue stain. The GeneSnap was used to capture the image.

A.4.1.3. Transformation of *nicA* constructs into *E. coli* BL21 (DE3)

E. coli DH10B is not a suitable expression host as it was designed to carry large plasmids for building metagenomic libraries [401]. Therefore, the *E. coli* strain BL21 (DE3), which is more suitable for heterologous protein expression [284, 402, 403], was chosen. This strain is an outer membrane protease (ompT) and T1 prophage receptor mutant. For the expression of Anor in *E. coli* BL21 (DE3) strain, plasmid DNA from colonies #26 and #44 were isolated from overnight cultures and

electroporated into *E. coli* BL21 (DE3). Thereafter, the *E. coli* cells were allowed to grow in SOC medium for 1 hour at 37˚C and were subsequently plated onto Luria agar containing kanamycin (50 µg.ml^{-1}). The plate was incubated at 37˚C for 18 hours. At random, five single colonies were selected from each construct and subjected to boiling for 10 minutes in dd H_2O. The cellular debris was collected by centrifugation (4000 ×*g* for 15 minutes at 4˚C) and the supernatant containing genomic DNA was used as a DNA template for PCR. As before, the PCR analysis with primer pairs of FnicA1-RnicA and FnicA2-RnicA were used to establish whether the colonies contained either pET-*nicA*1 or pET-*nicA*2. Figure A.4.4 presents the PCR products on a 0.8% agarose gel.

lane	vector	sample
1	Roche MwM III	
2	pET-*nicA*1	1
3		2
4		3
5		4
6		5
7	empty	
8	pET-*nicA*2	1
9		2
10		3
11		4
12	pET-*nicA*2 DNA	

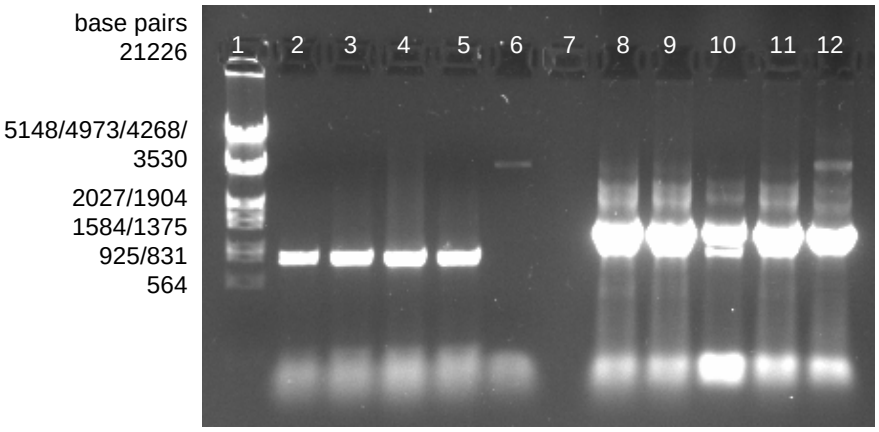

Figure A.4.4. Colony PCR products from *E. coli* BL21 (DE3) transformants. Transformants contained either pET-*nicA*1 and pET-*nicA*2. The PCR product was analysed with a 0.8% (v/w) agarose gel electrophoresis. The molecular weight marker III from Roche was used to estimate the molecular weight of the PCR products. The agarose gel was stained with ethidium bromide. The GeneSnap was used to capture the image.

The size of the PCR products from colonies transformed with pET-*nicA*1 were smaller than anticipated (lanes 1 to 5; 925/831 bp). However, the amplicon size generated from colonies transformed with pET-*nicA*2 were the expected ~1.4 kbps (lanes 8 to 12 in Figure A.4.4). Again, one colony containing either pET-*nicA*1 or pET-*nicA*2, was selected at random. The colony was used to inoculate Luria broth containing Kanamycin (50 µg.ml^{-1}) and cultured for 18 hours at 37˚C with 190 rpm agitation. This culture was used to prepare 80% glycerol stocks which were stored at -80˚C for further studies.

A.4.1.4. Sequence analysis of pET-*nicA*1 and pET-*nicA*2

Nucleotide sequences were viewed and edited with BioEdit Sequence Alignment Editor version 5.0.9 (USA). Sequence alignments and plasmid maps were constructed with DNAMAN version 5.2.9 (Lynnon BioSoft, Canada). Figure A.4.5 shows the sequence alignments from *nicA*1 and *nicA*2 with the gene sequence provided by GeneArt (refer to Appendix to Chapter 3, Section A.3.2.4). The plasmid maps are presented in Figure A.4.6.

The nucleotide sequence of the gene insert (PCR product, Section A. 4.1.1) on pET-*nicA*1 (colony #44) and pET-*nicA*2 (colony #26) was determined and aligned with *nicA*1 nucleotide sequence. Besides NcoI restriction site in the primers FnicA1 and FnicA2, another one was located 301 bp down stream of the ATP start codon. In the preparation of pET-*nicA*1 this site omitted 303 bp from nicA1. However, in pET-*nicA*2, the restriction enzyme did not cut at this second restriction site and hence the *nicA*2 nucleotide sequence aligned with 100% identity with *nicA*.

```
pET-nicA1    --------------------------------------------------
nicA1        GGTACCGCGGCCGCATGGTGTCCTTCACCTCCCTGCTCGCCGGCGTCGCC

pET-nicA1    --------------------------------------------------
nicA1        GCCATCTCTGGCGTCCTCGCTGCTCCTGCCGCCGAGGTCGAGTCCGTCGC

pET-nicA1    --------------------------------------------------
nicA1        CGTCGAGAAGCGCTTCCCCTTCGCTCGCCCTTCCGGCGACGAGCCCCCTG

pET-nicA1    --------------------------------------------------
nicA1        CCGAGTTCCACCGCCTCCTCCGCGAGTGCCCCGTGTCCCGCGTCGAGCTG

pET-nicA1    --------------------------------------------------
nicA1        TGGGATGGCTCCCACCCCTGGCTCGTCGTCAAGCACAAGGATGTCTGCGA

pET-nicA1    --------------------------------------------------
nicA1        GGTCCTCACCGATCCCCGCCTCTCCAAGGTCCGCCAGCGCGACGGCTTCC

pET-nicA1    --------------------------------------------------
nicA1        CCGAGATGTCCCCTGGCGGCAAGGCCGCTGCCCGCAACCGCCCCACCTTC

pET-nicA1    ----------------------------------------ATGGGGTCCGC
nicA1        GTCGATATGGATGCCCCCGATCACATGCACCAGCGCTCCATGGTGTCCGC

pET-nicA1    TTTCTTCAACGATGAGTACGTCGAGTCCCGCCTGCATCTCATCCGCGATA
nicA1        TTTCTTCAACGATGAGTACGTCGAGTCCCGCCTCCCCTTCATCCGCGATA

pET-nicA1    CCGTCCAGCACTACCTCGATCGCCTCATCCGCGCTGGCAAGGACGGCAAA
nicA1        CCGTCCAGCACTACCTCGATCGCCTCATCCGCGCTGGCAAGGACGGCAAA

pET-nicA1    GAAGTCGATCTCGTCAAGCACTTCGCCCTCCCCATCCCTTCCCACATCAT
nicA1        GAAGTCGATCTCGTCAAGCACTTCGCCCTCCCCATCCCTTCCCACATCAT

pET-nicA1    CTACGATATCCTCGGCATCCCCATCGAGGATTTCGAGTACCTCTCCGGCT
nicA1        CTACGATATCCTCGGCATCCCCATCGAGGATTTCGAGTACCTCTCCGGCT

pET-nicA1    GCGACGCCACCCGCACCAACGGCTCCTCCACCGCCGCTGCTGCCCAGGCC
nicA1        GCGACGCCACCCGCACCAACGGCTCCTCCACCGCCGCTGCTGCCCAGGCC
```

```
pET-nicA1    GCCAACAAAGAAATCCTCGAGTACCTCGAGCGCCTCGTCGATAAGAAAAC
nicA1        GCCAACAAAGAAATCCTCGAGTACCTCGAGCGCCTCGTCGATAAGAAAAC

pET-nicA1    CACCAACCCCTCCCACGATGTCATCTCCACCCTCGTCATCCAGCAGCTCA
nicA1        CACCAACCCCTCCCACGATGTCATCTCCACCCTCGTCATCCAGCAGCTCA

pET-nicA1    AGCCCGGCCACATCGAGAAGCTCGATGTCGTCCAGATCGCCTTCCTCCTC
nicA1        AGCCCGGCCACATCGAGAAGCTCGATGTCGTCCAGATCGCCTTCCTCCTC

pET-nicA1    CTCGTCGCCGGCAACGCCACTGTCGTGTCCATGATCGCTCTCGGCGTCGT
nicA1        CTCGTCGCCGGCAACGCCACTGTCGTGTCCATGATCGCTCTCGGCGTCGT

pET-nicA1    CACCCTCCTCGAGCACCCCGATCAGCTCTCCCGCCTCCTCGAGGATCCCT
nicA1        CACCCTCCTCGAGCACCCCGATCAGCTCTCCCGCCTCCTCGAGGATCCCT

pET-nicA1    CCCTCTCCAACCTCTTCGTCGAGGAACTCTGCCGCTTCCACACCGCCTCC
nicA1        CCCTCTCCAACCTCTTCGTCGAGGAACTCTGCCGCTTCCACACCGCCTCC

pET-nicA1    GCCTTGGCTACCCGTCGCGTCGCTACCGTCGATATCGAGCTGCGTGGCCA
nicA1        GCCTTGGCTACCCGTCGCGTCGCTACCGTCGATATCGAGCTGCGTGGCCA

pET-nicA1    GAAGATCCGGGCTGGCGAGGGCATCATCGCCTCCAACCAGGCCGCTAACC
nicA1        GAAGATCCGGGCTGGCGAGGGCATCATCGCCTCCAACCAGGCCGCTAACC

pET-nicA1    GTGATCCTGAGGTGTTCCCCGATCCCGATACCTTCGACATGTTCCGCAAG
nicA1        GTGATCCTGAGGTGTTCCCCGATCCCGATACCTTCGACATGTTCCGCAAG

pET-nicA1    CGCGGTCCCGAGGAAGCCCTCGGCTTCGGCTACGGCGATCATCGCTGTAT
nicA1        CGCGGTCCCGAGGAAGCCCTCGGCTTCGGCTACGGCGATCATCGCTGTAT

pET-nicA1    TGCCGAGATGCTCGCTCGCGCCGAGCTGGAAACCGTGTTCTCCACTCTCT
nicA1        TGCCGAGATGCTCGCTCGCGCCGAGCTGGAAACCGTGTTCTCCACTCTCT

pET-nicA1    TCCAGACCCTGCCCTCCCTGAAGCTCGCCATCCCCAAGTCCGAGATCCAG
nicA1        TCCAGACCCTGCCCTCCCTGAAGCTCGCCATCCCCAAGTCCGAGATCCAG

pET-nicA1    TGGACCCCCCCCACCCGTGACGTCGGCATCGTCGGCCTCCCCGTCACTTG
nicA1        TGGACCCCCCCCACCCGTGACGTCGGCATCGTCGGCCTCCCCGTCACTTG

pET-nicA1    GGATCGTGATGTCGACAATGCTTGCGGCCGCACTCGAGCACCACCACCAC
nicA1        GGATCGTGATTGAGCGGCCGCGAGCTC----------------------

pET-nicA1    CACCACTGA
nicA1        ---------


pET-nicA2    --------------------------------------------------
nicA2        GGTACCGCGGCCGCATGGTGTCCTTCACCTCCCTGCTCGCCGGCGTCGCC

pET-nicA2    ---------TTTCCCCCCTCCAAGAAATAATTTTGTTTAACTTTAAGAAG
nicA2        GCCATCTCTGGCGTCCTCGCTGCTCCTGCCGCCGAGGTCGAGTCCGTCGC

pET-nicA2    GAGATATACCATGGGCAACTCCGAGCCCGTCTACCCCCGCTTCCCCTTCG
nicA2        CGTCGAGAAGCGCATGAACTCCGAGCCCGTCTACCCCCGCTTCCCCTTCG

pET-nicA2    CTCGCCCTTCCGGCGACGAGCCCCCTGCCGAGTTCCACCGCCTCCTCCGC
nicA2        CTCGCCCTTCCGGCGACGAGCCCCCTGCCGAGTTCCACCGCCTCCTCCGC

pET-nicA2    GAGTGCCCCGTGTCCCGCGTCGAGCTGTGGGATGGCTCCCACCCCTGGCT
nicA2        GAGTGCCCCGTGTCCCGCGTCGAGCTGTGGGATGGCTCCCACCCCTGGCT

pET-nicA2    CGTCGTCAAGCACAAGGATGTCTGCGAGGTCCTCACCGATCCCCGCCTCT
nicA2        CGTCGTCAAGCACAAGGATGTCTGCGAGGTCCTCACCGATCCCCGCCTCT

pET-nicA2    CCAAGGTCCGCCAGCGCGACGGCTTCCCCGAGATGTCCCCTGGCGGCAAG
nicA2        CCAAGGTCCGCCAGCGCGACGGCTTCCCCGAGATGTCCCCTGGCGGCAAG

pET-nicA2    GCCGCTGCCCGCAACCGCCCCACCTTCGTCGATATGGATGCCCCCGATCA
nicA2        GCCGCTGCCCGCAACCGCCCCACCTTCGTCGATATGGATGCCCCCGATCA

pET-nicA2    CATGCACCAGCGCTCCATGGTGTCCGCTTTCTTCAACGATGAGTACGTCG
nicA2        CATGCACCAGCGCTCCATGGTGTCCGCTTTCTTCAACGATGAGTACGTCG

pET-nicA2    AGTCCCGCCTCCCCTTCATCCGCGATACCGTCCAGCACTACCTCGATCGC
```

```
nicA2       AGTCCCGCCTCCCCTTCATCCGCGATACCGTCCAGCACTACCTCGATCGC

pET-nicA2   CTCATCCGCGCTGGCAAGGACGGCAAAGAAGTCGATCTCGTCAAGCACTT
nicA2       CTCATCCGCGCTGGCAAGGACGGCAAAGAAGTCGATCTCGTCAAGCACTT

pET-nicA2   CGCCCTCCCCATCCCTTCCCACATCATCTACGATATCCTCGGCATCCCCA
nicA2       CGCCCTCCCCATCCCTTCCCACATCATCTACGATATCCTCGGCATCCCCA

pET-nicA2   TCGAGGATTTCGAGTACCTCTCCGGCTGCGACGCCACCCGCACCAACGGC
nicA2       TCGAGGATTTCGAGTACCTCTCCGGCTGCGACGCCACCCGCACCAACGGC

pET-nicA2   TCCTCCACCGCCGCTGCTGCCCAGGCCGCCAACAAAGAAATCCTCGAGTA
nicA2       TCCTCCACCGCCGCTGCTGCCCAGGCCGCCAACAAAGAAATCCTCGAGTA

pET-nicA2   CCTCGAGCGCCTCGTCGATAAGAAAACCACCAACCCCTCCCACGATGTCA
nicA2       CCTCGAGCGCCTCGTCGATAAGAAAACCACCAACCCCTCCCACGATGTCA

pET-nicA2   TCTCCACCCTCGTCATCCAGCAGCTCAAGCCCGGCCACATCGAGAAGCTC
nicA2       TCTCCACCCTCGTCATCCAGCAGCTCAAGCCCGGCCACATCGAGAAGCTC

pET-nicA2   GATGTCGTCCAGATCGCCTTCCTCCTCCTCGTCGCCGGCAACGCCACTGT
nicA2       GATGTCGTCCAGATCGCCTTCCTCCTCCTCGTCGCCGGCAACGCCACTGT

pET-nicA2   CGTGTCCATGATCGCTCTCGGCGTCGTCACCCTCCTCGAGCACCCCGATC
nicA2       CGTGTCCATGATCGCTCTCGGCGTCGTCACCCTCCTCGAGCACCCCGATC

pET-nicA2   AGCTCTCCCGCCTCCTCGAGGATCCCTCCCTCTCCAACCTCTTCGTCGAG
nicA2       AGCTCTCCCGCCTCCTCGAGGATCCCTCCCTCTCCAACCTCTTCGTCGAG

pET-nicA2   GAACTCTGCCGCTTCCACACCGCCTCCGCCTTGGCTACCCGACGCGTCGC
nicA2       GAACTCTGCCGCTTCCACACCGCCTCCGCCTTGGCTACCCGTCGCGTCGC

pET-nicA2   TACCGTCGATATCGAGCTGCGTGGCCAGAAGATCCCGGCTGGCGAGGGCA
nicA2       TACCGTCGATATCGAGCTGCGTGGCCAGAAGATCCGGGCTGGCGAGGGCA

pET-nicA2   TCATCGCCTCCAACCAGGCCGCTAACCGTGATCCTGGGGTGTTCCCCGAT
nicA2       TCATCGCCTCCAACCAGGCCGCTAACCGTGATCCTGAGGTGTTCCCCGAT

pET-nicA2   CCCGATACCTTCGACATGTTCCGCAAGCGCGGTCCCGAGGAAGCCCTCGG
nicA2       CCCGATACCTTCGACATGTTCCGCAAGCGCGGTCCCGAGGAAGCCCTCGG

pET-nicA2   CTTCGGCTACGGCGATCATCGCTGTATTGCCGAGATGCTCGCTCGCGCCG
nicA2       CTTCGGCTACGGCGATCATCGCTGTATTGCCGAGATGCTCGCTCGCGCCG

pET-nicA2   AGCTGGAAACCGTGTTCTCCACTCTCTTCCAGACCCTGCCCTCCCTGAAG
nicA2       AGCTGGAAACCGTGTTCTCCACTCTCTTCCAGACCCTGCCCTCCCTGAAG

pET-nicA2   CTCGCCATCCCCAAGTCCGAGATCCAGTGGACCCCCCCCCACCCGTGACGT
nicA2       CTCGCCATCCCCAAGTCCGAGATCCAGTGGACCCCCCCCCACCCGTGACGT

pET-nicA2   CGGCATCGTCGGCCTCCCCGTCACTTGGGATCGTGATTCGACAAGCTTGC
nicA2       CGGCATCGTCGGCCTCCCCGTCACTTGGGATCGTGATTGAGCGGCCGCGA

pET-nicA2   ACCGCACTCGAGCACCACCACCACCACCACTGAGATCCGGCTGCTAACAA
nicA2       GCTC----------------------------------------------
```

Figure A.4.5. DNA sequence alignment of pET-*nicA*1 and pET-*nicA*2. DNA sequence was aligned with *nicA*1 and *nicA*2 from GeneArt (respectively). Start and stop codon are indicated in red text and the restriction enzyme cutting sites are highlighted with green. The annealing site for the primers is shown by underlined text and the nucleotides encoding for the histidine residues are highlighted in grey. The nucleotide sequence alignment was done with BioEdit Sequence Alignment Editor version 5.0.9 (USA).

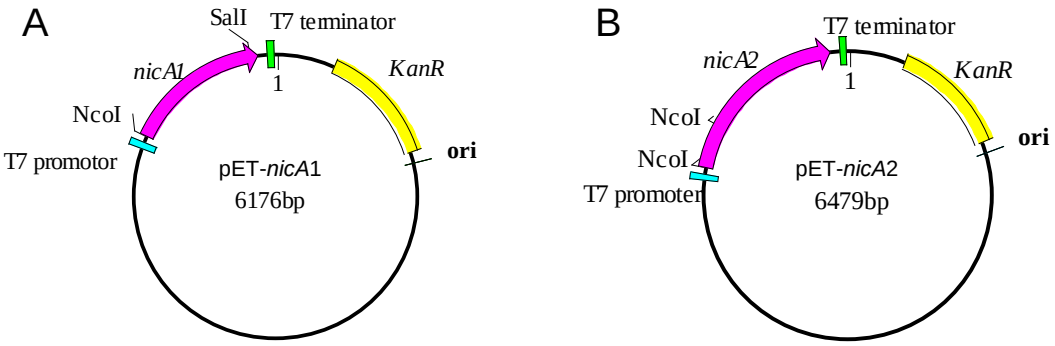

Figure A.4.6. Plasmid maps for pET-*nicA*1 and pET-*nicA*2. The coding sequence for *nicA*1 or *nicA*2 is indicated in pink which is flanked by the restriction enzyme sites NcoI and SalI. The T7 promoter (blue) and T7 terminator are indicated by the blue and green boxes. The kanamycin resistance gene is indicated in yellow. The plasmid map was constructed with DNAMAN (Lynnon BioSoft, Canada).

A.4.1.5. Tryptic digest fingerprinting of 45 kDa proteins from SDS-PAGE

The protein with the anticipated mobility on SDS-PAGE gel electrophoresis was excised and the amino acid sequenced was determined. The methods were adapted from Shevchenko *et al*. (2006) [239] and the analysis was done by Dr Stoyan Stoychev. In brief, a Dionex Ultimate 3000 RSLC system coupled to a QSTAR ELITE mass spectrometer was operated by Information Dependant Acquisition (IDA) using an Exit Factor of 2.0 and Maximum Accumulation Time of 2.5 sec. The amino acid sequences were identified with NCBI's msdb database and PEAKS v 6.1 proteomics software. The tryptic digest fingerprinting of the ~45 kDa protein from *E. coli* BL21[*nicA*2] presented a 87% coverage of Cytochrome P450nor (*A. oryzae*) with an accession number of Q8NKB4_ASPOR. For this analysis, the Unused ProtScore was set to 82.07%, which is a measurement of all the peptide evidence for a protein that is not better explained by a higher ranking protein [240]. For this analysis, *E. coli* BL21[*nicA*2] was cultured in Luria broth and 50 µg.ml^{-1} kanamycin supplemented with filtered haemoglobin. Gene expression was induced with 0.5 mM IPTG. The lysate was harvested after 18 hours as describe in Chapter 4, Section 4.3.5. Figure A.4.7 is an example of a fragment of amino acid sequence determined from a 45 kDa protein and in Figure A.4.8 the amino acids identified are shown.

A

Residue	b	y
S	88.039	1780.785
M	219.080	1693.753
V	318.148	1562.712
S	405.180	1463.644
A	476.217	1376.612
F	623.286	1305.575
F	770.354	1158.506
N	884.397	1011.438
D	999.424	897.395
E	1128.467	782.368
Y	1291.530	653.325
V	1390.598	490.262
E	1519.641	391.194
S	1606.673	262.151
R	1762.774	175.119

B

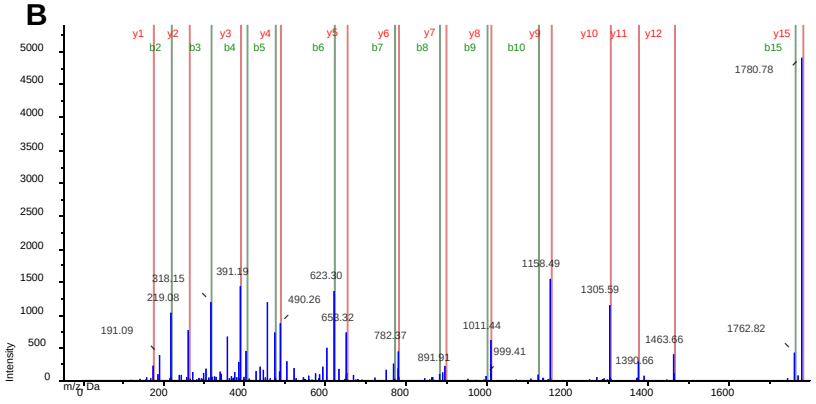

Figure A.4.7. Amino acid sequence analysis of a 45 kDa protein expressed by *E. coli* BL21[*nicA*2]. This fragment provided evidence of a Cytochrome P450nor from A. *oryzae* (Accession no. Q8NKB4_ASPOR) with a 87% coverage. The table in (A) presents the b and y ions from peptide sequence SMVSAFFNDEYVESR from N-terminus to C-terminus and C-terminus to N-terminus, respectively. The overlapping fragments are highlighted in green. The overlapping MS-MS fragments are resented in the mass spec chart (B), where b ions are in green and y-ions in red.

MNSEPVYPRFPFARPSGDEPPAEFHRLLRECPVSRVELWDGSHPWLVVKHKDVCEVLTDPRLSKV
RQRDGFPEMSPGGKAAARNRPTFVDMDAPDHMHQRSMVSAFFNDEYVESRLPFIRDTVQHYLDRL
IRAGKDGKEVDLVKHFALPIPSHIIYDILGIPIEDFEYLSGCDATRTNGSSTAAAAQAANKEILEYLERL
VDKKTTNPSHDVISTLVIQQLKPGHIEKLDVVQIAFLLLVAGNATVVSMIALGVVTLLEHPDQLSRLLED
PSLSNLFVEELCRFHTASALATRRVATVDIELRGQKIRAGEGIIASNQAANRDPEVFPDPDTFDMFRK
RGPEEALGFGYGDHRCIAEMLARAELETVFSTLFQTLPSLKLAIPKSEIQWTPPTRDVGIVGLPVTW
DRD

Figure A.4.8. Protein sequence coverage map of Anor expressed in *E. coli* BL21[*nicA*2]. Green indicates the peptide has been identified with at least 95% confidence and yellow at least 50% confidence (ProteinPilot™Software, version 3.0, Applied Biosystems & MDS Analytical Technologies). Red is less than 50% confidence. Underlined conserved sequences around the predicted haem-binding region and I-helix [151].

A.4.2. Culture medium supplementation

In the results shown in Chapter 3 (Section 3.4.2), it was observed that the supplementation of the culture media with haemoglobin resulted in an increase of specific NOR activity and thus it was hypothesised that it might also increase the NOR activity in the expression of Anor in *E. coli*. At first, a pilot study was conducted to determine whether the addition of haemoglobin did result in increased NOR activity. Thereafter, the Anor yield was compared to the supplementation of autoclaved haemoglobin vs. filtered haemoglobin. Hamilton-Miller (1966) [404] indicated that ethylenediaminetetra-acetic acid (EDTA) and penicillin would make *E. coli* cell membrane porous and thus facilitate the uptake of haemoglobin. Therefore, a pilot study was conducted to investigate whether the EDTA would improve Anor expression by facilitating haemoglobin uptake. And thirdly, the supplementation with the haem precursor, 5-aminolevulinic acid was compared to the protein expression obtained from *E. coli* cultured in haemoglobin supplemented media. *E. coli* BL21[*nicA*2] was chosen for these studies as it presented the highest NOR activity in the pilot study reported in Section A.4.1.2.

A.4.2.1. Autoclaved vs. filtered haemoglobin

The Anor yield from *E. coli* BL21[*nicA*2] cultured in Luria broth (50 µg.ml^{-1} kanamycin) supplemented either with autoclaved or filtered haemoglobin was detemrined. Here, it was hypothesised that the haem from the haemoglobin could

potentially improve the yield of the holo-protein. Therefore, *E. coli* BL21[*nicA*2] was cultured with denatured haemoglobin (autoclaved) and native haemoglobin (filter sterilised). For this study, 2 × 250 ml of culture medium were inoculated with *E. coli* BL21[*nicA*2] overnight starter culture and allowed to grow until the absorbance at 600 nm reached 0.4. At this point, IPTG was added and the culture was further incubated at 30˚C for 18 hours. The culture was harvested and Anor was purified as described in Section 4.3.5. The culture supplemented with autoclaved haemoglobin yielded a higher specific NOR activity. However, the filtered haemoglobin had two-fold higher total NOR yield (Table A.4.1).

Table A.4.1. Anor yield from *E. coli* BL21[*nicA*2] cultured in medium supplemented with autoclaved or filtered haemoglobin.

		Total protein	Total activity	Specific activity	Total P450	Specific P450
Haemoglobin	Sample	mg	Units	Units.mg^{-1}	nmol	nmol.mg^{-1}
autoclaved	L	10.1	89.7	8.9		
	UB	7.1	39.6	5.6		
	W	2.5	24.0	9.6		
	E	0.1	21.5	221.6	3.5	36.2
filtered	L	6.1	156.1	25.5		
	UB	5.5	63.3	11.4		
	W	0.0	33.5	0.0		
	E	0.2	24.7	209.7	8.7	73.8

L-lysate, UB- unbound, W- wash step, E-eluate

Not only was the total NOR activity higher from *E. coli* BL21[*nicA*2] when cultured in filtered haemoglobin, but also the P450 spectral analysis indicated twice as much P450 content (73.8 vs. 36.2 nmol.mg^{-1} P450 for filtered haemoglobin vs. autoclaved haemoglobin). The samples from the MagReSyn™ NTA purification process were analysed on the denaturing 4-12% gradient SDS-PAGE gel electrophoresis and presented another confirmation that filtered haemoglobin produced higher holoprotein (Fig. A.4.9). Therefore, it was concluded that filtered haemoglobin produces the higher functional Anor yield and was used as the haemoglobin supplementation for further studies.

Lane	samples	
1	Fermentas MwM	
2	autoclaved haemoglobin	Lysate
3		UB
4		Wash
5		Eluate
6		ReSyn
7	Fermentas MwM	
8	filtered haemoglobin	Lysate
9		UB
10		Wash
11		Eluate
12		ReSyn

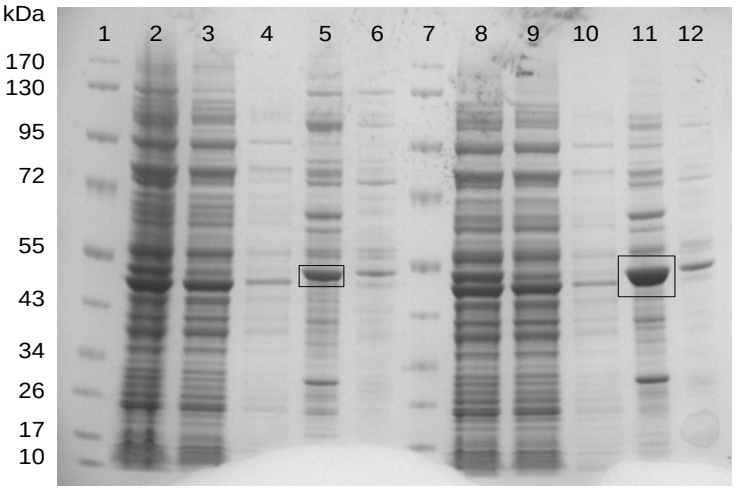

Figure A.4.9. Denaturing and reducing gradient SDS-PAGE analysis of Anor purified from *E. coli* BL21[*nicA*2]. *E. coli* BL21[*nicA*2] cultured either in autoclaved haemoglobin or in filtered haemoglobin. MagReSyn™ NTA was used to purify Anor with poly-histidines tag. The protein band anticipated to be Anor was boxed. An approximate 10 µg of protein was loaded onto the gel, which was stained with Colloidal Coomassie Blue overnight and was destained with dd H_2O as described in Chapter 4, Section 4.3.8. The gel was photographed with GeneSnap as before. UB- unbound; MwM- molecular weight marker.

A.4.2.2. Haemoglobin with and without EDTA

Hamilton-Miller (1966) [404] indicated that ethylenediaminetetra-acetic acid (EDTA) and penicillins compromise the bacterial permeability barriers, i.e. increase permeability of bacterial cell walls. Therefore we hypothesised that the addition of EDTA to haemoglobin supplemented culture media would facilitate the transport of haem across the cell membrane and increase holoprotein synthesis. To investigate this hypothesis, a pilot study was conducted in which 1 $g.L^{-1}$ filtered haemoglobin or haemoglobin with 10 mM EDTA were added to 2 × 250 ml of Luria broth (50 $\mu g.ml^{-1}$ kanamycin). The culture medium was inoculated with a overnight starter culture and the gene expression was induced with IPTG at a cellular density of 0.4 absorbance at 600 nm. The cells were further incubated with agitation at 30˚C for 18 hours. The cells were harvested as before and Anor was purified with NTA MagReSyn™ as described in Chapter 4, Section 4.3.5. Table A.4.2. presents the Anor yields obtained from each culture media supplementation. The specific NOR activity and % yield were very similar as observed in Fig. A.4.10. on the SDS-PAGE. However, the P450 content indicated that haemoglobin supplementation resulted in 4.5 × fold higher P450 content (25 $nmol.mg^{-1}$ P450) than the specific P450 content (5.6 $nmol.mg^{-1}$) obtained from haemoglobin and EDTA supplemented culture medium. Since EDTA

together with haemoglobin media supplementation did not result in a significant increase in enzyme activity, this medium supplementation was not further used.

Table A.4.2. Anor yield from *E. coli* BL21[*nicA*2] cultured in medium supplemented with EDTA and haemoglobin.

		Total protein	Total activity	Specific activity	Total P450	Specific P450
	Sample	mg	Units	Units.mg^{-1}	nmol	nmol.mg^{-1}
haemoglobin and EDTA	L	21.9	299.4	13.7		
	UB	16.4	167.4	10.2		
	W	3.6	165.7	46.5		
	E	1.6	4.3	2.8	2.6	5.6
haemoglobin	L	18.1	288.0	15.9		
	UB	15.0	120.5	8.0		
	W	3.8	71.4	18.7		
	E	0.9	1.7	1.9	7.7	24.9

L-lysate, UB- unbound, W- wash step, E-eluate

Lane	samples	
1	haemoglobin	Eluate
2	Fermentas MwM	
3	haemoglobin and ETDA	CM
4		Lysate
5		UB
6		ReSyn
7		Eluate
8	Fermentas MwM	
9	haemoglobin	CM
10		Lysate
11		UB
12		ReSyn

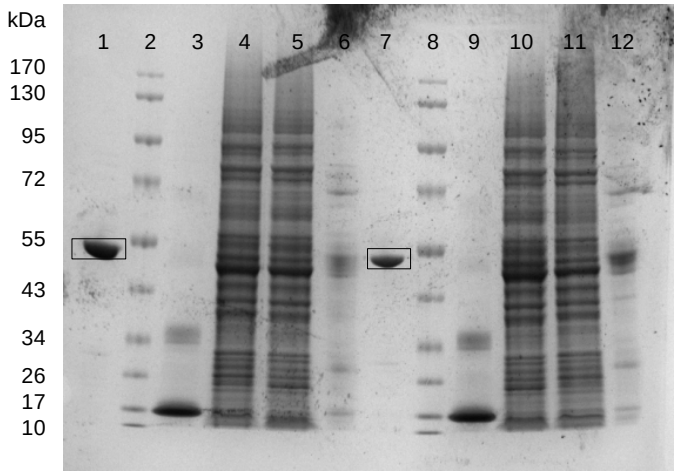

Figure A.4.10. Denaturing and reducing gradient SDS-PAGE analysis of Anor purified from *E. coli* BL21[*nicA*2]. *E. coli* BL21[*nicA*2] cultured either in filtered haemoglobin or in filtered haemoglobin in combination with 10 mM EDTA. MagReSyn™ NTA was used to purify Anor with poly-histidines tag. The protein band anticipated to be Anor is boxed. An approximate 12 µg of protein was loaded onto the gel, which was stained with Coomassi Blue overnight and was destained with dd H_2O as described in Chapter 4, Section 4.3.9. The gel was photographed with GeneSnap as before. MwM- molecular weight marker, CM- culture medium, UB- unbound.

A.4.2.3. 5-Aminolevulinic acid vs. haemoglobin

An initial study was conducted with a 50 ml culture of E. coli BL21[*nicA*2] to determine whether the addition of 5-aminolevulinic acid (A), haemoglobin (H) or a combination (A, H) of both would improve enzyme yield. Expression of Anor from *E.*

coli BL21[*nicA*2] was induced with IPTG and purified as described in Chapter 4 (Section 4.3.5). Table A.4.3 presents the yields obtained from *E. coli* BL21 (no plasmid) and *E. coli* BL21[*nicA*2] with the various medium supplementation (A; H; A, H). The NOR activity as well as the P450 content were compared to IPTG induced expression (I). NOR activity was measured in *E. coli* BL21 (0.4% of total NOR activity of *E. coli* BL21[*nicA*2] induced by IPTG only). 5-Aminolevulinic acid supplementation did increase total NOR activity by 20%, however, the P450 content remained similar. The NOR activity was increased three-fold after addition of haemoglobin, although the P450 content increased only marginally. The medium supplementation with haemoglobin or in combination of 5-aminolevulinic acid and haemoglobin resulted in the highest Anor yield. This study was repeated with a culture volume of 200 ml (refer to Section 4.4.3).

Table A.4.3. Anor yield from *E. coli* BL21[*nicA*2] with medium supplementation.

media supplementation	Total protein mg	Total activity Units	Specific activity Units.mg^{-1}	Total P450 nmoles	Specific P450 nmol.mg^{-1}
No plasmid	0.9	0.25	0.28	0	0
I	0.4	66	154	1.6	3.9
I, A	0.5	79	165	1.6	3.4
I, H	1.3	274	213	2.2	1.7
I, A, H	1.5	304	208	8.4	5.7

BL21- no plasmid; I- addition of IPTG to Luria broth; A- 5-aminolevulinic acid; H- haemoglobin; A, H- 5-aminolevulinic acid and haemoglobin.
50 ml culture volume

An SDS-PAGE gel analysis was used to investigate whether the NOR activity observed from *E. coli* BL21 was not related to Anor. Lanes 1 to 4 in Figure A.4.11 confirm that no Anor was expressed by *E. coli* BL21 (no plasmid) and that the NOR activity was most likely due to endogenous NADH-NO activity. The NOR activity determined from *E. coli* BL21[*nicA*2] cultured with haemoglobin was due to Anor expressed from pET-*nicA*2. A single protein of ~45 kDa was observed in lane 9 and 10 (eluate and remaining Anor on Mag ReSyn™ NTA). A commercial preparation of Anor (Wako Chemicals, Germany) was used as a size comparison (Fig. A.4.11, lane 12).

Lane	samples	
1	*E. coli* BL21(DE3)	Lysate
2		UB
3		Wash
4		Eluate
5	Fermentas MwM	
6	*E. coli* BL21[*nicA*2]	Lysate
7		UB
8		Wash
9		Eluate
10		ReSyn
11	Fermentas MwM	
12	wild-type NOR	

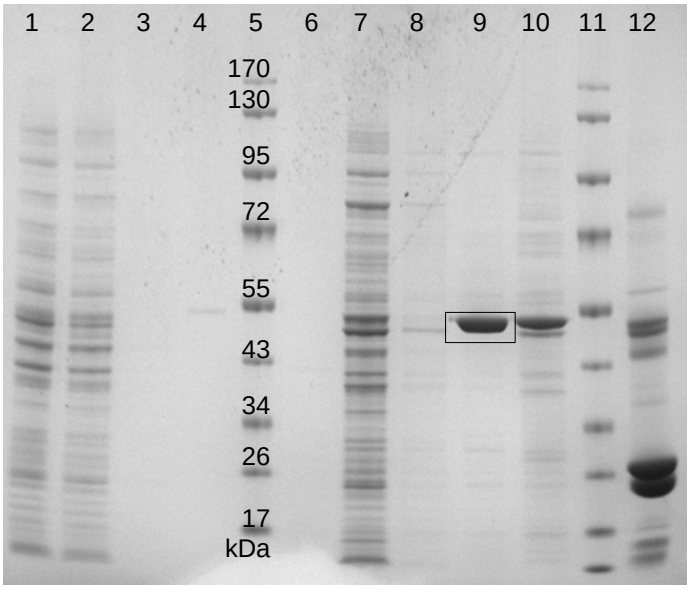

Figure A.4.11. Denaturing and reducing gradient SDS-PAGE analysis of Anor purified from *E. coli* BL21[*nicA*2]. *E. coli* BL21 containing pET-*nicA*2 and *E. coli* BL21 without the plasmid were cultured in filtered haemoglobin. MagReSyn™ NTA was used to purify poly histidine tagged Anor. The protein band anticipated to be Anor is boxed. An approximate 7-12 µg of protein was loaded onto the gel, which was stained with Colloidal Coomassie brilliant blue overnight and was destained with dd H_2O as described in Chapter 4, Section 4.3.8. The gel was photographed with GeneSnap. UB-unbound, MwM- molecular weight marker

The spectral analysis of Anor purified with MagReSyn™ NTA from *E. coli* BL21[*nicA*2] cultured with various medium supplementations (Table A.4.3) is shown in Figure A.4.12. As expected, eluates from *E. coli* cultured in Luria broth (containing 50 µg.ml^{-1} kanamycin) did not present a 410 nm peak nor a 450 nm peak after reduction and CO binding (Fig. A.4.12 A). Haemoglobin was also investigated and did present a 410 nm peak. This peak, as well as the 530 and 580 nm peaks are considered characteristic for haemoglobin. These relate to methaemoglobin upon reduction and CO binding as shown by the green line in Figure A. 4.12 B [405]. As for the other samples the spectral analysis indicated the presence a cytochrome P450 at various concentrations (Fig. A.4.12 C to D). These results show that the Anor expressed by E. coli BL21[*nicA*2] presented the characteristic Soret peak of a P450.

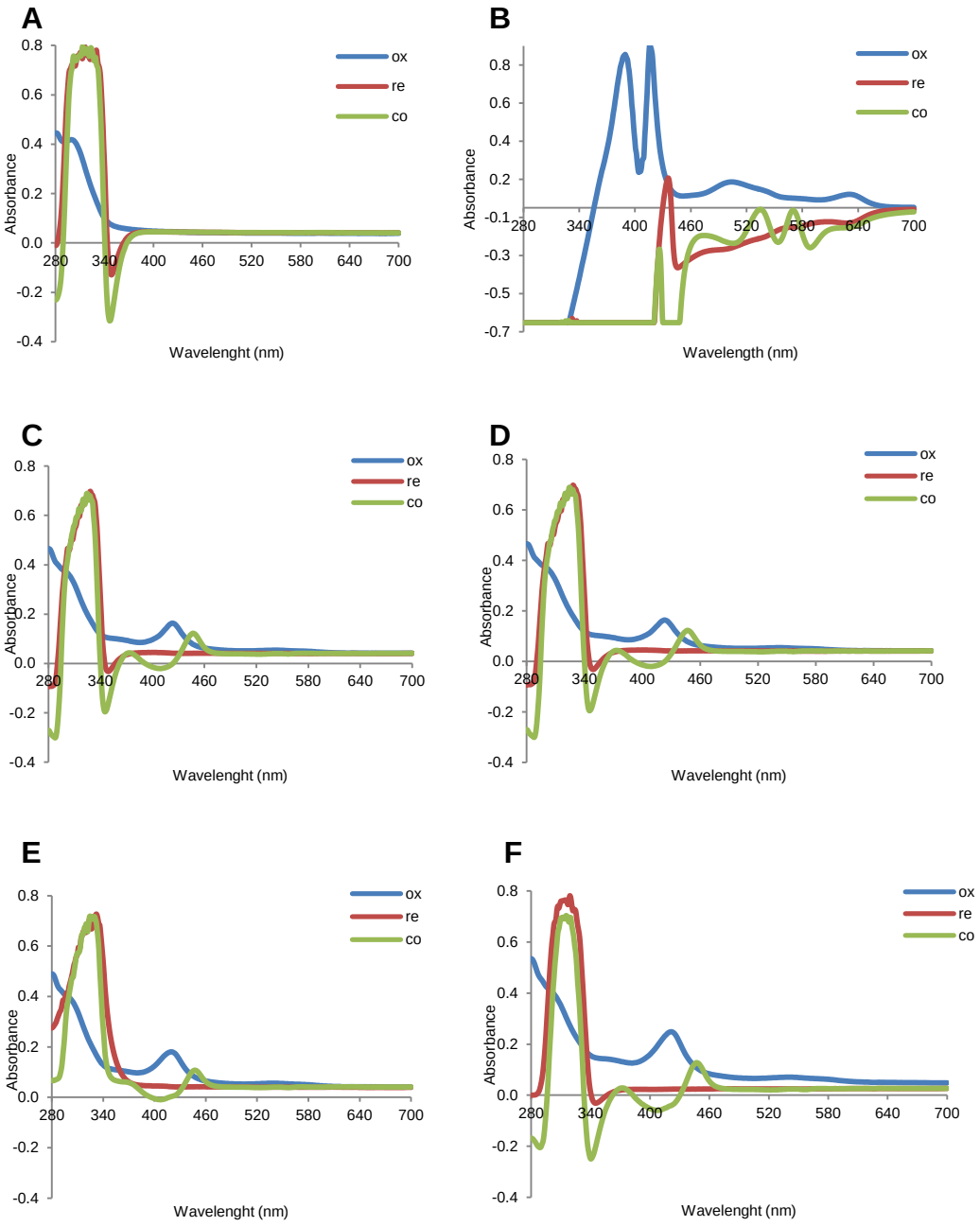

Figure A.4.12. P450 spectral analysis of Anor purified from *E. coli* BL21[*nicA*2]. *E. coli* BL21[*nicA*2] was cultured in various medium with supplementations as indicated and MagReSyn™ NTA was used to extract histidine tagged Anor. The blue line represents the protein in its resting state, i.e. oxidative state (ox). The red line is the absorbance after sodium dithionite reduction (re) and the green line is the absorbance after saturating the haem centre with carbon monoxide (CO). In (A): no IPTG, (B): haemoglobin, (C): IPTG, (D) aminolevulinic acid, (E) haemoglobin, (F) haemoglobin and aminolevulinic acid. A dilution of sample (eluate) in sodium phosphate buffer was prepared and the spectral analysis was done as described in Chapter 4, Section 4.3.6.

REFERENCES

[1] D.E. Koshland Jr, The molecule of the year, Science 258 (1992) 1861.

[2] R. SoRelle, Nobel Prize Awarded to Scientists for Nitric Oxide Discoveries, Circulation 98 (1998) 2365-2366.

[3] W.P. Arnold, C.K. Mittal, S. Katsuki, F. Murad, Nitric oxide activates guanylate cyclase and increases guanosine 3':5'-cyclic monophosphate levels in various tissue preparations, Proc. Natl. Acad. Sci. U. S. A. 74 (1977) 3203-3207.

[4] R.M. Rapoport, M.B. Draznin, F. Murad, Endothelium-dependent relaxation in rat aorta may be mediated through cyclic GMP-dependent protein phosphorylation, Nature 306 (1983) 174-176.

[5] R.M. Rapoport, F. Murad, Endothelium-dependent and nitrovasodilator-induced relaxation of vascular smooth muscle: role of cyclic GMP, J. Cyclic Nucleotide Protein Phosphor Res. 9 (1983) 281-296.

[6] R.R. Fiscus, R.M. Rapoport, F. Murad, Endothelium-dependent and nitrovasodilator-induced activation of cyclic GMP-dependent protein kinase in rat aorta, J. Cyclic Nucleotide Protein Phosphor Res. 9 (1983) 415-425.

[7] F. Murad, R.M. Rapoport, R. Fiscus, Role of cyclic-GMP in relaxations of vascular smooth muscle, J. Cardiovasc. Pharmacol. 7 Suppl 3 (1985) S111-8.

[8] R.M. Palmer, A.G. Ferrige, S. Moncada, Nitric oxide release accounts for the biological activity of endothelium-derived relaxing factor, Nature 327 (1987) 524-526.

[9] R.F. Furchgott, P.M. Vanhoutte, Endothelium-derived relaxing and contracting factors, FASEB J. 3 (1989) 2007-2018.

[10] A.J. Hobbs, L.J. Ignarro, Nitric oxide-cyclic GMP signal transduction system, Methods Enzymol. 269 (1996) 134-148.

[11] C. Nathan, Nitric oxide as a secretory product of mammalian cells, FASEB J. 6 (1992) 3051-3064.

[12] C.J. Lowenstein, J.L. Dinerman, S.H. Snyder, Nitric oxide: a physiologic messenger, Ann. Intern. Med. 120 (1994) 227-237.

[13] S. Moncada, R.M. Palmer, E.A. Higgs, Nitric oxide: physiology, pathophysiology, and pharmacology, Pharmacol. Rev. 43 (1991) 109-142.

[14] B. Dugas, P. Debre, S. Moncada, Nitric oxide, a vital poison inside the immune and inflammatory network, Res. Immunol. 146 (1995) 664-670.

[15] B.J. Whittle, Nitric oxide in physiology and pathology, Histochem J. 27 (1995) 727-737.

[16] P. Pacher, J.S. Beckman, L. Liaudet, Nitric oxide and peroxynitrite in health and disease, Physiol. Rev. 87 (2007) 315-424.

[17] J.S. Beckman, W.H. Koppenol, Nitric oxide, superoxide, and peroxynitrite: the good, the bad, and ugly, Am. J. Physiol. 271 (1996) C1424-37.

[18] S.H. Francis, J.L. Busch, J.D. Corbin, cGMP-Dependent Protein Kinases and cGMP Phosphodiesterases in Nitric Oxide and cGMP Action, Pharmacol. Rev. 62 (2010) 525.

[19] R. Korhonen, A. Lahti, H. Kankaanranta, E. Moilanen, Nitric oxide production and signaling in inflammation, Cur Drug Targets Inflamm Allergy 4 (2005) 471-479.

[20] M.N. Moller, Q. Li, J.R. Lancaster Jr, A. Denicola, Acceleration of nitric oxide autoxidation and nitrosation by membranes, IUBMB Life 59 (2007) 243-248.

[21] K.A. Broniowska, N. Hogg, The chemical biology of S-nitrosothiols, Antioxid. Redox Signaling 17 (2012) 969-980.

[22] D.D. Thomas, X. Liu, S.P. Kantrow, J.R. Lancaster Jr, The biological lifetime of nitric oxide: implications for the perivascular dynamics of NO and O_2, Proc. Natl. Acad. Sci. U. S. A. 98 (2001) 355-360.

[23] L.A. Blatter, W.G. Wier, Nitric oxide decreases $[Ca^{2+}]$i in vascular smooth muscle by inhibition of the calcium current, Cell Calcium 15 (1994) 122-131.

[24] F. Murad, Shattuck Lecture. Nitric oxide and cyclic GMP in cell signaling and drug development, NEJM 355 (2006) 2003-2011.

[25] M. Kelm, J. Schrader, Control of coronary vascular tone by nitric oxide, Circ Res. 66 (1990) 1561-1575.

[26] J.C. de Graaf, J.D. Banga, S. Moncada, R.M. Palmer, P.G. de Groot, J.J. Sixma, Nitric oxide functions as an inhibitor of platelet adhesion under flow conditions, Circulation 85 (1992) 2284-2290.

[27] D.R. Riddell, J.S. Owen, Nitric oxide and platelet aggregation, Vitam. Horm. 57 (1999) 25-48.

[28] K.M. Sanders, S.M. Ward, Nitric oxide as a mediator of nonadrenergic noncholinergic neurotransmission, Am. J. Physiol. 262 (1992) G379-92.

[29] N. Dugas, J.F. Delfraissy, M. Tardieu, Immune regulatory role of nitric oxide within the central nervous system, Res. Immunol. 146 (1995) 707-710.

[30] D.S. Bredt, P.M. Hwang, S.H. Snyder, Localization of nitric oxide synthase indicating a neural role for nitric oxide, Nature 347 (1990) 768-770.

[31] J. MacMicking, Q.W. Xie, C. Nathan, Nitric oxide and macrophage function, Annu. Rev. Immunol. 15 (1997) 323-350.

[32] H. Kolb, V. Kolb-Bachofen, Nitric oxide in autoimmune disease: cytotoxic or regulatory mediator?, Immunol. Today 19 (1998) 556-561.

[33] C. Bogdan, M. Rollinghoff, A. Diefenbach, The role of nitric oxide in innate immunity, Immunol. Rev. 173 (2000) 17-26.

[34] K.D. Kroncke, The Role of Nitric Oxide in Autoimmune Disease, Curr. Med. Chem.: Anti-Inflammatory Anti-Allergy Agents 3 (2004) 223-238.

[35] Y. Kobayashi, The regulatory role of nitric oxide in proinflammatory cytokine expression during the induction and resolution of inflammation, J. Leukocyte Biol. 88 (2010) 1157-1162.

[36] R.M. Clancy, A.R. Amin, S.B. Abramson, The role of nitric oxide in inflammation and immunity, Arthritis Rheum. 41 (1998) 1141-1151.

[37] M.B. Grisham, D. Jourd'Heuil, D.A. Wink, Nitric oxide. I. Physiological chemistry of nitric oxide and its metabolites: implications in inflammation, Am. J. Physiol. 276 (1999) G315-21.

[38] J.W. Denninger, M.A. Marletta, Guanylate cyclase and the NO/cGMP signaling pathway, Biochim. Biophys. Acta 1411 (1999) 334-350.

[39] M.W. Radomski, R.M. Palmer, S. Moncada, An L-arginine/nitric oxide pathway present in human platelets regulates aggregation, Proc. Natl. Acad. Sci. U. S. A. 87 (1990) 5193-5197.

[40] V.B. O'Donnell, B. Coles, M.J. Lewis, B.C. Crews, L.J. Marnett, B.A. Freeman, Catalytic consumption of nitric oxide by prostaglandin H synthase-1 regulates platelet function, J. Biol. Chem. 275 (2000) 38239-38244.

[41] H. Bult, G.E. Boeckxstaens, P.A. Pelckmans, F.H. Jordaens, Y.M. Van Maercke, A.G. Herman, Nitric oxide as an inhibitory non-adrenergic non-cholinergic neurotransmitter, Nature 345 (1990) 346-347.

[42] D.S. Bredt, C.E. Glatt, P.M. Hwang, M. Fotuhi, T.M. Dawson, S.H. Snyder, Nitric oxide synthase protein and mRNA are discretely localized in neuronal populations of the mammalian CNS together with NADPH diaphorase, Neuron 7 (1991) 615-624.

[43] F. Aktan, iNOS-mediated nitric oxide production and its regulation, Life Sciences 75 (2004) 639-653.

[44] J.S. Beckman, T.W. Beckman, J. Chen, P.A. Marshall, B.A. Freeman, Apparent hydroxyl radical production by peroxynitrite: implications for endothelial injury from nitric oxide and superoxide, Proc. Natl. Acad. Sci. U. S. A. 87 (1990) 1620-1624.

[45] C. Szabo, Multiple pathways of peroxynitrite cytotoxicity, Toxicol. Lett. 140-141 (2003) 105-112.

[46] C. Wang, W.M. Deen, Peroxynitrite delivery methods for toxicity studies, Chem. Res. Toxicol. 17 (2004) 32-44.

[47] D.W. Gilroy, T. Lawrence, M. Perretti, A.G. Rossi, Inflammatory resolution: new opportunities for drug discovery, Nat. Rev. Drug Discovery 3 (2004) 401-416.

[48] C.N. Serhan, S.D. Brain, C.D. Buckley, D.W. Gilroy, C. Haslett, L.A. O'Neill, M. Perretti, A.G. Rossi, J.L. Wallace, Resolution of inflammation: state of the art, definitions and terms, FASEB J. 21 (2007) 325-332.

[49] T. Lawrence, D.A. Willoughby, D.W. Gilroy, Anti-inflammatory lipid mediators and insights into the resolution of inflammation, Nat. Rev. Immunol. 2 (2002) 787-795.

[50] J.N. Fullerton, A.J. O'Brien, D.W. Gilroy, Pathways mediating resolution of inflammation: when enough is too much, J. Pathol. 231 (2013) 8-20.

[51] K.D. Kroncke, K. Fehsel, V. Kolb-Bachofen, Nitric oxide: cytotoxicity versus cytoprotection--how, why, when, and where?, Nitric Oxide-Biol. Ch. 1 (1997) 107-120.

[52] K.D. Kroncke, K. Fehsel, C. Suschek, V. Kolb-Bachofen, Inducible nitric oxide synthase-derived nitric oxide in gene regulation, cell death and cell survival, Int. Immunopharmacol. 1 (2001) 1407-1420.

[53] C. Bogdan, Nitric oxide and the immune response, Nat. Immunol. 2 (2001) 907-916.

[54] K.E. Kolodziejska, A.R. Burns, R.H. Moore, D.L. Stenoien, N.T. Eissa, Regulation of inducible nitric oxide synthase by aggresome formation, Proc. Natl. Acad. Sci. U. S. A. 102 (2005) 4854-4859.

[55] L. Pandit, K.E. Kolodziejska, S. Zeng, N.T. Eissa, The physiologic aggresome mediates cellular inactivation of iNOS, Proc. Natl. Acad. Sci. U. S. A. 106 (2009) 1211-1215.

[56] T. Wang, Y. Xia, Inducible nitric oxide synthase aggresome formation is mediated by nitric oxide, Biochem. Biophys. Res. Commun. 426 (2012) 386-389.

[57] P.R. Gardner, L.A. Martin, D. Hall, A.M. Gardner, Dioxygen-dependent metabolism of nitric oxide in mammalian cells, Free Radical Biol. Med. 31 (2001) 191-204.

[58] V.P. Reutov, Nitric oxide cycle in mammals and the cyclicity principle, Biochemistry c/c of Biokhimiia 67 (2002) 293-311.

[59] W.K. Alderton, C.E. Cooper, R.G. Knowles, Nitric oxide synthases: structure, function and inhibition, Biochem. J. 357 (2001) 593-615.

[60] R.G. Knowles, S. Moncada, Nitric oxide synthases in mammals, Biochem. J. 298 (1994) 249-258.

[61] U. Forstermann, W.C. Sessa, Nitric oxide synthases: regulation and function, Eur. Heart J. 33 (2012) 829-37, 837a-837d.

[62] U. Forstermann, H. Kleinert, Nitric oxide synthase: expression and expressional control of the three isoforms, Naunyn-Schmiedeberg's Arch. Pharmacol. 352 (1995) 351-364.

[63] D.A. Wink, K.M. Miranda, M.G. Espey, Cytotoxicity related to oxidative and nitrosative stress by nitric oxide, Exp. Biol. Med. 226 (2001) 621-623.

[64] J.R. Lancaster Jr (Ed.), Nitric Oxide. Principals and Actions, Academic Press Inc., USA, 1996.

[65] K. Schmidt, B. Mayer, Consumption of nitric oxide by endothelial cells: evidence for the involvement of a NAD(P)H-, flavin- and heme-dependent dioxygenase reaction, FEBS Lett. 577 (2004) 199-204.

[66] P.R. Gardner, A.M. Gardner, W.T. Brashear, T. Suzuki, A.N. Hvitved, K.D. Setchell, J.S. Olson, Hemoglobins dioxygenate nitric oxide with high fidelity, J. Inorg. Biochem. 100 (2006) 542-550.

[67] P.R. Gardner, Nitric oxide dioxygenase function and mechanism of flavohemoglobin, hemoglobin, myoglobin and their associated reductases, J. Inorg. Biochem. 99 (2005) 247-266.

[68] L.M. Blomberg, M.R. Blomberg, P.E. Siegbahn, A theoretical study of myoglobin working as a nitric oxide scavenger, J. Biol. Inorg. Chem. 9 (2004) 923-935.

[69] X. Zhao, N. Yeung, B.S. Russell, D.K. Garner, Y. Lu, Catalytic reduction of NO to N_2O by a designed heme copper center in myoglobin: implications for the role of metal ions, J. Am. Chem. Soc. 128 (2006) 6766-6767.

[70] M. Brunori, A. Giuffre, K. Nienhaus, G.U. Nienhaus, F.M. Scandurra, B. Vallone, Neuroglobin, nitric oxide, and oxygen: functional pathways and conformational changes, Proc. Natl. Acad. Sci. U. S. A. 102 (2005) 8483-8488.

[71] F. Trandafir, D. Hoogewijs, F. Altieri, P. Rivetti di Val Cervo, K. Ramser, S. Van Doorslaer, J.R. Vanfleteren, L. Moens, S. Dewilde, Neuroglobin and cytoglobin as potential enzyme or substrate, Gene 398 (2007) 103-113.

[72] S. Shiva, X. Wang, L.A. Ringwood, X. Xu, S. Yuditskaya, V. Annavajjhala, H. Miyajima, N. Hogg, Z.L. Harris, M.T. Gladwin, Ceruloplasmin is a NO oxidase and nitrite synthase that determines endocrine NO homeostasis, Nat. Chem. Biol. 2 (2006) 486-493.

[73] X. Wang, J.E. Tanus-Santos, C.D. Reiter, A. Dejam, S. Shiva, R.D. Smith, N. Hogg, M.T. Gladwin, Biological activity of nitric oxide in the plasmatic compartment, Proc. Natl. Acad. Sci. U. S. A. 101 (2004) 11477-11482.

[74] L.L. Pearce, A.J. Kanai, L.A. Birder, B.R. Pitt, J. Peterson, The catabolic fate of nitric oxide: the nitric oxide oxidase and peroxynitrite reductase activities of cytochrome oxidase, J. Biol. Chem. 277 (2002) 13556-13562.

[75] M.J. Coffey, R. Natarajan, P.H. Chumley, B. Coles, P.R. Thimmalapura, M. Nowell, H. Kuhn, M.J. Lewis, B.A. Freeman, V.B. O'Donnell, Catalytic consumption of nitric oxide by 12/15- lipoxygenase: inhibition of monocyte soluble guanylate cyclase activation, Proc. Natl. Acad. Sci. U. S. A. 98 (2001) 8006-8011.

[76] S.R. Clark, P.B. Anning, M.J. Coffey, A.G. Roberts, L.J. Marnett, V.B. O'Donnell, Depletion of iNOS-derived nitric oxide by prostaglandin H synthase-2 in inflammation-activated J774.2 macrophages through lipohydroperoxidase turnover, Biochem. J. 385 (2005) 815-821.

[77] H.M. Abu-Soud, S.L. Hazen, Nitric oxide modulates the catalytic activity of myeloperoxidase, J. Biol. Chem. 275 (2000) 5425-5430.

[78] H.M. Abu-Soud, S.L. Hazen, Nitric oxide is a physiological substrate for mammalian peroxidases, J. Biol. Chem. 275 (2000) 37524-37532.

[79] L. Brunelli, V. Yermilov, J.S. Beckman, Modulation of catalase peroxidatic and catalatic activity by nitric oxide, Free Radical Biol. Med. 30 (2001) 709-714.

[80] E.A. Jansson, L. Huang, R. Malkey, M. Govoni, C. Nihlen, A. Olsson, M. Stensdotter, J. Petersson, L. Holm, E. Weitzberg, J.O. Lundberg, A mammalian functional nitrate reductase that regulates nitrite and nitric oxide homeostasis, Nat. Chem. Biol. 4 (2008) 411-417.

[81] A.U. Igamberdiev, N.V. Bykova, W. Ens, R.D. Hill, Dihydrolipoamide dehydrogenase from porcine heart catalyzes NADH-dependent scavenging of nitric oxide, FEBS Lett. 568 (2004) 146-150.

[82] B.L. Godber, J.J. Doel, G.P. Sapkota, D.R. Blake, C.R. Stevens, R. Eisenthal, R. Harrison, Reduction of nitrite to nitric oxide catalyzed by xanthine oxidoreductase, J. Biol. Chem. 275 (2000) 7757-7763.

[83] S. Shiva, Z. Huang, R. Grubina, J. Sun, L.A. Ringwood, P.H. MacArthur, X. Xu, E. Murphy, V.M. Darley-Usmar, M.T. Gladwin, Deoxymyoglobin is a nitrite reductase that generates nitric oxide and regulates mitochondrial respiration, Circ Res. 100 (2007) 654-661.

[84] A.V. Kozlov, K. Staniek, H. Nohl, Nitrite reductase activity is a novel function of mammalian mitochondria, FEBS Lett. 454 (1999) 127-130.

[85] H. Nohl, K. Staniek, B. Sobhian, S. Bahrami, H. Redl, A.V. Kozlov, Mitochondria recycle nitrite back to the bioregulator nitric monoxide, Acta Biochim. Pol. (Engl. Transl.) 47 (2000) 913-921.

[86] S.B. Abramson, Osteoarthritis and nitric oxide, Osteoarthr. Cartil. 16 Suppl 2 (2008) S15-20.

[87] I.A. Clark, K.A. Rockett, W.B. Cowden, Proposed link between cytokines, nitric oxide and human cerebral malaria, Parasitol. Today 7 (1991) 205-207.

[88] K.D. Kroncke, Mechanisms and biological consequences of nitrosative stress, Biol. Chem. 384 (2003) 1341.

[89] K.D. Kroncke, Nitrosative stress and transcription, Biol. Chem. 384 (2003) 1365-1377.

[90] H.G. Seo, N. Fujiwara, H. Kaneto, M. Asahi, J. Fujii, N. Taniguchi, Effect of a nitric oxide synthase inhibitor, S-ethylisothiourea, on cultured cells and cardiovascular functions of normal and lipopolysaccharide-treated rabbits, J. Biochem. 119 (1996) 553-558.

[91] S.M. Bode-Böger, Effect of L-arginine supplementation on NO production in man, Eur. J. Clin. Pharmacol. 62 (2006) 91-99.

[92] J. Satriano, Arginine pathways and the inflammatory response: interregulation of nitric oxide and polyamines: review article, Amino Acids 26 (2004) 321-329.

[93] S.M. Morris Jr, Arginine metabolism: boundaries of our knowledge, J. Nutr. 137 (2007) 1602S-1609S.

[94] T.R. Billar, R.D. Curran, B.G. Harbrecht, D.J. Stuehr, A.J. Demetris, and R.L. Simmons, Modulation of Nitrogen Oxide Synthesis in Vivo: N^{G}-Monomethyl-L-Arginine inhibits Endotoxin-Induced Nitrite/Nitrate Biosynthesis While Promoting Hepatic Damage, J. Leukocyte Biol. 48 (1990) 565-569.

[95] M. Di Rosa, M. Radomski, R. Carnuccio, S. Moncada, Glucocorticoids inhibit the induction of nitric oxide synthase in macrophages, Biochem. Biophys. Res. Commun. 172 (1990) 1246-1252.

[96] J.M. Woodley in T. Sheper (Ed.), Adv. Biochem. Eng./Biotechnol. 70 (2000) 93-108. Springer-Verlag, Berlin Heidelberg.

[97] D.J. Pollard, J.M. Woodley, Biocatalysis for pharmaceutical intermediates: the future is now, Trends Biotechnol. 25 (2007) 66-73.

[98] J.M. Woodley, New opportunities for biocatalysis: making pharmaceutical processes greener, Trends Biotechnol. 26 (2008) 321-327.

[99] J.M. Woodley, M. Breuer, D. and Mink, A future perspective on the role of industrial biotechnology for chemicals production, Chem. Eng. Res. Des. (2013).

[100] J.M. Woodley, Protein engineering of enzymes for process applications, Curr. Opin. Chem. Biol. 17 (2013) 310-316.

[101] R.K. Singh, M.K. Tiwari, R. Singh, J.K. Lee, From protein engineering to immobilization: promising strategies for the upgrade of industrial enzymes, Int. J. Mol. Sci. 14 (2013) 1232-1277.

[102] R. Xue, J.M. Woodley, Process technology for multi-enzymatic reaction systems, Bioresour. Technol. 115 (2012) 183-195.

[103] W. Liu, P. Wang, Cofactor regeneration for sustainable enzymatic biosynthesis, Biotechnol. Adv. 25 (2007) 369-384.

[104] K. Nakahara, T. Tanimoto, K. Hatano, K. Usuda, H. Shoun, Cytochrome P-450 55A1 (P-450dNIR) acts as nitric oxide reductase employing NADH as the direct electron donor, J. Biol. Chem. 268 (1993) 8350-8355.

[105] D.C. Harrison, Glucose dehydrogenase: preparation and some properties of the enzyme and its coenzyme, Biochem. J. 27 (1933) 382-386.

[106] J. Yudkin, The dehydrogenases of Bacterium coli.: The coenzyme of glucose dehydrogenase, Biochem. J. 28 (1934) 1463-1473.

[107] H.J. Strecker, S. Korkes, Glucose dehydrogenase, J. Biol. Chem. 196 (1952) 769-784.

[108] H.K. Chenault, E.S. Simon, G.M. Whitesides, Cofactor regeneration for enzyme-catalysed synthesis, Biotechnol. Genet. Eng. Rev. 6 (1988) 221-270.

[109] H. Zhao, W.A. van der Donk, Regeneration of cofactors for use in biocatalysis, Curr. Opin. Biotechnol. 14 (2003) 583-589.

[110] A. Weckbecker, H. Groger, W. Hummel, Regeneration of nicotinamide coenzymes: principles and applications for the synthesis of chiral compounds, Adv. Biochem. Eng./Biotechnol. 120 (2010) 195-242.

[111] R. Yuryev, S. Strompen, A. Liese, Coupled chemo(enzymatic) reactions in continuous flow, Beilstein J. Org. Chem. 7 (2011) 1449-1467.

[112] A. Nunez, T.A. Foglia, G.J. and Piazza, Cofactor recycling in a coupled enzyme oxidation-reduction reaction: conversion of oxo-fatty acids to hydroxy and dicarboxylic acids, Biotechnol. Appl. Biochem. 29 (1999) 207.

[113] S.W. May, Applications of oxidoreductases, Curr. Opin. Biotechnol. 10 (1999) 370-375.

[114] B.V. Twala, B.T. Sewell, J. Jordaan, Immobilisation and characterisation of biocatalytic co-factor recycling enzymes, glucose dehydrogenase and NADH oxidase, on aldehyde functional ReSyn polymer microspheres, Enzyme Microb. Technol. 50 (2012) 331-336.

[115] W. Tischer, V. Kasche, Immobilized enzymes: crystals or carriers?, Trends Biotechnol. 17 (1999) 326-335.

[116] C. Mateo, J.M. Palomo, G. Fernandez-Lorente, J.M. Guisan, R. and Fernandez-Lafuente, Improvement of enzyme activity, stability and selectivity via immobilization techniques, Enzyme Microb. Technol. 40 (2007) 1451.

[117] D. Brady, J. Jordaan, Advances in enzyme immobilisation, Biotechnol. Lett. 31 (2009) 1639-1650.

[118] S. Datta, L.R. Christena, Y.R.S. and Rajaram, Enzyme Immobilization: an overview on techiques and support materials, 3 Biotech 3 (2013) 1.

[119] J.M. Bolivar, L. Wilson, S.A. Ferrarotti, R. Fernandez-Lafuente, J.M. Guisan, C. and Mateo, Evaluation of different immobilization stragegies to prepare an industrial biocatalyst of formate dehydrogenase from *Candida biodinii*, Enzyme Microb. Technol. 40 (2007) 540.

[120] Wang, Y. and Caruso, F., Mesoporous Silica Spheres as Supports for Enzyme Immobilization and Encapsulation, Chem. Mater. 17 (2005) 953-561.

[121] F. Lopez-Gallego, J.M. Guisan, L. Betancor, Glutaraldehyde-mediated protein immobilization, Methods Mol. Biol. (N. Y.) 1051 (2013) 33-41.

[122] C. Mateo, R. Torres, G. Fernandez-Lorente, C. Ortiz, M. Fuentes, A. Hildago, F. Lopez-Gallego, O. Abian, J.M. Palomo, L. Betancor, B.C.C. Pessela, J.M. Guisan, R. and Fernandez-Lafuente, Epoxy-Amino Groups: A New Tool for Improved Immobilization of Proteins by Epoxy Method, Biomacromolecules 4 (2003) 772.

[123] Z. Knezevic, N. Milosavic, D. Bezbradica, Z. Jakovljevic, R. and Prodanovic, Immobilization of lipase from *Candida rugosa* on Eupergit®C supports by covalent attachment, Biochem. Eng. J. 30 (2006) 269.

[124] F. Lopez-Gallego, G. Fernandez-Lorente, J. Rocha-Martin, J.M. Bolivar, C. Mateo, J.M. Guisan, Stabilization of enzymes by multipoint covalent immobilization on supports activated with glyoxyl groups, Methods Mol. Biol. (N. Y.) 1051 (2013) 59-71.

[125] J.M. Bolivar, J. Rocha-Martin, C. Mateo, F. Cava, J. Berenguer, D. Vega, R. Fernandez-Lafuente, J.M. and Guisan, Purification and stabilization of a glutamate dehydrogenase from *Thermus thermophilus* via oriented multisubunit plus multipoint covalent immobilization, J. Mol. Catal. B: Enzym. 58 (2009) 158.

[126] C. Mateo, O. Abian, G. Fernandez-Lorente, J. Pedroche, R. Fernandez-Lafuente, J.M. Guisan, A. Tam, M. Daminati, Epoxy sepabeads: a novel epoxy support for stabilization of industrial enzymes via very intense multipoint covalent attachment, Biotechnol. Prog. 18 (2002) 629-634.

[127] J.M. Bolivar, L. Wilson, S.A. Ferrarotti, J.M. Guisan, R. Fernandez-Lafuente, C. Mateo, Improvement of the stability of alcohol dehydrogenase by covalent immobilization on glyoxyl-agarose, J Biotec. 125 (2006) 85-94.

[128] L. Cao, Immobilised enzymes: science or art?, Curr. Opin. Chem. Biol. 9 (2005) 217-226.

[129] L. Wang, L. Wei, Y. Chen, R. Jiang, Specific and reversible immobilization of NADH oxidase on functionalized carbon nanotubes, J Biotec. 150 (2010) 57-63.

[130] C. Mateo, G. Fernandez-Lorente, O. Abian, R. Fernandez-Lafuente, J.M. Guisan, Multifunctional epoxy supports: a new tool to improve the covalent immobilization of proteins. The promotion of physical adsorptions of proteins on the supports before their covalent linkage, Biomacromolecules 1 (2000) 739-745.

[131] J.M. Bolivar, L. Wilson, S.A. Ferrarotti, R. Fernandez-Lafuente, J.M. Guisan, C. Mateo, Stabilization of a formate dehydrogenase by covalent immobilization on highly activated glyoxyl-agarose supports, Biomacromolecules 7 (2006) 669-673.

[132] J. Perdoche, M. del Mar Yust, C. Mateo, R. Fernandez-Lafuente, J. Giron-Calle, M. Alaiz, J. Vioque, J.M. Guisan, F. and Millan, Effect of the support and experimental conditions in the intensity of the multipoint covalent attachment of proteins on glyoxyl-agarose supports: Correlation between enzyme-support linkages and thermal stability, Enzyme Microb. Technol. 40 (2007) 1160.

[133] D. Brady, J. Jordaan, C. Simpson, A. Chetty, C. Arumugam, F.S. Moolman, Spherezymes: a novel structured self-immobilisation enzyme technology, BMC Biotechnol. 8 (2008) 8.

[134] N.L. Watmough, S.J. Field, R.J.L.a.R. Hughes D.J., The bacterial respiratory nitric oxide reductase, Biochem. Soc. Trans. 37 (2009) 392-399.

[135] W.G. Zumft, Nitric oxide reductases of prokaryotes with emphasis on the respiratory, heme-copper oxidase type, J. Inorg. Biochem. 99 (2005) 194-215.

[136] Y. Shiro, H. Sugimoto, T. Tosha, S. Nagano, T. Hino, Structural basis for nitrous oxide generation by bacterial nitric oxide reductases, Philos. Trans. R. Soc., B 367 (2012) 1195-1203.

[137] K. Usuda, N. Toritsuka, Y. Matsuo, D.H. Kim, H. Shoun, Denitrification by the fungus *Cylindrocarpon tonkinense*: anaerobic cell growth and two isozyme forms of cytochrome P-450nor, Appl. Environ. Microbiol. 61 (1995) 883-889.

[138] S. Kobasyashi, Y. Matsuo, A. Takimoto, S. Suzuki, F. Maruo, H. Shoun, Denitrification, a Novel Type of Respiratory Metabolism in Fungal Mitochondrion, J. Biol. Chem. 271 (1996) 16263.

[139] H. Shoun, S. Fushinobu, L. Jiang, S.W. Kim, T. Wakagi, Fungal denitrification and nitric oxide reductase cytochrome P450nor, Philos. Trans. R. Soc., B 367 (2012) 1186-1194.

[140] H. Shoun, T. Tanimoto, Denitrification by the Fungus *Fusarium oxysporum* and Involvment of Cytochrome P-450 in the Respiratory Nitrite Reduction, J. Biol. Chem. 266 (1991) 11078.

[141] A.M. Gardner, R.A. Helmick, P.R. Gardner, Flavorubredoxin, an inducible catalyst for nitric oxide reduction and detoxification in *Escherichia coli*, J. Biol. Chem. 277 (2002) 8172-8177.

[142] J. Hendriks, A. Oubrie, J. Castresana, A. Urbani, S. Gemeinhardt, M. Saraste, Nitric oxide reductases in bacteria, Biochim. Biophys. Acta 1459 (2000) 266-273.

[143] L. Zhang, T. Kudo, N. Takaya, H. Shoun, Distribution, structure and function of fungal nitric oxide reductase P450nor-recent advances, International Congress Series 1233 (2002) 197-202.

[144] L. Zhang, H. Shoun, Purification and Functional Analysis of Fungal Nitric Oxide Reductase Cytochrome P450nor, in: Robert K. Poole (Ed.) Methods Enzymol., Academic Press (2008)117-133.

[145] D.L. Harris, Cytochrome P450nor: A nitric oxide reductase- structure, spectra, and mechanism, Int. J. Quantum Chem. 88 (2002) 183-200.

[146] T. Kudo, N. Takaya, S.-. Park, Y. Shiro, H. Shoun, A Positively Charged Cluster Formed in the Heme-distal Pocket of Cytochrome P450nor Is Essential for Interaction with NADH, J. Biol. Chem. 276 (2001) 5020.

[147] L. Zhang, T. Kudo, N. Takaya, H. Shoun, The B' helix determines cytochrome P450nor specificity for the electron donors NADH and NADPH, J. Biol. Chem. 277 (2002) 33842-33847.

[148] T. Kudo, D. Tomura, D.L. Liu, X.Q. Dai, H. Shoun, Two isozymes of P450nor of *Cylindrocarpon tonkinense*: molecular cloning of the cDNAs and genes, expressions in the yeast, and the putative NAD(P)H-binding site, Biochimie 78 (1996) 792-799.

[149] S. Tsuruta, N. Takaya, L. Zhang, H. Shoun, K. Kimura, M. Hamamoto, T. Nakase, Denitrifcation by yeasts and occurance of cytochromo P450nor in *Trichosporon cutaneum*, FEMS Microbiol. Lett. 168 (1998) 105.

[150] N. Takaya, S. Suzuki, S. Kuwazaki, H. Shoun, F. Maruo, M. Yamaguchi, K. Takeo, Cytochrome P450nor, a Novel Class of Mitochondrial Cytochrome P450 Involved in Nitrate Respiration in the Fungus *Fusarium oxysporum*, Arch. Biochem. Biophys. 372 (1999) 340.

[151] L. Zhang, N. Takaya, T. Kitazume, T. Kondo, H. Shoun, Purification and cDNA cloning of nitric oxide reductase cytochrome P450nor (CYP55A4) from *Trichosporon cutaneum*, European J. Biochem. / FEBS 268 (2001) 3198-3204.

[152] M. Kaya, K. Matsumura, K. Higashida, Y. Hata, A. Kawato, Y. Abe, O. Akita, N. Takaya, H. Shoun, Cloning and enhanced expression of the cytochrome P450nor gene (nicA; CYP55A5) encoding nitric oxide reductase from *Aspergillus oryzae*, Bioscience, Biotechnology, and Biochemistry 68 (2004) 2040-2049.

[153] C.H. Wang, I.J. Stern, C.M. Gilmour, The catabolism of glucose and gluconate in Pseudomonas species, Arch. Biochem. Biophys. 81 (1959) 489-492.

[154] B. Siebers, V.F. Wendisch, R. Hensel, Carbohydrate metabolism in *Thermoproteus tenax*: *in vivo* utilization of the non-phosphorylative Entner-Doudoroff pathway and characterization of its first enzyme, glucose dehydrogenase, Arch. Microbiol. 168 (1997) 120-127.

[155] H.J. Lamble, N.I. Heyer, S.D. Bull, D.W. Hough, M.J. Danson, Metabolic pathway promiscuity in the archaeon *Sulfolobus solfataricus* revealed by studies on glucose dehydrogenase and 2-keto-3-deoxygluconate aldolase, J. Biol. Chem. 278 (2003) 34066-34072.

[156] A.H. Romano, T. Conway, Evolution of carbohydrate metabolic pathways, Res. Microbiol. 147 (1996) 448-455.

[157] A. Weckbecker and W. Hummel, Glucose Dehydrogenase for the Regeneration of NADPH and NADH, Methods in Biotechnology: in J.-L. Barredo (Ed.), Microbial Enzymes and Biotransformations 17 (2005) 225-237, Human Press.

[158] S.C. Davis, S.J. Jenne, P.A. Kebber, L.M. Newman, Glucose Dehydrogenase Polypeptides and Related Polynucleotides 10/915927 (2010).

[159] S. Chaykin, Nicotinamide coenzymes, Annu. Rev. Biochem. 36 (1967) 149-170.

[160] Y. Shiro, M. Fujii, T. Iizuka, S. Adachi, K. Tsukamoto, K. Nakahara, H. Shoun, Spectroscopic and Kinetic Studies on Reaction of Cytochrome P450nor with Nitric oxide, J. Biol. Chem. 270 (1995) 1617.

[161] K.K. Mak, U. Wollenberger, F.W. Scheller, R. Renneberg, An amperometric bi-enzyme sensor for determination of formate using cofactor regeneration, Biosens. Bioelectron. 18 (2003) 1095-1100.

[162] R. Wichmann, D. Vasic-Racki, Cofactor regeneration at the lab scale, Adv. Biochem. Eng./Biotechnol. 92 (2005) 225-260.

[163] M.W. Radomski, R.M. Palmer, S. Moncada, Glucocorticoids inhibit the expression of an inducible, but not the constitutive, nitric oxide synthase in vascular endothelial cells, Proc. Natl. Acad. Sci. U. S. A. 87 (1990) 10043-10047.

[164] R.M. Palmer, L. Bridge, N.A. Foxwell, S. Moncada, The role of nitric oxide in endothelial cell damage and its inhibition by glucocorticoids, Br. J. Pharmacol. 105 (1992) 11-12.

[165] C.I. Chang, J.C. Liao, L. Kuo, Arginase modulates nitric oxide production in activated macrophages, Am. J. Physiol. 274 (1998) H342-8.

[166] B. Heiss, K. Frunzke, W.G. Zumft, Formation of the N-N bond from nitric oxide by a membrane-bound cytochrome *bc* complex of nitrate-respiring (denitrifying) *Pseudomonas stutzeri*, J. Bacteriol. 171 (1989) 3288-3297.

[167] U.M. Stuendl, I. Schmidt, U. Scheller, R. Schmid, Schunck, W-H. and Schauer, F., Purification and Characterization of Cytosolic Cytochrome P450 Forms from Yeast Belonging to the Genus Trichosporon, Arch. Biochem. Biophys. 357 (1998) 313.

[168] L.Y. Chao, J. Rine, M.A. Marletta, Spectroscopic and kinetic studies of Nor1, a cytochrome P450 nitric oxide reductase from the fungal pathogen *Histoplasma capsulatum*, Arch. Biochem. Biophys. 480 (2008) 132-137.

[169] F.H. Thorndycroft, G. Butland, D.J. Richardson, N.J. Watmough, A new assay for nitric oxide reductase reveals two conserved glutamate residues form the entrance to a proton-conducting channel in the bacterial enzyme, Biochem. J. 401 (2007) 111-119.

[170] E. Forte, A. Urbani, M. Saraste, P. Sarti, M. Brunori, A. Giuffre, The cytochrome *cbb3* from *Pseudomonas stutzeri* displays nitric oxide reductase activity, Eur. J. Biochem. 268 (2001) 6486-6491.

[171] C. Butler, E. Forte, F. Maria Scandurra, M. Arese, A. Giuffre, C. Greenwood, P. Sarti, Cytochrome bo_3 from *Escherichia coli*: the binding and turnover of nitric oxide, Biochem. Biophys. Res. Commun. 296 (2002) 1272-1278.

[172] P. Girsch, S. de Vries, Purification and initial kinetic and spectroscopic characterization of NO reductase from *Paracoccus denitrificans*, Biochim. Biophys. Acta 1318 (1997) 202-216.

[173] M. Dermastia, T. Turk, T.C. Hollocher, Nitric oxide reductase. Purification from *Paracoccus denitrificans* with use of a single column and some characteristics, The J. Biol. Chem. 266 (1991) 10899-10905.

[174] T. Hayashi, M.T. Lin, K. Ganesan, Y. Chen, J.A. Fee, R.B. Gennis, P. Moenne-Loccoz, Accomodation of Two Diatomic Molecules in Cytochrome bo_3: Insights into NO Reductase Activity in Terminal Oxidases, Biochemistry 48 (2009) 883.

[175] Y. Shiro, Structure and function of bacterial nitric oxide reductases: nitric oxide reductase, anaerobic enzymes, Biochim. Biophys. Acta 1817 (2012) 1907-1913.

[176] H. Kizawa, D. Tomura, M. Oda, A. Fukamizu, T. Hoshino, O. Gotoh, T. Yasui, H. Shoun, Nucleotide sequence of the unique nitrate/nitrite-inducible cytochrome P-450 cDNA from *Fusarium oxysporum*, J. Biol. Chem. 266 (1991) 10632-10637.

[177] U.M. Stuendl, Patzak, D. and Schauer, F., Purification of a soluable cytochrome P450 from *Trichosporon montevideense*, J. Basic Microbiol. 40 (2000) 289.

[178] H. Shimizu, E. Obayashi, Y. Gomi, H. Arakawa, S.- Park, H. Nakamura, S. Adachi, H. Shoun, Y. Shiro, Proton Delivery in NO Reduction by Fungal Nitric oxide Reductase, J. Biol. Chem. 275 (2000) 4816.

[179] I.G. Zacharia, W.M. Deen, Diffusivity and solubility of nitric oxide in water and saline, Ann. Biomed. Eng. 33 (2005) 214-222.

[180] M. Kavdia, R.S. Lewis, Nitric oxide delivery in stagnant systems via nitric oxide donors: a mathematical model, Chem. Res. Toxicol. 16 (2003) 7-14.

[181] R.B. McComb, L.W. Bond, R.W. Burnett, R.C. Keech, G.N. Bowers Jr, Determination of the molar absorptivity of NADH, Clin. Chem. 22 (1976) 141-150.

[182] K. Kiianitsa, J.A. Solinger, W.D. Heyer, NADH-coupled microplate photometric assay for kinetic studies of ATP-hydrolyzing enzymes with low and high specific activities, Anal. Biochem. 321 (2003) 266-271.

[183] R.D. Allison, Kinetic Assay Methods, Curr Protoc in Protein Sci, John Wiley and Sons Inc, United States (2001) Unit 3.5.51-5.3.11

[184] C.M. Maragos, D. Morley, D.A. Wink, T.M. Dunams, J.E. Saavedra, A. Hoffman, A.A. Bove, L. Isaac, J.A. Hrabie, L.K. Keefer, Complexes of NO with nucleophiles as agents for the controlled biological release of nitric oxide. Vasorelaxant effects, J. Med. Chem. 34 (1991) 3242-3247.

[185] R.S. Lewis, W.M. Deen, Kinetics of the reaction of nitric oxide with oxygen in aqueous solutions, Chem. Res. Toxicol. 7 (1994) 568-574.

[186] A. Ramamurthi, R.S. Lewis, Measurement and modeling of nitric oxide release rates for nitric oxide donors, Chem. Res. Toxicol. 10 (1997) 408-413.

[187] K. Schmidt, W. Desch, P. Klatt, W.R. Kukovetz, B. Mayer, Release of nitric oxide from donors with known half-life: a mathematical model for calculating nitric oxide concentrations in aerobic solutions, Naunyn-Schmiedeberg's Arch. Pharmacol. 355 (1997) 457-462.

[188] J.A. Hrabie, J.R. Klose, D.A. Wink, L.K. Keefer, New Nitric Oxide-Releasing Zwitterions Derived from Polyamines, J. Org. Chem. 58 (1993) 1472-1476.

[189] L.K. Keefer, R.W. Nims, K.M. Davies, D.A. Wink, "NONOates" (1-substituted diazen-1-ium-1,2-diolates) as nitric oxide donors: convenient nitric oxide dosage forms, Methods Enzymol. 268 (1996) 281-293.

[190] D.A. Wink, J.F. Darbyshire, R.W. Nims, J.E. Saavedra, P.C. Ford, Reactions of the bioregulatory agent nitric oxide in oxygenated aqueous media: determination of the kinetics for oxidation and nitrosation by intermediates generated in the NO/O_2 reaction, Chem. Res. Toxicol. 6 (1993) 23-27.

[191] P.C. Ford, D.A. Wink, D.M. Stanbury, Autoxidation kinetics of aqueous nitric oxide, FEBS Lett. 326 (1993) 1-3.

[192] V.G. Kharitonov, A.R. Sundquist, V.S. Sharma, Kinetics of nitric oxide autoxidation in aqueous solution, J. Biol. Chem. 269 (1994) 5881-5883.

[193] K. Nakahara, H. Shoun, N-terminal processing and amino acid sequence of two isoforms of nitric oxide reductase cytochrome P450nor from *Fusarium oxysporum*, J. Biochem. 120 (1996) 1082-1087.

[194] N. Okamoto, K. Tsuruta, Y. Imai, D. Tomura, H. Shoun, Fungal P450nor: expression in *Escherichia coli* and site-directed mutageneses at the putative distal region, Arch. Biochem. Biophys. 337 (1997) 338-344.

[195] E. Obayashi, S. Takahashi, Y. Shir, Electronic Structure of Reaction Intermediate of Cytochrome P450nor in its Nitric oxide reduction, J. Am. Chem. Soc. 120 (1998) 12964-12965.

[196] H.J.M. van den Brink, R.F.M. van Gorcom, van den Hondel, C.A.M and Punt, P.J., Review: Cytochrome P450 Enzyme Systems in Fungi, Fungal Genet. Biol. 23 (1998) 1.

[197] D. Mansuy, The great diversity of reactions catalyzed by cytochromes P450, Comp. Biochem. Physiol., Part C: Pharmacol., Toxicol. Endocrinol. 121 (1998) 5-14.

[198] D. Werck-Reichhart, R. Feyereisen, Cytochromes P450: a success story, Genome Biol. 1 (2000) Reviews 3003.1-3003.9.

[199] D. Werck-Reichhart, S. Bak, S. Paquette, Cytochromes p450, The Arabidopsis book, 1 (2002) e0028, American Society of Plant Biologists.

[200] K.J. McLean, M. Sabri, K.R. Marshall, R.J. Lawson, D.G. Lewis, D. Clift, P.R. Balding, A.J. Dunford, A.J. Warman, J.P.Q. McVey A.-M., M.J. Sutcliffe, Scrutton, N.S. and Munro, A.W., Biodiversity of cytochrome P450 redox systems, Biochem. Soc. Trans. 33 (2005) 796.

[201] T. Omura, R. Sato, The Carbon Monoxide-Binding Pigment of Liver Microsomes. I. Evidence for its Hemoprotein Nature, J. Biol. Chem. 239 (1964) 2370-2378.

[202] T. Omura, R. Sato, The Carbon Monoxide-Binding Pigment of Liver Microsomes. Ii. Solubilization, Purification, and Properties, J. Biol. Chem. 239 (1964) 2379-2385.

[203] J.A. Peterson, S.E. Graham, A close family resemblance: the importance of structure in understanding cytochromes P450, Structure 6 (1998) 1079-1085.

[204] M. Hata, Y. Hirano, T. Hoshino, R. Nishida, M. Tsuda, Theoretical study on monooxygenation mechanism by cytochrome P450: an ultimate species in the substrate oxidation process, J. Mol. Struct.: THEOCHEM 722 (2005) 133.

[205] F. Hannemann, A. Bichet, Ewen, K.M. and Bernhardt, R., Cytochrome P450 systems-biological variations of electron transport chains, Biochim. Biophys. Acta 1770 (2007) 330.

[206] T.L. Poulos, Y. Madrona, Oxygen activation and redox partner binding in cytochromes P450, Biotechnol. Appl. Biochem. 60 (2013) 128-133.

[207] M. Otyepka, J. Skopalik, E. Anzenbacherova, P. Anzenbacher, What common structural features and variations of mammalian P450s are known to date?, Biochim. Biophys. Acta 1770 (2007) 376-389.

[208] T.L. Poulos, B.C. Finzel, A.J. Howard, High-resolution crystal structure of cytochrome P450cam, J. Mol. Biol. 195 (1987) 687-700.

[209] S.A. Martinis, W.M. Atkins, P.S. Stayton, S.G. and Sligar, A Conserved Residue of Cytochrome P-450 Is Involved in Heme-Oxygen Stability and Activation, J. Am. Chem. Soc. 111 (1989) 9252.

[210] Y. Shiro, Reaction mechanism of nitric oxide reductase and its relation to molecular structure, RIKEN Rev. 9 (1999) 56-58.

[211] A. Daiber, H. Shoun, V. Ullrich, Nitric oxide reductase (P450nor) from *Fusarium oxysporum*, J. Inorg. Biochem. 99 (2005) 185-193.

[212] N. Lehnert, V.K. Praneeth, F. Paulat, Electronic structure of iron(II)-porphyrin nitroxyl complexes: molecular mechanism of fungal nitric oxide reductase (P450nor), J. Comput. Chem. 27 (2006) 1338-1351.

[213] S.-. Park, H. Shimizu, S. Adachi, A. Nakagawa, I. Tanaka, K. Nakahara, H. Shoun, E. Obayashi, H. Nakamura, T. Iizuka, Y. Shiro, Cyrstal structure of nitric oxide reductase from denitrifying fungus *Fusarium oxysporum*, Nat. Struct. Biol. 4 (1997) 827.

[214] D. Tomura, K. Obika, A. Fukamizu, H. Shoun, Nitric oxide reductase cytochrome P-450 gene, CYP 55, of the fungus *Fusarium oxysporum* containing a potential binding-site for FNR, the transcription factor involved in the regulation of anaerobic growth of *Escherichia coli*, J. Biochem. 116 (1994) 88-94.

[215] R.S. Zitomer, C.V. Lowry, Regulation of gene expression by oxygen in *Saccharomyces cerevisiae*, Microbiol. Rev. 56 (1992) 1-11.

[216] C.V. Lowry, R.S. Zitomer, ROX1 encodes a heme-induced repression factor regulating ANB1 and CYC7 of *Saccharomyces cerevisiae*, Mol. Cell. Biol. 8 (1988) 4651-4658.

[217] D. Lubertozzi, J.D. Keasling, Developing *Aspergillus* as a host for heterologous expression, Biotechnol. Adv. 27 (2009) 53-75.

[218] C.A. van den Hondel, P.J. Punt, R.F. van Gorcom, Production of extracellular proteins by the filamentous fungus *Aspergillus*, Antonie van Leeuwenhoek 61 (1992) 153-160.

[219] P.J. Punt, C.A. van den Hondel, Transformation of filamentous fungi based on hygromycin B and phleomycin resistance markers, Methods Enzymol. 216 (1992) 447-457.

[220] P.J. Punt, N. van Biezen, A. Conesa, A. Albers, J. Mangnus, C. van den Hondel, Filamentous fungi as cell factories for heterologous protein production, Trends Biotechnol. 20 (2002) 200-206.

[221] J.Y. Shoji, M. Arioka, K. Kitamoto, Dissecting cellular components of the secretory pathway in filamentous fungi: insights into their application for protein production, Biotechnol. Lett. 30 (2008) 7-14.

[222] M.G. Wiebe, A. Karandikar, G.D. Robson, A.P. Trinci, J.L. Candia, S. Trappe, G. Wallis, U. Rinas, P.M. Derkx, S.M. Madrid, H. Sisniega, I. Faus, R. Montijn, C.A. van den Hondel, P.J. Punt, Production of tissue plasminogen activator (t-PA) in *Aspergillus niger*, Biotechnol. Bioeng. 76 (2001) 164-174.

[223] C.L. Gordon, V. Khalaj, A.F. Ram, D.B. Archer, J.L. Brookman, A.P. Trinci, D.J. Jeenes, J.H. Doonan, B. Wells, P.J. Punt, C.A. van den Hondel, G.D. Robson, Glucoamylase::green fluorescent protein fusions to monitor protein secretion in *Aspergillus niger*, Microbiology 146 (Pt 2) (2000) 415-426.

[224] S.H. Rose, W.H. van Zyl, Constitutive expression of the *Trichoderma reesei* beta-1,4-xylanase gene (*xyn2*) and the beta-1,4-endoglucanase gene (*egl*) in *Aspergillus niger* in molasses and defined glucose media, Appl. Microbiol. Biotechnol. 58 (2002) 461-468.

[225] D.C. la Grange, I.S. Pretorius, W.H. van Zyl, Expression of a *Trichoderma reesei* beta-xylanase gene (*xyn2*) in *Saccharomyces cerevisiae*, Appl. Environ. Microbiol. 62 (1996) 1036-1044.

[226] S.H. Rose, W.H. van Zyl, Exploitation of *Aspergillus niger* for the Heterologous Production of Cellulases and Hemicellulases, Open Biotechnol. J. 2 (2008) 167-175.

[227] R. Radzio, U. Kuck, Efficient synthesis of the blood-coagulation inhibitor hirudin in the filamentous fungus *Acremonium chrysogenum*, Appl. Microbiol. Biotechnol. 48 (1997) 58-65.

[228] L. Wang, D. Ridgway, T.a.M. Gu M., Effects of process parameters on heterologous protein production in *Aspergillus niger* fermentation, J. Chem. Technol. Biotechnol. 78 (2003) 1259-1266.

[229] Q. Li, L.M. Harvey, B. McNeil, The effects of bioprocess parameters on extracellular proteases in a recombinant *Aspergillus niger* B1-D, Appl. Microbiol. Biotechnol. 78 (2008) 333-341.

[230] Purwanto, L.A., Ibrahim, D., and Sudrajat, H., Effect of agitation speed on morphological changes in *Aspergillus niger* hyphae during production of tannase, World J. Chem. 4 (2009) 34-38.

[231] J. Xu, L. Wang, D. Ridgway, T. Gu, M. Moo-Young, Increased heterologous protein production in *Aspergillus niger* fermentation through extracellular proteases inhibition by pelleted growth, Biotechnol. Prog. 16 (2000) 222-227.

[232] M. Papagianni, Fungal morphology and metabolite production in submerged mycelial processes, Biotechnol. Adv. 22 (2004) 189-259.

[233] J. Sambrook, E.F. Fritsch and T. Maniatis (Ed.), Molecular Cloning A Laboratory Manual (1989), Cold Spring Harbor, New York.

[234] Y.Q. Cui, R.G. van der Lans, K.C. Luyben, Effect of agitation intensities on fungal morphology of submerged fermentation, Biotechnol. Bioeng. 55 (1997) 715-726.

[235] H. el-Enshasy, K. Hellmuth, U. Rinas, Fungal morphology in submerged cultures and its relation to glucose oxidase excretion by recombinant *Aspergillus niger*, Appl. Biochem. Biotechnol. 81 (1999) 1-11.

[236] S. Kelly, L.H. Grimm, J. Hengstler, E. Schultheis, R. Krull, D.C. Hempel, Agitation effects on submerged growth and product formation of *Aspergillus niger*, Bioprocess Biosyst. Eng. 26 (2004) 315-323.

[237] J.P. van den Hombergh, M.D. Sollewijn Gelpke, P.J. van de Vondervoort, F.P. Buxton, J. Visser, Disruption of three acid proteases in *Aspergillus niger*-effects on protease spectrum, intracellular proteolysis, and degradation of target proteins, European J. Biochem. 247 (1997) 605-613.

[238] A.C. Franken, B.C. Lokman, A.F. Ram, P.J. Punt, C.A. van den Hondel, S. de Weert, Heme biosynthesis and its regulation: towards understanding and improvement of heme biosynthesis in filamentous fungi, Appl. Microbiol. Biotechnol. 91 (2011) 447-460.

[239] A. Shevchenko, H. Tomas, J. Havlis, J.V. Olsen, M. Mann, In-gel digestion for mass spectrometric characterization of proteins and proteomes, Nat. Protoc. 1 (2006) 2856-2860.

[240] G. Hather, R. Higdon, A. Bauman, P.D. von Haller, E. Kolker, Estimating false discovery rates for peptide and protein identification using randomized databases, Proteomics 10 (2010) 2369-2376.

[241] R.J. Corbett, R.S. Roche, Use of high-speed size-exclusion chromatography for the study of protein folding and stability, Biochemistry 23 (1984) 1888-1894.

[242] V.L. Prabha, N.S. Punekar, Genetic transformation in Aspergilli: tools of the trade, Indian J. Biochem. Biophys. 41 (2004) 205-215.

[243] R.M. Berka, P. Schneider, E.J. Golightly, S.H. Brown, M. Madden, K.M. Brown, T. Halkier, K. Mondorf, F. Xu, Characterization of the gene encoding an extracellular laccase of Myceliophthora thermophila and analysis of the recombinant enzyme expressed in *Aspergillus oryzae*, Appl. Environ. Microbiol. 63 (1997) 3151-3157.

[244] T. Guillemette, N.N. van Peij, T. Goosen, K. Lanthaler, G.D. Robson, C.A. van den Hondel, H. Stam, D.B. Archer, Genomic analysis of the secretion stress response in the enzyme-producing cell factory *Aspergillus niger*, BMC Genomics 8 (2007) 158.

[245] A.A. Tokmakov, A. Kurotani, T. Takagi, M. Toyama, M. Shirouzu, Y. Fukami, S. Yokoyama, Multiple post-translational modifications affect heterologous protein synthesis, J. Biol. Chem. 287 (2012) 27106-27116.

[246] I.I. Karuzina, V.G. Zgoda, G.P. Kuznetsova, N.F. Samenkova, A.I. Archakov, Heme and apoprotein modification of cytochrome P450 2B4 during its oxidative inactivation in monooxygenase reconstituted system, Free Radical Biol. Med. 26 (1999) 620-632.

[247] S.M. Sadrzadeh, E. Graf, S.S. Panter, P.E. Hallaway, J.W. Eaton, Hemoglobin. A biologic fenton reagent, J. Biol. Chem. 259 (1984) 14354-14356.

[248] F.P. Guengerich, N.A. Hosea, A. Parikh, L.C. Bell-Parikh, W.W. Johnson, E.M. Gillam, T. Shimada, Twenty years of biochemistry of human P450s: purification, expression, mechanism, and relevance to drugs, Drug Metab. Dispos. 26 (1998) 1175-1178.

[249] F.P. Guengerich, N.A. Hosea, M.V. Martin, Purification of cytochromes P450: products of bacterial recombinant expression systems, Methods Mol. Biol. (N. Y.) 107 (1998) 77-83.

[250] C. Wandersman, I. Stojiljkovic, Bacterial heme sources: the role of heme, hemoprotein receptors and hemophores, Curr. Opin. Microbiol. 3 (2000) 215-220.

[251] I. Stojiljkovic, D. Perkins-Balding, Processing of heme and heme-containing proteins by bacteria, DNA Cell Biol. 21 (2002) 281-295.

[252] M. Schobert, D. Jahn, Regulation of heme biosynthesis in non-phototrophic bacteria, J. Mol. Microbiol. Biotechnol. 4 (2002) 287-294.

[253] S.C. Andrews, A.K. Robinson, F. Rodriguez-Quinones, Bacterial iron homeostasis, FEMS Microbiol. Rev. 27 (2003) 215-237.

[254] I.U. Heinemann, M. Jahn, D. Jahn, The biochemistry of heme biosynthesis, Arch. Biochem. Biophys. 474 (2008) 238-251.

[255] D. Jahn, E. Verkamp, D. Soll, Glutamyl-transfer RNA: a precursor of heme and chlorophyll biosynthesis, Trends Biochem. Sci. 17 (1992) 215-218.

[256] D. Jahn, C. Hungerer, B. Troup, Unusual pathways and environmentally regulated genes of bacterial heme biosynthesis, Die Naturwissenschaften 83 (1996) 389-400.

[257] N. Frankenberg, J. Moser, D. Jahn, Bacterial heme biosynthesis and its biotechnological application, Appl. Microbiol. Biotechnol. 63 (2003) 115-127.

[258] G. Layer, J. Reichelt, D. Jahn, D.W. Heinz, Structure and function of enzymes in heme biosynthesis, Protein Sci. 19 (2010) 1137-1161.

[259] M.J. Weickert, M. Pagratis, S.R. Curry, R. Blackmore, Stabilization of apoglobin by low temperature increases yield of soluble recombinant hemoglobin in *Escherichia coli*, Appl. Environ. Microbiol. 63 (1997) 4313-4320.

[260] M.J. Weickert, I. Apostol, High-fidelity translation of recombinant human hemoglobin in *Escherichia coli*, Appl. Environ. Microbiol. 64 (1998) 1589-1593.

[261] M.J. Weickert, D.H. Doherty, E.A. Best, P.O. Olins, Optimisation of heterologous protein production in *Escherichia coli*, Curr. Opin. Biotechnol. 7 (1996) 494-499.

[262] J. Sudhamsu, M. Kabir, M.V. Airola, B.A. Patel, S.R. Yeh, D.L. Rousseau, B.R. Crane, Co-expression of ferrochelatase allows for complete heme incorporation into recombinant proteins produced in *E. coli*, Protein Expression Purif. 73 (2010) 78-82.

[263] W.K. Philipp-Dormston, M. Doss, Over-production of porphyrins and heme in heterotrophic bacteria, Z. Naturforsch. C Bio. Sci. 30 (1975) 425-426.

[264] M.L. McConville, H.P. Charles, Mutants of *Escherichia coli* K12 permeable to haemin, J. Gen. Microbiol. 113 (1979) 165-168.

[265] M.L. McConville, H.P. Charles, Isolation of haemin-requiring mutants of *Escherichia coli* K12, J. Gen. Microbiol. 113 (1979) 155-164.

[266] J.M. Li, O. Brathwaite, S.D. Cosloy, C.S. Russell, 5-Aminolevulinic acid synthesis in *Escherichia coli*, J. Bacteriol. 171 (1989) 2547-2552.

[267] E. Verderber, L.J. Lucast, J.A. Van Dehy, P. Cozart, J.B. Etter, E.A. Best, Role of the hemA gene product and delta-aminolevulinic acid in regulation of *Escherichia coli* heme synthesis, J. Bacteriol. 179 (1997) 4583-4590.

[268] N.J. Jacobs, E.R. Maclosky, S.F. Conti, Effects of oxygen and heme on the development of a microbial respiratory system, J. Bacteriol. 93 (1967) 278-285.

[269] N.J. Jacobs, J.M. Jacobs, H.E. Morgan Jr, Comparative effect of oxygen and nitrate on protoporphyrin and heme synthesis from delta-aminolevulinic acid in bacterial cultures, J. Bacteriol. 112 (1972) 1444-1445.

[270] M. Nishimoto, J.E. Clark, B.S. Masters, Cytochrome P450 4A4: expression in *Escherichia coli*, purification, and characterization of catalytic properties, Biochemistry 32 (1993) 8863-8870.

[271] E.M. Gillam, Z. Guo, M.V. Martin, C.M. Jenkins, F.P. Guengerich, Expression of cytochrome P450 2D6 in *Escherichia coli*, purification, and spectral and catalytic characterization, Arch. Biochem. Biophys. 319 (1995) 540-550.

[272] C.L. Varnado, D.C. Goodwin, System for the expression of recombinant hemoproteins in *Escherichia coli*, Protein Expression Purif. 35 (2004) 76-83.

[273] P.E. Graves, D.P. Henderson, M.J. Horstman, B.J. Solomon, J.S. Olson, Enhancing stability and expression of recombinant human hemoglobin in *E. coli*: Progress in the development of a recombinant HBOC source, Biochim. Biophys. Acta 1784 (2008) 1471-1479.

[274] V. Kery, D. Elleder, J.P. Kraus, Delta-aminolevulinate increases heme saturation and yield of human cystathionine beta-synthase expressed in *Escherichia coli*, Arch. Biochem. Biophys. 316 (1995) 24-29.

[275] I.N. Harnastai, A.A. Gilep, S.A. Usanov, The development of an efficient system for heterologous expression of cytochrome P450s in *Escherichia coli* using hemA gene co-expression, Protein Expression Purif. 46 (2006) 47-55.

[276] L. Fecker, V. Braun, Cloning and expression of the fhu genes involved in iron(III)-hydroxamate uptake by *Escherichia coli*, J. Bacteriol. 156 (1983) 1301-1314.

[277] D. Law, K.M. Wilkie, R. Freeman, F.K. Gould, The iron uptake mechanisms of enteropathogenic *Escherichia coli*: the use of haem and haemoglobin during growth in an iron-limited environment, J. Med. Microbiol. 37 (1992) 15-21.

[278] D. Law, J. Kelly, Use of heme and hemoglobin by *Escherichia coli* O157 and other Shiga-like-toxin-producing *E. coli* serogroups, Infect. Immun. 63 (1995) 700-702.

[279] J.J. Woodward, N.I. Martin, M.A. Marletta, An *Escherichia coli* expression-based method for heme substitution, Nat. Methods 4 (2007) 43-45.

[280] G. Hannig, S.C. Makrides, Strategies for optimizing heterologous protein expression in *Escherichia coli*, Trends Biotechnol. 16 (1998) 54-60.

[281] P. Gatti-Lafranconi, A. Natalello, D. Ami, S.M. Doglia, M. Lotti, Concepts and tools to exploit the potential of bacterial inclusion bodies in protein science and biotechnology, FEBS J. 278 (2011) 2408-2418.

[282] J. Grodberg, J.J. Dunn, ompT encodes the *Escherichia coli* outer membrane protease that cleaves T7 RNA polymerase during purification, J. Bacteriol. 170 (1988) 1245-1253.

[283] K. Obika, D. Tomura, A. Fukamizu, H. and Shoun, Expression of the fungal cytochrome P-450nor cDNA in *Escherichia coli*, Biochem. Biophys. Res. Commun. 196 (1993) 1255-1260.

[284] F.W. Studier, B.A. Moffatt, Use of bacteriophage T7 RNA polymerase to direct selective high-level expression of cloned genes, J. Mol. Biol. 189 (1986) 113-130.

[285] F.P. Guengerich, M.V. Martin, C.D. Sohl, Q. Cheng, Measurement of cytochrome P450 and NADPH-cytochrome P450 reductase, Nat. Protoc. 4 (2009) 1245-1251.

[286] K. Nakahigashi, K. Nishimura, K. Miyamoto, H. Inokuchi, Photosensitivity of a protoporphyrin-accumulating, light-sensitive mutant (visA) of *Escherichia coli* K-12, Proc. Natl. Acad. Sci. U. S. A. 88 (1991) 10520-10524.

[287] A. Sasarman, M. Surdeanu, G. Szegli, T. Horodniceanu, V. Greceanu, A. Dumitrescu, Hemin-deficient mutants of *Escherichia coli* K-12, J. Bacteriol. 96 (1968) 570-572.

[288] A. Rogers, Y. Gibon, J. Schwender (Ed.), Chapter 4: Enzyme Kinetics: Theory and Practice in Plant Metabolic Networks, Springer Science+Business media, LLC, 2009, 71-103.

[289] L. Michaelis, M.L. Menten, K.A. Johnson, R.S. Goody, The original Michaelis constant: translation of the 1913 Michaelis-Menten paper, Biochemistry 50 (2011) 8264-8269.

[290] J.W. Williams, D.B. Northrop, Substrate specificity and structure-activity relationships of gentamicin acetyltransferase I. The dependence of antibiotic resistance upon substrate V_{max}/K_m values, J. Biol. Chem. 253 (1978) 5908-5914.

[291] D.E. Koshland, The application and usefulness of the ratio k_{cat}/K_m, Bioorg. Chem. 30 (2002) 211-213.

[292] E.A. Ceccarelli, N. Carrillo, O.A. Roveri, Efficiency function for comparing catalytic competence, Trends Biotechnol. 26 (2008) 117-118.

[293] R.J. Fox, M.D. Clay, Catalytic effectiveness, a measure of enzyme proficiency for industrial applications, Trends Biotechnol. 27 (2009) 137-140.

[294] N. Carrillo, E. Ceccarelli, O. Roveri, Usefulness of kinetic enzyme parameters in biotechnological practice, Biotechnol. Genet. Eng. Rev. 27 (2010) 367-382.

[295] C.A. Genco, D.W. Dixon, Emerging strategies in microbial haem capture, Mol. Microbiol. 39 (2001) 1-11.

[296] V. Braun, M. Braun, Iron transport and signaling in *Escherichia coli*, FEBS Lett. 529 (2002) 78-85.

[297] V. Braun, Iron uptake by *Escherichia coli*, Front. Biosci. 8 (2003) s1409-21.

[298] W.W. Ho, H. Li, S. Eakanunkul, Y. Tong, A. Wilks, M. Guo, T.L. Poulos, Holo- and apo-bound structures of bacterial periplasmic heme-binding proteins, J. Biol. Chem. 282 (2007) 35796-35802.

[299] Y. Tong, M. Guo, Bacterial heme-transport proteins and their heme-coordination modes, Arch. Biochem. Biophys. 481 (2009) 1-15.

[300] J. Tao, J.H. Xu, Biocatalysis in development of green pharmaceutical processes, Curr. Opin. Chem. Biol. 13 (2009) 43-50.

[301] J. Turkova, Oriented immobilization of biologically active proteins as a tool for revealing protein interactions and function, J. Chromatogr. B: Biomed. Sci. Appl. 722 (1999) 11-31.

[302] C. Mateo, O. Abian, R. Fernandez-Lafuente, J.M. and Guisan, Increase in confirmational stability of enzymes immobilized on epoxy-activated supports by favoring addtional multipoint covalent attachment, Enzyme Microb. Technol. 26 (2000) 509.

[303] F. Lopez-Gallego, L. Betancor, A. Hidalgo, C. Mateo, J.M. Guisan, R. Fernandez-Lafuente, Optimisation of an industrial biocatalyst of glutaryl acylase: stabilization of the enzyme by multipoint covalent attachment onto new amino-epoxy Sepabeads, J Biotec. 111 (2004) 219-227.

[304] R.C. Rodrigues, C. Ortiz, A. Berenguer-Murcia, R. Torres, R. Fernandez-Lafuente, Modifying enzyme activity and selectivity by immobilization, Chem. Soc. Rev. 42 (2013) 6290-6307.

[305] L. Wilson, L. Betancor, G. Fernandez-Lorente, M. Fuentes, A. Hidalgo, J.M. Guisan, B.C. Pessela, R. Fernandez-Lafuente, Cross-linked aggregates of multimeric enzymes: a simple and efficient methodology to stabilize their quaternary structure, Biomacromolecules 5 (2004) 814-817.

[306] B.C. Pessela, C. Mateo, M. Fuentes, A. Vian, J.L. Garcia, A.V. Carrascosa, J.M. Guisan, R. Fernandez-Lafuente, Stabilization of a multimeric beta-galactosidase from Thermus sp. strain T2 by immobilization on novel heterofunctional epoxy supports plus aldehyde-dextran cross-linking, Biotechnol. Prog. 20 (2004) 388-392.

[307] R. Fernandez-Lafuente, Stabilization of multimeric enzymes: Strategies to prevent subunit dissociation, Enzyme Microb. Technol. 45 (2009) 405.

[308] J.M. Bolivar, J. Rocha-Martin, C. Mateo, F. Cava, J. Berenguer, R. Fernandez-Lafuente, J.M. Guisan, Coating of soluble and immobilized enzymes with ionic polymers: full stabilization of the quaternary structure of multimeric enzymes, Biomacromolecules 10 (2009) 742-747.

[309] S. Sharma, B.J. Berne, S.K. Kumar, Thermal and structural stability of adsorbed proteins, Biophysical Journal 99 (2010) 1157-1165.

[310] M. Dragomirescu, G. Preda, T. Vintila, B. Vlad-Oros, D. Bordean, C. and Savii, The effect of immobization on activity and stability of a protease preparation obtained by an indigenous strain, *Bacillus licheniformis* B40, Academia Romana 57 (2012) 77.

[311] T. Yamazaki, W. Tsugawa, K. and Sode, Increased thermal stability of glucose dehydrogenase by cross-linking chemical modification, Biotechnol. Lett. 21 (1999) 199.

[312] D.A. Cowan, R. Fernandez-Lafuente, Enhancing the functional properties of thermophilic enzymes by chemical modification and immobilization, Enzyme Microb. Technol. 49 (2011) 326-346.

[313] D.A. Wood, T.L. Whateley, A study of enzyme and protein microencapsulation--some factors affecting the low apparent enzymic activity yields, J. Pharm. Pharmacol. 34 (1982) 552-557.

[314] K. Yamamoto, G. Kurisu, M. Kusunoki, S. Tabata, I. Urabe, S. Osaki, Crystal structure of glucose dehydrogenase from *Bacillus megaterium* IWG3 at 1.7 A resolution, J. Biochem. 129 (2001) 303-312.

[315] H.E. Pauly, G. Pfleiderer, D-glucose dehydrogenase from *Bacillus megaterium* M 1286: purification, properties and structure, Biol. Chem. Hoppe-Seyler 356 (1975) 1613-1623.

[316] H.E. Pauly, G. Pfleiderer, Conformational and functional aspects of the reversible dissociation and denaturation of glucose dehydrogenase, Biochemistry 16 (1977) 4599-4604.

[317] Y. Fujita, R. Ramaley, E. Freese, Location and properties of glucose dehydrogenase in sporulating cells and spores of *Bacillus subtilis*, J. Bacteriol. 132 (1977) 282-293.

[318] G. Hermanson (Ed.), Bioconjugate Techniques (2008), Academic press.

[319] J.K. Grady, N.D. Chasteen, D.C. Harris, Radicals from "Good's" buffers, Anal. Biochem. 173 (1988) 111-115.

[320] M. Kirsch, E.E. Lomonosova, H.G. Korth, R. Sustmann, H. de Groot, Hydrogen peroxide formation by reaction of peroxynitrite with HEPES and related tertiary amines. Implications for a general mechanism, J. Biol. Chem. 273 (1998) 12716-12724.

[321] M. Baron, J.D. Fontana, M.F. Guimaraes, J. Woodward, Stabilization and reutilization of *Bacillus megaterium* glucose dehydrogenase by immobilization, Appl. Biochem. Biotechnol. 63-65 (1997) 257-268.

[322] V. Grazu, O. Abian, C. Mateo, F. Batista-Viera, R. Fernandez-Lafuente, J.M. Guisan, Stabilization of enzymes by multipoint immobilization of thiolated proteins on new epoxy-thiol supports, Biotechnol. Bioeng. 90 (2005) 597-605.

[323] C. Mateo, V. Grazu, B.C. Pessela, T. Montes, J.M. Palomo, R. Torres, F. Lopez-Gallego, R. Fernandez-Lafuente, J.M. Guisan, Advances in the design of new epoxy supports for enzyme immobilization-stabilization, Biochem. Soc. Trans. 35 (2007) 1593-1601.

[324] C. Mateo, O. Abian, R. Fernandez-Lafuente, J.M. Guisan, Increase in conformational stability of enzymes immobilized on epoxy-activated supports by favoring additional multipoint covalent attachment, Enzyme Microb. Technol. 26 (2000) 509-515.

[325] C. Wong, D.G. Drueckhammer, H.M. and Sweers, Enzymatic vs. Fermantative Synthesis: Thermostable Glucose Dehydrogenase Catalyzed Regeneration of NAD(P)H for use in Enzymatic Synthesis, J. Am. Chem. Soc. 107 (1985) 4028.

[326] S. Pandey, D.K. Agrawal, Immunobiology of Toll-like receptors: emerging trends, Immunol. Cell Biol. 84 (2006) 333-341.

[327] Y. Vodovotz, G. Constantine, J. Faeder, Q. Mi, J. Rubin, J. Bartels, J. Sarkar, R.H. Squires Jr, D.O. Okonkwo, J. Gerlach, R. Zamora, S. Luckhart, B. Ermentrout, G. An, Translational systems approaches to the biology of inflammation and healing, Immunopharmacol. Immunotoxicol. 32 (2010) 181-195.

[328] L.A. Baxt, A.C. Garza-Mayers, M.B. Goldberg, Bacterial subversion of host innate immune pathways, Science 340 (2013) 697-701.

[329] S. Agarwal, N.P. Piesco, L.P. Johns, A.E. Riccelli, Differential expression of IL-1 beta, TNF-alpha, IL-6, and IL-8 in human monocytes in response to lipopolysaccharides from different microbes, J. Dent. Res. 74 (1995) 1057-1065.

[330] D. Zeidler, U. Zahringer, I. Gerber, I. Dubery, T. Hartung, W. Bors, P. Hutzler, J. Durner, Innate immunity in *Arabidopsis thaliana*: lipopolysaccharides activate nitric oxide synthase (NOS) and induce defense genes, Proc. Natl. Acad. Sci. U. S. A. 101 (2004) 15811-15816.

[331] P. Ma, X. Cui, S. Wang, J. Zhang, E.V. Nishanian, W. Wang, R.A. Wesley, R.L. Danner, Nitric oxide post-transcriptionally up-regulates LPS-induced IL-8 expression through p38 MAPK activation, J. Leukocyte Biol. 76 (2004) 278-287.

[332] A.A. Azenabor, P. Kennedy, J. York, Free intracellular Ca2+ regulates bacterial lipopolysaccharide induction of iNOS in human macrophages, Immunobiology 214 (2009) 143-152.

[333] K. Mao, S. Chen, M. Chen, Y. Ma, Y. Wang, B. Huang, Z. He, Y. Zeng, Y. Hu, S. Sun, J. Li, X. Wu, X. Wang, W. Strober, C. Chen, G. Meng, B. Sun, Nitric oxide suppresses NLRP3 inflammasome activation and protects against LPS-induced septic shock, Cell Res. 23 (2013) 201-212.

[334] D.W. Gilroy, P. Vallance, Resolution for sepsis?, Circulation 111 (2005) 2-4.

[335] I.J. Elenkov, D.G. Iezzoni, A. Daly, A.G. Harris, G.P. Chrousos, Cytokine dysregulation, inflammation and well-being, Neuroimmunomodulation 12 (2005) 255-269.

[336] A. Cauwels, P. Brouckaert, Nitrite regulation of shock, Cardiovasc. Res. 89 (2011) 553-559.

[337] C.A. Feghali, T.M. Wright, Cytokines in acute and chronic inflammation, Front. Biosci. 2 (1997) d12-26.

[338] L.J. Hofseth, S. Saito, S.P. Hussain, M.G. Espey, K.M. Miranda, Y. Araki, C. Jhappan, Y. Higashimoto, P. He, S.P. Linke, M.M. Quezado, I. Zurer, V. Rotter, D.A. Wink, E. Appella, C.C. Harris, Nitric oxide-induced cellular stress and p53 activation in chronic inflammation, Proc. Natl. Acad. Sci. U. S. A. 100 (2003) 143-148.

[339] T. Lawrence, D.W. Gilroy, Chronic inflammation: a failure of resolution?, Int. J. Exp. Pathol. 88 (2007) 85-94.

[340] I. Tabas, C.K. Glass, Anti-inflammatory therapy in chronic disease: challenges and opportunities, Science 339 (2013) 166-172.

[341] X. Liu, P.S. Silverstein, V. Singh, A. Shah, N. Qureshi, A. Kumar, Methamphetamine increases LPS-mediated expression of IL-8, TNF-alpha and IL-1beta in human macrophages through common signaling pathways, PloS one 7 (2012) e33822.

[342] W. Cao, L. Cheng, J. Behar, C. Fiocchi, P. Biancani, K.M. Harnett, Proinflammatory cytokines alter/reduce esophageal circular muscle contraction in experimental cat esophagitis, Am. J. Physiol. 287 (2004) G1131-9.

[343] S.J. Wu, L.T. Ng, Tetrandrine inhibits proinflammatory cytokines, iNOS and COX-2 expression in human monocytic cells, Biol. Pharm. Bull. 30 (2007) 59-62.

[344] K.H. Yip, Y. Huang, M.M. Waye, H.Y. Lau, Induction of nitric oxide synthases in primary human cultured mast cells by IgE and proinflammatory cytokines, Int. Immunopharmacol. 8 (2008) 764-768.

[345] G. Rawadi, S. Roman-Roman, Mycoplasma membrane lipoproteins induced proinflammatory cytokines by a mechanism distinct from that of lipopolysaccharide, Infect. Immun. 64 (1996) 637-643.

[346] L.P. Grattage, I.F. McKenzie, P.M. Hogarth, Effects of PMA, cytokines and dexamethasone on the expression of cell surface Fc receptors and mRNA in U937 cells, Immunol. Cell Biol. 70 (Pt 2) (1992) 97-105.

[347] A.K. Nussler, M. Di Silvio, T.R. Billiar, R.A. Hoffman, D.A. Geller, R. Selby, J. Madariaga, R.L. Simmons, Stimulation of the nitric oxide synthase pathway in human hepatocytes by cytokines and endotoxin, J. Exp. Med. 176 (1992) 261-264.

[348] M. Shimizu, K. Ogura, I. Mizoguchi, Y. Chiba, K. Higuchi, H. Ohtsuka, J. Mizuguchi, T. Yoshimoto, IL-27 promotes nitric oxide production induced by LPS through STAT1, NF-kappaB and MAPKs, Immunobiology 218 (2013) 628-634.

[349] A.R. Brasier, The nuclear factor-kappaB-interleukin-6 signalling pathway mediating vascular inflammation, Cardiovasc. Res. 86 (2010) 211-218.

[350] T. Lawrence, C. Fong, The resolution of inflammation: anti-inflammatory roles for NF-kappaB, Int. J. Biochem. Cell Biol. 42 (2010) 519-523.

[351] Z. Xing, J. Gauldie, G. Cox, H. Baumann, M. Jordana, X.F. Lei, M.K. Achong, IL-6 is an antiinflammatory cytokine required for controlling local or systemic acute inflammatory responses, J. Clin. Invest. 101 (1998) 311-320.

[352] T. Ohama, M. Hori, E. Momotani, M. Elorza, W.T. Gerthoffer, H. Ozaki, IL-1beta inhibits intestinal smooth muscle proliferation in an organ culture system: involvement of COX-2 and iNOS induction in muscularis resident macrophages, Am. J. Physiol. 292 (2007) G1315-22.

[353] M.O. Li, R.A. Flavell, Contextual regulation of inflammation: a duet by transforming growth factor-beta and interleukin-10, Immunity 28 (2008) 468-476.

[354] I.P. Oswald, T.A. Wynn, A. Sher, S.L. James, Interleukin 10 inhibits macrophage microbicidal activity by blocking the endogenous production of tumor necrosis factor alpha required as a costimulatory factor for interferon gamma-induced activation, Proc. Natl. Acad. Sci. U. S. A. 89 (1992) 8676-8680.

[355] M.C. Defer, B. Dugas, N. Paul-Eugene, K. Yamaoka, J.P. Kolb, C. Damais, Role of interleukin-4 in the regulation of nitric oxide production by normal human monocytes, C. R. Acad. Sci. 317 (1994) 1021-1025.

[356] Z. Guo, L. Shao, Q. Du, K.S. Park, D.A. Geller, Identification of a classic cytokine-induced enhancer upstream in the human iNOS promoter, FASEB J. 21 (2007) 535-542.

[357] C.L. Tham, C.Y. Liew, K.W. Lam, A.S. Mohamad, M.K. Kim, Y.K. Cheah, Z.A. Zakaria, M.R. Sulaiman, N.H. Lajis, D.A. Israf, A synthetic curcuminoid derivative inhibits nitric oxide and proinflammatory cytokine synthesis, Eur. J. Pharmacol. 628 (2010) 247-254.

[358] Harris, P. and Ralph, P., Human Leukemic Models of Myelomonocytic Development: A Review of the HL-60 and U937 cell lines, J. Leukocyte Biol. 37 (1985) 407-422.

[359] I.M. Garrelds, P.T. van Hal, R.C. Haakmat, H.C. Hoogsteden, P.R. Saxena, F.J. Zijlstra, Time dependent production of cytokines and eicosanoids by human monocytic leukaemia U937 cells; effects of glucocorticosteroids, Mediators Inflammation 8 (1999) 229-235.

[360] D. Franchimont, H. Martens, M.T. Hagelstein, E. Louis, W. Dewe, G.P. Chrousos, J. Belaiche, V. Geenen, Tumor necrosis factor alpha decreases, and interleukin-10 increases, the sensitivity of human monocytes to dexamethasone: potential regulation of the glucocorticoid receptor, J. Clin. Endocrinol. Metab. 84 (1999) 2834-2839.

[361] M. Ishiyama, Y. Miyazono, K. Sasamoto, Y. Ohkura, K. Ueno, A highly water-soluble disulfonated tetrazolium salt as a chromogenic indicator for NADH as well as cell viability, Talanta 44 (1997) 1299-1305.

[362] O. Huet, J.M. Petit, M.H. Ratinaud, R. Julien, NADH-dependent dehydrogenase activity estimation by flow cytometric analysis of 3-(4,5-dimethylthiazolyl-2-yl)-2,5-diphenyltetrazolium bromide (MTT) reduction, Cytometry 13 (1992) 532-539.

[363] D.T. Vistica, P. Skehan, D. Scudiero, A. Monks, A. Pittman, M.R. Boyd, Tetrazolium-based assays for cellular viability: a critical examination of selected parameters affecting formazan production, Cancer Res. 51 (1991) 2515-2520.

[364] C. Korzeniewski, D.M. Callewaert, An enzyme-release assay for natural cytotoxicity, J. Immunol. Methods 64 (1983) 313-320.

[365] T. Decker, M.L. Lohmann-Matthes, A quick and simple method for the quantitation of lactate dehydrogenase release in measurements of cellular cytotoxicity and tumor necrosis factor (TNF) activity, J. Immunol. Methods 115 (1988) 61-69.

[366] M. Drent, N.A. Cobben, R.F. Henderson, E.F. Wouters, M. van Dieijen-Visser, Usefulness of lactate dehydrogenase and its isoenzymes as indicators of lung damage or inflammation, Eur. Respir. J. 9 (1996) 1736-1742.

[367] S. Depraetere, B. Vanhaesebroeck, W. Fiers, J. Willems, M. Joniau, Polar agents with differentiation inducing capacity potentiate tumor necrosis factor-mediated cytotoxicity in human myeloid cell lines, J. Leukocyte Biol. 57 (1995) 141-151.

[368] F.H. Guo, S.C. Erzurum, Characterization of inducible nitric oxide synthase expression in human airway epithelium, Environ. Health Perspect. 106 Suppl. 5 (1998) 1119-1124.

[369] S. Kwon, S.C. George, Synergistic cytokine-induced nitric oxide production in human alveolar epithelial cells, Nitric Oxide-Biol Ch 3 (1999) 348-357.

[370] A. Cauwels, J. Bultinck, P. Brouckaert, Dual role of endogenous nitric oxide in tumor necrosis factor shock: induced NO tempers oxidative stress, Cell. Mol. Life Sci. 62 (2005) 1632-1640.

[371] A.S. Farias, C. de la Hoz, F.R. Castro, E.C. Oliveira, J.R. Ribeiro dos Reis, J.S. Silva, F. Langone, L.M.B. Santos, Nitric Oxide and TNF alpha: Effects in Experimental Autoimmune Encephalomyelitis Demyelination, Neuroimmunomodulation 14 (2007) 32-38.

[372] H. Muhl, J.H. Chang, A. Huwiler, M. Bosmann, J. Paulukat, R. Ninic, M. Nold, M. Hellmuth, J. Pfeilschifter, Nitric oxide augments release of chemokines from monocytic U937 cells: modulation by anti-inflammatory pathways, Free Radical Biol. Med. 29 (2000) 969-980.

[373] L. Yan, S. Wang, S.P. Rafferty, R.A. Wesley, R.L. Danner, Endogenously produced nitric oxide increases tumor necrosis factor-alpha production in transfected human U937 cells, Blood 90 (1997) 1160-1167.

[374] S. Wang, L. Yan, R.A. Wesley, R.L. Danner, Nitric oxide increases tumor necrosis factor production in differentiated U937 cells by decreasing cyclic AMP, J. Biol. Chem. 272 (1997) 5959-5965.

[375] M.B. Gorbet, M.V. Sefton, Endotoxin: the uninvited guest, Biomaterials 26 (2005) 6811-6817.

[376] K. Turpaev, D. Litvinov, J. Justesen, Redox modulation of NO-dependent induction of interleukin 8 gene in monocytic U937 cells, Cytokine 23 (2003) 15-22.

[377] K. Turpaev, C. Bouton, J.C. Drapier, Nitric oxide-derived nitrosating species and gene expression in human monocytic cells, Biochemistry 43 (2004) 10844-10850.

[378] S.A. Fulton, J.M. Johnsen, S.F. Wolf, D.S. Sieburth, W.H. Boom, Interleukin-12 production by human monocytes infected with *Mycobacterium tuberculosis*: role of phagocytosis, Infect. Immun. 64 (1996) 2523-2531.

[379] H. Naruse, T. Hisamatsu, Y. Yamauchi, J.E. Chang, K. Matsuoka, M.T. Kitazume, K. Arai, S. Ando, T. Kanai, N. Kamada, T. Hibi, Intracellular bacteria recognition contributes to maximal interleukin (IL)-12 production by IL-10-deficient macrophages, Clin. Exp. Immunol. 164 (2011) 137-144.

[380] H. Nagura, J. Asai, Y. Katsumata, K. Kojima, Role of electric surface charge of cell membrane in phagocytosis, Acta Pathol. Jpn. 23 (1973) 279-290.

[381] N.P. Ziats, K.M. Miller, J.M. Anderson, *In vitro* and *in vivo* interactions of cells with biomaterials, Biomaterials 9 (1988) 5-13.

[382] M.D. McGeough, C.A. Pena, J.L. Mueller, D.A. Pociask, L. Broderick, H.M. Hoffman, S.D. Brydges, Cutting edge: IL-6 is a marker of inflammation with no direct role in inflammasome-mediated mouse models, J. Immunol. 189 (2012) 2707-2711.

[383] H. Tilg, E. Trehu, M.B. Atkins, C.A. Dinarello, J.W. Mier, Interleukin-6 (IL-6) as an anti-inflammatory cytokine: induction of circulating IL-1 receptor antagonist and soluble tumor necrosis factor receptor p55, Blood 83 (1994) 113-118.

[384] J.A. Cairns, G.R. Guy, Y.H. Tan, Interleukin-6 regulates the cytotoxic effect of tumour necrosis factor on U937 cells, Immunology 75 (1992) 669-673.

[385] A.M. Deakin, A.N. Payne, B.J. Whittle, S. Moncada, The modulation of IL-6 and TNF-alpha release by nitric oxide following stimulation of J774 cells with LPS and IFN-gamma, Cytokine 7 (1995) 408-416.

[386] J. Siednienko, J. Nowak, P.N. Moynagh, W.A. Gorczyca, Nitric oxide affects IL-6 expression in human peripheral blood mononuclear cells involving cGMP-dependent modulation of NF-kappaB activity, Cytokine 54 (2011) 282-288.

[387] R.T. Villavicencio, S. Liu, M.R. Kibbe, D.L. Williams, R.W. Ganster, K.F. Dyer, D.J. Tweardy, T.R. Billiar, B.R. Pitt, Induced nitric oxide inhibits IL-6-induced stat3 activation and type II acute phase mRNA expression, Shock 13 (2000) 441-445.

[388] S. Vlahopoulos, I. Boldogh, A. Casola, A.R. Brasier, Nuclear factor-kappaB-dependent induction of interleukin-8 gene expression by tumor necrosis factor alpha: evidence for an antioxidant sensitive activating pathway distinct from nuclear translocation, Blood 94 (1999) 1878-1889.

[389] J.R. Bradley, TNF-mediated inflammatory disease, J Pathol. 214 (2008) 149-160.

[390] J.P. Waters, J.S. Pober, J.R. Bradley, Tumour necrosis factor in infectious disease, J Pathol. 230 (2013) 132-147.

[391] J.L. Swantek, M.H. Cobb, T.D. Geppert, Jun N-terminal kinase/stress-activated protein kinase (JNK/SAPK) is required for lipopolysaccharide stimulation of tumor necrosis factor alpha (TNF-alpha) translation: glucocorticoids inhibit TNF-alpha translation by blocking JNK/SAPK, Mol. Cell. Biol. 17 (1997) 6274-6282.

[392] C. Mendoza-Milla, C. Machuca Rodriguez, E. Cordova Alarcon, A. Estrada Bernal, E.M. Toledo-Cuevas, E. Martinez Martinez, A. Zentella Dehesa, NF-kappaB activation but not PI3K/Akt is required for dexamethasone dependent protection against TNF-alpha cytotoxicity in L929 cells, FEBS Lett. 579 (2005) 3947-3952.

[393] L. Cole, R. Bellomo, D. Journois, P. Davenport, I. Baldwin, P. Tipping, High-volume haemofiltration in human septic shock, Intensive Care Med. 27 (2001) 978-986.

[394] L. Cole, R. Bellomo, P. Davenport, P. Tipping, S. Uchino, C. Tetta, C. Ronco, The effect of coupled haemofiltration and adsorption on inflammatory cytokines in an ex vivo model, Dial., Transplant., Nephrol. 17 (2002) 1950-1956.

[395] J. Jiang, N. Malavia, V. Suresh, S.C. George, Nitric oxide gas phase release in human small airway epithelial cells, Respir. Res. 10 (2009) 3.

[396] V. Neuhoff, N. Arold, D. Taube, W. Ehrhardt, Improved staining of proteins in polyacrylamide gels including isoelectric focusing gels with clear background at nanogram sensitivity using Coomassie Brilliant Blue G-250 and R-250, Electrophoresis 9 (1988) 255-262.

[397] L. Wang, D. Ridgway, T. Gu, M. Moo-Young, Bioprocessing strategies to improve heterologous protein production in filamentous fungal fermentations, Biotechnol. Adv. 23 (2005) 115-129.

[398] R. Sharma, Katoch, M. and Srivastava, P.S., Approaches for refining heterolous protein production in filamentous fungi, World J. Microbiol. Biotechnol. 25 (2009) 2083-2094.

[399] C.L. Gordon, D.B. Archer, D.J. Jeenes, J.H. Doonan, B. Wells, A.P. Trinci, G.D. Robson, A glucoamylase::GFP gene fusion to study protein secretion by individual hyphae of *Aspergillus niger*, J. Microbiol. Methods 42 (2000) 39-48.

[400] A. Conesa, C.A. van den Hondel, P.J. Punt, Studies on the production of fungal peroxidases in *Aspergillus niger*, Appl. Environ. Microbiol. 66 (2000) 3016-3023.

[401] T. Durfee, R. Nelson, S. Baldwin, G. Plunkett 3rd, V. Burland, B. Mau, J.F. Petrosino, X. Qin, D.M. Muzny, M. Ayele, R.A. Gibbs, B. Csorgo, G. Posfai, G.M. Weinstock, F.R. Blattner, The complete genome sequence of *Escherichia coli* DH10B: insights into the biology of a laboratory workhorse, J. Bacteriol. 190 (2008) 2597-2606.

[402] H. Jeong, V. Barbe, C.H. Lee, D. Vallenet, D.S. Yu, S.H. Choi, A. Couloux, S.W. Lee, S.H. Yoon, L. Cattolico, C.G. Hur, H.S. Park, B. Segurens, S.C. Kim, T.K. Oh, R.E. Lenski, F.W. Studier, P. Daegelen, J.F. Kim, Genome sequences of *Escherichia coli* B strains REL606 and BL21(DE3), J. Mol. Biol. 394 (2009) 644-652.

[403] F.W. Studier, P. Daegelen, R.E. Lenski, S. Maslov, J.F. Kim, Understanding the differences between genome sequences of *Escherichia coli* B strains REL606 and BL21(DE3) and comparison of the *E. coli* B and K-12 genomes, J. Mol. Biol. 394 (2009) 653-680.

[404] J.M. Hamilton-Miller, Damaging effects of ethylenediaminetetra-acetate and penicillins on permeability barriers in Gram-negative bacteria, Biochem. J. 100 (1966) 675-682.

[405] C.C. Winterbourn, Free-radical production and oxidative reactions of hemoglobin, Environ. Health Perspect. Suppl. 64 (1985) 321-330.

[406] M.M. Bradford, A rapid and sensitive method for the quantitation of microgram quantities of protein utilizaing the principle of protein-dye binding. Anal. Biochem. 72 (1976) 248-254.

[407] U.K. Laemmli, Cleavage of structural proteins during the assembly of the head of bacteriophage T4, Nature 227 (1970) 680-685.

[408] M. Daigneault, J.A. Preston, H.M. Marriot, M.K. Whyte and D.H. Dockrell, The indentification of macrophage differentiation in PMA-stimulated THP-1 cells and monocyte-derived macrophages, PLoS one 5 (2010) e8668 1-10.